UNIVERSIDADE FEDERAL DE MINAS GERAIS
Instituto de Ciência Biológicas
Programa de Pós-graduação em Patologia

Ana Paula Vargas Garcia

ESTUDO COMPARATIVO DA CORRELAÇÃO ENTRE MACRÓFAGOS ASSOCIADOS AO TUMOR E AS ALTERAÇÕES DAS FIBRAS COLÁGENAS EM NEOPLASIAS MAMARIAS HUMANAS E CANINAS

Belo Horizonte
2024

Ana Paula Vargas Garcia

ESTUDO COMPARATIVO DA CORRELAÇÃO ENTRE MACRÓFAGOS ASSOCIADOS AO TUMOR E AS ALTERAÇÕES DAS FIBRAS COLÁGENAS EM NEOPLASIAS MAMARIAS HUMANAS E CANINAS

Tese apresentada ao Programa de Pós-graduação em Patologia da Universidade Federal de Minas Gerais, como requisito parcial à obtenção do título de Doutora em Patologia Investigativa.

Orientador: Prof. Dr. Geovanni Dantas Cassali

Coorientadora: Prof.ª Dr.ª Ana Maria de Paula

Belo Horizonte
2024

043 Garcia, Ana Paula Vargas.
Estudo comparativo da correlação entre macrófagos associados ao tumor e as alterações das fibras colágenas em neoplasias mamarias humanas e caninas [manuscrito] / Ana Paula Vargas Garcia. – 2024.
161 f. : il. ; 29,5 cm.

Orientador: Prof. Dr. Geovanni Dantas Cassali. Coorientadora: Prof.ª Dr.ª Ana Maria de Paula.
Tese (doutorado) – Universidade Federal de Minas Gerais, Instituto de Ciências Biológicas. Programa de Pós-Graduação em Patologia.

1. Patologia. 2. Colágeno. 3. Neoplasias da Mama. 4. Matriz Extracelular. 5. Microambiente Tumoral. 6. Macrófagos associados a tumores. I. Cassali, Geovanni Dantas. II. Paula, Ana Maria de. III. Universidade Federal de Minas Gerais. Instituto de Ciências Biológicas. IV. Título.

CDU: 616

Ficha catalográfica elaborada pela bibliotecária Fabiane C M Reis – CRB 6 – 2680

UNIVERSIDADE FEDERAL DE MINAS GERAIS
INSTITUTO DE CIÊNCIAS BIOLÓGICAS
PROGRAMA DE PÓS-GRADUAÇÃO EM PATOLOGIA DA UFMG - ICB/UFMG

FOLHA DE APROVAÇÃO

ANA PAULA VARGAS GARCIA

TÍTULO:

"ESTUDO COMPARATIVO DA CORRELAÇÃO ENTRE MACRÓFAGOS ASSOCIADOS AO TUMOR E AS ALTERAÇÕES DAS FIBRAS COLÁGENAS EM NEOPLASIAS MAMÁRIAS HUMANAS E CANINAS"

Tese submetida à Banca Examinadora designada pelo Colegiado do Programa de **Pós-Graduação em Patologia**, como requisito para obtenção do grau de **Doutor** em **PATOLOGIA**, área de concentração **PATOLOGIA INVESTIGATIVA**.

Aprovada em 23 de agosto de 2024, pela banca constituída pelos membros:

Profa. Dra. Karine Araujo Damasceno, Fiocruz-BA
Prof. Dr. Diego Carlos dos Reis, The Institute of Cancer Research - London
Profa. Dra. Cecilia Bonolo de Campos, University Health Network Princess Margaret Cancer
Profa. Dra. Helenice Gobbi, UFTM
Profa. Dra. Ana Maria de Paula, ICEx/UFMG - COORIENTADORA
Prof. Dr. Geovanni Dantas Cassali, ICB/UFMG - ORIENTADOR

Belo Horizonte, 23 de agosto de 2024.

Documento assinado eletronicamente por **Geovanni Dantas Cassali**, **Professor do Magistério Superior**, em 17/09/2024, às 16:51, conforme horário oficial de Brasília, com fundamento no art. 5º do Decreto nº 10.543, de 13 de novembro de 2020.

Documento assinado eletronicamente por **Ana Maria de Paula**, **Professora do Magistério Superior**, em 19/09/2024, às 22:19, conforme horário oficial de Brasília, com fundamento no art. 5º do Decreto nº 10.543, de 13 de novembro de 2020.

Documento assinado eletronicamente por **Helenice Gobbi**, **Usuário Externo**, em 20/09/2024, às 14:32, conforme horário oficial de Brasília, com fundamento no art. 5º do Decreto nº 10.543, de 13 de novembro de 2020.

Documento assinado eletronicamente por **Karine Araujo Damasceno**, **Usuária Externa**, em 20/09/2024, às 15:14, conforme horário oficial de Brasília, com fundamento no art. 5º do Decreto nº 10.543, de 13 de novembro de 2020.

Documento assinado eletronicamente por **Cecilia Bonolo de Campos**, **Usuária Externa**, em 23/10/2024, às 11:33, conforme horário oficial de Brasília, com fundamento no art. 5º do Decreto nº 10.543, de 13 de novembro de 2020.

Documento assinado eletronicamente por **Diego Carlos dos Reis**, **Usuário Externo**, em 30/10/2024, às 07:23, conforme horário oficial de Brasília, com fundamento no art. 5º do Decreto nº 10.543, de 13 de novembro de 2020.

A autenticidade deste documento pode ser conferida no site https://sei.ufmg.br/sei/controlador_externo.php?acao=documento_conferir&id_orgao_acesso_externo=0, informando o código verificador **3487766** e o código CRC **F14297AC**.

Referência: Processo nº 23072.247469/2024-48 SEI nº 3487766

Dedico este trabalho a todos os pacientes e àqueles que confiaram no meu trabalho e tornaram possível a geração dos novos conhecimentos presentes aqui, permitindo que hoje possamos compartilhá-los com o mundo, esperançosos de melhorar a vida dos que virão.

AGRADECIMENTOS

Ao meu mentor e orientador, professor Geovanni: obrigada por acreditar em mim e por permitir que este trabalho fosse desenvolvido. Obrigada por me ensinar diariamente a importância de estar sempre disposta a aprender coisas novas. Sou grata por todos os conselhos, oportunidades e ensinamentos que tem me transformado em uma profissional cada vez mais qualificada.

À professora Ana Maria: obrigada por acreditar no nosso trabalho, por possibilitar a realização deste trabalho e por abrir portas para novas descobertas e conhecimentos. Sou profundamente grata por todo o apoio e pelos valiosos ensinamentos que me guiaram neste novo mundo.

À CAPES, agradeço a concessão da bolsa que permitiu minha dedicação integral aos estudos e à pesquisa.

Aos meus pais, Viviane e Cristian, ao meu irmão, Victor, e aos meus avós, Olinda e Tito (in memorian): obrigada por serem meu porto seguro e minha sustentação ao longo deste período. Sem vocês, essa jornada não teria sido possível. Essa conquista não é só minha, mas nossa! Obrigada por tanto amor! Eu amo vocês!

À Kamilla, que foi meu alicerce durante esses quatro anos: você me ouviu, me aconselhou, enxugou minhas lágrimas e me acolheu todas as vezes que pensei em desistir. Obrigada por estar ao meu lado e por não me deixar renunciar a esse sonho, que se tornou nosso ao longo desse tempo. Eu te amo!

Agradeço aos meus queridos gatos Theo (*in memorian*), Frida, Léo, Maninho, Pituco e Mostarda, que foram minha companhia constante ao longo deste tempo. Vocês são e sempre serão uma parte especial da minha vida. Eu amo vocês!

Às amigas que este período me trouxe: Laiz, Amanda, Júlia, Marina e Marisa. Obrigada por tornarem meus dias mais leves, especialmente nos momentos em que eu duvidei da minha capacidade. Agradeço pelas discussões, pelos aprendizados, pelo auxílio nos experimentos, pelas conversas, pelas sessões de terapia em grupo e, acima de tudo, pelas incontáveis risadas. Aprendi muito com cada uma de vocês. Obrigada por tanto!

Aos funcionários do Laboratório Celulavet! Mesmo à distância, vocês foram incríveis! Agradeço pela ajuda, pela paciência e por todas as vezes que facilitaram meu trabalho no LPC. Vocês tornaram essa experiência muito mais leve e produtiva.

À Luana, Bárbara e Luisa: obrigada por todo o auxílio nos experimentos e por todos os momentos maravilhosos que compartilhamos no laboratório, especialmente durante as intermináveis medições das lâminas.

Aos demais colegas do Laboratório de Patologia Comparada, que, mesmo sem tanto tempo compartilhado, contribuíram de alguma forma para o desenvolvimento deste trabalho da melhor maneira possível.

Um agradecimento especial à Cintya, secretária do programa de pós-graduação em Patologia, cuja dedicação e presteza foram imprescindíveis para a realização desta tese. Sua ajuda com as burocracias, sempre com atenção e eficiência, permitiu que eu me concentrasse na pesquisa e no desenvolvimento deste trabalho. Agradeço imensamente por sua paciência, seu conhecimento e sua constante disponibilidade.

Deixo expresso, também, meu reconhecimento aos estimados professores que compuseram a banca examinadora desta tese. Agradeço profundamente à Dra. Cecília Bonolo de Campos, ao Dr. Diego Carlos Reis, à Dra. Karine Araújo Damasceno e à Dra. Helenice Gobbi, não apenas pela gentileza de sua presença, mas também pelas valiosas contribuições e arguições que, sem dúvida, enriqueceram este trabalho e o conduziram a um patamar de maior excelência.

Aos professores, técnicos e demais profissionais do Departamento de Patologia do ICB/UFMG, ao Departamento de Física do ICEx/UFMG, às agências de fomento, CNPq e FAPMIG e a todos aqueles que contribuíram para que este trabalho fosse realizado de forma excepcional, meu muito obrigada! Todos vocês fazem parte dessa história e dessa conquista!

“É muito melhor lançar-se em busca de conquistas grandiosas, mesmo expondo-se ao fracasso, do que alinhar-se com os pobres de espírito, que nem gozam muito nem sofrem muito, porque vivem numa penumbra cinzenta onde não conhecem nem vitória, nem derrota.”

(Theodore Roosevelt, 1858-1919)

RESUMO

A identificação das alterações nos componentes do microambiente tumoral em neoplasias mamárias é fundamental para compreender os mecanismos que influenciam os diferentes comportamentos dos carcinomas mamários e contribuir para um diagnóstico mais preciso. Apesar dos avanços no entendimento do câncer de mama, ainda existe uma lacuna significativa no conhecimento sobre como as interações entre o colágeno e os macrófagos associados ao tumor influenciam a progressão tumoral e o prognóstico. Trata-se de um estudo retrospectivo de 19 amostras de glândula mamária normal, 12 amostras de fibroadenoma, 04 amostras de carcinoma tubular, 16 amostras de carcinoma invasor grau I, 21 amostras de carcinoma invasor grau III e 17 amostras de carcinoma micropapilar invasor na espécie humana e 20 amostras de glândula mamária normal, 15 amostras de tumor misto benigno, 14 amostras de carcinoma em tumor misto, 06 casos de carcinossarcoma, 16 amostras de carcinoma micropapilar invasor e 23 casos de carcinomas de arranjo sólido na espécie canina. Foram avaliadas lâminas coradas com eosina e hematoxilina de 15 áreas representativas em cada amostra. Imagens por geração de segundo harmônico e microscopia de fluorescência excitada por dois fótons foram realizadas para avaliar os parâmetros de colágeno e segmento celular. Os resultados indicam que nos carcinomas mamários humanos e caninos, as fibras colágenas estão mais alinhadas em relação ao tecido normal. Nos carcinomas, o número de fibras e a área coberta por elas são maiores, enquanto a área coberta por células é menor, em comparação ao tecido normal, tanto em tumores humanos quanto caninos. No carcinoma mamário humano, as fibras colágenas são mais lineares em comparação com o tecido normal. Além disso, os carcinomas com prognóstico desfavorável possuem fibras colágenas mais curtas e os parâmetros de colágeno se correlacionam com os dados clínicos e patológicos nas espécies humana e canina. Há uma clara associação entre o comprimento médio das fibras com os tempos de sobrevida global em cães, em que pacientes diagnosticados com carcinomas com fibras colágenas mais curtas têm pior sobrevida. Nossos achados demonstraram uma correlação significativa entre os parâmetros do colágeno e os dados clínicos e patológicos nas espécies humana e canina. Identificamos uma associação clara entre o comprimento médio das fibras colágenas e o tempo de sobrevida global em cães, evidenciando que pacientes diagnosticados com carcinomas exibindo fibras colágenas mais curtas apresentam um pior prognóstico. O estudo também revelou que os macrófagos associados ao tumor (TAMs) infiltrados em carcinomas com prognóstico favorável (como o carcinoma tubular e o carcinoma invasor grau I em humanos, e o carcinoma em tumor misto em cães) expressam simultaneamente marcadores dos tipos M1 e M2, demonstrando a plasticidade dessas células. Em contraste, os TAMs presentes em carcinomas com prognóstico desfavorável (como o carcinoma invasor grau III e o carcinoma micropapilar invasor em humanos, e o carcinossarcoma, carcinoma micropapilar invasor e carcinoma com arranjo sólido em cães) apresentam um perfil predominantemente do tipo M2-like. As descobertas ressaltam a importância da interação entre as fibras colágenas e TAMs na progressão do câncer de mama e sugerem que atingir essa interação pode representar uma nova abordagem terapêutica. Neste trabalho, demonstrou-se que a espécie canina é um bom modelo de estudo para avaliar as alterações estromais em tecidos mamários neoplásicos humanos. Nossos resultados expandem o entendimento das alterações estromais em carcinomas mamários, tanto em humanos quanto em cães, corroborando com o uso dos modelos comparativos para a investigação das características tumorais, potencialmente influenciando futuras abordagens em pesquisa oncológica.

Palavras-chave: arquitetura do colágeno; organização do colágeno; câncer de mama; remodelação da matriz extracelular; microambiente tumoral; macrófagos associados a tumor.

ABSTRACT

The identification of alterations in the components of the tumor microenvironment in mammary neoplasms is essential for understanding the mechanisms that influence the different behaviors of mammary carcinomas and contribute to more accurate diagnoses. Despite advances in the understanding of breast cancer, there remains a significant gap in knowledge regarding how the interactions between collagen and tumor-associated macrophages (TAMs) influence tumor progression and prognosis. This is a retrospective study of 19 normal mammary gland samples, 12 fibroadenoma samples, 4 tubular carcinoma samples, 16 grade I invasive carcinoma samples, 21 grade III invasive carcinoma samples, and 17 invasive micropapillary carcinoma samples in humans, as well as 20 normal mammary gland samples, 15 benign mixed tumor samples, 14 carcinoma in mixed tumor samples, 6 cases of carcinosarcoma, 16 invasive micropapillary carcinoma samples, and 23 cases of solid arrangement carcinomas in dogs. Hematoxylin and eosin-stained slides of 15 representative areas from each sample were evaluated. Second harmonic generation and two-photon excited fluorescence microscopy images were used to assess collagen parameters and cell segment. The results indicate that in both human and canine mammary carcinomas, collagen fibers are more aligned compared to normal tissue. In carcinomas, the number of fibers and the area covered by them are greater, while the area covered by cells is smaller, compared to normal tissue, in both human and canine tumors. In human breast carcinoma, collagen fibers are more linear compared to normal tissue. Additionally, carcinomas with poor prognosis have shorter collagen fibers, and collagen parameters correlate with clinical and pathological data in both human and canine species. There is a clear association between the average fiber length and overall survival times in dogs, where patients diagnosed with carcinomas exhibiting shorter collagen fibers have poorer survival. Our findings demonstrated a significant correlation between collagen parameters and clinical and pathological data in both human and canine species. We identified a clear association between the average collagen fiber length and overall survival time in dogs, showing that patients diagnosed with carcinomas displaying shorter collagen fibers have a worse prognosis. The study also revealed that tumor-associated macrophages (TAMs) infiltrating carcinomas with favorable prognosis (such as tubular carcinoma and grade I invasive carcinoma in humans, and carcinoma in mixed tumor in dogs) simultaneously express both M1 and M2 markers, demonstrating the plasticity of these cells. In contrast, TAMs present in carcinomas with poor prognosis (such as grade III invasive carcinoma and invasive micropapillary carcinoma in humans, and carcinosarcoma, invasive micropapillary carcinoma, and solid arrangement carcinoma in dogs) exhibit a predominantly M2-like profile. These findings highlight the importance of the interaction between collagen fibers and TAMs in breast cancer progression and suggest that targeting this interaction may represent a new therapeutic approach. This work demonstrates that the canine species is a good model for studying stromal changes in human neoplastic mammary tissues. Our results expand the understanding of stromal changes in mammary carcinomas in both humans and dogs, supporting the use of comparative models to investigate tumor characteristics, potentially influencing future approaches in cancer research.

Key-words: collagen architecture; collagen organization; breast cancer; extracellular matrix remodelling; tumour microenvironment; tumour-associated macrophages

LISTA DE FIGURAS

LISTA DE ABREVIATURAS E SIGLAS

αSMA - α actina de músculo liso
BCL- linfoma de células B
BMT- benign in mixed tumor
BRCA1 - breast cancer 1
BRCA2 - breast cancer 2
CEA- carcinoembryogenic antigen
CAS - carcinomas com arranjo sólido
CCL- chemokine ligand
CK - citoqueratina
CM - carcinoma micropapilar
CMT - carcinoma in mixed tumor
CMI - carcinoma micropapilar invasivo
CS - carcinosarcoma
CSA - carcinoma with solid arrangement
CSF-1- fator estimulante de colônias 1
CSS - carcinossarcoma
CT - carcinoma tubular
CTM - carcinoma em tumor misto
CXCL- CX motif chemokine ligand
DM - dichroic mirror
EAT - estroma associado ao tumor
EGFR - epidermal growth factor receptor
EMA- epithelial membrane antigen
FAP- fibroblast activation protein
FAC- fibroblastos associados ao câncer
Fb- fibroadenoma
GATA- guanina-adenina-timina-adenina gene
HER-2 - (receptor de crescimento epidérmico humano 2)
H&E - eosina e hematoxilina
ICB - Instituto de Ciências Biológicas
ICEx - Instituto de Ciências Exatas
IL- interleucina
IFNγ- interferon γ
INCA - Instituto Nacional do Câncer
LPS- lipopolissacarídeo
LPC- Laboratório de Patologia Comparada
M - presença de metástases à distância
N - envolvimento neoplásico de linfonodos regionais
MAT - macrófagos associados ao tumor
MCF- Michigan Cancer Foundation
MCP-1- proteína quimiotática de monócitos
MMT - metaloproteinases de matriz
MRTF- myocardin-related transcription factor
MVD- densidade microvascular
OMS - Organização Mundial da Saúde
p63- proteína 63
PAX- paired box genes

PMT - photomultiplier (fotomultiplicadora)
RE - receptor de estrógeno
RP - receptor de progesterona
SDF1- stromal cell-derived factor 1
SHG - second harmonic generation (geração de segundo harmônico)
T - tamanho do tumor
TGF - fator de crescimento transformador
TNF- tumor necrosis factor
TTF- thyroid transcription factor
TMB - tumor misto benigno
UFMG - Universidade Federal de Minas Gerais
uPA- urokinase-type plasminogen activator
VEGF- vascular endothelial growth factor
WT1- Wilms' Tumor protein

SUMÁRIO

1. INTRODUÇÃO

O câncer de mama é a neoplasia maligna mais comum entre mulheres em todo o mundo, motivando extensos estudos sobre prevenção e diagnóstico precoce para reduzir a morbimortalidade associada a essa condição (Toríbio et al., 2012). Na Medicina Veterinária, essa neoplasia também desperta grande interesse devido à elevada prevalência de tumores malignos em cadelas, que frequentemente resulta em diagnóstico tardio, comprometendo o tratamento e reduzindo a taxa de sobrevida dos animais (Cavalcanti & Cassali, 2006; Andrade et al., 2010; Estrela-Lima, 2010). Notavelmente, as neoplasias mamárias em cadelas e em mulheres compartilham similaridades epidemiológicas, clínicas, biológicas e genéticas, permitindo o uso da cadela como um modelo comparativo experimental relevante (Cassali, 2000; Cassali, 2002; Misdorp, 2002; Uva et al., 2009; Rivera & Von Euler, 2011; Markkanen, 2019).

O microambiente tumoral (MAT), composto por uma complexa interação de células não tumorais, como fibroblastos, macrófagos, células imunes, células vasculares e adipócitos, juntamente com a matriz extracelular (MEC), é fundamental tanto na iniciação quanto na progressão de diversas neoplasias, incluindo o câncer de mama (Pollard, 2010; Markkanen, 2019). Cada um desses componentes exerce influências específicas no comportamento das células tumorais, modulando processos como a proliferação, a invasão e a resposta ao tratamento. Entre esses componentes, os macrófagos associados a tumor (MATs) desempenham um papel especialmente crucial. Estes macrófagos, particularmente na forma polarizada M2, são prevalentes no MAT e estão fortemente associados a prognósticos desfavoráveis. Eles promovem a progressão tumoral através da secreção de fatores de crescimento e pró-angiogênicos, contribuindo para a formação do estroma e a angiogênese, além de suprimirem a resposta imunológica antitumoral (Gyorki & Lindeman, 2008; Mantovani & Sica, 2010; Mahmoud et al., 2012). A presença de MATs está correlacionada a piores prognósticos em diversos tipos de câncer, incluindo o câncer de mama em humanos (Ueno et al., 2000; Wyckoff et al., 2004; Goswami et al., 2005; Qiu et al., 2018; Munir et al., 2021; Xiao et al., 2021; Xu et al., 2021) e caninos (Monteiro et al., 2018).

Estudos clínicos e pré-clínicos têm ligado os MAT à iniciação, desenvolvimento e metástase em neoplasias mamárias (Krol et al., 2011; Raposo et al., 2014; SchmiedeR et al., 2012). A expressão de marcadores de transição epitelial-mesenquimal (EMT) e a presença de macrófagos M2 no MAT sugerem um papel ativo dessas células na progressão do câncer

(Monteiro et al., 2018; Zhu et al., 2019; Jiang & Zhan, 2020; Orecchioni et al., 2019; DeNardo & Ruffell, 2019; Locati & Mantovani, 2020). Por isso, torna-se crucial investigar se as alterações ocorridas nas fibras colágenas durante a progressão de neoplasias mamárias têm correlação com o aumento da expressão de MATs. Essa investigação pode fornecer *insights* valiosos para novas abordagens terapêuticas, visando o desenvolvimento de terapias direcionadas que interrompam essa interação e, consequentemente, a progressão tumoral, tanto em oncologia humana quanto veterinária.

Além dos macrófagos, a MEC também desempenha um papel central na progressão tumoral. O colágeno, um dos componentes principais da MEC, tem uma função particularmente significativa no desenvolvimento de metástases em carcinomas mamários. Ele influencia diretamente a atividade das metaloproteinases de matriz (MMPs), que são enzimas críticas na degradação e remodelamento da MEC, processos essenciais para a invasão e disseminação tumoral. A interação entre colágeno e MMPs tem sido amplamente estudada no contexto do prognóstico e terapias para o câncer, especialmente no câncer de mama (Hompland et al., 2008; Burke et al., 2013; Burke et al., 2015; Golaraei et al., 2016; Barcus et al., 2017; Case et al., 2017; Conklin et al., 2018; Reis et al., 2020; Garcia et al., 2021; Garcia et al., 2024).

Estudos têm demonstrado que, em comparação com a mama saudável, as glândulas mamárias neoplásicas exibem fibras colágenas mais organizadas e alinhadas, e essa organização correlaciona-se com prognósticos desfavoráveis (Case et al., 2017; Conklin et al., 2018; Natal et al., 2018; Natal et al., 2019; Reis et al., 2020; Garcia et al., 2021; Garcia et al., 2024). Alterações na densidade e na organização das fibras de colágeno não só refletem a agressividade do tumor, mas também estão associadas ao grau tumoral e à sobrevida global das pacientes, tanto em carcinomas mamários humanos quanto em caninos (Case et al., 2017; Garcia et al., 2021). Essas descobertas reforçam a importância da MEC e dos MATs na modulação do MAT, influenciando diretamente o comportamento das células cancerosas e o desfecho clínico.

2. REVISÃO DE LITERATURA

2.1 Câncer de mama

O câncer de mama é o tipo de câncer mais frequentemente diagnosticado em mulheres em todo o mundo, correspondendo a aproximadamente 24% de todos os casos de câncer feminino. As neoplasias malignas da mama representam cerca de 11,6% dos cânceres em ambos os sexos, sendo o segundo tipo mais comum na população geral (WHO, 2022). Em 2021, foram estimados 66.280 novos casos de câncer de mama no Brasil, com um risco estimado de 61,61 casos a cada 100 mil mulheres. Além disso, é a principal causa de morte por câncer entre as mulheres no Brasil, com uma taxa de mortalidade ajustada por idade de 12,23 por 100 mil mulheres. As regiões sul e sudeste apresentam as maiores taxas de incidência da doença (INCA, 2023).

Estudos nos Estados Unidos revelaram variações nos subtipos de câncer de mama dependendo das características da população. Em populações rastreadas, o câncer de mama positivo para receptores hormonais é o subtipo mais comum, com cânceres HER2-positivos constituindo 10-15% e os tumores negativos para receptores hormonais/HER2-negativo correspondendo a 13-17%. Em populações não triadas, a frequência é diferente, com maior proporção de cânceres RE-negativo/HER2-negativo (20-40%) e HER2-positivo (15-25%) (WHO, 2019).

A biologia do câncer de mama também varia conforme a etnia, influenciando as taxas de mortalidade globalmente (Razzak, 2019). Por exemplo, mulheres afro-americanas apresentam maiores taxas de carcinomas triplos negativos e doença metastática, além de maior proporção de carcinomas pouco diferenciados, todos associados a uma menor sobrevida. O câncer de mama metastático representa 9% dos diagnósticos entre mulheres negras não hispânicas, comparado a 5-6% em outras mulheres (Harbeck et al., 2019).

A origem do carcinoma da glândula mamária é multifatorial, sendo hormônios, dieta, fatores reprodutivos e genéticos os principais fatores de risco (WHO, 2021). Dados epidemiológicos sugerem que o estilo de vida ocidental, caracterizado por dieta hipercalórica, falta de exercício físico, obesidade, idade avançada para o primeiro parto, menor paridade e menor duração da lactação, está associado ao aumento da incidência da doença. A doença é mais frequente entre mulheres que têm menarca precoce, permanecem nulíparas, têm poucos filhos ou têm o primeiro filho em idade avançada. A utilização de esteroides exógenos

(estrógenos ou progestágenos) também desempenha um papel importante no desenvolvimento de carcinomas mamários (WHO, 2021).

A taxa de incidência do câncer de mama aumenta mais rapidamente antes da menopausa (~8% ao ano) do que após a menopausa (~2% ao ano), quando a síntese de estrógeno e progesterona pelos ovários cessa, e a produção de andrógenos ovarianos diminui gradualmente. O consumo de álcool está consistentemente associado a um aumento moderado no risco de câncer de mama, particularmente em cânceres positivos para receptores hormonais (WHO, 2021). Embora o tabagismo ativo não tenha sido associado diretamente ao câncer de mama, mulheres que começam a fumar antes do primeiro parto apresentam um risco aumentado. Além disso, níveis mais altos de atividade física estão associados a uma redução no risco da doença, enquanto a associação entre índice de massa corporal e risco de câncer de mama é mais forte em mulheres na pós-menopausa (WHO, 2021).

A identificação de genes de susceptibilidade ao câncer de mama esclareceu alguns aspectos da patogênese da doença esporádica e hereditária (Razzak, 2019). As características moleculares mais relevantes clinicamente estão relacionadas ao receptor de crescimento epidérmico humano 2 (HER2), aos receptores hormonais (estrógeno e progesterona) e às mutações BRCA, dados que orientam o tratamento e a pesquisa clínica (Razzak, 2019).

A malignidade e a progressão neoplásica dependem tanto do comportamento intrínseco das células tumorais quanto das mudanças no MAT que as rodeia (Rimal et al., 2022). O MAT desempenha um papel crítico no suporte ao crescimento tumoral e na facilitação de sua disseminação. A MEC, composta por colágeno, fibronectina e outras proteínas estruturais, também é constantemente remodelada e ajustada para facilitar a invasão e migração das células tumorais. A interação dinâmica entre esses elementos celulares e não celulares dentro do MAT cria um ambiente propício para o crescimento contínuo do tumor, resistência ao tratamento e eventual disseminação metastática. Essas complexas interações tornam o MAT um alvo promissor para o desenvolvimento de novas estratégias terapêuticas que busquem interromper o suporte fornecido pelo microambiente às células tumorais (Piersma et al., 2020).

2.1.1 Caracterização histológica da glândula mamária humana saudável e neoplásica

As glândulas mamárias possuem entre 15 a 25 lóbulos de glândulas tubuloalveolares compostas, cuja função é secretar leite para a nutrição do recém-nascido. Cada lóbulo é uma glândula individualizada com seu próprio ducto excretor, chamado ducto galactóforo, que mede entre 2 a 4,5 cm de comprimento. Esses ductos emergem independentemente no mamilo. Os

lóbulos são separados entre si por tecido conjuntivo denso e abundante tecido adiposo (Junqueira & Carneiro, 2017).

Na mulher adulta, o lóbulo, estrutura característica da glândula, desenvolve-se a partir das extremidades dos ductos menores. Um lóbulo consiste em vários ductos intralobulares que se unem em um ducto interlobular terminal. Ao redor de cada lóbulo há tecido conjuntivo intralobular, mais frouxo e muito celularizado. Em contrapartida, o tecido conjuntivo interlobular, que separa os lóbulos, é mais denso e menos celularizado (figura 01). O tecido conjuntivo em torno dos alvéolos contém uma abundância de linfócitos e plasmócitos, importantes para conferir imunidade passiva ao recém-nascido (Junqueira & Carneiro, 2017).

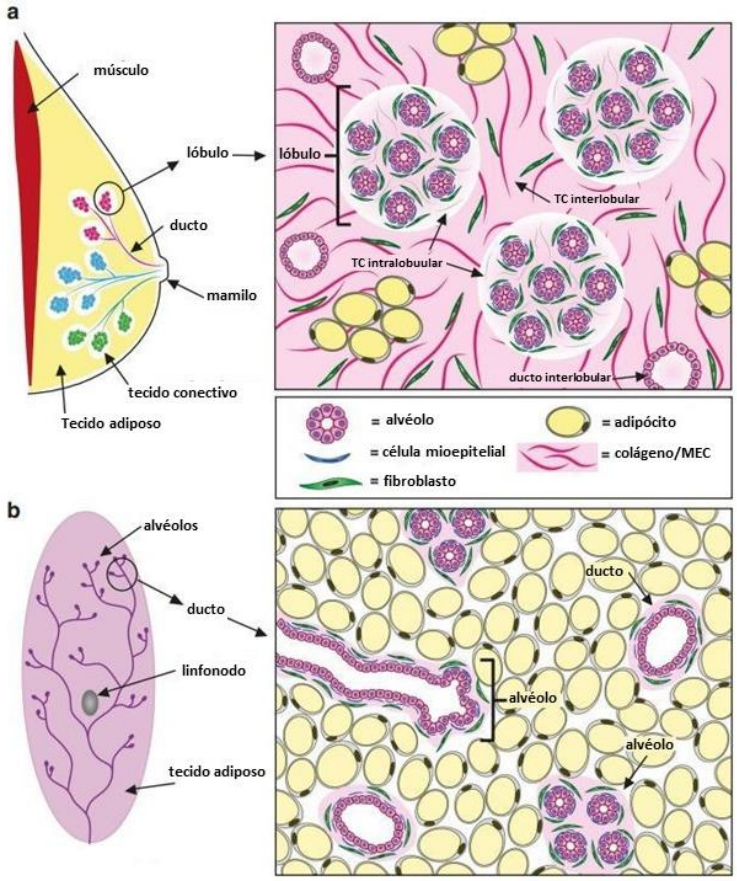

Figura 01- Desenho esquemático representando a glândula mamária humana consistindo em ductos e lóbulos localizados em um ambiente rico em matriz extracelular (tecido conectivo intra e interlobular). Adaptado de J. M. Houthuijzenl & J. Jonkers, 2018.

Dentro desse contexto de organização tecidual, podem alterações patológicas nos ductos ou nas unidades lobulares da mama, que são as unidades funcionais do tecido mamário. Entre elas, destaca-se o fibroadenoma, uma neoplasia benigna circunscrita do tecido lobular do ducto terminal, caracterizada por proliferação bifásica de células epiteliais e componentes estromais. Estes tumores podem apresentar um padrão de crescimento estromal ao redor dos ductos abertos

de forma circunferencial e/ou em padrão intracanalicular com compressão estromal de ductos em fendas. Mitoses são incomuns, mas podem estar presentes em adenomas-fibrosos em pacientes jovens ou grávidas (WHO, 2019).

Enquanto os fibroadenomas representam uma condição benigna, o espectro das neoplasias mamárias inclui patologias mais graves, como os carcinomas invasivos. Esses carcinomas abrangem um grupo heterogêneo de neoplasias epiteliais malignas, cuja classificação é baseada na presença ou ausência de expressão dos receptores hormonais (RE e RP) e da proteína HER2: RE-positivo, HER2-negativo; RE-positivo, HER2-positivo; RE-negativo, HER2-positivo; e RE-negativo, HER2-negativo (WHO, 2019).

Os carcinomas invasivos apresentam um amplo espectro histológico, descrito através de quatro características principais: (1) subtipo histológico, (2) Graduação de Nottingham, (3) presença ou ausência de invasão angiolinfática, e (4) componente in situ associado. A graduação histológica é baseada na formação de túbulos, pleomorfismo nuclear e contagem mitótica, resultando em uma pontuação que classifica os tumores como grau 1 (bem diferenciado), grau 2 (moderadamente diferenciado) ou grau 3 (pouco diferenciado) (WHO, 2019).

A expressão nuclear do receptor de estrogênio (RE) deve ser avaliada nos carcinomas mamários invasivos, devido à sua utilidade em prever o benefício da terapia endócrina. A expressão do receptor de progesterona (RP) tende a variar mais do que a do receptor de estrogênio, auxiliando na estratificação prognóstica dos casos RE-positivos, embora os limiares de RP específicos para essa finalidade ainda não estejam totalmente definidos (WHO, 2019).

Existem também carcinomas mamários que apresentam características histológicas únicas, classificados como carcinomas invasivos de tipo especial. O carcinoma tubular (CT), por exemplo, é um câncer de mama invasivo, porém de baixa agressividade, caracterizado por túbulos bem estruturados, revestidos por uma única camada de células cancerígenas. Com uma prevalência de aproximadamente 1,6% de todos os carcinomas mamários invasivos, o CT tem um excelente prognóstico, com taxas de sobrevida de 5 anos variando de 88% a 96% (WHO, 2019).

O carcinoma micropapilar invasivo (CMI) é outro tipo de carcinoma mamário invasivo, composto por aglomerados de células malignas rodeados por espaços claros, com padrão de crescimento de dentro para fora. Os CMI são raros, representando 0,9 a 2% dos casos, e frequentemente apresentam metástases para linfonodos axilares. A morfologia micropapilar está associada a um pior prognóstico em relação aos carcinomas não especiais de mesmo tamanho (WHO, 2019).

2.2 Neoplasias da glândula mamária na medicina veterinária

Os carcinomas mamários são a forma mais comum de neoplasia em cadelas (Nunes et al., 2018). Interessantemente, a maioria das cadelas com lesões mamárias está clinicamente saudável no momento do diagnóstico, com essas lesões geralmente sendo identificadas pelo proprietário ou durante exames físicos de rotina (Sorenmo, 2003). As neoplasias mamárias costumam manifestar-se como nódulos circunscritos, variando em tamanho, consistência e mobilidade em relação à pele e aos músculos subjacentes. Podem estar associados a ulcerações na pele e reações inflamatórias. Múltiplos nódulos em uma única glândula mamária ou em várias glândulas simultaneamente são comuns, com diferentes tipos histológicos (Kurzman et al., 1986; Misdorp, 1999).

O estadiamento clínico da neoplasia é fundamental para estabelecer um prognóstico e planejar o tratamento, oferecendo indicações precisas ao patologista sobre o material a ser analisado (Cassali et al., 2020). O estadiamento é determinado conforme o Sistema TNM, estabelecido pela Organização Mundial da Saúde para tumores mamários caninos. Esse sistema avalia o tamanho da lesão primária (T), a extensão de sua disseminação para linfonodos regionais (N) e a presença ou ausência de metástases à distância (M) (Owen, 1999). Esses parâmetros apresentam significativa correlação com a agressividade tumoral.

Além do estadiamento clínico, o grau histológico é outro fator crucial na avaliação das neoplasias mamárias, baseado na análise do índice de formação tubular, pleomorfismo nuclear e contagem mitótica. O grau histológico é determinado por uma pontuação que resulta em um valor total que varia de 3 a 9 (Cassali et al., 2020). A classificação mais amplamente adotada é a de Misdorp et al. (1999), atualizada no último Consenso de *Diagnóstico, Prognóstico e Tratamento de Tumores Mamário Caninos e Felinos* - 2019, publicado em 2020 (Cassali et al., 2020).

2.2.1 Caracterização histológica da glândula mamária canina saudável e neoplásica

A glândula mamária canina é constituída por adenômeros bem desenvolvidos, característicos de sua classificação como glândula exócrina composta, tubuloacinosa ou tubuloalveolar, apócrina. Cada glândula é formada por um corpo mamário e uma papila mamária, onde desembocam numerosos ductos lactíferos principais. Abaixo do tecido subcutâneo, há um conjunto de estruturas conjuntivas que sustentam o parênquima glandular, composto por adenômeros do tipo tubuloacinosos. Esses adenômeros são constituídos por

parede epitelial e cavidade contendo secreção, e ductos lactíferos. Os lúmens das glândulas tubuloacinares contêm secreção acidófila de aspecto homogêneo ou granular, na maioria dos casos. Os ductos excretores glandulares subdividem-se em intralobulares, interlobulares e principais, recebendo o leite produzido pelos tubuloácinos e conduzindo-o aos diferentes ductos principais que desembocam no ápice da papila mamária. O epitélio de revestimento dos ductos é simples e baixo nos segmentos intralobulares, tornando-se cúbico ou biestratificado nos ductos de maior calibre (Cassali et al., 2023).

Embora a glândula mamária canina seja fundamental para o desenvolvimento de sua função exócrina, ela também é suscetível ao desenvolvimento de neoplasias, como os tumores mistos benignos (TMB). Esses tumores são caracterizados pela proliferação benigna de células epiteliais e mesenquimais, que produzem cartilagem, osso e/ou tecido adiposo, frequentemente combinados com proliferação de tecido fibroso (Misdorp et al., 1999). A proliferação de células mioepiteliais em associação com a matriz mixoide é a origem da cartilagem ectópica observada nesses tumores, sugerindo ser resultado da transição epitelial-mesenquimal ou mesenquimal-mioepitelial (Erdelyi et al., 1991). Algum grau de pleomorfismo e atipia é frequentemente observado nesses casos, tornando o diagnóstico diferencial com o carcinoma em tumor misto mais desafiador. O TMB é o tumor benigno mais comum em cães (Misdorp et al., 1999; Cassali et al., 2017), enquanto em humanos, embora raro nas glândulas mamárias, ocorre de forma rotineira nas glândulas salivares, onde é denominado tumor misto ou adenoma pleomórfico (Voz et al., 2000).

No entanto, a transformação maligna de tumores mistos benignos pode dar origem ao carcinoma em tumor misto (CTM). Este tipo de tumor, que representa cerca de 44% das neoplasias malignas da glândula mamária canina (Nunes et al., 2018), exibe um padrão histológico mais complexo, envolvendo componentes epiteliais e mesenquimais, dos quais alguns podem se tornar malignos, resultando no desenvolvimento de carcinomas. O CTM se caracteriza pela presença de células epiteliais com elevado pleomorfismo e mitoses atípicas, além de um crescimento infiltrativo, identificado pela descontinuidade da camada basal/mioepitelial e a penetração de aglomerados de células tumorais no estroma. Apesar dessa agressividade, o prognóstico é relativamente bom, com alta taxa de sobrevida global (Nunes et al., 2018; Cassali et al., 2017).

Já os carcinossarcomas (CSS), que são menos frequentes, apresentam um prognóstico significativamente pior. Embora raros em humanos, os CSS são mais prevalentes na espécie canina, e apresentam comportamento clínico e patológico semelhante em ambas as espécies. Esses tumores são compostos por células que se assemelham a epitélio, exibindo diferentes

tipos de diferenciação, como áreas sólidas, escamosas, mucinosas, anaplásicas e sarcomatosas, com diferenciação fibro, condro e osteomatosa (Misdorp et al., 1973; Cassali et al., 2017). A alta taxa de metástase dos CSS contribui para seu pior prognóstico em relação aos CTMs. Devido às similaridades morfológicas entre os CTMs e CSS nas glândulas mamárias de humanos e cães, essas neoplasias são frequentemente usadas como modelos comparativos para estudos de progressão tumoral (Cassali et al., 2017).

Outro tipo raro de neoplasia mamária é o carcinoma micropapilar, associado a linfotropismo e prognóstico desfavorável (Cassali et al., 2020). Microscopicamente, esses tumores são caracterizados por espaços císticos bem definidos, que lembram vasos linfáticos, e estão distribuídos pela glândula mamária. Dentro desses espaços, aglomerados de células epiteliais formam padrões micropapilares, exibindo citoplasma eosinofílico, pleomorfismo nuclear evidente e nucléolos proeminentes. O índice mitótico é variável, e a presença de metástases em linfonodos é frequentemente observada (Cassali et al., 1999a; Cassali et al., 2000; Cassali et al., 2020). O comportamento biologicamente agressivo do carcinoma micropapilar, com altas taxas de metástase e menor sobrevida global, ressalta a necessidade de estudos mais aprofundados (Gama et al., 2008; Gamba et al., 2013; Nunes et al., 2018).

Por outro lado, os carcinomas com arranjo sólido apresentam um padrão de proliferação distinto, com células epiteliais organizadas em cordões, folhas ou aglomerados sólidos. Essas células tumorais são indiferenciadas, com pequenos núcleos hipercromáticos e um alto índice mitótico. Em alguns casos, as células podem apresentar citoplasma vacuolado, possivelmente de origem mioepitelial. A quantidade de estroma varia de pequena a moderada, e áreas de necrose são frequentemente observadas (Cassali et al., 2002a; Cassali et al., 2020). Assim como os carcinomas micropapilares, os carcinomas sólidos também estão associados a um prognóstico mais reservado, com menor sobrevida global (Nunes et al., 2018; Nakagaki et al., 2021).

Um estudo realizado por Nunes e colaborares em 2022, investigou a distribuição e o valor prognóstico dos imunofenótipos em carcinomas mamários caninos, utilizando um painel imuno-histoquímico conforme as recomendações da classificação de St. Gallen (Goldhirsch et al., 2011). A classificação dos subtipos luminais foi subdividida em luminal A (RE e/ou RP positivo, Ki67 /=20%) e luminal B HER+ (RE e/ou RP positivo, HER2 positivo, Ki67 >/=20%). O subtipo mais comum diagnosticado foi o luminal B HER2 negativo, seguido do luminal A.

Os imunofenótipos luminal B HER2- e HER2+ foram associados a pior sobrevida, maiores tamanhos tumorais, metástases linfonodais ou distantes, tipos histológicos mais agressivos e invasão angiolinfática. Esses achados têm implicações importantes para a

definição do prognóstico e planejamento de terapias adjuvantes. Embora a classificação imunofenotípica seja um fator preditivo/prognóstico estabelecido no câncer de mama humano, terapias individualizadas para cada imunofenótipo ainda não estão amplamente disponíveis na oncologia veterinária (Nunes et al., 2022). Além disso, a expressão aumentada de Ki67 e a diminuição dos receptores hormonais também indicam um pior prognóstico e sugerem a necessidade de quimioterapia adjuvante (Cassali et al., 2019).

2.3 Neoplasias mamárias em cadelas como modelo translacional

A diversidade e complexidade das neoplasias mamárias humanas refletem-se também na medicina veterinária, onde os carcinomas mamários são as neoplasias mais frequentes em cadelas idosas (De Nardi et al., 2002; Nunes et al., 2018). Essas similaridades destacam a importância de estudos comparativos e a necessidade de abordagens detalhadas no diagnóstico e tratamento dessas neoplasias em humanos e animais.

Devido à fisiopatologia intimamente relacionada, as neoplasias que se desenvolvem naturalmente em cães domésticos têm sido progressivamente utilizadas como uma valiosa fonte de informações para compreender melhor a biologia do câncer de mama em mulheres (Sorenmo et al., 2009; Queiroga et al., 2011b; Abadie et al., 2017; Nguyen et al., 2017; Markkanen, 2019). Muitos estudos têm se concentrado em avaliar os aspectos moleculares das células tumorais em cães, comparando-as com as células tumorais humanas (Sorenmo et al., 2009; Queiroga et al., 2011b; Abadie et al., 2017; Markkanen, 2019; Vieira et al., 2022).

Entre várias neoplasias, as neoplasias mamárias espontâneas em cães são vistas como excelentes modelos de estudo para o câncer de mama humano (Sorenmo et al., 2009; Queiroga et al., 2011b; Abadie et al., 2017; Markkanen, 2019; Vieira et al., 2022). A oncologia comparativa visa abordar algumas deficiências das pesquisas tradicionais, ampliando seu foco desde modelos clássicos de roedores até neoplasias espontâneas que se desenvolvem em animais. Essa abordagem é percebida como uma oportunidade para complementar e aprimorar a compreensão de doenças complexas, como o câncer, particularmente no que diz respeito ao desenvolvimento neoplásico, fatores de risco e mecanismos de tumorigênese. Devido a muitas semelhanças compartilhadas entre cães e humanos, o cão doméstico é considerado um dos melhores exemplos de oncologia comparada (Sorenmo et al., 2009; Queiroga et al., 2011b; Abadie et al., 2017; Nguyen et al., 2017; Markkanen, 2019).

O número de genes em cães e humanos é comparável evolutivamente, e as alterações conservadas no genoma são compartilhadas entre essas espécies (Karlsson & Lindblad-Toh,

2008; Liu et al., 2014; Rowell et al., 2011). O câncer de mama se desenvolve espontaneamente em ambas as espécies, apresentando fisiopatologia, manifestações clínicas e histologia semelhantes (Queiroga et al., 2011; Liu et al., 2014; Bundesamt For Statistik, 2015; Markkanen, 2019). Assim, o desenvolvimento de neoplasias espontâneas em cães apresenta fortes paralelos com o desenvolvimento e a progressão do câncer em humanos, sendo considerado o modelo animal mais próximo do homem. A maior expectativa de vida dos cães, em comparação aos modelos de roedores, e os fatores ambientais compartilhados entre cães e humanos, combinados com o fato de os cães frequentemente receberem um alto nível de assistência médica, fortalecem ainda mais essa análise comparativa (Sorenmo et al., 2009; Queiroga et al., 2011; Abadie et al., 2017; Nguyen et al., 2017; Markkanen, 2019).

Além disso, foi demonstrado que certas raças de cães possuem genes de predisposição para certos tipos de câncer, facilitando as comparações entre alelos de risco responsáveis pela doença em mulheres. Essas ideias enfatizam o potencial de utilização do cão como modelo para o câncer humano e oferecem a possibilidade de melhorar a compreensão da biologia tumoral e descoberta de novos biomarcadores (Queiroga et al., 2011; Rowell et al., 2011; Bundesamt For Statistik, 2015; Carvalho et al., 2016; Markkanen, 2019).

Em termos relativos, ou seja, ao converter "anos do cão" em "anos humanos", a idade para início da vida reprodutiva é comparável em cadelas e mulheres. A incidência de neoplasias mamárias começa a aumentar após os 6 anos de idade (equivalente a 40 anos em mulheres), com picos entre os 8 e 14 anos (equivalente a 50 e 70 anos em mulheres) (INCA, 2022). Além disso, o câncer de mama é o câncer mais frequentemente diagnosticado em mulheres – excetuando-se câncer de pele não melanoma - e cães (Queiroga et al., 2011; Rowell et al., 2011; Bundesamt For Statistik, 2015; Carvalho et al., 2016; WHO, 2019; Markkanen, 2019).

A anatomia da glândula mamária normal é semelhante em cães e mulheres. Os alvéolos e ductos da glândula mamária consistem em células epiteliais luminais revestidas por células mioepiteliais, sendo separados do tecido conjuntivo circundante pela membrana basal (Liu et al., 2014; Santos & Matos, 2015). Em ambas as espécies, a formação de neoplasias é vista como um processo dinâmico, iniciando-se com lesões hiperplásicas benignas que podem evoluir para carcinoma in situ (Markkanen, 2019). Posteriormente, essas neoplasias podem se tornar invasivas, marcadas pela ruptura da membrana basal e potencial de metástase. No nível molecular, muitas das principais alterações provocadas pelo câncer de mama em mulheres são reproduzidas em carcinomas mamários caninos, incluindo mutações da linhagem germinativa em BRCA1, BRCA2 e TP53, associadas a um risco aumentado de câncer de mama hereditário em humanos (Karlsson & Lindbland, 2008; Markkanen, 2019).

Além dos fatores clínicos, como tamanho tumoral, envolvimento linfonodal e estágio clínico, o valor prognóstico de aspectos histopatológicos, como tipo e grau histológicos e subtipos moleculares (luminal A, luminal B, HER-2 positivo e triplo negativo basal-like), está conservado em carcinomas mamários caninos e humanos. As semelhanças entre as neoplasias nas duas espécies sugerem homologias abrangentes na biologia tumoral. Estudos em cães oferecem a oportunidade de identificar novos biomarcadores, não apenas para uso veterinário, mas também para benefícios em pacientes humanos (Gilbertson et al., 1983; Burstein et al., 2004; Simpson et al., 2005; Sorenmo et al., 2009; Markkanen, 2019). A utilização de modelos comparativos pode auxiliar na diferenciação das vias moleculares da doença, pois os principais genes relacionados estão conservados nas duas espécies (Liu et al., 2014; Santos & Matos, 2015). Além disso, ensaios clínicos em cães podem ser realizados em um período mais curto em comparação aos estudos em humanos, devido à vida útil reduzida dos cães e à manifestação clínica precoce da doença nas cadelas (Gilbertson et al., 1983; Burstein et al., 2004; Simpson et al., 2005; Sorenmo et al., 2009; Markkanen, 2019).

A sinergia entre médicos veterinários, médicos e outros profissionais da saúde e do meio ambiente promove uma iniciativa conhecida como "One Health", que visa melhorar a vida de todas as espécies através da integração da pesquisa médica e veterinária. Essa abordagem pode ser mais eficiente e contribuir significativamente para o entendimento e tratamento do câncer de mama em mulheres e cães simultaneamente (Case et al., 2017; Markkanen, 2019).

Aproximadamente metade das neoplasias da glândula mamária canina são malignas e, dependendo do subtipo histológico, estágio e grau histológico, podem estar associadas a um risco significativo de recorrência local e distante (metástase). Tal como ocorre em humanos, dois grandes obstáculos limitam os resultados bem-sucedidos em cães com carcinomas mamários: a identificação precisa de cães com alto risco de recorrência e a seleção de terapias eficazes para esses indivíduos. A falta de indicadores prognósticos precisos resulta em aumento da morbimortalidade, devido ao excesso de tratamento em pacientes com neoplasias malignas de baixo potencial metastático e terapias inadequadas para aqueles que requerem intervenção precoce e agressiva (Burke et al., 2015; Barcus et al., 2017; Conklin et al., 2018; Markkanen, 2019).

2.4 Microambiente durante a progressão tumoral

A maioria das neoplasias origina-se de células epiteliais que, ao se tornarem tumorais, ignoram as barreiras dos tecidos onde normalmente residem. No entanto, essas células não

vivem em um ambiente isolado e dependem fortemente do MAT para sobreviver e crescer (Hanahan, 2022). Esse microambiente é um sistema complexo de interações entre diferentes tipos de células não tumorais, como fibroblastos, células imunes, células vasculares e adipócitos, além da MEC, todos fundamentais para a progressão do câncer (Hanahan, 2022; Anderson & Simon, 2020; Markkanen, 2019; Vitale et al., 2019; Binnewies et al., 2018; Quail & Joyce, 2017).

Entre os principais componentes desse microambiente, destacam-se as células vasculares, como o endotélio e os pericitos, que desempenham um papel crucial na angiogênese, processo essencial para a progressão tumoral. A formação de novos vasos sanguíneos garante o suprimento de oxigênio e nutrientes ao tumor em expansão. O endotélio regula o fluxo sanguíneo e interage diretamente com as células tumorais, facilitando sua invasão nos tecidos circundantes e a disseminação através da corrente sanguínea.

Por sua vez, os pericitos fornecem suporte estrutural e regulam a permeabilidade dos vasos, permitindo a migração das células cancerígenas para outros órgãos, promovendo a formação de metástases (Carmeliet & Jain, 2011; Ribatti et al., 2015). Esse processo de angiogênese é frequentemente estimulado por fatores de crescimento secretados pelas células tumorais e pelos fibroblastos associados ao câncer (FACs), como o VEGF, que orquestram o desenvolvimento vascular em prol da progressão tumoral (Hanahan, 2022).

Além das células vasculares, o MAT também interage com o sistema nervoso. Recentes descobertas apontam para o papel das terminações nervosas na progressão tumoral, em um fenômeno conhecido como neurogênese tumoral. Essa interação entre nervos e tumor estimula o crescimento do câncer, uma vez que os nervos liberam neurotransmissores que aumentam a proliferação, motilidade e invasividade das células tumorais. Assim, as conexões nervosas podem facilitar o avanço da doença e aumentar o potencial metastático do tumor (Zahalka & Frenette, 2020).

As células imunes também são componentes centrais do MAT, desempenhando um papel paradoxal. Inicialmente, algumas dessas células, como os neutrófilos, podem ter um papel antitumoral, combatendo diretamente as células cancerígenas. No entanto, à medida que o tumor se estabelece, os neutrófilos associados ao tumor (NATs) passam a apoiar a progressão tumoral, favorecendo a angiogênese e suprimindo a resposta imune. Além disso, os eosinófilos podem secretar citocinas que criam um ambiente mais permissivo para o crescimento tumoral, contribuindo para a imunossupressão (Fridlender et al., 2009; Carretero et al., 2015).

Outro grupo importante de células imunes no MAT são os linfócitos T reguladores (Tregs). Esses linfócitos têm a capacidade de suprimir a resposta imune antitumoral, impedindo

a ativação eficaz dos linfócitos T citotóxicos, que são essenciais na destruição de células tumorais. Com a presença elevada de Tregs, o tumor é capaz de escapar do sistema imune e continuar sua progressão. Além disso, as células dendríticas, normalmente responsáveis pela apresentação de antígenos e ativação das células T, podem ser inativadas pelo tumor, comprometendo sua função e permitindo que o câncer se dissemine sem ser detectado pelo sistema imune (Binnewies et al., 2018; Salmon et al., 2016).

Outro elemento fundamental do MAT são as células-tronco tumorais (CTTs). Essas células são capazes de se autorrenovar e gerar diferentes tipos de células dentro do tumor, sendo frequentemente associadas à resistência ao tratamento e à recidiva. Sua capacidade de evadir a morte celular torna-as mais resistentes a terapias convencionais, como quimioterapia e radioterapia, e, por isso, representam um desafio significativo no controle do câncer (Yang et al., 2020; Batlle & Clevers, 2017).

Dentro do microambiente, os fibroblastos associados ao câncer (FACs) desempenham um papel duplo. Eles são responsáveis pela produção da MEC, que não só fornece suporte estrutural ao tumor, mas também regula a sinalização celular que promove a proliferação e migração das células tumorais. Além de produzirem proteínas como colágeno e fibronectina, os FACs secretam fatores de crescimento e citocinas que facilitam a invasão tumoral, promovendo o remodelamento do estroma e a transição epitelial-mesenquimal (Sahai et al., 2020; Kalluri, 2016).

Os adipócitos, tradicionalmente conhecidos como células de armazenamento de gordura, também têm um papel crucial no MAT. Em tumores, como o de mama, os adipócitos associados ao tumor (AACs) fornecem ácidos graxos livres e outros metabólitos para as células cancerígenas, apoiando seu metabolismo acelerado e facilitando a progressão metastática. Além disso, esses adipócitos secretam citocinas pró-inflamatórias que promovem a transição epitelial-mesenquimal (TEM), o que favorece a invasão e a disseminação das células tumorais (Nieman et al., 2013; Dirat et al., 2011).

Por fim, a MEC é outro componente dinâmico do MAT, sendo continuamente remodelada pelas células tumorais e estromais. A MEC é composta por uma rede de proteínas, como colágeno e fibronectina, que regulam diretamente a sinalização celular e o comportamento das células cancerígenas. A rigidez da MEC está associada a um comportamento mais agressivo das células tumorais, promovendo a proliferação, migração e invasão. Esse desequilíbrio na produção e degradação da MEC favorece a invasão tumoral e a formação de metástases, tornando a matriz um alvo importante para terapias que visam interromper a progressão do câncer (Pickup et al., 2014; Mouw et al., 2014).

Assim, todos esses componentes – desde células vasculares, imunes, adipócitos e fibroblastos até a MEC – interagem de maneira dinâmica e orquestrada para promover o crescimento e disseminação do tumor. Isso demonstra que o câncer não é apenas uma doença das células tumorais, mas também do seu microambiente, sendo essencial considerar as complexas interações celulares e moleculares para o desenvolvimento de novas abordagens terapêuticas (Hanahan, 2022; Anderson & Simon, 2020; Markkanen, 2019; Vitale et al., 2019; Binnewies et al., 2018; Quail & Joyce, 2017).

No início da formação do tumor, ele enfrenta sinais de inibição do crescimento, principalmente modulados por linfócitos T citotóxicos, macrófagos M1 e fibroblastos. As células do câncer de mama superam esses mecanismos estimulando as células do estroma hospedeiro a adquirirem características que favorecem o crescimento da neoplasia (Joyce & Pollard, 2009; Hanahan & Coussens, 2012). Citocinas liberadas pela inflamação, como TGF-β, IL-1β e TNF-α, induzem a diferenciação de fibroblastos normais em fibroblastos associados ao câncer (CAFs). Estes, por sua vez, secretam proteínas da MEC e fatores solúveis (TGF-β, CXCL12, IL-6) que estimulam a transição epitelial-mesenquimal (TEM), o crescimento e a progressão do tumor. Neutrófilos também podem induzir a TEM e promover a progressão tumoral através da liberação de citocinas (Engblom et al., 2016; Zhu et al., 2019; Jiang & Zhan, 2020). Adipócitos fornecem metabólitos de alta energia para alimentar o crescimento tumoral (Dirat et al., 2011; Nieman et al., 2013; Vaysse et al., 2014). Os MAT apoiam vários processos no MAT, incluindo crescimento e invasão do câncer, por meio da secreção de citocinas e fatores de crescimento pró-tumorigênicos (Qian et al., 2010; Noy et al., 2014; Mantovani & Allavena, 2015; Vitale et al., 2016; Zhu et al., 2017; DeNardo & Ruffell, 2019; Cassetta & Pollard, 2020).

Durante a expansão do tumor, citocinas presentes no ambiente, como CXCL5-CXCR2 e TGF-β, estimulam o recrutamento de células T reguladoras (Treg) e células supressoras derivadas de mieloides (MDSCs), que prejudicam a vigilância imunológica, inibindo linfócitos T citotóxicos, macrófagos M1 e células natural killer. As células do câncer de mama também podem escapar da vigilância imunológica superexpressando o ligante PD-L1 (Gajewski et al., 2013; Weber et al., 2018; Binnewies et al., 2018; Bruno et al., 2020).

Esses eventos permitem que as células tumorais adquiram um fenótipo móvel e invasivo. Fatores secretados, como MMPs e VEGF, facilitam a entrada das células tumoraisna circulação, onde interagem com plaquetas, macrófagos M2, neutrófilos e fibroblastos, que contribuem para sua proteção e evasão do sistema imunológico (Labelle & Hynes, 2011; DeNardo & Ruffell, 2019; Fisher et al., 2021). As plaquetas aderem às células tumorais, formando um escudo protetor que as ajuda a evitar a destruição pelo sistema imunológico,

enquanto macrófagos M2 e outros elementos do MAT secretam citocinas e fatores de crescimento que promovem a sobrevivência e migração celular. Juntas, essas interações permitem que as células tumorais sejam escoltadas até os locais secundários, onde interagem com células endoteliais e pericitos, promovendo a extravasão e colonização de novos tecidos (Labelle & Hynes, 2011; DeNardo & Ruffell, 2019; Fisher et al., 2021). O local preferencial de metástase pode ser influenciado pelo subtipo do câncer de mama (Weigelt et al., 2005; Smid et al., 2008; Kennecke et al., 2010).

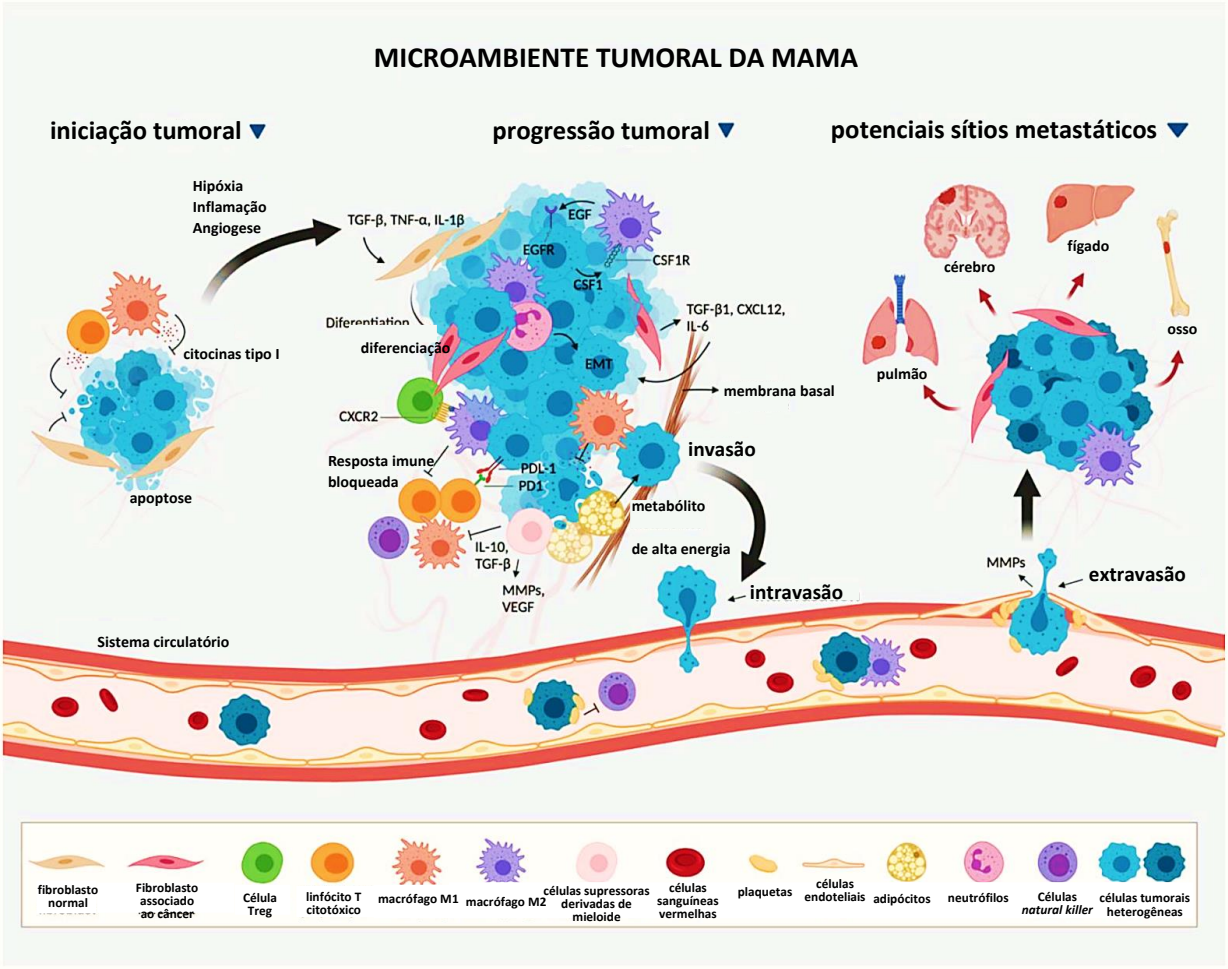

Figura 02- Microambiente tumoral e a progressão do câncer de mama. Fonte: Adaptado de Terceiro et al., 2021.

2.4.1 Fibras colágenas

A homeostasia tecidual requer a manutenção de sua estrutura e função, com a composição, organização e rigidez da MEC desempenhando papéis críticos nesse processo. A tensão do citoesqueleto modula a estrutura do tecido, e condições patológicas associadas ao enrijecimento da MEC resultam em distúrbios na estrutura e função tecidual (Piersma et al.,

2020). Diversos estudos mostram que as propriedades físicas associadas à rigidez da MEC são componentes importantes do MAT, responsáveis pela transformação maligna e regulação da agressividade tumoral (Friedl & Brocker, 2019; Duchez et al., 2019; Ebata et al., 2019; Mierke, 2019; Moriyama & Kidoaki, 2019; Zhang, 2019; Piersma et al., 2020).

Neoplasias sólidas são geralmente mais rígidas do que o tecido saudável, característica essa que tem sido explorada no diagnóstico do câncer de mama através da palpação física ou de modalidades de imagem, como ressonância magnética, tomografia computadorizada e elastografia (Piersma et al., 2020). O câncer de mama e o adenocarcinoma ductal pancreático estão associados a uma MEC mais rígida, e modelos experimentais demonstram relações causais entre a mecânica tecidual e a malignidade (Piersma et al., 2020).

Estudos mostram que durante o desenvolvimento de neoplasias há um aumento na deposição de fibras colágenas, sugerindo que o colágeno desempenha uma função essencial nesse processo (Hanahan & Coussens, 2012; Markkanen, 2019; Garcia et al., 2022; Garcia et al., 2024). Essa deposição, conhecida como desmoplasia, aumenta a rigidez do tumor e do tecido adjacente, estimulando a progressão do câncer em ambientes com MEC mais rígida (Souza et al., 2018; Garcia et al., 2022; Garcia et al., 2024). Além disso, as neoplasias podem remodelar ativamente a MEC circundante. Fibras de colágeno do tipo 1 e tipo 3, quando alinhadas, aumentam a rigidez da MEC, e isso prediz piores prognósticos, especialmente em cânceres receptores de estrogênio positivos (Barcus et al., 2017; Souza et al., 2018).

Estudos recentes sugerem que a rigidez da MEC é fundamental nos processos de migração celular, invasão e metastatização do câncer (Friedl & Brocker, 2019; Duchez et al., 2019; Ebata et al., 2019; Mierke, 2019; Moriyama & Kidoaki, 2019; Zhang, 2019; Garcia et al., 2021; Garcia et al., 2024). O colágeno desempenha um papel crítico no MAT, exercendo influência no crescimento neoplásico e na disseminação de células tumorais devido à sua capacidade de fornecer orientações físicas, bioquímicas e biomecânicas (Friedl & Brocker, 2019; Duchez et al., 2019; Ebata et al., 2019; Mierke, 2019; Moriyama & Kidoaki, 2019; Zhang, 2019; Garcia et al., 2021; Garcia et al., 2024).

A abundância de colágeno fibrilar em um câncer de mama primário é um fator de risco significativo para a sobrevivência do paciente (Hasebe et al., 1997). Essa abundância está associada à metástase à distância em carcinomas mamários triplos negativos, promovendo agressividade tumoral e metástases em modelos experimentais (Provenzano et al., 2008). Análises de transcriptoma completo demonstraram mudanças drásticas e consistentes na expressão gênica dentro da população de fibroblastos e células mioepiteliais associadas ao câncer de mama, sendo possível derivar uma assinatura genética prognóstica que poderia prever

a sobrevida livre de recidiva dos pacientes (Ma et al., 2009). A "assinatura de cicatrização de feridas", identificada por microarray de fibroblastos, previu a sobrevida de pacientes com câncer de mama (Chang et al., 2005), enquanto outro estudo identificou uma assinatura de expressão gênica estromal associada à resistência à quimioterapia neoadjuvante (Farmer et al., 2005).

A movimentação celular através da MEC é um processo dinâmico e complexo, englobando atividades como a formação de lamelipódios, adesão focal, locomoção mediada por contração de actina e fixação (Mierke, 2019). A motilidade celular é importante em processos fisiológicos, como cicatrização de feridas, resposta imune e desenvolvimento de órgãos e tecidos, além de processos patológicos como a progressão tumoral. Em geral, uma neoplasia pode se transformar em doença sistêmica maligna quando as células cancerosas migram do sítio primário através do estroma tumoral circundante (Friedl & Brocker, 2019; Duchez et al., 2019; Mierke, 2019; Moriyama & Kidoaki, 2019; Zhang, 2019).

O movimento direcional das células é essencial nos organismos vivos, sendo influenciado por gradientes de produtos químicos, rigidez, corrente elétrica, luz e gravidade. A durotaxia, que envolve o movimento celular em direção a regiões de maior rigidez na MEC, desempenha um papel crucial nesse processo. A durotaxia está envolvida em diversos processos de desenvolvimento e progressão de doenças (Moriyama & Kidoaki, 2019; Zhang, 2019; Garcia et al., 2021; Garcia et al., 2024). Além da durotaxia, outro conceito importante é a "mecanoreciprocidade", que descreve como uma célula ajusta a tensão do citoesqueleto em resposta à rigidez da MEC e como esse fenótipo contrátil intrínseco remodela e enrijece a matriz local até que um equilíbrio mecânico seja alcançado (Paszek & Weaver, 2004; Piersma et al., 2020).

2.4.2 Macrófagos associados ao tumor

Os macrófagos, componentes essenciais do sistema imunológico inato, fazem parte do sistema fagocitário mononuclear e desempenham funções cruciais, como a fagocitose de patógenos, a modulação da inflamação e a coordenação do reparo tecidual (Condeelis et al., 2006; Kim et al., 2019). Nesse contexto, os MATs desempenham um papel particularmente importante. A maioria desses MATs é derivada de monócitos da medula óssea, recrutados para o local do tumor em resposta a quimiocinas e citocinas, como a proteína quimiotática de monócitos 1 (MCP-1/CCL2) e o fator estimulante de colônias 1 (CSF-1) (Qian & Pollard, 2011; Murray et al., 2011; Wynn & Pollard, 2013; Yona & Gordon, 2015).

A origem dos MATs tem sido objeto de debate, com evidências sugerindo que podem derivar tanto de monócitos circulantes quanto de macrófagos de origem embrionária. Estudos recentes indicam uma origem mista, na qual ambos os tipos contribuem para o crescimento tumoral (Mass et al., 2016; Guilliams & Scott, 2017; Zhu et al., 2017; Bain & Jenkins, 2018). Dependendo da origem dos MATs, diferentes funções são atribuídas a essas células. Por exemplo, enquanto os macrófagos teciduais residentes derivados do saco vitelino estão relacionados à proliferação celular e fibrose, os macrófagos derivados dos monócitos da medula óssea estão associados à apresentação de antígenos, afetando o crescimento e metástase das células tumorais (Guilliams & Scott, 2017; Zhu et al., 2017; Bain & Jenkins, 2018; Xu et al., 2021).

Os macrófagos podem ser classificados em um espectro de estados de ativação, com os extremos representados pelos macrófagos M1, classicamente ativados, e os macrófagos M2, alternativamente ativados. Os macrófagos M1, induzidos principalmente por interferon-γ (IFN-γ), lipopolissacarídeo (LPS) e fator estimulante de colônias de granulócitos-macrófagos (GM-CSF), exercem efeitos citotóxicos sobre as células cancerígenas. Em contraste, os macrófagos M2, estimulados por IL-4, IL-6, IL-10, IL-13, TGF-β, VEGF e outras citocinas específicas, fornecem uma vantagem nutricional para as células tumorais, promovendo seu crescimento e sobrevivência. No entanto, além dessas duas categorias, diversos estudos têm identificado subtipos de macrófagos que não se encaixam perfeitamente no modelo M1/M2.

Por exemplo, em condições específicas os macrófagos M4, encontrados em placas ateroscleróticas e induzidos pela proteína quimiotática de monócitos-1 (MCP-1). Esses macrófagos exibem propriedades anti-inflamatórias e expressam MMPs, desempenhando um papel chave na degradação da MEC (Krakauer, 2012; Zhang et al, 2021). Os macrófagos Mox, por sua vez, surgem em resposta ao estresse oxidativo, como a exposição ao peróxido de hidrogênio (H_2O_2), e são caracterizados pela expressão elevada de genes antioxidantes. Esse subtipo é frequentemente associado a processos inflamatórios crônicos, como a aterosclerose (Forstreuter et al., 2017; Rahman et al., 2020). Além disso, os macrófagos reguladores (Mregs) desempenham um papel fundamental na promoção da tolerância imunológica, especialmente em contextos como transplantes, onde ajudam a prevenir a rejeição do enxerto (Turner et al., 2013; Huttner & Strawbridge, 2021).

Essa diversidade funcional demonstra que os macrófagos não seguem apenas um padrão fixo de ativação M1/M2, mas sim adotam uma ampla gama de estados intermediários e subtipos especializados, dependendo do microambiente patológico em que se encontram. Essa plasticidade é essencial para a capacidade dos macrófagos de responderem de maneira dinâmica

a diferentes desafios biológicos, incluindo tumores e inflamações crônicas (Heusinkveld et al., 2011; Monteiro et al., 2018; De Nola et al., 2019; Orecchioni et al., 2019; Zhu et al., 2019; DeNardo & Ruffell, 2019; Nakamura et al., 2020; Jiang & Zhan, 2020; Locati & Mantovani, 2020).

Muitos estudos mostraram que os MATs são amplamente polarizados em direção ao fenótipo M2, promovendo a progressão tumoral e restringindo a resposta imune antitumoral (Monteiro et al., 2018; Orecchioni et al., 2019; Zhu et al., 2019; DeNardo & Ruffell, 2019; Nakamura et al., 2020; Jiang & Zhan, 2020; Locati & Mantovani, 2020; Xu et al., 2021). Embora os MATs sejam frequentemente classificados como pró-inflamatórios (M1) ou imunossupressores (M2), eles existem em um espectro de estados de ativação intermediários, em resposta às condições heterogêneas do MAT (Martinez & Gordon, 2014; Xue et al., 2014; Orecchioni et al., 2019; Locati & Mantovani, 2020; Guilliams et al., 2021).

O MAT orquestra notavelmente os mecanismos moleculares que programam esses macrófagos (Alessandrini et al., 2019; Viola et al., 2019; Van Den Bossche et al., 2017). Dada a heterogeneidade dos MATs e a falta de marcadores específicos e confiáveis para atingir seletivamente os subconjuntos desejados, as abordagens atuais para a classificação dos macrófagos enfrentam desafios. Portanto, é essencial realizar análises mais detalhadas dos diferentes subconjuntos de MATs, considerando sua localização no tumor, para desenvolver terapias mais eficazes. Tecnologias avançadas, como imunofluorescência multiplex e citometria de massa, estão permitindo uma compreensão mais profunda da diversidade e plasticidade dos MATs, revelando a complexidade de suas funções no MAT e fornecendo evidências para o desenvolvimento de novas estratégias de pesquisa (Martinez & Gordon, 2014; Xue et al., 2014; Orecchioni et al., 2019; Locati & Mantovani, 2020; Guilliams et al., 2021).

Em termos de ativação e plasticidade, os MATs exibem uma variedade de estados funcionais. Embora geralmente tendam ao fenótipo M2, associado à promoção tumoral, também expressam marcadores característicos do fenótipo M1, reconhecido por suas propriedades antitumorais (Qian & Pollard, 2010; Biswas & Mantovani, 2010; Mantovani et al., 2017; Orecchioni et al., 2019; Locati & Mantovani, 2020; Guilliams et al., 2021). Além disso, a localização dos MATs no tumor é um fator determinante de suas funções específicas, influenciando diretamente seu comportamento e impacto no MAT. Nas áreas invasivas do tumor, os MATs desempenham um papel facilitador na invasão de células cancerosas, liberando enzimas, citocinas e fatores de crescimento que degradam a MEC e promovem a migração celular (Condeelis & Pollard, 2006; Qian & Pollard, 2010; Laoui et al., 2014; Ruffell &

Coussens, 2015; Cassetta & Fragkogianni, 2020; Xue et al., 2021; Liu et al., 2022; Hosseini & Vatanmakanian, 2022).

Dados clínicos revelam uma correlação entre altas concentrações de MATs na frente invasiva do tumor e um prognóstico desfavorável em determinados tipos de câncer, enquanto em outros, os MATs estão associados a desfechos mais positivos. Nessa região de fronte tumoral, os MATs podem expressar moléculas imunossupressoras, como PD-L1, que inibem a resposta imune efetora, ou moléculas coestimuladoras, como CD80 e CD86, que potencializam a ativação de células T (Zhu et al., 2014; Noy & Pollard, 2014; Mantovani et al., 2017; Pyonteck et al., 2019; Locati et al., 2020; Müller & Salem, 2021; Hosseini & Vatanmakanian, 2022).

Evidências sugerem que os MATs participam de diferentes estágios e aspectos do desenvolvimento tumoral, secretando diversos fatores, como IL-1/6/8/10, IGFI, VEGF, MMP-7/9, uPA, TNF-α e TGF-β. Estudos demonstraram que os MATs secretam IL-6, uma citocina associada à tumorigênese, que desempenha um papel importante na proliferação, diferenciação e sobrevivência das células tumorais (Yao et al., 2014; Dong et al., 2020; Zhong et al., 2020). Outro membro da família das interleucinas, CXCL8 (IL-8), também está amplamente envolvido na tumorigênese devido à sua pluripotência, incluindo angiogênese e efeitos mitogênicos. A CXCL8 é principalmente secretada por macrófagos mononucleares, e estudos mostram que os MATs diminuem a expressão do receptor de estrogênio em tecidos de carcinoma mamário através da secreção excessiva de CCL8, associada à invasão tumoral e pior prognóstico (Shah et al., 2013).

A infiltração de MATs está intimamente associada à expressão de VEGF e densidade microvascular (MVD), que afetam conjuntamente o prognóstico dos pacientes. Outro estudo demonstrou que macrófagos M2 secretam MMP-9, responsável por promover a progressão da neoplasia em cânceres de mama e cólon, sendo considerados marcadores prognósticos e potenciais alvos de estudo (Azevedo et al., 2020; Gonzalez-Avila et al., 2020). Em cânceres de mama receptores de estrogênio positivos, a MMP-9 secretada por MATs foi associada a pior sobrevida global; porém, em cânceres de mama receptores de estrogênio negativos ou triplos negativos, essas associações não foram relatadas (Pelekanou et al., 2018).

No nicho perivascular, os MATs exibem características particulares, expressando altos níveis de TIE2 e promovendo processos como angiogênese tumoral, metástase e recidiva pós-tratamento. A frequência desses MATs perivasculares correlaciona-se positivamente com a densidade de microvasos em determinadas neoplasias humanas, evidenciando sua contribuição para a vascularização neoplásica (Lewis & Pollard, 2006; Venneri et al., 2007; De Palma & Naldini, 2009; Coffelt et al., 2010; Harney et al., 2015; Larionova & Patysheva, 2020; Moradi

et al., 2021; Mazzieri & De Palma, 2021; Zhu & Wang, 2021). Além disso, estão implicados na revascularização e na recidiva tumoral após intervenções terapêuticas. Em sítios metastáticos, como os pulmões, um subconjunto específico de macrófagos facilita a extravasão de células cancerosas e a formação de metástases (Qian & Pollard, 2010; Harney et al., 2015; DeNardo & Ruffell, 2019).

Áreas hipóxicas ou necróticas dentro do tumor também influenciam o comportamento dos MATs. Nesses microambientes, elevados números de MATs estão associados ao aumento da angiogênese tumoral, metástase, redução da sobrevida livre de recidiva e diminuição da sobrevida global, especialmente em cânceres de mama, endometrial e cervical (Noy & Pollard, 2014; Chiarugi & Cirri, 2019; Hughes & Qian, 2020; Komohara & Fujiwara, 2021; Mulder & Van, 2021). A hipóxia estimula os MATs a promoverem angiogênese, evasão imunológica e disseminação metastática. Esse ambiente também induz alterações metabólicas nos macrófagos, que afetam diretamente as funções das células tumorais adjacentes, como a liberação de HMGB1 pelas células cancerosas, estimulando a produção de IL-10 pelos MATs (Chiarugi & Cirri, 2019; Hughes & Qian, 2020; Komohara & Fujiwara, 2021; Li et al., 2021).

A IL-10 é uma citocina multicelular com efeitos imunossupressores, capaz de inibir a liberação de antígenos pelo sistema fagocítico mononuclear (Saraiva et al., 2010; Mannino et al., 2015). Um estudo demonstrou que a IL-10 promove a transformação de macrófagos em macrófagos do tipo M2 no MAT e que esses macrófagos M2 polarizados, por sua vez, secretam altos níveis de IL-10 (Liu et al., 2020). No câncer de mama, a superexpressão de IL-10 derivada de macrófagos resultou no desenvolvimento do tumor por meio da ineficiência das respostas dependentes de células T CD8+ à quimioterapia. Além disso, a IL-10 é um fator independente para o prognóstico adverso em pacientes com câncer de mama negativo para o RE (Ruffell et al., 2014). Para as células T, o VEGF bloqueia a diferenciação das células T progenitoras em linfócitos CD4+ e CD8+, enfraquecendo a função imunológica dessas células. Por outro lado, o VEGF aumenta a infiltração dos MATs, gerando um feedback positivo para a presença de VEGF e MATs (Mandic et al., 2014).

Os MATs também exercem importante função na metastização das células tumorais, liberando o ativador de plasminogênio tipo uroquinase (uPA) e regulando positivamente a expressão do receptor para uPA (uPAR), que pertence ao sistema fibrinolítico. A combinação uPA-uPAR inicia as reações para o remodelamento da MEC, degradando seus componentes e induzindo a migração de células tumorais do sítio primário da neoplasia (Mahmood et al., 2018). O aumento do uPAR também pode induzir a agregação de macrófagos ao tecido normal mediante um feedback positivo. Nos carcinomas ductais mamários in situ e invasores, os

monócitos sanguíneos com níveis mais altos de uPAR podem ser recrutados seletivamente em tecidos neoplásicos e induzir níveis elevados de uPAR nos MATs através da ação parácrina (Hildenbrand et al., 1999). Como membro dos fatores de crescimento transformadores, o TGF-β é uma citocina multifuncional que atua como um potente supressor tumoral no estágio inicial do câncer, mas em estágios mais avançados, participa da indução da transição epitelial-mesenquimal (Xu et al., 2021). Assim, os MATs estão envolvidos na secreção de citocinas e fatores de crescimento que influenciam o remodelamento da matriz, crescimento tumoral, metástase e progressão (Xu et al., 2021).

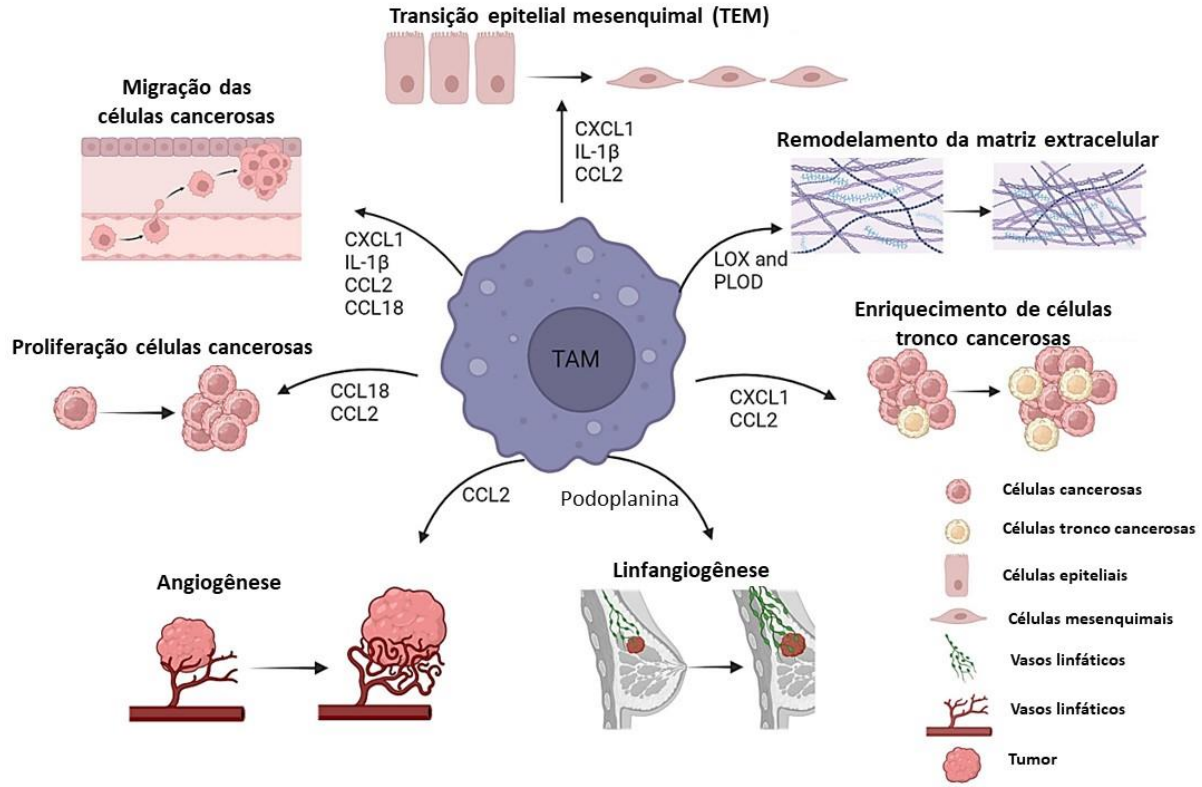

Figura 03- Macrófagos associados ao tumor (TAMs) na progressão e metástase do câncer de mama. Os TAMs estão envolvidos em múltiplos mecanismos que levam à progressão tumoral e metástase. Esses mecanismos de promoção tumoral incluem a transição epitelial-mesenquimal, o remodelamento da matriz extracelular, o enriquecimento de células-tronco cancerígenas e a angiogênese. Citocinas, enzimas e outros fatores derivados dos TAMs são mediadores chave desses processos. Fonte: Adaptado de Stavrou and Constantinidou, 2024.

Assim como nas mulheres, nas cadelas a infiltração de MAT está relacionada com a progressão e o prognóstico do câncer de mama e com a sobrevida das pacientes, reforçando o potencial dessas células como indicadores prognósticos no carcinoma mamário invasivo canino. O estudo realizado por Monteiro e colaboradores em 2018, mostrou que uma contagem mais alta de MATs apresenta uma correlação positiva com invasão e progressão do CTM,

havendo uma mudança de MAT M1 em TMB a MAT M2 em CTMs. Contagens mais altas de MAT foram associadas a maior densidade, maiores taxas de proliferação celular, presença de invasão e metástase linfonodal, bem como sobrevida global. Altos níveis de infiltração de MAT foram associados com características clinicopatológicas agressivas em carcinomas mamários caninos. Altas contagens de MAT estromal e total foram correlacionadas com metástase em linfonodo e com pior prognóstico, uma característica esperada uma vez que os macrófagos possuem a capacidade de remodelar o estroma tumoral, aumentando a migração e invasão das células neoplásicas (Monteiro *et al.*, 2018).

Essas características reforçam o papel dos macrófagos na progressão do carcinoma mamário canino. Neste trabalho não foram encontradas associações entre o aumento da infiltração dos MAT e o grau histológico (Monteiro *et al.*, 2018). Tanto as células epiteliais neoplásicas como as células estromais produzem substâncias capazes de remodelar a MEC, induzir a migração celular, atuar como quimioatraentes e promover proliferação e sobrevivência celular. Contagens mais altas de MATs intratumorais e MATs estromais também estão correlacionados com a diminuição da sobrevida e pior prognóstico (Monteiro *et al.*, 2018).

2.5 Microscopia por absorção de dois fótons

2.5.1 Microscopia por geração de segundo harmônico

A geração de segundo harmônico (SHG do inglês *second harmonic generation*) é um processo coerente no qual dois fótons de energia mais baixa são convertidos para exatamente o dobro da frequência incidente (metade do comprimento de onda) de um laser de excitação (figura 04). A imagem biológica obtida por SHG foi relatada pela primeira vez em 1986 quando Freund investigou a polaridade das fibras de colágeno no tendão da cauda de um rato com uma resolução de 50 micrômetros. Em 2011, Mohler e Campagnola relataram a implementação prática de imagens de tecidos em alta resolução e aquisição rápida de dados utilizando o escaneamento a laser e, desde então, a microscopia por SHG tem sido uma ferramenta cada vez mais utilizada. A maioria dos relatos recentes sobre imagens microscópicas por SHG concentra-se na visualização de fibras colágenas na matriz extracelular em uma variedade de tecidos conjuntivos e órgãos internos (Campagnola & Dong, 2011). A figura 05 mostra a montagem experimental para obtenção das imagens de microscopia por SHG utilizando o microscópio confocal.

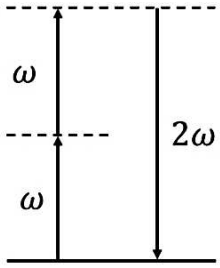

Figura 04- Representação de dois fótons com frequência ω gerando um fóton com o dobro da frequência.

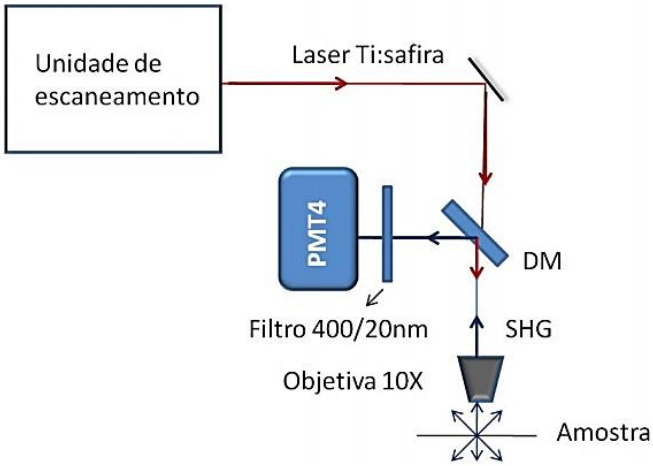

Figura 05- Montagem experimental para obtenção das imagens de microscopia multifotônica utilizando o microscópio confocal.

O colágeno tipo I é o componente predominante da matriz extracelular e do tecido conjuntivo. O colágeno é uma tripla hélice, com aproximadamente 300 kilodaltons. As moléculas individuais, chamadas de tropocolágeno, se associam covalentemente em fibrilas de aproximadamente 20-250 nanômetros de diâmetro para posteriormente formar fibras de aproximadamente 500 nanômetros a vários mícrons de diâmetro (Falzon et al., 2008; Campagnola & Dong, 2011; Case et al., 2017; Barcus et al., 2017; Wang et al., 2017; Conklin et al., 2018; Reis et al., 2020; Garcia et al., 2021; Garcia et al., 2024). A microscopia por SHG tem várias vantagens que a tornam ideal para a obtenção de imagens de tecidos in vivo. Um atributo particularmente forte é que a microscopia por SHG visualiza a estrutura do tecido porque o contraste é produzido puramente a partir de espécies endógenas (Campagnola & Dong, 2011). Por outro lado, imagens com corantes exógenos e proteínas coloridas só podem inferir aspectos estruturais. Os sinais de SHG surgem de uma polarização induzida ao invés de uma absorção, o que leva a uma fotodegradação e fototoxicidade substancialmente reduzidas em relação aos métodos de fluorescência. Além disso, como os comprimentos de onda fundamentais do laser estão no infravermelho (entre 700-1000 nanômetros) a microscopia por SHG pode obter imagens com melhor

resolução para profundidades de várias centenas de mícrons (Campagnola & Dong, 2011; Case et al., 2017; Barcus et al., 2017; Wang et al., 2017).

Diversos estudos na área humana identificaram, por meio da microscopia por SHG, que durante a progressão tumoral do câncer de mama as fibras colágenas se tornam mais alinhadas em comparação a tecidos mamários saudáveis, predizendo prognósticos desfavoráveis (Falzon et al., 2008; Campagnola & Dung, 2011; Barcus et al., 2017; Wang et al., 2017; Conklin et al., 2018; Garcia et al., 2018; Natal et al., 2018; Natal et al., 2019; Reis et al., 2020; Garcia et al., 2021; Garcia et al., 2024). Um estudo realizado por Case e colaboradores, em 2017, examinou o papel potencial do colágeno na modulação do metabolismo biológico e no comportamento das neoplasias mamárias em cães. Neste estudo ficou confirmado que a organização e o alinhamento das fibras colágenas, reveladas por imagens de SHG em carcinomas mamários caninos, são preditivos de resultados clínicos agressivos. Os pesquisadores identificaram que a falta de um limite definido entre estroma e neoplasia e um aumento na largura das fibras colágenas estão associados a prognósticos desfavoráveis. Essas descobertas direcionam para a hipótese de que o colágeno pode ser utilizado como um biomarcador prognóstico de neoplasias mamárias caninas, melhorando o sucesso terapêutico em cães (Case et al., 2017).

Semelhante ao câncer de mama humano, a densidade mamográfica em biópsias de carcinomas está inversamente relacionada à sobrevida de pacientes da espécie canina. Apesar da densidade não ser um dado útil para melhorar o prognóstico da doença, os dados do estudo sugerem que estratégias terapêuticas que suprimem respostas desmoplásicas, particularmente aquelas que estimulam a deposição de colágeno, podem melhorar a sobrevida dos cães (Case et al., 2017). Estudos recentes revelaram que a organização do colágeno e a rigidez da matriz extracelular são tão importantes quanto a densidade na mediação do crescimento e invasão tumorais (Conklin et al., 2018; Garcia et al., 2018; Natal et al., 2018; Natal et al., 2019; Reis et al., 2020; Garcia et al., 2021; Garcia et al., 2024).

2.5.2 Fluorescência excitada por dois fótons

A absorção de dois fótons é o processo pelo qual uma molécula ou material absorve um par de fótons, cuja soma de energia é igual à energia de transição. A probabilidade de uma molécula sofrer a absorção de dois fótons quando exposta à luz de uma determinada energia de fótons (ou combinação de energia de fótons) depende de certas características do material e do ambiente em que a molécula está imersa. Assim, a espectroscopia por absorção de dois fótons pode ser utilizada como uma ferramenta para sondar as propriedades das moléculas, por exemplo para descobrir a energia dos estados ativos de dois fótons por meio da força das transições na absorção por dois fótons e as diferenças de estrutura eletrônica entre o estado fundamental e os estados excitados do sistema. Desde a primeira demonstração

experimental da absorção por dois fótons, houve um interesse nesse tipo de espectroscopia para o estudo de propriedades básicas de materiais e de interações matéria-luz (Rumi & Perri, 2010).

O processo de excitação de um material por dois fótons consiste em um processo ótico não linear que envolve a absorção quase simultânea de dois fótons por um dado material quando a energia desses fótons é combinada (os fótons podem ter energias iguais E1+E1 ou diferentes E1+E2, podendo ser obtida com lasers diferentes) de forma suficiente para induzir uma transição do estado fundamental para um estado excitado) (Imiolek, 2014). A figura 06 mostra o tipo mais simples de excitação por absorção de dois fótons, onde dois fótons com a mesma energia são combinados.

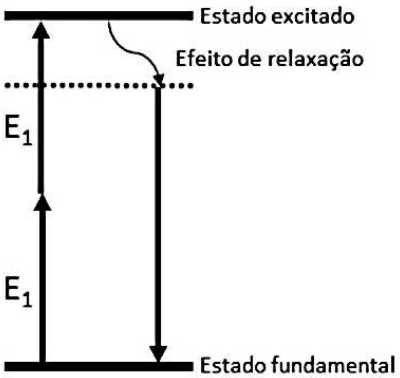

Figura 06- Fótons com mesma energia E1 absorvidos pelo material quase simultaneamente e depois decai emitindo a fluorescência. Fonte: Adaptado de Rumi & Perri, 2010.

A microscopia por absorção de dois fótons é uma das invenções recentes mais importantes da instrumentação de microscopia óptica, pois permitiu imagens tridimensionais não invasivas de amostras biológicas com excelente resolução. As principais vantagens deste tipo de microscopia incluem danos fototóxicos reduzidos, possibilitando a criação de imagens de materiais vivos e detecção de alta sensibilidade sem contaminação do sinal de fluorescência pela luz de excitação (Imiolek, 2014). Os principais elementos de um microscópio de absorção de dois fótons são: laser de safira dopado com titânio de femtossegundo usado como fonte de luz, tubos fotomultiplicadores para detecção de fluorescência e várias partes da óptica de microscopia (*scanner* acionado por galvanômetro, espelho dicróico, objetiva, entre outros). Utilizando essa instrumentação, pode-se obter fotografias de excitação de células marcadas com diferentes corantes (Rumi & Perri, 2010; Imiolek, 2014). Neste trabalho, a microscopia por absorção de dois fótons foi utilizada para se obter mais informações a respeito do tecido em análise, uma vez que a eosina é o principal corante que pode ser excitado em tecidos corados com H&E.

3. HIPÓTESE

Os carcinomas mamários humanos e caninos associados a prognósticos desfavoráveis têm fibras colágenas mais curtas e maior infiltração de macrófagos M2.

4. OBJETIVOS

4.1 Objetivo geral

Avaliar a organização, quantidade, ondulação e comprimento das fibras colágenas na glândula mamária saudável e nas neoplasias mamárias humanas e caninas e correlacionar com os dados clínico-patológicos e sobrevida das pacientes.

4.2 Objetivos específicos

- Avaliar a organização, quantidade, ondulação e comprimento das fibras colágenas na glândula mamária saudável e nas neoplasias mamárias humanas e caninas, a partir de imagens obtidas por geração de segundo harmônico e fluorescência excitada por dois fótons;
- Caracterizar o fenótipo molecular dos carcinomas mamários humanos e caninos, pela técnica de imuno-histoquímica;
- Correlacionar a organização, quantidade, ondulação e comprimento das fibras colágenas com o fenótipo molecular e com os dados clínico-patológicos das pacientes;
- Correlacionar a organização, quantidade, ondulação e comprimento das fibras colágenas nos carcinomas mamários humanos e caninos com a sobrevida das pacientes;
- Avaliar a infiltração de macrófagos na glândula mamária saudável e nas neoplasias mamárias humanas e caninas, pela técnica de imuno-histoquímica;
- Caracterizar o fenótipo dos macrófagos infiltrantes na glândula mamária saudável e nas neoplasias mamárias humanas e caninas, pela técnica de imunofluorescência;
- Correlacionar a infiltração de macrófagos e a organização, quantidade, ondulação e comprimento das fibras colágenas na glândula mamária saudável e nas neoplasias mamárias humanas e caninas.
- Correlacionar a infiltração de macrófagos nos carcinomas mamários humanos e caninos com a sobrevida das pacientes.

5. MATERIAL E MÉTODO

5.1 Seleção das amostras humanas

Este é um estudo retrospectivo de 20 amostras de glândula mamária saudável e 69 casos de neoplasias mamárias benignas e malignas. Foram incluídas amostras com informações sobre o tamanho tumoral, presença ou ausência de metástases linfonodais, grau histológico, subtipo molecular e taxa de proliferação celular. As amostras foram obtidas no setor de biópsia da Faculdade de Medicina da Universidade Federal de Minas Gerais (UFMG), Brasil. As amostras foram provenientes do Hospital das Clínicas da UFMG. As lâminas foram confeccionadas a partir de fragmentos de glândula mamária saudável ou neoplásico obtidos de biópsias de setorectomia, mastectomia simples, mastectomia radical unilateral ou bilateral dependendo do tamanho tumoral, estadiamento clínico, drenagem linfática e localização da neoplasia. Amostras de glândula mamária humana saudável foram adquiridas a partir de mamoplastias realizadas no Hospital das Clínicas da Faculdade de Medicina da UFMG.

5.2 Seleção das amostras caninas

Este é um estudo retrospectivo de 12 amostras de glândula mamária saudável e 74 casos de neoplasias mamárias benignas e malignas, de ocorrência espontânea. Foram incluídas amostras com informações sobre o tamanho tumoral, presença ou ausência de metástases linfonodais, grau histológico, subtipo molecular e taxa de proliferação celular. As amostras foram obtidas dos arquivos do Laboratório de Patologia Comparada da Universidade Federal de Minas Gerais (UFMG), Brasil. O material foi encaminhado do Hospital Veterinário da UFMG para o Laboratório de Patologia Comparada. As lâminas foram confeccionadas a partir de fragmentos de glândula mamária saudável ou neoplásico obtidos de biópsias de setorectomia, mastectomia simples, mastectomia radical unilateral ou bilateral dependendo do tamanho tumoral, estadiamento clínico, drenagem linfática e localização da neoplasia. Amostras de glândula mamária canina saudável foram adquiridas a partir de tecidos mamários sem alterações das cadeias mamárias recebidas no Laboratório de Patologia Comparada.

5.3 Avaliação histopatológica

As amostras cirúrgicas foram fixadas em solução de formalina tamponada neutra a 10%. Seções representativas foram processadas rotineiramente, incluídas em parafina, cortadas em seções de 4 μm de espessura e coradas com hematoxilina e eosina (H&E) para exame em microscopia de luz. As amostras humanas foram coletadas no período de 2010 e 2020 e foram classificadas histologicamente com base nos critérios descritos na Organização Mundial da Saúde (WHO, 2019) incluindo os tipos histológicos fibroadenoma (Fb, n=12), carcinoma tubular (CT, n=4), carcinoma invasivo (CI, n=37) e carcinoma micropapilar (CM, n=16). As amostras caninas foram coletadas no período de 2009 a 2020 e foram classificadas histologicamente com base nos critérios descritos no *Consensus for the Diagnosis, Prognosis and Treatment of Canine Mammary Tumors* (Cassali *et al.,* 2020) incluindo os tipos histológicos benigno em tumor misto (TMB, n=15), carcinoma em tumor misto (CTM, n=14), carcinossarcoma (CSS, n=6), carcinoma micropapilar (MP, n=16) e carcinoma com arranjo sólido (CAS, n=23).

Informações sobre o tamanho tumoral (T), acometimento neoplásico de linfonodos regionais (N) e presença de metástases à distância (M) foram apresentados como variáveis isoladas, uma vez que informações sobre metástase à distância não são devidamente relatadas devido às dificuldades de diagnosticar esta variável. O grau histológico foi estabelecido conforme o sistema de Nottingham.

5.4 Microscopia por absorção de dois fótons

O sistema de imagem empregado neste estudo combinou imagens SHG e TPEF usando uma configuração personalizada que compreende uma unidade de varredura a laser confocal Olympus FV300 conectada a um microscópio vertical BX61. Para amostras humanas, 1.200 seções representativas de tecido mamário humano normal e tipos histológicos humanos avaliados foram escolhidos de lâminas coradas com H&E. Para amostras caninas, 1.304 seções representativas de tecido mamário normal e tipos histológicos caninos avaliados de seções coradas com H&E foram definidos. Nos casos em que as lâminas histológicas incluíam regiões mamárias normais, imagens das 10 áreas mais representativas em amostras humanas e caninas foram capturadas. Em relação aos tecidos neoplásicos, 10 a 15 regiões intratumorais altamente representativas foram selecionadas para medições. Os sinais SHG e TPEF de áreas selecionadas

foram medidos para análises posteriores. Além disso, imagens de microscopia de campo claro de tecido corado com H&E foram adquiridas das mesmas áreas medidas usando o microscópio Olympus BX41 acoplado à câmera SPOT Insight Color para fins comparativos. O software de captura usado foi o *SPOT Advanced*.

Para a aquisição das imagens de microscopia de absorção de dois fótons, foram utilizadas lâminas histológicas coradas com eosina e hematoxilina a partir de tecidos fixados em formalina e embebidos em parafina. Foram selecionadas O sistema de imagem de geração de segundo harmônico (SHG) é uma instalação que utiliza um microscópio confocal de varredura a laser Olympus FV300. Nesse sistema utiliza-se um laser de Ti-Safira sintonizável (Coherent Chameleon) de 140fs com taxa de repetição de 80MHz ajustado para um comprimento de onda de 800nm. O feixe de laser, com polarização linear, passa através dos espelhos de varredura, de um espelho dicróico e é então focado na amostra em incidência normal por uma lente objetiva de 20x (N.A. 0,90). A potência média na amostra é de 5mW. O sinal de retroespalhamento na Geração de Segundo Harmônico é coletado pela mesma objetiva e direcionado pelo espelho dicróico insensível à polarização (Semrock FF665-Di02) para o detector (um tubo fotomultiplicador). Um filtro de banda fina (20nm de largura de banda) centrado no comprimento de onda do Segundo Harmônico (400nm) é usado para remover completamente a luz dispersa do laser. Todas as polarizações do Segundo Harmônico são coletadas, ou seja, não se utiliza nenhum polarizador-analisador na frente do detector. Isso garante que as fibras colágenas em todas as orientações da amostra possam ser observadas. Há apenas uma pequena diminuição na intensidade das fibras na polarização ortogonal à polarização linear do laser. Essa intensidade é de cerca de 80% em comparação à direção paralela.

As imagens de microscopia de fluorescência por absorção de dois fótons (TPEF) serão obtidas por meio da mesma montagem experimental da microscopia por geração de segundo harmônico, com algumas modificações. O feixe de laser com comprimento de onda de 800nm percorre o mesmo caminho até chegar à unidade de escaneamento. Para que se tenha uma comparação direta das posições nas imagens, foram obtidas imagens para as mesmas posições da amostra em que coletamos o sinal de SHG. O feixe de laser que sai da unidade de escaneamento passa por um espelho e é focado na amostra pela objetiva. A luz transmitida pela amostra é coletada por uma lente no interior do condensador focalizado em uma fotomultiplicadora (PMT3). A fluorescência é coletada pela mesma objetiva de focalização por retro-espalhamento. Após passar pela objetiva, ela passa novamente pelo espelho dicroico DM1. O sinal de fluorescência passa por uma lente e por uma íris que barram a luz proveniente

de espelhamento e de outros planos, garantindo que apenas a luz proveniente do plano focal chegue até as fotomultiplicadoras PMT1 e PMT2, utilizadas para obtenção das imagens de diferentes regiões da banda de fluorescência. Após passar pela região confocal, o laser passa por um espelho dicroico DM1 em 505nm. Um filtro passa banda (560-600nm) é utilizado antes da fotomultiplicadora para eliminar o restante de laser espalhado e selecionar a banda de fotoluminescência a ser coletada pela PMT2. Esta faixa de comprimento de onda é escolhida para medir a fluorescência da eosina.

5.5 Aquisição e Análise de Imagens de SHG e TPEF

A análise quantitativa dos parâmetros das fibras de colágeno e segmentos celulares foi obtida usando um pacote de software de código aberto chamado PyFibre (Python Fibrous Image Analysis Toolkit) que foi desenvolvido para realizar uma segmentação automatizada de imagens em regiões de colágeno e células e extrair seus parâmetros (disponível gratuito no GitHub) (Langford, 2020). No procedimento de análise, os sinais SHG e TPEF, bem como uma cópia dos dados da transmissão do laser, são usados para melhor identificar as fibras de colágeno e as características celulares nas imagens. O sinal SHG permite identificar as fibras de colágeno. Para mapear as localizações das fibras de colágeno como uma rede, usamos uma versão modificada do algoritmo FIbeR Extraction (FIRE) (Stein et al., 2008; Bredfeldt et al., 2014). Informações adicionais do TPEF e sinais de transmissão são então usadas para refinar ainda mais o limite entre as áreas fibrosas e celulares. A análise do PyFibre gera um banco de dados com todas as métricas extraídas das imagens para análise, cujos detalhes podem ser encontrados na documentação online do software (Langford, 2020). A segmentação da imagem permite que os cálculos sejam realizados especificamente para as regiões celulares e de fibras colágenas da imagem. Os valores das métricas avaliadas são utilizados como parâmetros de comparação entre os tecidos normais e o tecido neoplásico. As medidas de coerência das fibras SHG caracterizam a organização das fibras colágenas como regiões puramente isotrópicas (valor 0) e regiões em que as fibras colágenas estão perfeitamente alinhadas, ou anisotrópicas (valor 1). A rede de fibras de colágeno extraída permite medir também o número de fibras e o comprimento da fibra. A ondulação média da fibra é uma medida da linearidade das fibras colágenas extraídas das regiões estromais, onde 1 significa fibras totalmente lineares e 0 fibras totalmente onduladas. Os parâmetros da área de cobertura da fibra e da área de cobertura do segmento celular são a porcentagem da imagem coberta pelos recursos de fibra e celular,

respectivamente. Uma forte correlação negativa entre o segmento de fibra e os parâmetros de cobertura do segmento celular talvez seja esperada, mas não é garantida pelo método de análise.

5.6 Imuno-histoquímica e imunofluorescência

Foram utilizados cortes histológicos de 4µm de espessura para as reações de imuno-hitoquímica. Foi utilizado um kit comercial de detecção anti-mouse/anti-rabbit (Novolink Polymer Detection System, Leica Biosystems, Newcastle Upon Tyne, Reino Unido) conforme as instruções do fabricante. Para a recuperação dos antígenos dos receptores de estrogênio (RE), progesterona (RP), Ki67 e HER2 foi utilizada o calor a vapor (Pascal®) com citrato pH 6,0 (Dako Cytomation Target Retrieval Solution, Dako, Glostrup, Dinamarca). As lâminas com os cortes histológicos foram incubadas com o anticorpo primário apropriado por 16 horas em câmara úmida a 4ºC. Os dados dos anticorpos primários utilizados estão na tabela 1. A imunorreatividade foi visualizada com o cromógeno 3'-diaminobenzidina (DAB Substrate System, Dako, Carpinteria, CA, EUA) e contrastada com a hematoxilina de Mayer (RE, RP, Ki67, HER2 e CD68). Amostras de fragmentos de mama positivas para RE, RP, HER-2, Ki67 e CD68 serão utilizadas como controles positivos das reações. Para os controles negativos, o anticorpo primário foi substituído por solução salina tamponada com fosfato (PBS).

Anticorpo	**Clone**	**Diluição**	**Fabricante**	**Recuperação antigênica**	**Incubação**
RE	1D5	1:50	*Dako*	RCU	16h/4ºC
RP	hPRa2	1:50	*Neomarkers*	RCU	16h/4ºC
Ki67	MIB-1	1:50	*Dako*	RCU	16h/4ºC
HER-2	Policlonal	1:200	*Dako*	RCU	16h/4ºC
CD68	KP1	Pronto para uso	*Dako*	RCU	16h/4ºC

Tabela 1- Informações dos anticorpos utilizados na imuno-histoquímica. RCU: recuperação com calor úmido.

A coloração por imunofluorescência foi realizada conforme descrito em um estudo anterior por Rodrigues et al. (2016) e Monteiro et al. (2018). Resumidamente, seções de 5 µm de fragmentos de neoplasias mamárias caninas e humanas embebidos em parafina foram colocadas em lâminas previamente revestidas com gelatina. As amostras foram submetidas à recuperação antigênica em solução Trilogy sob calor úmido a 120°C por 20 minutos. Após a recuperação antigênica, as seções foram lavadas em solução salina tamponada com fosfato

(PBS) e, em seguida, permeabilizadas com PBS contendo 0,5% de Triton-X-100 (Sigma-Aldrich). Posteriormente, a ligação não específica foi bloqueada usando PBS suplementado com 1% de albumina sérica bovina (BSA, Sigma-Aldrich). Os dados dos anticorpos primários utilizados estão na tabela 2. Para a detecção de iNOS2, as seções foram incubadas com anticorpo secundário Alexa Fluor 647 goat anti-rabbit IgG (1:1000, Life Technologies). Posteriomente os núcleos foram contracorados com DAPI (dados do DAPI) e em seguida as lâminas foram montadas usando o reagente Prolong Gold Antifade (Life Technologies). Controles negativos foram incluídos em todas as reações, omitindo os anticorpos primários. As seguintes configurações de excitação/emissão foram usadas: DAPI (405 nm/415-480 nm), FITC (488 nm/500-525 nm), R-PE (543 nm/550-630 nm) e Alexa Fluor 647 (630 nm/>650 nm). As imagens foram adquiridas em microscópio confocal invertido Zeiss LSM 880 (CAPI). Os anticorpos utilizados foram padronizados em nossa rotina laboratorial, e sua especificidade antigênica foi confirmada por meio de nossa própria pesquisa e por referência a outros estudos publicados (Rodrigues et al., 2016; Monteiro et al., 2018).

Anticorpo	**Fonte**	**Clone**	**Diluição**	**Fabricante**	**Conjugado**	**Recuperação antigênica**	**Incubação**
S100A8/A9 *Complex*	Camundongo	MAC387	1:400	*Abcam*	FITC	RCU	16h/4ºC
CD206	Camundongo	3.29B1.10	1:100	*Beckman Coulter*	R-PE	RCU	1 hora, TA
NOS2	Coelho	Policlonal	1:100	*Santa Cruz*	-	RCU	16h/4ºC

Tabela 2 - Informações dos anticorpos utilizados na imunofluorescência. RCU: recuperação com calor úmido.

5.6.1 Avaliação da imunoexpressão para determinação do imunofenótipo

A leitura das lâminas para determinação dos imunofenótipos foi realizada conforme a Organização Mundial da Saúde (WHO, 2019) para as neoplasias mamárias humanas e conforme o *Consensus for the Diagnosis, Prognosis and Treatment of Canine Mammary Tumors* (Cassali et al., 2020) para as neoplasias mamárias caninas. Avaliamos a imunomarcação do Ki67, dos receptores hormonais (RE e RP) e HER2, de modo a determinar os imunofenótipos das amostras neoplásicas. A imunomarcação para Ki67 foi feita

considerando a expressão nuclear em 500 células tumorais, observadas com uma ampliação de 400x. A porcentagem de células positivas foi usada para classificar a expressão de Ki67 em baixa (≤ 20%) ou alta (>20%). Em relação aos receptores hormonais, a imunomarcação foi avaliada pela intensidade da marcação nuclear, com quatro categorias de positividade: (+) entre 1-25%, (++) entre 26-50%, (+++) entre 51-75% e (++++) para mais de 75% das células com imunomarcação positiva.

A imunomarcação para HER2 foi avaliada considerando a imunoexpressão membranar das células neoplásicas. A classificação foi feita em quatro níveis: (-) para ausência de marcação ou marcação fraca/incompleta, (+) para marcação fraca/incompleta em 10% ou mais das células tumorais, (++) para marcação moderada/incompleta em mais de 10% das células tumorais e (+++) para marcação completa e intensa em mais de 10% das células.

Com base nesses parâmetros, as amostras foram categorizadas em quatro grupos de imunofenótipos. O grupo Luminal A incluiu tumores com Ki67≤20%, receptores hormonais positivos em qualquer intensidade e HER2 negativo. O grupo Luminal B incluiu tumores com Ki67>20%, receptores hormonais positivos em qualquer intensidade e HER2 negativo. O fenótipo HER2 superexpresso incluiu tumores com qualquer percentual de Ki67, receptores hormonais negativos e HER2 positivo. Finalmente, os tumores classificados como Triplo Negativo apresentaram qualquer percentual de Ki67, receptores hormonais negativos e HER2 negativo.

5.6.2 Imunoexpressão e quantificação dos macrófagos

A imunorreação foi considerada positiva para os anticorpos direcionados aos macrófagos quando foi observada marcação citoplasmática difusa ou granular, sem envolvimento do núcleo. A identificação dos macrófagos foi baseada na imunorreatividade positiva ao anticorpo específico, além de características morfológicas típicas dessas células. A contagem foi realizada sem conhecimento prévio da condição clínica dos pacientes, com a análise sendo conduzida em cinco áreas de maior infiltração ("hot-spots") identificadas inicialmente sob baixa magnificação (100x) e, em seguida, imagens capturadas com aumento de 400x. A escolha das áreas de maior infiltração, em vez de áreas aleatórias, foi baseada em sua relevância biológica (Leek et al., 1996; Takeuchi et al., 2004).

5.7 Comitê de ética

O estudo com amostras caninas foi realizado conforme os princípios éticos fundamentais estabelecidos pela lei n.º 11.794, de 8 de outubro de 2008, e pelo decreto n.º 6.899, de julho de 2009, bem como pelas normas emitidas pelo Conselho Nacional de Controle de Experimentação Animal (CONCEA) e as diretrizes internacionais para pesquisa em animais: Animal Research: Reporting of In Vivo Experiments (ARRIVE). Todos os protocolos experimentais foram aprovados pela "Comissão de Ética no Uso de Animais" da UFMG, sob o número 83/2021.

A pesquisa com amostras de tecido humano foi previamente aprovada pela "Comissão de Ética em Pesquisa" da UFMG (COEP-UFMG), sob o número 43947521.3.0000.5149/2021. Todos os experimentos foram conduzidos conforme a Declaração de Helsinque. Por se tratar de um estudo retrospectivo, realizado em lâminas histopatológicas de arquivo, a necessidade de consentimento informado de todos os sujeitos e/ou seus responsáveis legais foi dispensada pela COEP-UFMG.

5.8 Análises estatísticas

A distribuição dos dados foi avaliada utilizando o teste de Shapiro-Wilk para amostras menores e o teste de Kolmogorov-Smirnov para amostras maiores. Para os dados paramétricos, foram empregados os testes ANOVA e HSD de Tukey para múltiplas comparações de médias entre grupos. Para os dados não paramétricos, foram empregados os testes Kruskal Wallis e o teste de Dunn para múltiplas comparações de médias entre grupos. O coeficiente de correlação de postos de Spearman foi utilizado para investigar a relação entre parâmetros clinicopatológicos, as características das fibras de colágeno e a infiltração de macrófagos nas neoplasias mamárias. Curvas de Kaplan-Meier foram geradas para estimar as taxas de sobrevida específicas para o câncer, e as comparações entre grupos foram realizadas utilizando o teste de log-rank de Mantel-Cox. Para as correlações feitas entre os parâmetros de colágeno e os dados de sobrevida global das pacientes, foram incluídas apenas pacientes tratados cirurgicamente. A pontuação 1 foi atribuída aos pacientes que morreram de câncer de mama e 0 aos pacientes vivos. Pacientes que morreram por outros motivos foram censuradas. O teste qui-quadrado e o teste exato de Fisher foram utilizados para examinar a potencial associação entre as características das fibras de colágeno, infiltração de macrófagos (como variável categórica) e

os dados clinicopatológicos, como grau histológico, estadiamento clínico, taxa de proliferação celular e subtipo molecular. Tabelas de contingência foram utilizadas para apresentar essas associações. Todas as análises estatísticas foram realizadas utilizando o Prism (versão 8.0, GraphPad, San Diego, CA, Estados Unidos), com um nível de significância estabelecido em $p<0,05$. Valores de p menores que 0,0001, 0,001, 0,01 e 0,05 são denotados por ****, ***, ** e *, respectivamente.

6. RESULTADOS E DISCUSSÃO

Os tópicos “Resultados e Discussão” serão apresentados nesta sessão sob a forma de dois artigos científicos. O artigo 01 foi publicado na revista *Scientific Reports* (anexo 01).

Identificação do artigo publicado:

Garcia APV, Reis LA., Nunes FC., Longford FGJ, Frey JG, De Paula AM, Cassali GD. Canine mammary cancer tumour behaviour and patient survival time are associated with collagen fibre characteristics. Scientific Reports, v. 11, p. 5668, 2021.

6.1 Artigo 01 - Comparative evaluation of collagen modifications in breast cancer in human and canine carcinomas

Ana Paula Vargas Garcia[1], Luana Aparecida Reis[2], Bárbara Regina Melo Ribeiro[2], Cristiana Buzelin Nunes[3], Ana Maria de Paula[2*], Geovanni Dantas Cassali[1]

[1]Department of General Pathology, Institute of Biological Sciences, Federal University of Minas Gerais. Av. Pres. Antônio Carlos, 6627, Pampulha, Belo Horizonte, MG, Brazil. 31270-901.

[2]Department of Physics, Institute of Exact Sciences, Federal University of Minas Gerais. Av. Pres. Antônio Carlos, 6627, Pampulha, Belo Horizonte, MG, Brazil. 31270-901.

[3]Department of Anatomic Pathology, Faculty of Medicine, Federal University of Minas Gerais. Av. Prof. Alfredo Balena, 190, Santa Efigênia, Belo Horizonte, MG, Brazil. 30130-100.

Ana Paula Vargas Garcia - vargas.biomedicina@gmail.com (ORCID: 0000-0002-0898-6295)

Luana Aparecida Reis - lareis@unicamp.br (ORCID: 0000-0002-8404-9463)

Bárbara R. M. Ribeiro - barbara-melo@ufmg.br

Cristiana Buzelin Nunes - cbn@medicina.ufmg.br (ORCID: 0000-0002-5266-6870)

*Ana Maria de Paula - ana@fisica.ufmg.br (ORCID: 0000-0002-8551-5948)

Geovanni Dantas Cassali - gcassali@ufmg.br (ORCID: 0000-0002-5650-6743)

*Corresponding author

Present address Luana Aparecida Reis: Institute of Physics “Gleb Wataghin”, University of Campinas, Campinas, SP, Brazil.

ABSTRACT

New diagnostic and therapeutic approaches have been increasingly demanded due to the high morbidity and mortality associated with breast cancer. Recently, changes in the collagen fibres in mammary neoplasms have been shown to provide information that can be helpful for more accurate diagnosis. We aimed to conduct a comparative analysis of the tumour stroma in human and canine mammary neoplasms to assess the relationship between collagen modifications and the behaviour of carcinomas in both species, by multiphoton microscopy. We present a retrospective study of 70 cases of human mammary tumour and 74 cases of canine mammary tumour. We analysed sections stained with haematoxylin and eosin from 1,200 representative areas of normal mammary tissue, fibroadenoma, grade I invasive carcinoma, grade III invasive carcinoma and invasive micropapillary carcinoma in human species and 1,304 representative areas of normal mammary tissue, benign mixed tumour, mixed carcinoma, carcinosarcoma, invasive micropapillary carcinoma and solid carcinoma in canine species. We obtained that both human and canine mammary carcinomas present lower density of collagen fibres, higher density of cells and the collagen fibres are more aligned than in normal tissue. For human mammary carcinomas, the collagen fibres are more linear as compared to normal tissue. In addition, we demonstrated that the carcinomas with unfavourable prognosis present shorter collagen fibres, and these collagen changes correlate with the clinical and pathological data in human and canine species. For dogs, there is a correlation between the mean fibre length with the specific survival times. Thus, we demonstrate that dogs provide an excellent comparative perspective for studying how changes in the tumour stroma affect patient survival.

Key-words: collagen fibre; collagen alignment; tumour microenvironment; breast cancer; matrix remodelling; tumour-associated stroma.

Mammary gland neoplasms are characterized by collagen deposition, remodelling, and linearisation of the extracellular matrix, leading to fibrosis that promotes malignancy[1,2]. The stiffened stroma enhances tumour cell growth, survival, and migration, driving an epithelial-mesenchymal transition. A rigid stroma also induces angiogenesis, hypoxia, and compromises antitumour immunity[3]. It is a well-established fact that the tumour microenvironment, also known as the tumour-associated stroma, is composed of a diverse combination of non-tumour cells, such as fibroblasts, macrophages and other immune cells, vascular cells, adipocytes, and others, in addition to the extracellular matrix. Studies demonstrated that tumour-associated stroma plays a key role in the initiation and progression of a wide variety of neoplasms, having multiple roles in tumour biology[4,5]. Collagen, specifically, plays a crucial role in metastasis development in breast cancer, as well as in matrix metalloprotease activity, that has been the subject of a considerable number of planned and therapeutic studies of many types of cancer[6-9] and specifically in breast cancer[10-18]. It has been shown that the neoplastic mammary glands present more organized and defined collagen fibres when compared to the healthy breast. Therefore, collagen organization is correlated with unfavourable prognosis[1,15-21]. Furthermore, changes in collagen density and fibre organization were associated with tumour grade and overall survival in human[15] and canine[18] breast carcinomas.

Neoplasms naturally developed in domestic dogs have increasingly been used as a valuable source of information to better understand the biology of breast cancer development in women. The canine species presents pathophysiological similarities with the human species and can help in research for new diagnoses and therapies related to this neoplasm[22-28]. The field of comparative oncology aims to approach some existing research deficiency, broadening its focus from classic rodent models to spontaneous tumours that develop in animals. This additional perspective is perceived as a chance to complement and improve the understanding of complex diseases, such as cancer, in relation to tumour development, risk factors and mechanisms of tumourigenesis. Due to the many similarities shared between dogs and humans, the domestic dog has been considered one of the best examples of comparative oncology[21,22,25,26,28-30]. Thus, the aim of this study was to carry out a comparative analysis of the tumour stroma in human and canine mammary neoplasms to evaluate the links between changes in collagen fibres and the behaviour of carcinomas in both species. The study was based on morphological, clinicopathological, immunophenotypic data and imaging by second harmonic generation (SHG) and two-photon excited fluorescence (TPEF) microscopy in cases of human mammary and canine mammary tumour.

Materials and Methods

Case selection

This retrospective study involved the analysis of 70 cases of human mammary neoplasms, 74 samples of canine mammary tumours, 20 healthy samples of human mammary tissue, and 12 healthy samples of canine mammary tissue. The canine mammary tissue samples were obtained from the archives of the Comparative Pathology Laboratory at the Federal University of Minas Gerais (UFMG), Brazil. The human mammary tissue samples were collected from the biopsy sector archives of the Faculty of Medicine at the Federal University of Minas Gerais (UFMG), Brazil. Both the canine and human samples were sourced from naturally occurring tumours in patients undergoing treatment at the UFMG Veterinary Hospital and the UFMG Hospital das Clínicas. Healthy canine mammary tissue samples were acquired from mammary tissues without mammary chain abnormalities received at the Comparative Pathology Laboratory. Healthy samples of human breast tissue were obtained from breast reduction surgeries performed at the Hospital das Clínicas of UFMG. The selection process encompassed samples with comprehensive information regarding tumour size, presence or absence of regional or distant metastasis, and histological grade.

The two-photon microscopy images were performed on histological slides stained with haematoxylin and eosin (H&E). The slides were prepared using sections of healthy or neoplastic mammary tissue sourced from biopsies involving procedures such as setorectomy, simple mastectomy, or unilateral/bilateral radical mastectomy, determined by factors including tumour size, tumour site, lymphatic involvement, and clinical stage. The selected canine samples were collected between 2009 and 2020 and submitted to histological classification according to the Classification and Grading of Canine Mammary Tumors[31,32] and Consensus for the Diagnosis, Prognosis and Treatment of Canine and Feline Mammary Tumours[33-36]. The selected human samples were collected from 2010 to 2020 a were classified histologically based on the criteria described in the World Health Organization[37]. For correlations between collagen fibre organization parameters, number, waviness and mean fibre length, collagen density and cell density and patient-specific survival, only data from patients treated with surgery alone were included. Score 1 was assigned to patients who died from breast cancer and 0 to living patients. Patients who died for reasons other than mammary cancer were not included.

The canine sample study was performed in view of the fundamental ethical principles under law no. 11.794, of October 8, 2008 and of decree no. 6.899 of July 2009, and with the rules issued by the National Council for the Control of Animal Experimentation (CONCEA) and the international Animal Research: Reporting of In Vivo Experiments (ARRIVE). All experimental protocols were approved by the "Ethics Committee on the Use of Animals" at UFMG, under number 83/2021.

The research on human tissue sample was previously approved by the "Research Ethics Committee" at UFMG (COEP-UFMG) under No. 43947521.3.0000.5149/2021. All experiments were carried out in accordance with the Declaration of Helsinki. As a retrospective study, performed on archive histopathological slides, the need for informed consent from all subjects and/or their legal guardian(s) was waived by the COEP-UFMG.

Performing immunohistochemistry

Histological sections, measuring 4 µm thick, were prepared for immunohistochemical analysis. A commercial anti-mouse/anti-rabbit detection kit (Novolink Polymer Detection System, Leica Biosystems, Newcastle Upon Tyne, United Kingdom, REF RE7158, LOT 6092583), was used following the manufacturer's instructions. Antigen retrieval for estrogen receptor (ER), progesterone receptor (PR), Ki67 and HER2 was performed using steam heat (*Pascal*®) with citrate pH 6.0 (Invitrogen by Thermo Fisher Scientific, 10X low pH, REF 00-4955-58, LOT 2410220, Life Technologies' Corp., 5781 Van Allen Way, Carlsbad, CA92008). The histological sections were incubated with the corresponding primary antibodies for 1 hour in a humid chamber at 4 °C. Primary antibodies used included ER (Dako Cat# ER-14-0481, RRID:AB_1545347, goat anti-human EP1 receptor, PTGER1 antibody, unconjugated, LOT 11303512, REF IR084, ready-to-use), PR (LSBio LifeSpan Cat# LS-C26712, RRID:AB_2283822, progesterone receptor (PGR) mouse monoclonal (hPRa2+hPRa3) antibody, anti-human/mouse/rat, unconjugated, LOT XI3703736, REF MA512642, 0.4mg/mL, 1:50), HER2 (Dako Cat# AP7629e, RRID: AB_2262284, rabbit anti-human HER2, polyclonal antibody, unconjugated, REF A0485, LOT 00060381, 0.50g/mL, 1:200), and Ki67 (Thermo Fisher Scientific Cat# MA5-31796, RRID:AB_2787419, mouse anti-human MIB1 receptor, 2A7B1 antibody, unconjugated, LOT 20067572, REF M7240, 46 mg/mL, 1:50). Immunoreactivity was visualized using 3,3'-diaminobenzidine chromogen (Novolink Polymer Detection System, Leica Biosystems, Newcastle Upon Tyne, United Kingdom, REF RE7158, LOT 6092583) and counterstained with Mayer's haematoxylin. Positive controls for the

reactions consisted of fragments of canine and human mammary tissues positive for HER-2, ER, PR and Ki67. The primary antibody was omitted and chromogen was added to both for negative controls. The evaluation of the slides, the quantification of immunoreactive and the classification of immunophenotypes were carried out in accordance with the World Health Organization[32] guidelines (for human samples) and the criteria established by Nunes et al.[33] (for dog samples). The antibodies used were standardized in our laboratory routine, and their antigenic specificity was confirmed through our own research and by reference to others published studies[33-38].

Image acquisition and analyses

The imaging system employed in this study combined SHG and TPEF imaging using a custom setup comprising an Olympus FV300 confocal scanning laser unit connected to a BX61- upright microscope. The SHG images allow to extract information from the collagen fibres and the TPEF allows to extract details of the cell arrangements in the tissue. Details of the image acquisition methodology is described in our previous publications[17,18,39]. In brief, we used 140 fs pulses centred at the wavelength of 800 nm. The beam is focused on the sample microscope slab by a 20X objective with a high numerical aperture (NA=0.9) and the images are obtained in back scattering geometry. The SHG is measured at 400 nm using a filter with bandwidth of 20 nm by directing the signal to a non-descanned detector placed just above the objective. The fluorescence signal from the eosin dye staining the tissue is measured by the standard de-scanned detector of the confocal unit at the wavelength band of 560 to 600 nm. The transmitted laser image is also collected by the condenser of the microscope. We measured images at the optimized focus position and at ±1 μm from this position to allow for noise filtering by the software. The images were acquired for areas of 0.47x0.47 mm^2. For human samples, 1,200 representative sections of normal human breast tissue (NMTh) and evaluated human histological types were chosen from H&E-stained slides. For canine samples, 1,304 representative sections of normal mammary tissue (NMTc) and canine histological types evaluated from sections stained with H&E were defined. In cases where histological slides included normal mammary regions, images of the 10 most representative areas in human and canine samples were captured. Regarding neoplastic tissues, 10 to 15 highly representative intratumoural regions were selected for measurements. SHG and TPEF signals from selected areas were measured for further analyses. Additionally, brightfield microscopy images of H&E-stained tissue were acquired from the same measured areas using the Olympus BX41

microscope coupled to the *SPOT Insight Color* camera for comparative purposes. The capture software used was *SPOT Advanced*.

Our quantitative analyses of collagen fibre and cell segment parameters utilized PyFibre, an open-source software package (Python Fibrous Image Analysis Toolkit), that we specifically designed for automated segmentation of images into cellular and collagen regions, allowing extraction of pertinent parameters. PyFibre is openly accessible on GitHub[40]. During the analyses process, the integration of SHG and TPEF signals along with laser transmission data was employed to improve the accurate identification of collagen fibres and cellular features in the images. This approach utilized the TPEF and SHG signals, in addition to a copy of the laser transmission data, to better discern collagen fibres and cellular features in the images. Data were extracted and analysed according to Reis et al.[17], Garcia et al.[18] and Gomes et al.[39].

Statistical analysis

The Shapiro-Wilk test was employed to assess normality in small sample groups, while the Kolmogorov-Smirnov test was used for larger sample groups. Due to the non-parametric nature of the data, the Kruskal Wallis test and the Dunn test were performed for multiple comparisons of the medians between groups. We employed Spearman's Correlation Coefficient and linear regression statistical tests to establish correlations between clinicopathological data of patients and collagen fibre parameters. The cancer-specific survival rate was estimated using the Kaplan–Meier curve, and the comparisons between groups were performed using the Mantel-Cox log rank test. To evaluate the independence or association between the categorical variables mean fibre length and histological grading, clinical staging, cell proliferation and significant molecular subtype between categorical variables using the chi-square test and Fisher's Exact Test. The graphs were presented in contingency graphs. These analyses were performed using *Prism* (version 8.0, GraphPad, San Diego, CA, United States). A value of $p < 0.05$ was considered statistically significant for all analyses. The p values less than 0.001 are denoted by (***), p less than 0.01 are denoted by (**) and p less than (0.05) are denoted by (*).

Results

Details of the analysed samples

Table 1 presents the details of the histological subtypes analysed, number of samples, patient age, clinical staging, histological grading, molecular subtype and survival information for human breast neoplasms. Table 2 provides equivalent details for canine mammary neoplasms. The analysis of correlations between collagen fibre parameters and clinicopathological data did not include Fibroadenoma (Fb) in women and benign mixed tumours (BMT) in dogs. It should be noted that the canine data presented in this article comprise a different data set from that used in our previously published works. Importantly, there is no overlap between the samples included in this study and those analysed in our previous publications[18,41]. For this study, we selected more recent cases, ensuring a more accurate assessment of potential changes in the genetic, environmental, and social conditions of the animals involved. Additionally, we prioritised cases with comprehensive descriptions of clinical-pathological data, which allowed us to deepen the analysis of additional prognostic factors. Nonetheless, due to the low occurrence of carcinosarcomas in clinical practice, we used some of the same carcinosarcoma cases described in our previous publication[18]. However, all the other cases selected are new, and the analyses performed in this work are original, providing new insights into tumour progression.

The women were followed up for a minimum of 05 years and a maximum of 10 years. At the conclusion of the study, we completed the follow-up of 43 patients. Of these, 06 women had died and 37 were still alive. Follow-up was not possible for 11 patients. The distribution of women based on clinical staging was as follows: 04 women with TC (02 alive, 02 not followed up), 16 women with ICgI (01 died, 14 alive, 01 not followed up), 21 women with ICgIII (18 alive, 03 not followed up), and 17 women with IMC (05 died, 09 alive, 03 not followed up). All patients had complete information on clinical staging.

The female dogs were followed up for a minimum of 02 years and a maximum of 05 years. At the conclusion of the study, we completed the follow-up of 55 bitches. Of these, 46 patients had died and 09 were still alive. Follow-up was not possible for 04. The distribution of patients based on clinical staging was as follows: 14 patients with MC (07 died, 07 alive), 16 with IMC (14 died, 02 not followed up), 06 with CS (all died), and 23 with SC (19 died, 02 alive, 02 not followed up). Three patients with IMC did not have complete information to define the clinical staging. Women with Fb and dogs with BMT were not followed up.

Histological type	n	Age (year)	Staging (TNM)					Histological grades			Molecular subtype				Survival (months)
			I	II	III	IV	V	I	II	III	HR+/ Ki67 < 20%	HR+/ Ki67 >20%	HR+/- HER2+	HR-/ HER2-	
Fb	12	34.2	NA	NA	NA	NA	NA	NA	NA	NA	NA	NA	NA	NA	NA
TC	4	71.3	2	2	0	0	0	4	0	0	4	0	0	0	66.0
ICgI	16	68.4	5	7	0	3	1	16	0	0	13	3	0	0	86.3
ICgIII	21	59.6	5	2	2	10	2	0	0	21	2	12	4	3	79.1
IMC	17	52.3	4	3	1	9	0	3	8	2	3	8	6	0	59.5
Total	**70**	**-**	**16**	**14**	**3**	**22**	**3**	**23**	**8**	**23**	**22**	**23**	**9**	**4**	**-**

Table 1. Clinicopathological features of human mammary neoplasms. For the age and the survival, the data are the mean values with the standard deviation in brackets. Fibroadenoma (Fb), tubular carcinoma (TC), grade I invasive carcinoma (ICgI), grade III invasive carcinoma (ICgIII), invasive micropapillary carcinoma (IMC). N= number of cases. NA= not evaluated. HR= hormonal receptor.

Histological type	n	Age (year)	Staging (TNM)					Histological grades			Molecular subtype				Survival (days)
			I	II	III	IV	V	I	II	III	HR+/ Ki67 < 20%	HR+/ Ki67 >20%	HR+/- HER2+	HR- /HER2-	
BMT	15	10	NA	NA	NA	NA	NA	NA	NA	NA	NA	NA	NA	NA	NA
MC	14	11	7	3	4	0	0	11	2	1	13	1	0	0	1116.2
CS	6	8.5	0	0	4	0	2	0	0	6	2	4	0	0	321.8
IMC	16	10.8	0	1	2	10	3	2	9	5	1	7	3	5	293.9
SC	23	11.8	5	4	4	9	1	2	10	11	3	17	2	1	279.5
Total	**74**	**-**	**12**	**8**	**14**	**19**	**6**	**15**	**21**	**23**	**19**	**29**	**5**	**6**	**-**

Table 2. Clinicopathological features of canine mammary neoplasms. For the age and the survival, the data are the mean values with the standard deviation in brackets. benign mixed tumour (BMT), mixed carcinoma (MC), invasive micropapillary carcinoma (IMC), carcinosarcoma (CS), solid carcinoma (SC). N= number of cases. NA= not evaluated.

Images and extract parameters

Figure 1 present representative images of the human histological sections studied to illustrate the imaging procedure. The histological types in the columns are indicated as NMTh (Figure 1A, 1E, 1I and 1M), Fb (1B, 1F, 1J and 1N), ICgI (1C, 1G, 1K and 1O) and IMC (1D, 1H, 1L, 1P) for the normal mammary gland, fibroadenoma, grade I invasive carcinoma and invasive micropapillary carcinoma, respectively. The fourth row presents images of individual fibres, displayed in varying colours, extracted using our image analysis methodology (1M-1P). The SHG signal is from the collagen fibres, that are non-centrosymmetric fibres, and the TPEF signal corresponds to the fluorescence emission of the dye eosin. The SHG and TPEF represent false colour representations of normalized intensity maps to accentuate various features. Comparing the two images allows to segment the tissue into collagen and cellular regions, and thus extract quantitative parameters. The images of the extracted collagen fibres are presented in Figure 1M, 1N 1O 1P. For the canine samples, the methodology for acquiring the images and extracting the parameters has already been thoroughly exemplified in previous articles[17,18,39]. More details about measurements and image analyses can be found in the 'Materials and Methods' section.

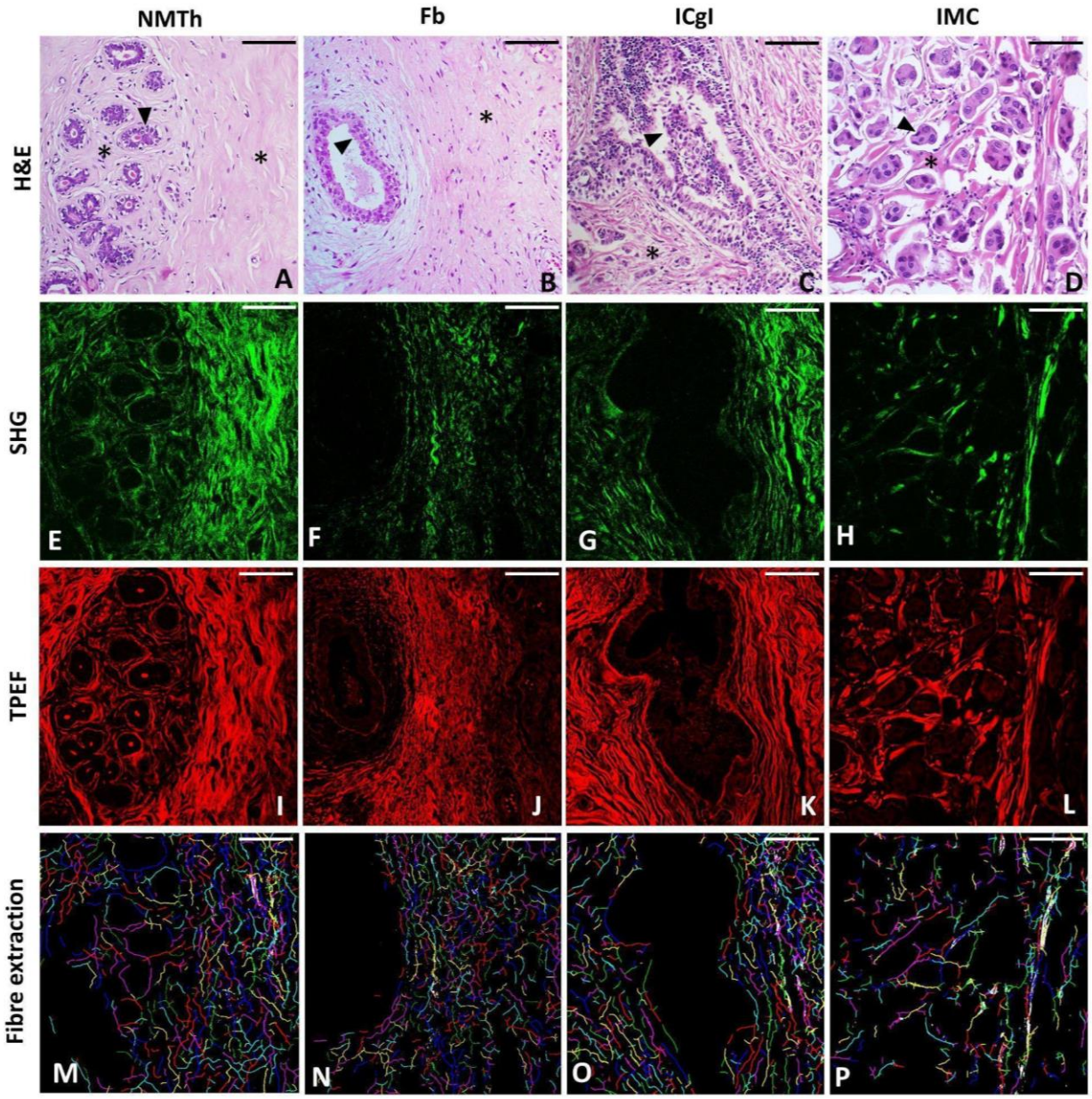

Figure 1. Acquired images (20X objective). The optical microscopy H&E (A-D), second harmonic generation microscopy (E-H), two-photon excited fluorescence microscopy (I-L) and the extracted collagen fibres with each fibre in a random colour (M-P) for the human normal mammary tissue (A, E, I and M), fibroadenoma (B, F, J and N), grade I invasive carcinoma (C, G, K and O) and invasive micropapillary carcinoma (D, H, L and P). Asterisk HE: stroma. HE arrowhead: epithelial cells. The scale bar is 100 μm.

Human mammary tissue (NNMTh, Fig 1) is composed of lobes, ducts, and an interconnected network of connective tissue (indicated by the asterisk in Fig. 1A). connective tissue, abundant collagen fibres are found surrounding the parenchyma, which exhibit different orientations within the breast tissue (Fig. 1E). In benign neoplasms of the mammary gland, such as fibroadenoma (Fb) in women (Fig. 1B), and also benign mixed tumours (BMT) in dogs, an abundance of collagen fibres is visible in the adjacent connective tissue, exhibiting a pattern of diverse orientation similar to that of NNMTh (Fig. 1F) and NMTc. However, in grade I invasive carcinoma (ICgI) and invasive micropapillary carcinoma (IMC), there is a reduction in collagen density and collagen fibres are organized in a preferential direction (Figs. 1G-1H and 1O-1P). ICgI has a favourable prognosis, while IMC is associated with an unfavourable prognosis[31,32,35]. Mixed carcinomas (MC) originates from the malignant transformation of benign mixed tumours, presenting a complex histological pattern and favourable prognosis[31,32-36,42,43]. On the other hand, carcinosarcoma (CS) is characterized by the coexistence of malignant epithelial and mesenchymal components, presenting an extremely aggressive biological behaviour, with a high incidence of metastases to regional lymph nodes and lower overall survival[29,31,34,36]. In IMC and SC, decrease in collagen density and an increased alignment of collagen fibres in the surrounding connective tissue are also noticeable.

Our image analysis and fibre and cell extraction procedures allowed the quantification of many of these microscopic features described. Collagen fibre organization parameters (fibre segment SHG coherence), number of collagen fibres (no. fibres), mean fibre length, collagen density (fibre segment coverage) and cell density (cell segment coverage) for all histological types of human and canine mammary neoplasms and for NMTh and NMTc that are presented in figure 2.

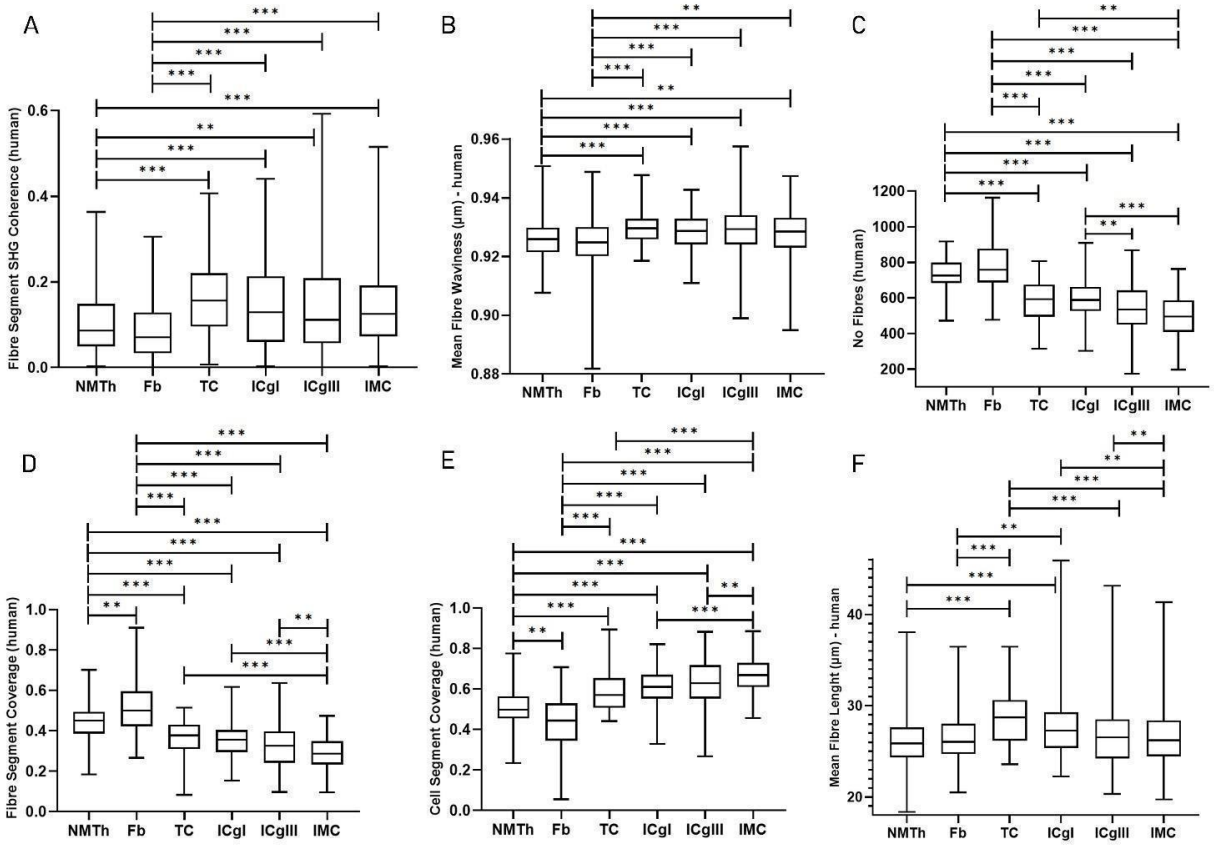

Figure 2. Parameters of the human mammary gland analysed by second harmonic generation and two-photon excited fluorescence techniques. Kruskal Wallis test and the Dunn test. Boxplot graphics showing the calculated parameters for the fibre segment SHG coherence, mean fibre waviness, mean fibre length, number of fibres, fibre segment coverage and cell segment coverage for human normal mammary tissue (NMTh, n=20), fibroadenoma (Fb, n=12), tubular carcinoma (TC, n=04), invasive carcinoma grade I (ICgI, n=16), invasive carcinoma grade III (ICgIII, n=21), invasive micropapillary carcinoma (IMC, n=17) in human samples (n=90). The centre lines show the medians, the box limits indicate the 25th and 75th percentiles, the whiskers extend 1.5 times the interquartile range from the 25th and 75th percentiles and the outliers are represented by dots. The p values less than 0.001 denoted by (***), p less than 0.01 are denoted by (**) and p less than (0.05) are denoted by (*).

Carcinomas present aligned fibres, lower fibre density and higher cell density

The collagen fibre organization parameter assesses the degree of alignment of collagen fibres within the tissue, with values spanning from zero (indicating a random arrangement) to one

(indicating highly oriented and aligned fibres along a specific direction). As depicted in Figures 2A human mammary carcinomas exhibit a greater degree of collagen fibre alignment when compared to NMTh. Canine neoplastic tissues exhibit the same behaviour (see Supplementary Fig. S1). These results clearly delineate a distinction between normal and carcinomatous tissue in both species.

Figures 2B show the waviness of the collagen fibres for human mammary tissues. This parameter evaluates the straightness of the collagen fibres extracted from the stromal regions, where 1 means perfectly linear fibres and 0 means perfectly wavy fibres. In human mammary tissues, carcinomas present more linear fibres compared to NBTh and Fb. In canine mammary tissue (see Supplementary Fig. S1), it was not possible to verify this same behaviour. We observed that none of the histological types present statistically significant differences with NBTc. SC has more linear collagen fibres compared to BMT and ICM, and CS has more linear fibres compared to BMT and IMC.

The number of collagen fibres, the fibre coverage area and the cell coverage area determine the collagen density and cell density in the measured regions. These are important parameters to evaluate changes related to the stromal and epithelial components of human (Fig. 2C to 2E) and canine (see Supplementary Fig. S1) mammary carcinomas. Figures 2C and 2D show that the number of collagen fibres and the area covered by fibres decrease in carcinomas compared to NMTh and neoplastic tissues benign. Comparatively, figures 2E show that carcinomas present a larger area covered by cells compared to NMTh and benign neoplastic tissues. We observed similar behaviour in the canine species (see Supplementary Fig. S1), however we did not observe significant differences in the number of collagen fibres, area covered by fibres and area covered by cells between CS with NMTc and BMT.

Furthermore, the collagen fibre length is an important parameter for evaluating the stromal changes that occur in neoplastic mammary tissues[1,9,18,44]. Figure 2F show that the mean fibre length is different between the histological types in humans. Carcinomas with favourable prognosis (TC and ICgI) present a higher mean fibre length as compared to carcinomas with unfavourable prognosis (ICgIII and IMC). In canine mammary carcinomas, we identified the same behaviour (see Supplementary Fig. S1 online). Carcinoma with favourable prognosis (MC) presents the highest average fibre length as compared to carcinomas with reserved to unfavourable prognosis (CS, IMC and SC).

More aggressive carcinomas present lower fibre density, higher cell density and shorter collagen fibres

To evaluate the influence of the tumour stroma on the behaviour of human and canine mammary carcinomas, we verified whether the density of collagen fibres, cell density and fibre length correlate with the clinicopathological data. Immunohistochemistry was performed on a sample of 58 human and 59 canine mammary tissue samples, all diagnosed with mammary carcinoma. Figure 3 shows these correlations. Here, the increased aggressiveness of carcinomas was associated with cases that presented the following characteristics: higher histological grade, larger probability of developing local and/or distant metastases, higher rate of cellular proliferation and larger probability of presenting molecular expressions of the “triple-negative” and “Her2 overexpressed”. For the correlations, the cell proliferation rate was obtained from the Ki67 count and the molecular subtype of human and canine mammary carcinomas were categorized as follows: 1 for luminal A (positive hormone receptors, negative HER-2 and proliferative rate less than 20%), 2 for luminal B (positive hormone receptors, negative HER-2 and proliferative rate greater than 20%), 3 for HER-2 positive (positive or negative hormone receptors and positive HER-2 independent of the proliferative rate) and 4 for triple negative (negative hormone receptors, negative HER2 regardless of proliferative rate).

We note that the mean fibre length inversely correlates with histological grade (Fig. 3A and 3B), clinical staging (Fig. 3C and 3D), cell proliferation (Fig. 3E and 3F) and molecular subtype (Fig. 3G and 3H) in women and dogs. Here, we show data correlating the increased tumour aggressiveness with the smaller collagen mean fibre length. It is important to note that while human molecular subtypes have been adapted for use in canine mammary carcinomas, their prognostic value in dogs remains controversial, particularly for HER2 overexpression. Conflicting results in the literature have made it difficult to establish a consistent correlation between HER2 status and clinical outcome in dogs. Despite this limitation, we found that mean fibre length inversely correlates with histological grade (Fig. 3A and 3B), clinical staging (Fig. 3C and 3D), cell proliferation (Fig. 3E and 3F) and molecular subtype (Fig. 3G and 3H) in both women and dogs. Here, we show data correlating the increased tumour aggressiveness with the smaller collagen mean fibre length.

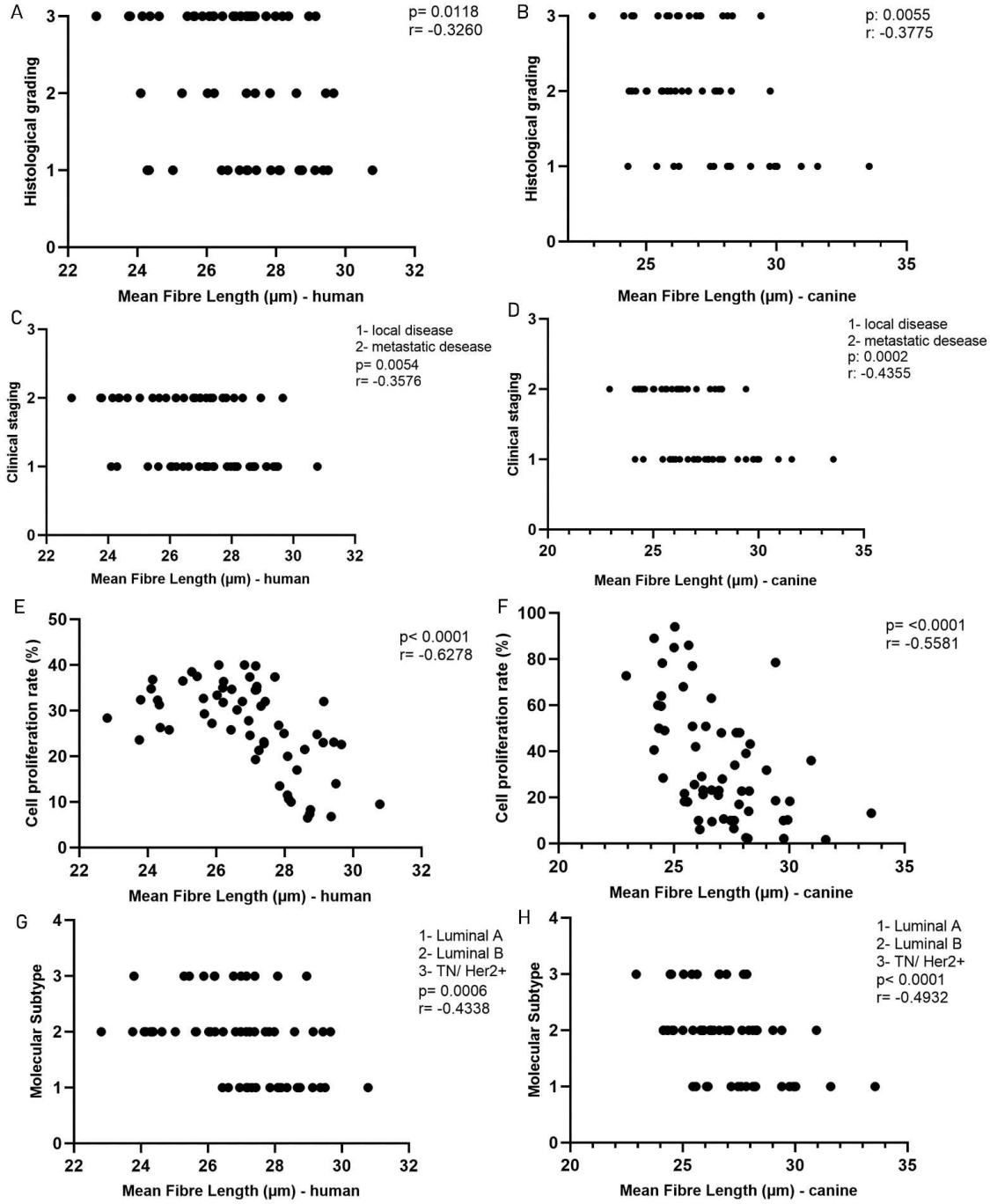

Figure 3. Correlation between clinicopathological parameters and mean fibre length in women and dogs. Spearman's correlation between histological grading and mean fibre length in women (A, n=58) and dogs (B, n=59). Spearman's correlation between clinical standing and mean fibre length in women (C, n=58) and dogs (D, n=59). Linear regression between cell proliferation and mean fibre length in women (E, n=58) and dogs (F, n=59). Spearman's correlation between molecular subtype and mean fibre length in women (G, n=58) and dogs (H, n=59).

To determine the influence of mean fibre length on patient survival, we established a cut-off point disregarding histological subtype, histological grade, clinical staging, cell proliferation rate and molecular subtype. For this, the data were organized in ascending order and the median fibre length value was calculated. Therefore, the value 27 µm was determined as the cut-off point, categorizing patients into two groups based on this cut-off point. Those diagnosed with carcinomas with fibres smaller than 27 µm were grouped in the first category, while those with carcinomas with collagen fibres larger than 27 µm were grouped in the second category. We assigned 0 to patients alive at the end of the study and 1 to patients who died from mammary carcinoma. For those diagnosed with carcinomas with collagen fibres larger than 27 µm (represented by the red line), the average survival was 150 days. On the other hand, patients with carcinomas with fibres larger than 27 µm (shown by the blue line) had a median survival of 849 days. Notably, more aggressive carcinomas with an unfavourable prognosis had shorter collagen fibres compared to less aggressive carcinomas with a favourable prognosis. In Figure 4A, we show survival curves for dogs. We extend this method to define cut-off points for SHG coherence, mean fibre waviness, number of fibres, fibre segment coverage, and cell segment coverage. However, no significant correlations were observed between these metrics and dog-specific survival. These findings support the data from our current study and are in line with our previously published work[18]. It should be noted that the canine dataset examined in this study differs from our previous assessment.

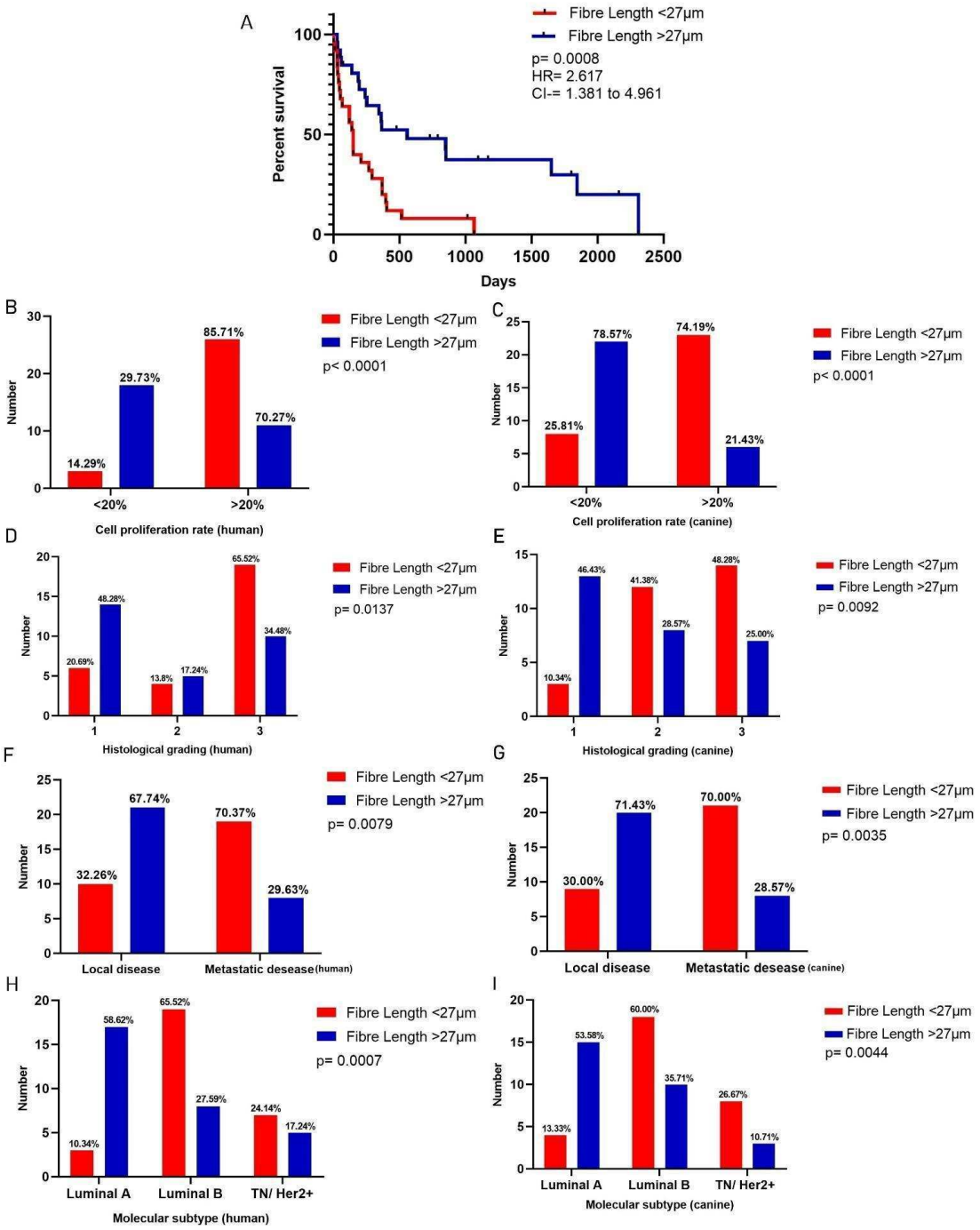

Figure 4. Survival curve for dogs and association between clinicopathological parameters and mean fibre length in women and dogs. Kaplan–Meier curve showing the separation of cases by mean fibre length in dogs; red line for fibre length <27 µm and blue line for fibre length > 27. (A, n= 59). Contingency plots presenting data from chi-square analysis (D, E, H ad I) and Fisher's exact test (B, C, F and G) to evaluate the association between clinicopathological data and the mean fibre length categorized in women and dogs. The clinicopathological data are presented on the x-axis, the absolute frequency (n) on the y-axis

and the proportion in percentage at the end of each bar. Association between cell proliferation rate (B, n=58), histological grade (D, n=58), local or metastatic disease (F, n=58), molecular subtype (H, n=58) and mean fibre length categorized by the 27 µm cut-off point in women. Association between cell proliferation rate (C, n=58), histological grade (E, n=58), presence or absence of metastatic disease (G, n=58) and molecular subtype (I, n=58) and mean fibre length categorized by the cut-off point 27 µm in dogs. Error bar not included because it is the evaluation of categorical data.

In humans, it was not possible to establish a specific survival curve for cancer using the same methodology as used for dogs. This is because approximately 85% of the patients in the study are alive and still under medical supervision. Thus, the median survival was not reached in any of the stratified groups, making it impossible to carry out and evaluate the analysis. However, to demonstrate the clinical importance of these findings for breast oncology, we established an association between the mean fibre length and clinicopathological data[32] that directly influence patient survival. For this analysis, the same cut-off point defined for the analysis of the dog's survival curve (Fig. 4A) was considered. Using the cut-off point of 27 µm, women and dogs were stratified into two groups: those diagnosed with carcinomas with collagen fibres smaller than 27 µm were categorized into the first group, while those diagnosed with carcinomas with collagen fibres larger than 27 µm were grouped into the second group (Fig. 4B-4I). To verify the association or independence between the mean fibre length and the clinicopathological data, we performed an analysis using the Fisher's Exact Test and the chi-square test. The data indicate that a higher proliferative rate, higher histological grade, presence of local and/or distant metastases and the “triple negative” and “Her2 overexpressed” molecular subtypes are associated with carcinomas with collagen fibres smaller than 27 µm in women (Fig. 4B, 4D, 4F and 4H) and dogs (Fig. 4C, 4E, 4G, 4I). Finally, we observed that collagen density presents an inverse correlation with histological grade (Fig. 5A and 5B), cell proliferation rate (Fig. 5C and 5D) and molecular subtype (Fig. 5E) in human breast carcinomas. Cell density has a direct correlation with molecular subtype (Fig. 5F). The same correlations were established for dogs, but no statistically significant correlations were obtained.

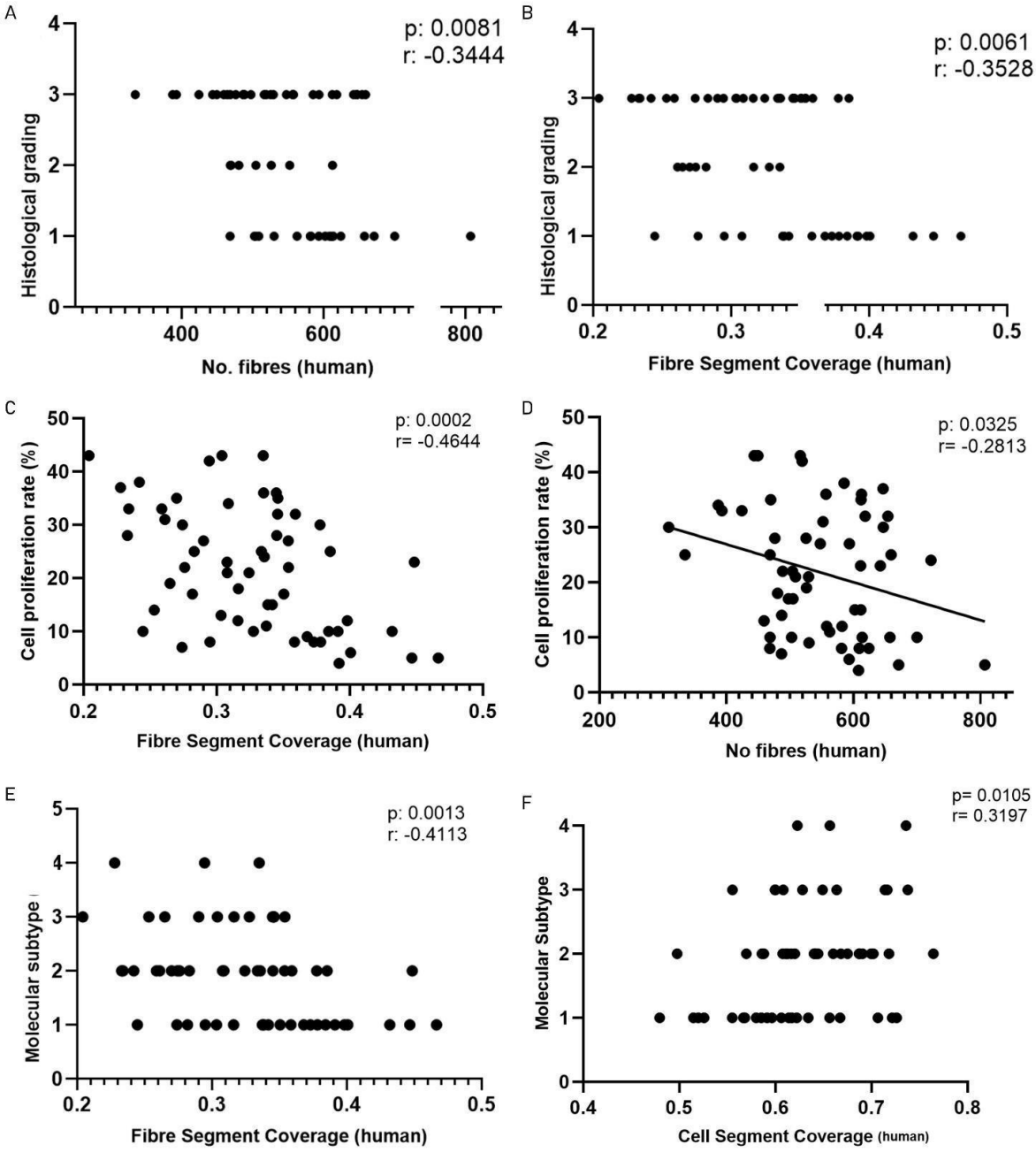

Figure 5. Correlation between clinicopathological parameters and metrics extracted by second harmonic generation and two-photon fluorescence techniques in women. Spearman's correlation between the number of fibres (A, n=58), fibre segment coverage (B, n=58), cell segment coverage (C, n=58) and histological grading. Spearman's correlation between fibre segment coverage (G, n=58) and cell segment coverage (H, n=58) and molecular subtype. Linear regression between the fibre segment coverage (D, n=58), number of fibres (E, n=58) and cell segment coverage (F, n=58) and cell proliferation rate.

Discussion

Numerous studies indicate that collagen plays a key role in the tumour micro-environment, playing a critical role in the regulation of neoplastic growth and tumour cell dissemination, due to its ability to provide physical, biochemical, and biomechanical guidance for tumour and non-tumour cells[18,45-51]. Tumours can actively remodel the surrounding extracellular matrix. Type 1 and type 3 collagen fibres, when aligned, increase the stiffness of the extracellular matrix and this predicts worse outcomes[50,57] and the expression of COL11A1 may have a potential role in the aggressiveness of carcinoma in situ in women through collagen remodelling and regulation of the cellular stimulation mechanism[1]. Recent studies have described that this stiffness of the extracellular matrix is fundamental in the process of cell migration, invasion, and metastasis of tumour cells[18,44-49,51-65]. Here, we demonstrated that in human and canine mammary carcinomas, collagen fibres orient themselves in a preferential direction, becoming more organized.

In human mammary carcinomas, we observed that collagen fibres are more linear compared to NMTh and Fb. We did not observe this behaviour in canine mammary carcinomas. The composition of carcinomas in mixed tumours and carcinosarcomas may explain this difference. As previously stated, the MC arises from epithelial malignant transformation into benign mixed tumours[31,42,43]. It has components of malignant epithelial origin and normal or benign mesenchymal components. CS are characterized by malignant components of epithelial and mesenchymal origin, leading to intense proliferation of the extracellular matrix. MC and CS exhibit a complex histological pattern[31,34,33,36]. Thus, we noticed that canine mammary carcinomas exhibit significant heterogeneity in their composition, unlike mammary carcinomas in women, which exhibit homogeneity in epithelial and mesenchymal components. Despite exhibiting distinct features, we selected these tumours for our study because they commonly affect the female dogs, as we aim to understand the behaviour of these carcinomas in regard to the more common breast carcinomas in women.

The larger organization and alignment of collagen fibres in the tumour and peritumoural areas collected in the evaluated samples makes the stroma more rigid. We believe that this increased alignment and linearity of collagen fibres in carcinomas is associated with extracellular matrix remodelling and increased stromal stiffness. The rigid extracellular stroma, which surrounds neoplastic cells, may offer a durotactic escape route from the potentially hypoxic and necrotic environment for tumour cells. Inhospitable conditions can induce an innate mechanical

sensitivity to direct cancer cells to an environment where conditions are more favourable[17,45]. The study by Toss et al., 2019[1] and Sprague et al., 2021[66] showed that the deposition and reorganization of collagen around breast carcinoma in situ plays a role in tumour progression and recurrence. The larger linearity of collagen fibres was associated with an increased risk of breast cancer recurrence in these women. Several studies show that the stiffness of the extracellular matrix and the high contractility of tumour cells severely disturb tumoural homeostasis. Matrix remodelling and cross-linking stiffens the extracellular matrix as positive feedback to further stiffen, remodel and reorient the matrix. In a transformed epithelium, increased cell tension stimulates cell growth, disturbs cell-cell adhesion, compromises tissue polarity, and promotes stromal invasion by tumour cells[66-70].

We observed that in human and canine mammary carcinomas there is an exacerbated growth of epithelial components contributing to the loss of balance between stromal and parenchymal components. Therefore, the tumours present lower density of collagen fibres and higher cell density. CS does not follow this growth pattern because it has malignant epithelial and mesenchymal components. Thus, a malignant mesenchymal component induces exaggerated deposition of stromal components[31]. We therefore observed higher stromal density and lower cell density compared to other canine mammary carcinomas. In Fb, we observed higher collagen density and lower cell density compared to other histological types and NMT in humans, since the deposition of stromal elements is increased in this tumour[32].

Correlating the parameters, number of fibres, area covered by fibres and area covered by cells with the histological grade, TNM, cell proliferation rate and molecular subtype, we observed that the most aggressive human mammary carcinomas[32] present lower density of collagen fibres and higher cell density (Fig. 3). Maller et al., 2013[71] showed that the abundance of collagen in the extracellular matrix of pregnant rats was associated with reduced tumour growth and invasion compared to the tumour micro-environment of nulliparous rats. Using methods including second harmonic generation imaging, the authors showed that the abundant collagen in the mammary glands of pregnant rats is less linearised and that high-density collagen induces tumour suppressive attributes[65]. Other authors have also shown that the decrease in collagen density and increase in fibre organization is correlated with more aggressive tumour behaviour[9,62].

Another important characteristic of collagen fibres that stood out was the identification that shorter collagen fibres are associated with an unfavourable prognosis (Fig. 2F, 3A-3F and 4B-

4I). In addition, we demonstrated that canine mammary carcinomas with shorter collagen fibres are associated with lower patient survival (Fig. 4A). Unlike women, most dogs diagnosed with mammary carcinoma are treated exclusively with surgery, without the use of chemotherapy. This fact is important to allow the study of progression of spontaneous breast carcinomas, without the interference of chemotherapy drugs that impact the growth and development of neoplasms. Furthermore, studying mammary carcinomas in dogs avoids the bias associated with induced experimental models that are carried out within controlled environments. Thus, a comparative study using dogs as a model provides accurate data on patient survival and the behaviour of mammary carcinomas in a short period of time, since these tumours progress more quickly compared to tumours in women.

Although we were unable to plot survival curves for women, we established correlations between the number of collagen fibres, collagen fibre density, and cell density with clinicopathological data that are known to play a crucial role in patients' survival[32]. Similarly, to what occurs in the canine species, we observed that a lower number and density of fibres, a higher cell density, and shorter collagen fibres are associated with carcinomas with an unfavourable prognosis. These are important findings. It can be hypothesized that this behaviour is related to the stromal changes that occur during tumour progression, as shown in our previous work[18]. TC and ICgI in humans and MTC in dogs are carcinomas that present well-defined tubular structures, differentiated cells, low mitotic rate and low cellular and nuclear pleomorphism. The stromal component is preserved and the rate of epithelial proliferation is low. These characteristics are associated with local growth, low probability of local and/or distant metastases and favourable prognosis[31-34.] In contrast, ICgIII and IMC in humans and CS, IMC and SC in dogs present expansive growth, undifferentiated cells, high mitotic rate and high cellular and nuclear pleomorphism. The stromal component is replaced by epithelial growth because the proliferation rate of these components is high. CS does not present this behaviour because the mesenchymal component is also malignant, making it more aggressive. Thus, these carcinomas are commonly associated with local and/or distant metastases and with an unfavourable prognosis[31,32,35].

We believe that in carcinomas with a favourable prognosis and low proliferative rate, collagen fibres are larger because they limit neoplastic growth. However, in carcinomas with an unfavourable prognosis, with loss of cellular differentiation and a high proliferative rate, the collagen fibres are unable to limit this growth, and thus they rupture, allowing the tumour to

expand. In this way, the fibres become fragmented and shorter compared to the fibres of carcinomas with less aggressive behaviour. Furthermore, we believe that this "shortening" of collagen fibres is associated with remodelling of the extracellular matrix to guide the metastatic invasion of tumour cells (Fig. 6). Studies show that while collagen can potentially form a protective barrier and prevent cancer cells from escaping their original location, collagen fibres also serve as a "highway" that facilitates the migration of cancer cells to remote locations, impacting survival of patients[7,9,16,62-75].

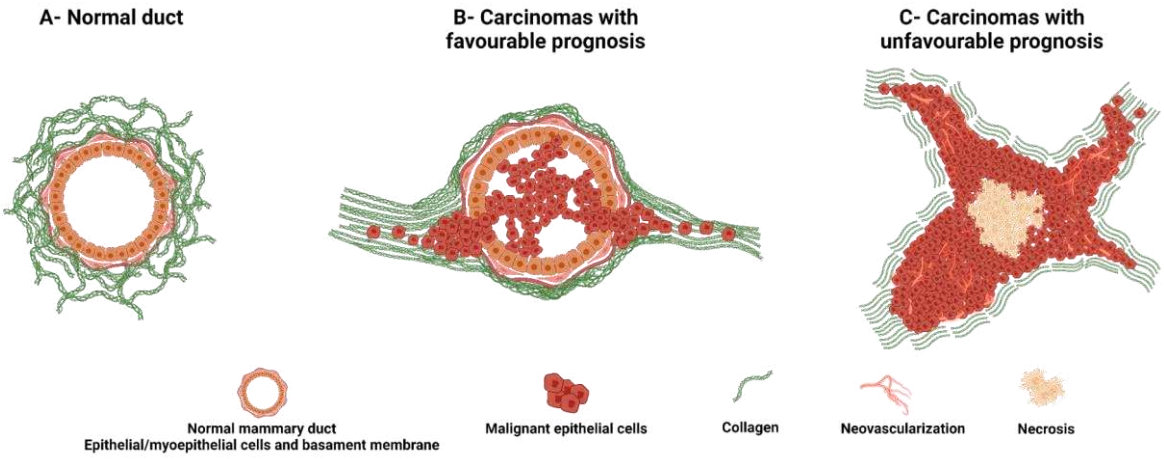

Figure 6. Carcinomas with an unfavourable prognosis present shorter fibre. Mammary carcinomas present more organized fibres (B and C) compared to normal mammary tissue (A). Carcinomas with a favourable prognosis and low proliferative rate present longer collagen fibres, capable of limiting neoplastic growth (B). In carcinomas with an unfavourable prognosis and high proliferative rates, collagen fibres are shorter and unable to limit this growth, allowing tumour expansion (C). This "shortening" of collagen fibres may be associated with remodelling of the tumour stroma that creates rigid pathways to help cancer cells escape necrotic and hypoxic environments. Thus, the fibres become capable of guiding tumour cells towards locations with greater vascularization (C). Created by BioRender.

Conclusions

In conclusion, our study revealed similarities in collagen changes between human and canine mammary neoplasms, showing the association of these changes with clinicopathological factors in both species. Employing second harmonic generation, two-photon excited fluorescence techniques, and automated image analysis, we identified similar changes in the tumour stroma of human and canine mammary neoplasms. We observed that human and canine mammary

carcinomas present more organized fibres. Carcinomas with higher histological grade, higher cell proliferation rate, with local and/or distant metastasis and molecular classifications of triple negative type and overexpressed Her2 present lower collagen density and higher cell density. We have also established a relation between the collagen fibre length and clinicopathological characteristics in women and dogs with mammary carcinomas, showing significant associations between shorter fibres and unfavourable clinical characteristics. Furthermore, we established a cut-off for the mean fibre length and specific survival time in dogs. The correlation between collagen modifications and clinicopathological factors may also have implications for diagnosis, prognosis, and the development of targeted therapies. Thus, the use of nonlinear microscopy provides new tools for assessing collagen in breast cancer.

DECLARATIONS

Ethics approval and consent to participate

The canine sample study was performed in view of the fundamental ethical principles under law no. 11.794, of October 8, 2008 and of decree no. 6.899 of July 2009, and with the rules issued by the National Council for the Control of Animal Experimentation (CONCEA) and the international Animal Research: Reporting of In Vivo Experiments (ARRIVE). All experimental protocols were approved by the "Ethics Committee on the Use of Animals" at UFMG, under number 83/2021.

The research on human tissue sample was previously approved by the "Research Ethics Committee" at UFMG (COEP-UFMG) under No. 43947521.3.0000.5149/2021. All experiments were carried out in accordance with the Declaration of Helsinki. As a retrospective study, performed on archive histopathological slides, the need for informed consent from all subjects and/or their legal guardian(s) was waived by the COEP-UFMG.

Consent for publication

Not applicable.

Availability of data and materials

The image datasets used during the current study are available from the corresponding author at https://mega.nz/folder/4xBylTIS#CWBOMzE-6TFRnZ3u6ys5Ig.

Competing interests

The authors declare that they have no conflict of interest.

Funding

This work was supported by Fundação de Amparo à Pesquisa do Estado de Minas Gerais (FAPEMIG) [Rede Mineira de Pesquisa Translacional em Imunobiológicos e Biofármacos no Câncer (REMITRIBIC, RED-00031-21)]; Conselho Nacional de Desenvolvimento Científico e Tecnológico (CNPq) and Coordenação de Aperfeiçoamento de Pesssoal de Nível Superior (Capes), Brazil.

Authors' contributions

APVG selected and prepared the samples, analysed the patients' clinical and pathological data, selected the fields for data acquisition in SHG and TPEF imaging, performed the immunohistochemistry technique and marker analysis, prepared the figures and tables, and drafted the manuscript. BRMR participated in acquisition and analysis of SHG and TPEF image data and image analysis of human samples. LAR participated in the acquisition and analysis of SHG and TPEF image data and image analysis of canine samples. CBN participated in the selection of human samples. GDC and AMdP guided APVG throughout all project phases, reviewed and edited the manuscript. GDC participated in the selection of canine samples and reviewed the clinical-pathological and immunohistochemical data. AMdP supervised all stages of SHG and TPEF data acquisition and image analysis. All authors read and approved the final paper.

REFERENCES

1. Toss MS, Miligy IM, Gorringe K L et al. Geometric characteristics of collagen have independent prognostic significance in breast ductal carcinoma in situ: an image analysis study. Mod Pathol. 2019; 32:1473-85. doi: 10.1038/s41379-019-0296-7.

2. Piersma B, Hayward MK, Weaver VM. Fibrosis and cancer: A strained relationship. Biochim Biophys Acta Rev Cancer. 2020 1873 (2):188356. doi: 10.1016/j.bbcan.2020.188356.

3. Harbeck N, Penault-Llorca F, Cortes J. et al. Breast Cancer. Nat. Rev. Dis. Primers. 2019; 5:66. doi: 10.1038/s41572-019-0111-2.

4. Pollard JW. Macrophages define the invasive microenvironment in breast cancer. J Leukoc Biol. 2008. 84(3):623-30. doi: 10.1189/jlb.1107762.

5. Markkanen, E. Know thy model: charting molecular homology in stromal reprogramming between canine and human mammary tumors. Front. Cell Develop. Biol. 2019; 7:348. https://doi.org/10.3389/fcell.2019.00348.

6. Ajeti, V, Nadiarnykh O, Ponik SM, Keely PJ, Eliceiri KW, Campagnola PJ. Structural changes in mixed Col I/Col V collagen gels probed by SHG microscopy: implications for probing stromal alterations in human breast cancer. Biomed. Opt. Express. 2011; 2:2307-16. doi: 10.1364/BOE.2.002307.

7. Conklin MW, Eickhoff JC, Riching KM et al. Aligned collagen is a prognostic signature for survival in human breast carcinoma. 2011. Am. J. Pathol. 178, 1221-32. doi: 10.1016/j.ajpath.2010.11.076.

8. Garcia AM, Magalhaes FL, Soares JS et al. Second harmonic generation imaging of the collagen architecture in prostate cancer tissue. 2017. Biomed. Phys. Eng. Express 4, 025026. doi: 10.1088/2057-1976/aaa379.

9. Almici E, Arshakyan M, Carrasco JL et al. Quantitative Image Analysis of Fibrillar Collagens Reveals Novel Diagnostic and Prognostic Biomarkers and Histotype-Dependent Aberrant Mechanobiology in Lung Cancer. 2023; 36:100155. doi: 10.1016/j.modpat.2023.100155.

10. Hompland T, Erikson A, Lindgren M, Lindmo T, de Lange Davies C. Second-harmonic generation in collagen as a potential cancer diagnostic parameter. J. Biomed. Opt. 2008; 13(5):054050. doi: 10.1117/1.2983664.

11. Burke K, Tang P, Brown E B. Second harmonic generation reveals matrix alterations during breast tumor progression. J. Biomed. Opt. 2012; 18:031106. doi: 10.1117/1.JBO.18.3.031106.

12. Burke K, Smid M, Dawes RP et al. Using second harmonic generation to predict patient outcome in solid tumors. BMC Cancer. 2015; 15:929. doi: 10.1186/s12885-015-1911-8.

13. Golaraei A, Kontenis L, Cisek R et al. Changes of collagen ultrastructure in breast cancer tissue determined by second-harmonic generation double Stokes-Mueller polarimetric microscopy. Biomed. Opt. Express. 2016; 7:4054-68. doi: 10.1364/BOE.7.004054.

14. Barcus CE, O'Leary K, Brockman JL et al. Elevated collagen-I augments tumor progressive signals, intravasation and metastasis of prolactin-induced estrogen receptor alpha positive mammary tumour cells. Breast Cancer Res. 2017; 19:1-13. doi: 10.1186/s13058-017-0801-1.

15. Case A, Brisson BK, Durham AC. et al. Identification of prognostic collagen signatures and potential therapeutic stromal targets in canine mammary gland carcinoma. PLoS ONE. 2017; 12:1-19. doi: 10.1186/s12885-015-1911-8.

16. Conklin MW, Gangnon RE, Sprague BL et al. Collagen Alignment as a Predictor of Recurrence after Ductal Carcinoma *in situ.* Cancer Epidemiol Biomarkers Prev. 2018; 27(2):138-145. doi: 10.1158/1055-9965.EPI-17-0720.

17. Reis LA, Garcia APV, Gomes EFA et al. Canine mammary cancer diagnosis from quantitative properties of nonlinear optical images. Biomed. Opt. Express. 2020; 11, 6413-27. doi: 10.1364/BOE.400871.

18. Garcia APV, Reis LA, Nunes FC et al. Canine mammary cancer tumour behaviour and patient survival time are associated with collagen fibre characteristics. Sci Rep. 2021; 11:5668. doi: 10.1038/s41598-021-85104-w.

19. Natal RA, Vassalo J, Paiva GR et al. Collagen analysis by second-harmonic generation microscopy predicts outcome of luminal breast cancer. Tumor Biol. 2018; 40. doi: 1010428318770953.

20. Natal R A, Paiva GR, Pelegati VB et al. Exploring collagen parameters in pure special types of invasive breast cancer. Sci. Rep. 2019; 9:7715. doi: 10.1038/s41598-019-44156-9.

21. Sorenmo KU, Durham AC, Kristiansen V et al. The estrogen effect: clinical and histopathological evidence of dichotomous influences in dogs with spontaneous mammary carcinomas. PLoS ONE. 2019; 14:e0224504. doi: 10.1371/journal.pone.0224504.

22. Queiroga FL, Raposo T, Carvalho MI, Prada J, Pires I. Canine mammary tumours as a model to study human breast cancer: most recent findings. In Vivo. 2011; 25(3):455-65.

23. Uva P, Aurisicchio L, Watters J et al. Comparative expression pathway analysis of human and canine mammary tumors. BMC Genom. 2009; 10:135. doi: 10.1186/1471-2164-10-135.

24. Rivera P & Von Euler H. Molecular biological aspects on canine and human mammary tumors. Vet. Pathol. 2011; 48:132-146. doi: 10.1177/0300985810387939.

25. Markkanen E. Know thy model: charting molecular homology in stromal reprogramming between canine and human mammary tumors. Front. Cell Develop. Biol. 2019; 7:348. doi: 10.3389/fcell.2019.00348.

26. Abadie J, Nguyen F, Loussouarn et al. Canine invasive mammary carcinomas as models of human breast cancer. Part 2: immunophenotypes and prognostic significance. Breast Cancer Res. Treat. 2018; 167:459-468. doi: 10.1007/s10549-017-4542-8.

27. Gray M, Meehan J, Martínez-Pérez C et al. Naturally-occurring canine mammary tumors as a translational model for human breast cancer. Front. Oncol. 2020; 10:617. doi: 10.3389/fonc.2020.00617.

28. Nguyen BN, Moriarty RA, Kamalitdinov T, Etheridge JM, Fisher JP. Collagen hydrogel scaffold promotes mesenchymal stem cell and endothelial cell coculture for bone tissue engineering. J Biomed Mater Res A. 2017; 105(4):1123-31. doi: 10.1002/jbm.a.36008.

29. Cassali, G. D. Comparative mammary oncology: canine model. BMC Proceedings. 2013; 7:K6. doi: 10.1186/1753-6561-7-S2-K6.

30. Owen LN & World Health Organization. Veterinary Public Health Unit and WHO Collaborating Center for Comparative Oncology. TNM classification of tumours in domestic animals, edited by L.N. Owen (1980). https://apps.who.int/iris/handle/10665 /68618.

31. Goldschmidt M, Peña L, Rasotto R, Zappulli V. Classification and grading of canine mammary tumors. Vet Pathol. 2011;48(1):117-131. doi:10.1177/0300985810393258.

32. Peña L, De Andrés PJ, Clemente M, Cuesta P, Pérez-Alenza MD. Prognostic value of histological grading in noninflammatory canine mammary carcinomas in a prospective study with two-year follow-up: relationship with clinical and histological characteristics. Vet Pathol. 2013; 50(1). 94-105. doi: 10.1177/0300985812447830.

33. Nunes FC, Bertagnolli AC, Lavalle GE, Silveira TL, Balabram D, Cassali GD. The prognostic significance of immunophenotypes in canine malignant mammary tumors. Arq. Bras. Med. Vet. Zootec. 2022; 74:2. doi: 10.1590/1678-4162-12273.

34. Cassali GD, Bertagnolli AC, Ferreira E, Damasceno KA, Gamba CO, Campos CB. Canine mammary mixed tumours: a review. Vet. Med. Int. 2012; 1-7: 274608. doi: 10.1155/2012/274608.

35. Gamba C, Dias EJ, Ribeiro LGR et al. Histopathological and immunohistochemical assessment of invasive micropapillary mammary carcinoma in dogs: a retrospective study. Vet. J. 2013; 196:241-246. doi: 10.1016/j.tvjl.2012.08.022.

36. Damasceno KA, Ferreira E, Estrela-Lima A et al. Relationship between the expression of versican and EGFR, HER-2, HER-3 and CD44 in matrix-producing tumours in the canine mammary gland. Histol. Histopathol. Cell. Mol. Biol. 2016. 31:675-88 (2016). doi: 10.14670/HH-11-705.

37. World Health Organization. Classification of Tumors. Breast Cancer. 5th ed.

38. Nakagaki KYR, Nunes MM, Garcia APV, Nunes FC, Schmitt F, Cassali GD. Solid Carcinoma of the Canine Mammary Gland: A Histological Type or Tumour Cell Arrangement? J. Comp. Pat. 2022; 190:1-12. doi: 10.1016/j.jcpa.2021.10.011.

39. Gomes EF et al. Prostate cancer tissue classification by multiphoton imaging, automated image analysis and machine learning. J Biophotonics. 2023; 16(6) e202200382. doi: 10.1002/jbio.202200382.

40. Longford FG. Pyfibre: Python fibrous image analysis toolkit. 2023. https://github.com/franklongford/PyFibre, Version 2.1.1.

41. Garcia APV, Taborda DYO, Reis LA, de Paula AM, Cassali GD. Collagen modifications predictive of lymph node metastasis in dogs with carcinoma in mixed tumours. Front Vet Sci. 2024 Mar 6;11:1362693. doi: 10.3389/fvets.2024.1362693.

42. Moulton JE, Taylor DON, Dorn CR, Andersen AC. Canine Mammary Tumors. Vet. Pat.1970; 7:4. doi: 10.1177/030098587000700401.

43. Misdorp W. Histological classification of the mammary tumors of the dog and the cat. World Health Organ. Int. Histol. Classif. Tumors Domestic Anim. 2ª ed. 1999.

44. Ouellette JN, Drifka CR, Pointer KB et al. Navigating the Collagen Jungle: The Biomedical Potential of Fiber Organization in Cancer. Bioengineering. 2021; 8:17. doi: 10.3390/bioengineering8020017.

45. DuChez BJ, Doyle AD, Dimitriadis EK, Yamada KM. Durotaxis by human cancer cells. Biophys. J. 2019; 116:670-683. doi: 10.1016/j.bpj.2019.01.009.

46. Toss MS, Miligy IM, Gorringe KL et al. Collagen (XI) alpha-1 chain is an independent prognostic factor in breast ductal carcinoma in situ. Mod Pat. 2019; 32:1460–1472. doi: 10.1038/s41379-019-0286-9.

47. Mierke CT. The Pertinent Role of Cell and Matrix Mechanics in Cell Adhesion and Migration. Front Cell Dev Biol. 2021; 9:720494. doi: 10.3389/fcell.2021.720494.

48. Moriyama K, Kidoaki S. Cellular durotaxis revisited: initial-position-dependent determination of the threshold stiffness gradient to induce durotaxis. Langmuir. 2018. 35:7478-7486. doi: 10.1021/acs.langmuir.8b02529.

49. Zhang K, Corsa CA, Ponik SM et al. The collagen receptor discoidin domain receptor 2 stabilizes SNAIL1 to facilitate breast cancer metastasis. Nat. Cell Biol. 2013; 15:677-687.

50. Souza FP, Pérez-Guerrero JA, Gomes MJP, Cavalcante FL, Filho MSMS, Castro-Silva II. Development and characterization of poultry collagen-based hybrid hydrogels for bone regeneration. Acta Cir. Bras. 2022; 37:3. doi:10.1590/acb370302.

51. Weigelin B, Friedl P. A three-dimensional organotypic assay to measure target cell killing by cytotoxic T lymphocytes. *Biochem Pharmacol.* 2010; **80**(12):2087-91. doi: 10.1016/j.bcp.2010.09.004.

52. Bredfeldt JS, Liu Y, Pehlke CA et al. Computational segmentation of collagen fibres from second-harmonic generation images of breast cancer. J. Biomed. Opt. 2014. 19:016007. doi: 10.1117/1.JBO.19.1.016007.

53. Tuer AE, Krouglov S, Prent N et al. Nonlinear optical properties of type I collagen fibres studied by polarization dependent second harmonic generation microscopy. J. Phys. Chem. B. 2011; 115:12759-12769. doi: 10.1021/jp206308k.

54. Burke K, Tang P, Brown E. Second harmonic generation reveals matrix alterations during breast tumor progression. J. Biomed. Opt. 2012; 18:031106. doi: 10.1117/1.JBO.18.3.031106.

55. Brabrand A, Kariuki II, Engstrøm MJ et al. Alterations in collagen fibre patterns in breast cancer. A premise for tumour invasiveness? APMIS. 2015; 123:1-8. doi: 10.1111/apm.12298.

56. Hall MS, Alisafaei F, Ban E, Feng X, Hui CY, Shenoy V, Wu M. Fibrous nonlinear elasticity enables positive mechanical feedback between cells and ECMs. Proc. Natl. Acad. Sci. 2016. 113:14043-14048. doi: 10.1073/pnas.1613058113.

57. Barcus CE, Longmore GD. Collagen Linearization within Tumors. Cancer Res. 2021; 81(22):5611-5612. doi: 10.1158/0008-5472.CAN-21-2939.

58. Guo S, Deng C X. Effect of stromal cells in tumor microenvironment on metastasis initiation. Int. J. Biol. Sci. 2018; 14:2083. doi: 10.7150/ijbs.25720.

59. Wang K, Wu F, Seo BR, Fischbach C, Chen W, Hsu L, Gourdon D. Breast cancer cells alter the dynamics of stromal fibronectin–collagen interactions. Matrix Biol. 2017. 60-61:86-95. doi: 10.1016/j.matbio.2016.08.001.

60. Rezakhaniha R, Agianniotis A, Schrauwen JTC et al. Experimental investigation of collagen waviness and orientation in the arterial adventitia using confocal laser scanning microscopy. Biomech. Model. Mechanobiol. 2012; 11:461-473. doi: 10.1007/s10237-011-0325-z.

61. Ávila FJ, Bueno JM. Analysis and quantification of collagen organization with the structure tensor in second harmonic microscopy images of ocular tissues. Appl. Opt. 2015. 54:9848-9854. doi: 10.1364/AO.54.009848.

62. Brett EA, Sauter MA, Machens HG, Duscher D. Tumor-associated collagen signatures: pushing tumor boundaries. Can & Metab. 2020; 8:14. doi: 10.1186/s40170-020-00221-w.

63. Xu S, Xu H, Wang W et al. The role of collagen in cancer: from bench to bedside. Journal of Translational Medicine. 2019; 17:309. doi: 10.1186/s12967-019-2058-1.

64. Gole L, Yeong J, Lim JCT et al. Quantitative stain-free imaging and digital profiling of collagen structure reveal diverse survival of triple negative breast cancer patients. Breast Cancer Res. 2020; 22:42. doi: 10.1186/s13058-020-01282-x.

65. Cox TR. The matrix in cancer Thomas R. Cox. Nat. Rev. Can. 2021; 21:217-238. doi: 10.1038/s41568-020-00329-7.

66. Sprague BL, Vacek PM, Mulrow SE et al. Collagen organization in relation to ductal carcinoma in situ pathology and outcomes. Cancer Epidemiol Biomarkers Prev. 2021; 30(1): 80–88. doi: 10.1158/1055-9965.EPI-20-0889.

67. Wu YH, Chou CY. Collagen XI Alpha 1 Chain, a Novel Therapeutic Target for Cancer Treatment. Front Oncol. 2022; 12: 925165. doi: 10.3389/fonc.2022.925165

68. Song K, Yu Z, Zu X, Li G, Hu Z Xue Y. Collagen Remodeling along Cancer Progression Providing a Novel Opportunity for Cancer Diagnosis and Treatment. Int J Mol Sci. 2022. 23(18):10509. doi: 10.3390/ijms231810509.

69. Huang J, Zhang L, Wan D et al. Extracellular matrix and its therapeutic potential for cancer treatment. Sig. Transd. Targ. Ther. 2021; 6:153. doi: 10.1038/s41392-021-00544-0.

70. W J, Ogunniyan AA, Metcalf KJ, Werb Z. Concepts of extracellular matrix remodelling in tumour progression and metastasis. Nat. Comm. 2020; 11:5120. doi: 10.1038/s41467-020-18794-x.

71. Maller O, Hansen KC, Lyons TR, Acerbi I, Weaver VM, Prekeris R, et al. Collagen architecture in pregnancy-induced protection from breast cancer. J Cell Sci. 2013; 126:4108-10. doi: 10.1242/jcs.121590

72. Provenzano PP, Eliceiri KW, Campbell JM et al. Collagen reorganization at the tumor-stromal interface facilitates local invasion. BMC Med. 2006; 4(1):38. doi: 10.1186/1741-7015-4-38.PMID: 17190588.

73. Provenzano PP, Inman DR, Eliceiri KW et al. Collagen density promotes mammary tumor initiation and progression. BMC Med. 2008; 28:6:11. doi: 10.1186/1741-7015-6-11.

74. Giorello MB, Borzone FR, Labovsky V, Piccioni FV, Chasseing NA. Cancer-associated fibroblasts in the breast tumor microenvironment. J. Mammary Gl. Biol. Neoplasia. 2021; 26(2):135-155. doi: 10.1007/s10911-020-09475-y.

75. Bourgot I, Primac I, Lois T, Noel A, Maquoi E. Reciprocal Interplay Between Fibrillar Collagens and Collagen-Binding Integrins: Implications in Cancer Progression and Metastasis. Front. Oncol. 2020; 10. doi: 10.3389/fonc.2020.01488.

SUPPLEMENTARY MATERIAL

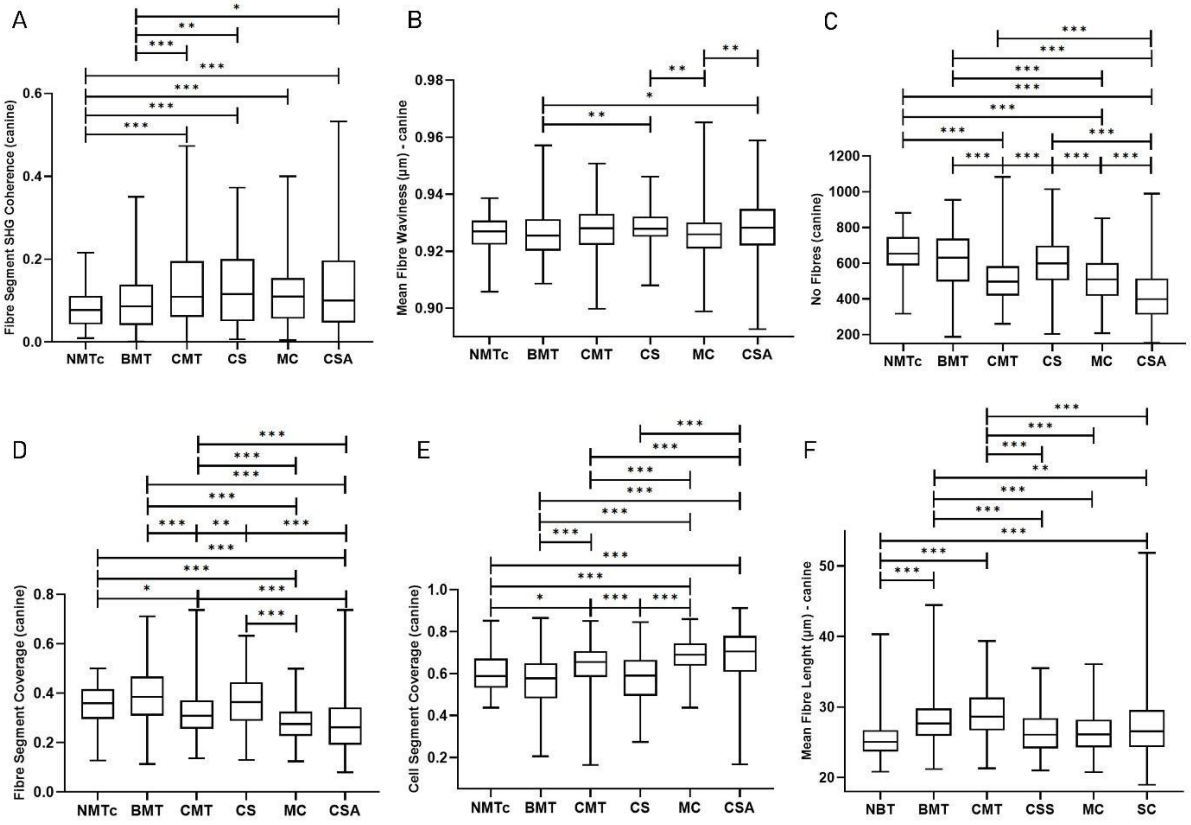

Parameters of the canine mammary gland analysed by second harmonic generation and two-photon excited fluorescence techniques. Kruskal Wallis test and the Dunn test. Boxplot graphics showing the calculated parameters for the fibre segment SHG coherence, mean fibre waviness, mean fibre length, number of fibres, fibre segment coverage and cell segment coverage for canine normal mammary tissue (NMTc, n=12), benign mixed tumour (BMT, n=15), mixed carcinoma (MC, n=14), carcinosarcoma (CS, n=06), invasive carcinoma micropapillary (ICM, n=16) and solid carcinoma (CS, n=23) in canine samples (n=86). The centre lines show the medians, the box limits indicate the 25th and 75th percentiles, the whiskers extend 1.5 times the interquartile range from the 25th and 75th percentiles and the outliers are represented by dots. The p values less than 0.001 denoted by (***), p less than 0.01 are denoted by (**) and p less than (0.05) are denoted by (*).

6.2 Artigo 02

Title: Comparative study of the prognostic significance of macrophage-collagen interactions in breast cancer

Ana Paula Vargas Garcia[1], Marisa Salvi[1], Luana Aparecida Reis[2], Bárbara R. M. Ribeiro[2], Cristiana Buzelin Nunes[3], Ana Maria de Paula[2], Geovanni Dantas Cassali[1*]

[1]Department of General Pathology, Institute of Biological Sciences, Federal University of Minas Gerais. Av. Pres. Antônio Carlos, 6627, Pampulha, Belo Horizonte, MG, Brazil. 31270-901.

[2]Department of Physics, Institute of Exact Sciences, Federal University of Minas Gerais. Av. Pres. Antônio Carlos, 6627, Pampulha, Belo Horizonte, MG, Brazil. 31270-901.

[3]Department of Anatomic Pathology, Faculty of Medicine, Federal University of Minas Gerais. Av. Prof. Alfredo Balena, 190, Santa Efigênia, Belo Horizonte, MG, Brazil. 30130-100.

Ana Paula Vargas Garcia - vargas.biomedicina@gmail.com (ORCID: 0000-0002-0898-6295)

Marisa Salvi - salvimarisa21@gmail.com (ORCID: 0000-0003-2434-3393)

Luana Aparecida Reis - lareis@unicamp.br (ORCID: 0000-0002-8404-9463)

Bárbara R. M. Ribeiro - barbara-melo@ufmg.br

Cristiana Buzelin Nunes - cbn@medicina.ufmg.br (ORCID: 0000-0002-5266-6870)

Ana Maria de Paula - ana@fisica.ufmg.br (ORCID: 0000-0002-8551-5948)

[*]Geovanni Dantas Cassali - gcassali@ufmg.br (ORCID: 0000-0002-5650-6743)

[*]Corresponding author

Present address Luana Aparecida Reis: Institute of Physics “Gleb Wataghin”, University of Campinas, Campinas, SP, Brazil.

ABSTRACT

This study evaluated 70 human and 74 canine mammary tumours to investigate the relationship between collagen fibre organization and tumour-associated macrophage (TAM) infiltration. Using histological and imaging analyses, we found that aggressive tumours exhibited shorter collagen fibres and higher TAM infiltration compared to less aggressive subtypes. Canine tumours, including carcinosarcomas and invasive micropapillary carcinomas, mirrored the patterns observed in human breast cancers, demonstrating the translational value of the canine model. TAM density was quantified through CD68 immunostaining, and collagen fibre organization was assessed via second harmonic generation microscopy. The study highlights the phenotypic diversity of TAMs, with the identification of macrophage populations expressing both M1 and M2 markers. A strong correlation between TAM infiltration and clinicopathological parameters, such as histological grade, cell proliferation rate, and molecular subtype, was observed. While TAM infiltration was associated with shorter collagen fibres and tumour aggressiveness, no direct evidence of extracellular matrix remodelling by TAMs was demonstrated, requiring further investigation to establish causal relationships. Our findings underscore the prognostic importance of TAMs and collagen fibre modifications in breast cancer progression. The canine model provided unique insights into the tumour microenvironment, supporting its use in comparative oncology. These results suggest that targeting TAM infiltration could be a promising therapeutic strategy, although additional studies are needed to validate this approach and explore the mechanistic role of TAMs in collagen remodelling.

Keywords: collagen fibres, tumour-associated macrophages, breast cancer, tumour microenvironment, comparative oncology.

Introduction

Breast cancer, a major global health challenge, remains a leading cause of morbidity and mortality in women worldwide[1]. The quest for more accurate diagnostic methods and targeted therapies has spurred research across multiple fronts, including investigating the role of the tumour microenvironment (TME) in disease progression[2-24]. The TME, a complex ecosystem comprising tumour cells, stromal cells, extracellular matrix (ECM) components, and a myriad of signalling molecules, plays a pivotal role in regulating tumour growth, invasion, and metastasis[5,22-24]. Within this intricate microenvironment, collagen fibres, the primary structural component of the ECM, emerge as key players in orchestrating tumour progression[2-4,6-21]. Beyond their structural role, collagen fibres influence TME stiffness, cell migration, angiogenesis, and the immune response. Recent studies have demonstrated that alterations in the organization, density, and alignment of collagen fibres are associated with a poorer prognosis in various cancer types, including breast cancer[8,10-13,15-21].

In addition to the ECM, the TME is also populated by a variety of immune cells, including tumour-associated macrophages (TAMs)[5,22-24]. These highly plastic and adaptable cells can exert both pro-tumoural and anti-tumoural functions, depending on the signals present in the microenvironment[5,25-32]. The infiltration of TAMs, particularly those with a pro-tumoural M2 phenotype, has been linked to a worse prognosis, therapy resistance, and decreased survival in breast cancer patients[29,33-35]. Recent evidence suggests an intricate interplay between collagen fibres and TAMs within the breast cancer TME. Collagen fibre organization can influence the recruitment, polarization, and function of TAMs, while TAMs can remodel the ECM, including collagen fibres, through the secretion of proteases and other factors[36-44]. This bidirectional interaction underscores the importance of investigating the relationship between collagen alterations and macrophage density in the context of breast cancer.

In this study, we investigated the relationship between modifications in collagen fibre organization and macrophage density in carcinomas with distinct prognoses in both human and canine species. We also conducted a comparative analysis of macrophage infiltration in human and canine mammary neoplasms, correlating this infiltration with clinicopathological data and tumour collagen characteristics.

Materials and Methods

Ethical aspects

This retrospective study adhered to the fundamental ethical principles outlined in Brazilian law no. 11.794 (October 8, 2008) and decree no. 6.899 (July 2009), as well as the guidelines set forth by the National Council for the Control of Animal Experimentation (CONCEA) and the international Animal Research: Reporting of In Vivo Experiments (ARRIVE) guidelines. All experimental protocols involving canine tissues were approved by the Ethics Committee on the Use of Animals at UFMG (protocol number 83/2021).

The research on human tissue samples was conducted in accordance with the Declaration of Helsinki and received prior approval from the Research Ethics Committee at UFMG (COEP-UFMG) under protocol number 43947521.3.0000.5149/2021. As this study utilized archival histopathological slides, the requirement for informed consent from individual subjects was waived by the COEP-UFMG.

Case selection

This retrospective study encompassed the analysis of 59 human breast tumour samples and 65 canine mammary tumour samples. The canine samples were obtained from the archives of the Comparative Pathology Laboratory at the Federal University of Minas Gerais (UFMG), Brazil, while the human samples were retrieved from the biopsy sector archives of the Faculty of Medicine at UFMG. Both the canine and human tumour samples originated from naturally occurring neoplasms in patients receiving treatment at the UFMG Veterinary Hospital and the UFMG Hospital das Clínicas, respectively. Healthy canine mammary tissue samples were collected from mammary tissues without apparent abnormalities located in the same mammary chain of dogs diagnosed with benign tumours or carcinomas in mixed tumours, which are associated with a favourable prognosis. Healthy human breast tissue samples were obtained from breast reduction surgeries conducted at the UFMG Hospital das Clínicas. Samples were selected based on the availability of comprehensive information regarding tumour size, presence or absence of regional or distant metastasis, and histological grade. Samples were selected based on the availability of comprehensive information regarding tumour size, presence or absence of regional or distant metastasis, and histological grade.

Performing immunohistochemistry

For immunohistochemical analysis, tissue sections were prepared at a thickness of 4 μm. The staining procedure was conducted using a commercially available anti-mouse/anti-rabbit detection kit (Novolink Polymer Detection System, Leica Biosystems, Newcastle Upon Tyne, United Kingdom, REF RE7158, LOT 6092583) according to the manufacturer's guidelines. Antigen retrieval for ER, PR, Ki67, and HER2 was achieved through steam heating (Pascal®) in a citrate buffer (Invitrogen by Thermo Fisher Scientific, 10X low pH, REF 00-4955-58, LOT 2410220, Life Technologies' Corp., 5781 Van Allen Way, Carlsbad, CA92008). The sections were then incubated with the respective primary antibodies for 1 hour at 4 °C in a humidified chamber. The primary antibodies employed in this study included ER (Dako Cat# ER-14-0481, RRID:AB_1545347, goat anti-human EP1 receptor, PTGER1 antibody, unconjugated, LOT 11303512, REF IR084, ready-to-use), PR (LSBio LifeSpan Cat# LS-C26712, RRID:AB_2283822, progesterone receptor (PGR) mouse monoclonal (hPRa2+hPRa3) antibody, anti-human/mouse/rat, unconjugated, LOT XI3703736, REF MA512642, 0.4mg/mL, 1:50), HER2 (Dako Cat# AP7629e, RRID: AB_2262284, rabbit anti-human HER2, polyclonal antibody, unconjugated, REF A0485, LOT 00060381, 0.50g/mL, 1:200), Ki67 (Thermo Fisher Scientific Cat# MA5-31796, RRID:AB_2787419, mouse anti-human MIB1 receptor, 2A7B1 antibody, unconjugated, LOT 20067572, REF M7240, 46 mg/mL, 1:50) and CD68 (Dako; clone KP1, FLEX RTU; monoclonal mouse anti-human; unconjugated; ready-to-use antibody).

The visualization of immunoreactivity was accomplished using 3,3'-diaminobenzidine chromogen (Novolink Polymer Detection System, Leica Biosystems, Newcastle Upon Tyne, United Kingdom, REF RE7158, LOT 6092583) and counterstaining with Mayer's haematoxylin. Positive controls for the reactions utilized fragments of canine and human mammary tissues known to express HER-2, ER, PR, Ki67, and CD68. Negative controls were prepared by omitting the primary antibody and proceeding with the addition of chromogen. The evaluation of the slides, quantification of immunoreactivity, and classification of immunophenotypes adhered to the World Health Organization guidelines for human samples (WHO, 2019)[52] and the criteria established by Nunes et al. (2022)[46] for canine samples. The antibodies used in this study have been standardized in our laboratory routine, and their specificity has been validated through our research and corroborated by findings in published studies[45-51,53-55].

The cell proliferation rate was determined based on Ki67 counts. The molecular subtypes of both human mammary carcinomas were categorized as follows: 1 for luminal A (positive hormone receptors, HER2-negative, and proliferative rate <20%), 2 for luminal B (positive hormone receptors, HER2-negative, and proliferative rate >20%), 3 for HER2-positive (positive or negative hormone receptors and HER2-positive, regardless of proliferative rate), and 4 for triple-negative (negative hormone receptors and HER2-negative, regardless of proliferative rate).

The presence of CD68-positive macrophages was determined by observing cytoplasmic diffuse or granular staining (excluding nuclear staining) in cells exhibiting macrophage morphology, characterized by large, irregularly shaped cells with abundant cytoplasm. Macrophages typically present a kidney-shaped or oval nucleus and may show varying degrees of cytoplasmic vacuolation. These cells are distinguishable from other cell types by their distinct morphology, which includes a relatively large size, uneven cellular boundaries, and the presence of clear, well-defined cytoplasm surrounding the nucleus. The number of stained TAMs was quantified within each tumour by identifying five 'hot spot' areas at low magnification and subsequently capturing images at x400 magnification. The selection of these hot spots was performed without prior knowledge of the patients' clinical data, as these regions are considered to be biologically significant in tumour progression[54,55]. The median TAM count was used as a cut-off point to classify tumours into high and low TAM groups.

Performing immunofluorescence

Immunofluorescence staining was conducted as outlined in a previous study by Rodrigues et al. (2016)[53] and Monteiro et al. (2018)[54]. Briefly, 5-µm sections of paraffin-embedded tumours were placed on slides previously coated with gelatin. The samples were subjected to antigen retrieval in Trilogy solution under moist heat at 120°C for 20 min. Following antigen retrieval, sections were rinsed in phosphate-buffered saline (PBS) and then permeabilized with PBS containing 0.2% Triton-X-100 (Sigma-Aldrich). Subsequently, non-specific binding was blocked using PBS supplemented with 1% bovine serum albumin (BSA, Sigma-Aldrich). Immu nostaining was performed with antibodies S100A8/A9 complex (anti-mouse; clone MAC387; 1:400; ABCAM; FITC-conjugated; incubated for 16 hours at 4ºC); iNOS (anti-rabbit; polyclonal; 1:100; Santa Cruz; incubated for 16 hours at 4ºC) and CD206 (anti-mouse; clone 3.29b1.10; 1:100; Beckman Coulter; R-PE-conjugated; incubated for 1 hour at room

temperature). For iNOS detection, sections were further incubated with Alexa Fluor 647 goat anti-rabbit IgG secondary antibody (1:1000, Life Technologies). The nuclei were counterstained with DAPI. After three washes in PBS, samples were mounted using Prolong Gold Antifade reagent (Life Technologies). Negative controls were included in all reactions by omitting the primary antibodies. The following excitation/emission settings were used: DAPI (405 nm/415-480 nm), FITC (488 nm/500-525 nm), R-PE (543 nm/550-630 nm), and Alexa Fluor 647 (630 nm/>650 nm). Images were acquired on an inverted Zeiss LSM 880 confocal microscope (CAPI). The antibodies used were standardized in our laboratory routine, and their antigenic specificity was confirmed through our own research and by reference to others published studies[53-55].

Acquisition and analysis of images generated from multiphoton microscopy

Two-photon microscopy was performed on haematoxylin and eosin (H&E) stained histological slides prepared from healthy or neoplastic mammary tissue biopsies. Biopsies were obtained through procedures such as setorectomy, simple mastectomy, or unilateral/bilateral radical mastectomy, depending on factors including tumour size, location, lymphatic involvement, and clinical stage. The canine samples, collected between 2009 and 2020, were histologically classified according to the Consensus for the Diagnosis, Prognosis and Treatment of Canine and Feline Mammary Tumours[45-51]. The human samples, collected between 2010 and 2020, were classified according to the World Health Organization criteria[52].

The imaging system employed in this study combined SHG and TPEF imaging using a custom setup comprising an Olympus FV300 confocal scanning laser unit connected to a BX61- upright microscope. The acquisition and analysis of second harmonic generation (SHG) and two-photon excited fluorescence (TPEF) images were performed as previously described (Reis et al., 2019; Garcia et al., 2021; Garcia et al., 2024). Briefly, 1,200 representative sections of normal human breast tissue (NMTh) and evaluated human histological types were chosen from H&E-stained slides. For canine samples, 1,304 representative sections of normal mammary tissue (NMTc) and canine histological types evaluated from sections stained with H&E were defined. The SHG and TPEF signals were acquired from selected intratumoural and normal areas and further analysed using PyFibre, an open-source software package that we specifically designed for the automated segmentation of images and extraction of collagen fibre and cell

segment parameters. Data were extracted and analysed according to Reis et al. (2020)[18], Garcia et al. (2021)[19], Gomes et al. (2023)[56], and Garcia et al. (2024)[21].

Statistical analysis

The distribution of the data was assessed using the Shapiro-Wilk test. Given the data characteristics, we employed ANOVA and Tukey's HSD test for multiple comparisons of means between groups. Spearman's rank correlation coefficient was utilized to investigate the relationship between clinicopathological parameters and macrophage infiltration.

For the analysis of correlations between collagen fibre organization parameters, macrophage infiltration in tumours, and patient-specific survival, data were included only from patients treated with surgery alone. Survival was assessed by assigning a score of 1 to patients who succumbed to breast cancer and 0 to those who remained alive. Patients who died from causes unrelated to breast cancer were excluded from this analysis. Kaplan-Meier curves were generated to estimate cancer-specific survival rates, and group comparisons were conducted using the Mantel-Cox log-rank test.

The chi-square test and Fisher's exact test were used to examine the potential association between macrophage infiltration (as a categorical variable) and other categorical variables, including histological grade, clinical stage, cell proliferation status, and molecular subtype. Contingency tables were used to present these associations. All statistical analyses were performed using Prism (version 8.0, GraphPad, San Diego, CA, United States), with a significance level set at $p < 0.05$. P-values less than 0.0001, 0.001, 0.01 and 0.05 are denoted by ****, ***, ** *and* *, respectively.

Results

Caracterization of the analyzed samples

In the human cohort, patient follow-up ranged from 05 to 10 years, with complete follow-up data available for 43 out of 59 patients. At the study's conclusion, 06 women had died, and 37 were alive. The distribution of patients across clinical stages was as follows: 04 with TC (02 alive, 02 lost to follow-up), 16 with ICgI (1 deceased, 14 alive, 01 lost to follow-up), 21 with

ICgIII (18 alive, 03 lost to follow-up), and 17 with IMC (05 deceased, 09 alive, 03 lost to follow-up).

The canine cohort was followed up for a minimum of 02 years and a maximum of 05 years, with complete follow-up data available for 55 out of 65 dogs. At the study's end, 46 patients had died, and 09 were alive. The distribution of patients based on clinical staging was as follows: 14 with CMT (07 deceased, 07 alive), 16 with MC (14 deceased, 20 lost to follow-up), 06 with CSS (all deceased), and 23 with CAS (19 deceased, 02 alive, 02 lost to follow-up). Complete clinical staging information was unavailable for three patients with IMC. Women with Fb and dogs with BMT were not included in the follow-up analysis.

Increased TAM infiltration is associated with tumours of poor prognosis

Figure 1 and figure 2 illustrate the immunostaining of intratumoral macrophages in canine and human mammary carcinomas. Figure 1 depicts positive immunostaining for CD68 in carcinoma in mixed tumours in dogs (A), invasive carcinoma grade I in women (B), carcinoma with a solid arrangement in dogs (C), invasive carcinoma grade III in women (D), invasive micropapillary carcinoma in dogs (E), and invasive micropapillary carcinoma in women (F). Figure 2 highlights the comparative analysis of macrophage infiltration in tumours with favourable prognosis (CMT and TC) versus those with unfavourable prognosis (CSA, ICgIII, canine IMC, and human IMC). These data reveal greater macrophage infiltration in carcinomas associated with an unfavourable prognosis.

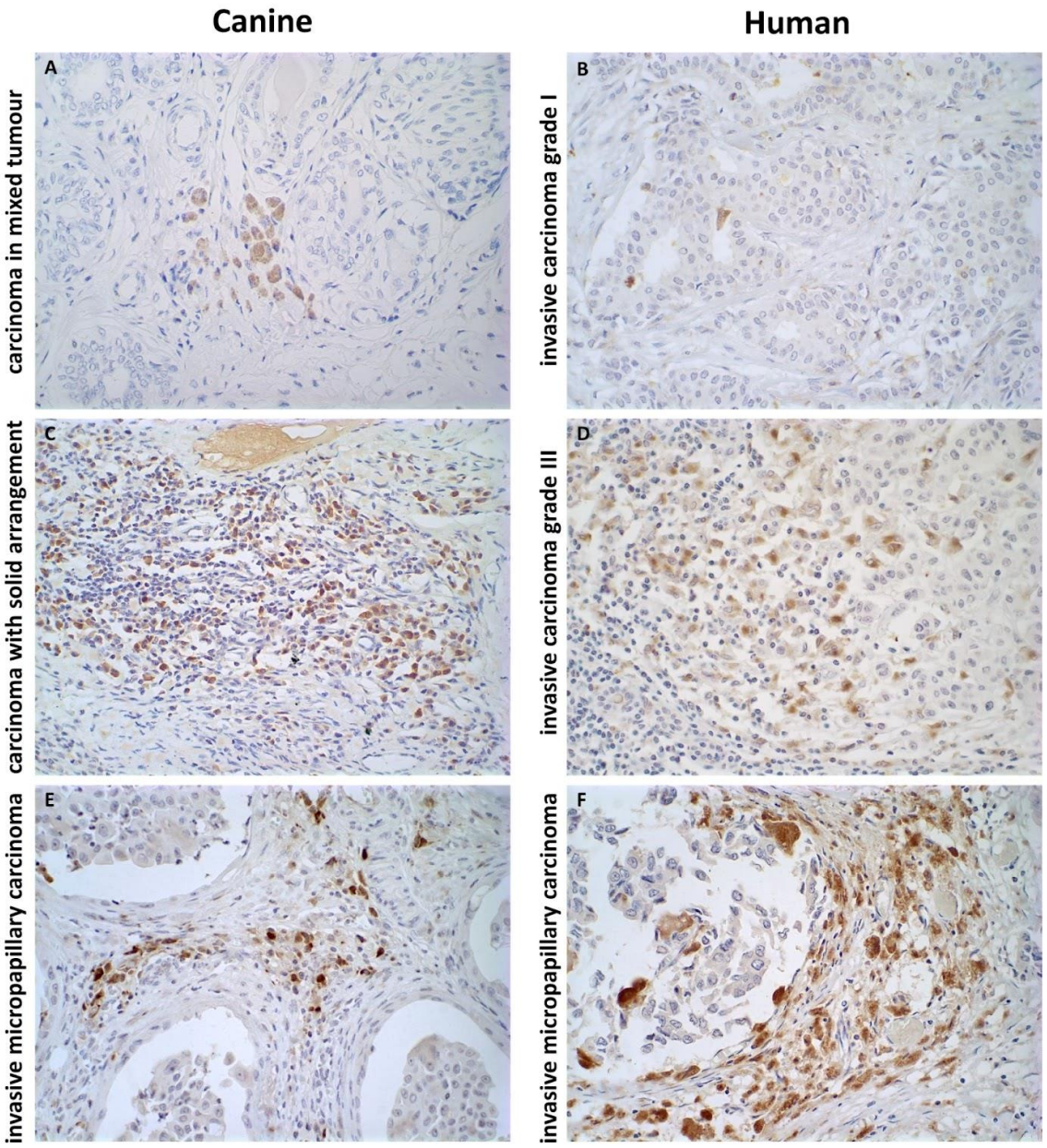

Figure 01: Immunohistochemical staining of intratumoral macrophages in canine and human mammary carcinomas. Intratumoral macrophages in carcinoma in mixed tumour in dogs (A), invasive carcinoma grade I in women (B), carcinoma with solid arrangement in dogs (C), invasive carcinoma grade III in women (D), invasive micropapillary carcinoma in dogs (E) and invasive micropapillary carcinoma in women (F).

Figure 2A and 2B present the comparison of macrophage infiltration across different histological subtypes of canine (CMT, CS, CAS, and IMC) and human (TC, ICgI, ICgIII, and IMC) mammary neoplasms. Each data point in the figures represents the macrophage count in

an individual tumour, while the box plots display the median and interquartile range for the distributions. Statistically significant differences between groups are indicated by asterisks.

Analysis of macrophage infiltration in canine mammary neoplasms revealed that CMT, the carcinoma with the most favourable prognosis, exhibited lower macrophage infiltration compared to the more aggressive tumour subtypes (CS, CAS, and IMC) (Figure 2A). Additionally, we observed greater variability in macrophage infiltration within the CS, CAS, and IMC subtypes, with some tumours displaying substantially higher infiltration compared to the majority within the same subtype. Similarly, in human mammary neoplasms, the less aggressive tumours (TC and ICgI) showed lower macrophage infiltration compared to the more aggressive subtypes (ICgIII and IMC) (Figure 2B). A similar trend of increased variability in macrophage infiltration was also noted in the ICgIII and IMC subtypes, with certain tumours exhibiting markedly higher infiltration compared to others within the same subtype.

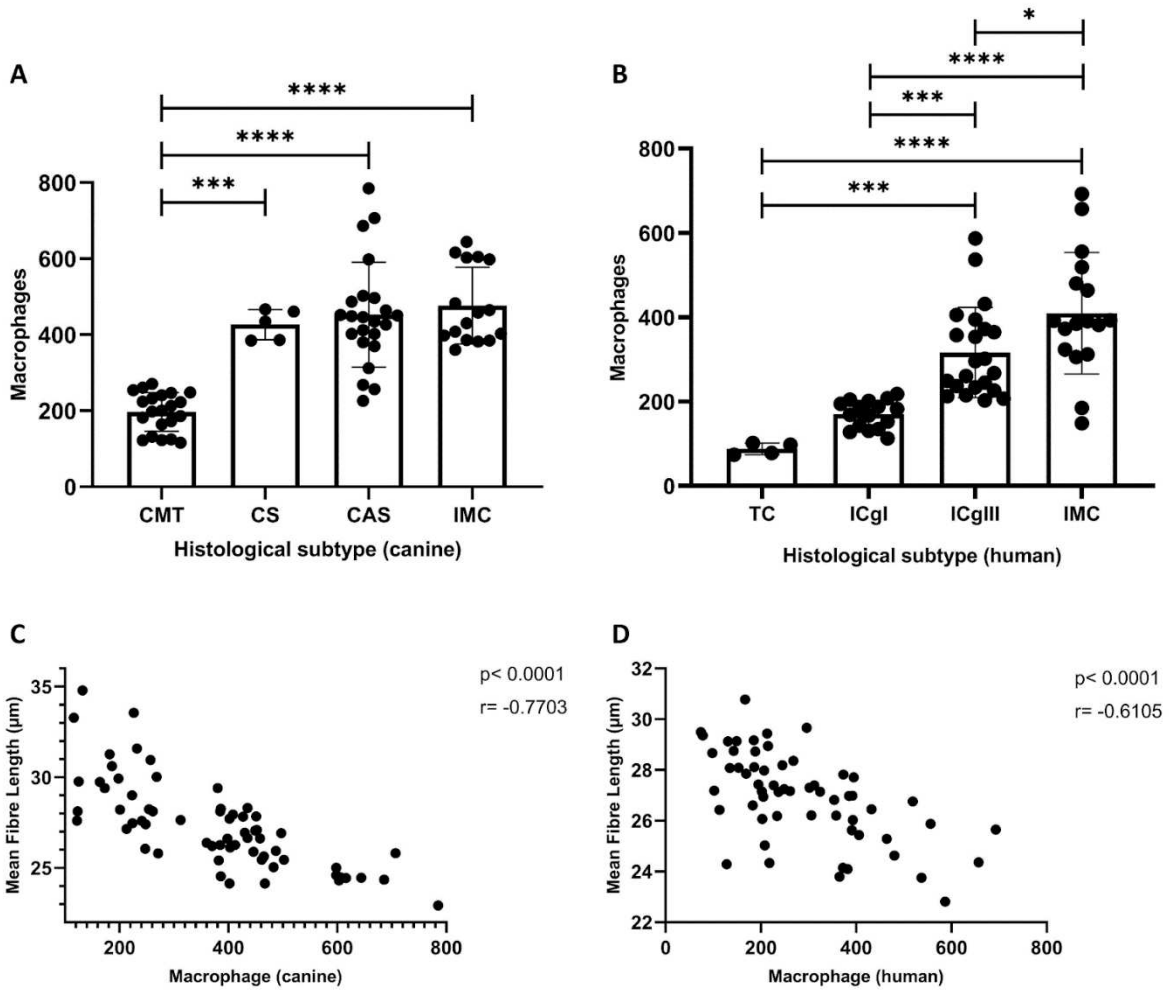

Figure 02: Macrophage infiltration in canine and human mammary carcinomas. The figure presents the results of the ANOVA and Tukey tests comparing the amount of infiltrating macrophages between the histological subtypes carcinoma in mixed tumor (CMT, n=21), carcinosarcoma (CS, n=05), carcinoma with solid arrangement (CAS, n=23) and invasive micropapillary carcinoma (IMC, n=16) in the canine species (A) and between the histological subtypes tubular carcinoma (TC, n=04), invasive carcinoma grade 1 (ICgI, n=16), invasive carcinoma grade III (ICgIII, n=22) and invasive micropapillary carcinoma (IMC, n=17) in the human species (B). The figure also presents Spearman's correlation test between macrophage infiltration and the mean fibre length in canine (C) and human (D) mammary neoplasms.

Carcinomas with shorter collagen fibres have the highest TAM infiltration

Figure 2C and 2D illustrate the relationship between macrophage infiltration and collagen fibre length in mammary carcinomas. Figure 2C shows a scatter plot with a strong negative correlation ($p < 0.0001$, $r = -0.7703$) between the quantity of infiltrating macrophages and the mean length of collagen fibres in canine mammary carcinomas, indicating that tumours with higher macrophage infiltration tend to present shorter collagen fibres. Similarly, figure 2D presents a scatter plot demonstrating a moderate negative correlation ($p < 0.0001$, $r = -0.6105$) in human breast carcinomas, suggesting that tumours with higher macrophage infiltration also exhibit shorter collagen fibres.

More aggressive carcinomas exhibit higher TAM infiltration

To investigate the impact of TAM infiltration on the behaviour of human and canine mammary carcinomas, we examined the relationship between macrophage infiltration and various clinicopathological parameters, including clinical stage, cell proliferation rate, molecular subtype, and histological grade. Immunohistochemical analysis was performed on 58 human and 59 canine mammary carcinoma samples. The results of these correlations are presented in figure 3. In this analysis, increased carcinoma aggressiveness was associated with factors such as higher histological grade, increased likelihood of local and/or distant metastasis, elevated cell proliferation rate, and a greater probability of exhibiting "triple-negative" or "HER2-overexpressed" molecular subtypes.

The application of human molecular subtypes to canine mammary carcinomas, while common, has yielded inconsistent prognostic value, particularly concerning HER2 overexpression. The literature presents conflicting results regarding the correlation between HER2 status and clinical outcomes in dogs. Despite this limitation, we observed a direct correlation between TAM infiltration and clinical stage (Figs. 3A-3D), cell proliferation rate (Figs. 3E and 3F), molecular subtype (Figs. 3G and 3H) and a histological grading (Figs. 3I and 3J) in both canine and human subjects. These data highlight the association between increased tumour aggressiveness and elevated TAM infiltration. Our findings suggest that macrophage infiltration in both canine and human mammary carcinomas is linked to features indicative of heightened tumour aggressiveness, including advanced clinical stage, high cell proliferation rate, unfavourable molecular subtypes and highest histological grade.

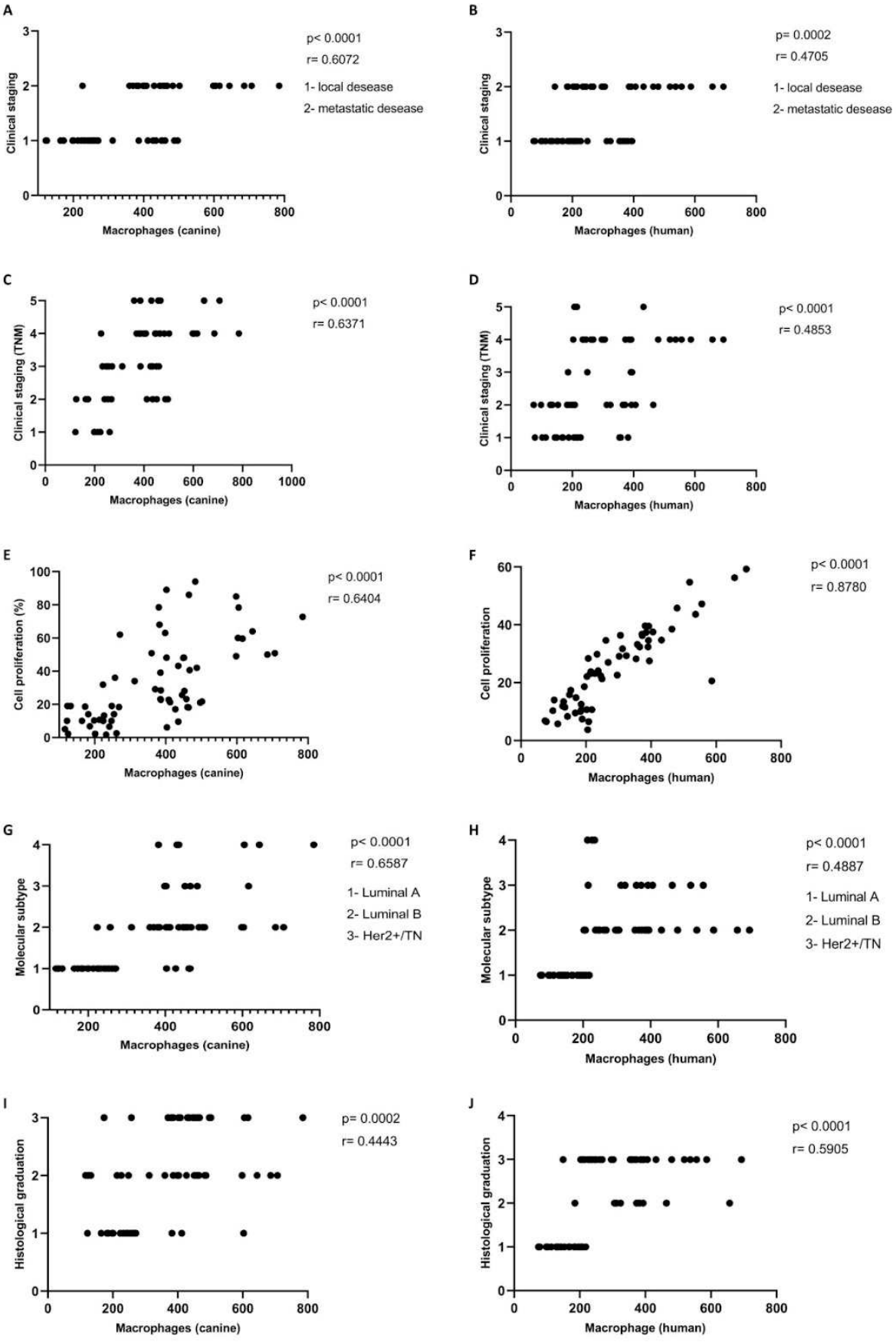
A
Clinical staging
Macrophages (canine)
p< 0.0001
r= 0.6072
1- local desease
2- metastatic desease
B
Clinical staging
Macrophages (human)
p= 0.0002
r= 0.4705
1- local desease
2- metastatic desease
C
Clinical staging (TNM)
Macrophages (canine)
p< 0.0001
r= 0.6371
D
Clinical staging (TNM)
Macrophages (human)
p< 0.0001
r= 0.4853
E
Cell proliferation (%)
Macrophages (canine)
p< 0.0001
r= 0.6404
F
Cell proliferation
Macrophages (human)
p< 0.0001
r= 0.8780
G
Molecular subtype
Macrophages (canine)
p< 0.0001
r= 0.6587
1- Luminal A
2- Luminal B
3- Her2+/TN
H
Molecular subtype
Macrophages (human)
p< 0.0001
r= 0.4887
1- Luminal A
2- Luminal B
3- Her2+/TN
I
Histological graduation
Macrophages (canine)
p= 0.0002
r= 0.4443
J
Histological graduation
Macrophage (human)
p< 0.0001
r= 0.5905

Figure 03: Correlation between clinicopathological parameters and macrophage infiltration in dogs and women. Spearman's correlation between clinical staging and macrophage infiltrate in dogs (A and C, n=65) and women (B and D, n=59). Spearman's correlation between cell proliferation and macrophage infiltrate in dogs (E, n=65) and women (F, n=59). Spearman's correlation between molecular subtype and macrophage infiltrate in dogs (G, n=65) and women (H, n=59). Spearman's between histological graduation and macrophage infiltrate in dogs (G, n=65) and women (H, n=59).

To assess the impact of TAM infiltration on patient survival in dogs, we established a cut-off point independent of histological subtype, grade, clinical stage, cell proliferation rate, and molecular subtype. The median TAM infiltration value (400) was calculated from the data arranged in ascending order and used to categorize patients into two groups. The first group included dogs with carcinomas exhibiting less than 400 infiltrating macrophages, while the second group comprised those with carcinomas showing more than 400 infiltrating macrophages. Survival status was assigned as 0 for dogs alive at the study's end and 1 for those that died from mammary carcinoma. The Kaplan-Meier survival curve (Figure 4A) demonstrates that dogs with carcinomas and higher macrophage infiltration (dashed red line) had a median survival of 168 days. In contrast, those with lower macrophage infiltration (blue line) had a median survival of 558 days. These findings underscore that more aggressive carcinomas, associated with an unfavourable prognosis, exhibit a greater degree of macrophage infiltration compared to less aggressive carcinomas with a favourable prognosis.

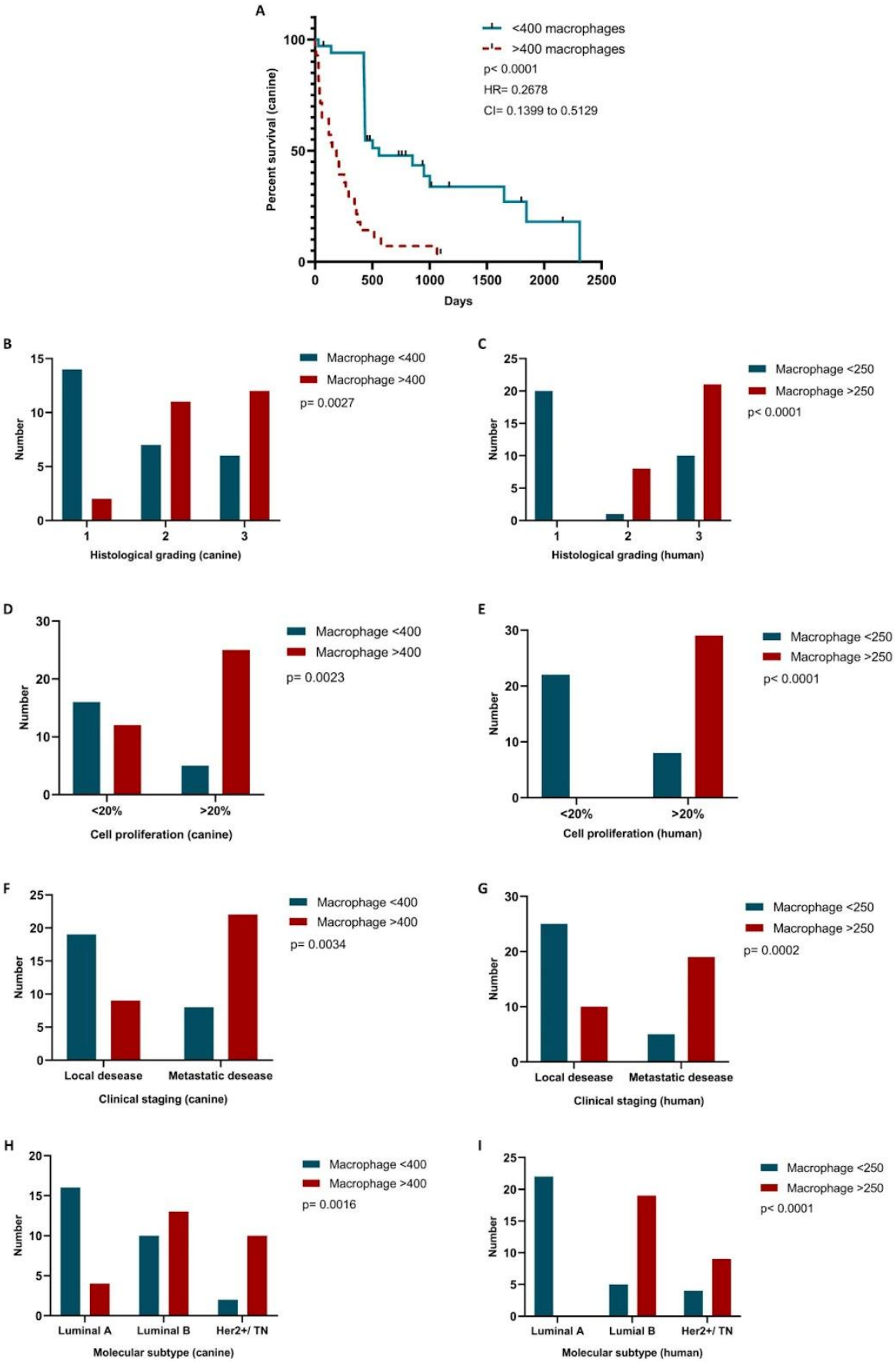
A
<400 macrophages
>400 macrophages
p< 0.0001
HR= 0.2678
CI= 0.1399 to 0.5129
Percent survival (canine)
Days
B
Macrophage <400
Macrophage >400
p= 0.0027
Number
Histological grading (canine)
C
Macrophage <250
Macrophage >250
p< 0.0001
Number
Histological grading (human)
D
Macrophage <400
Macrophage >400
p= 0.0023
Number
Cell proliferation (canine)
E
Macrophage <250
Macrophage >250
p< 0.0001
Number
Cell proliferation (human)
F
Macrophage <400
Macrophage >400
p= 0.0034
Number
Clinical staging (canine)
G
Macrophage <250
Macrophage >250
p= 0.0002
Number
Clinical staging (human)
H
Macrophage <400
Macrophage >400
p= 0.0016
Number
Molecular subtype (canine)
I
Macrophage <250
Macrophage >250
p< 0.0001
Number
Molecular subtype (human)

Figure 04: Survival curve for dogs and association between clinicopathological parameters and macrophage infiltration in women and dogs. Kaplan–Meier curve showing the separation of cases by mean macrophage infiltrate (A, n= 59). Contingency plots presenting data from chi-square analysis (B and C) and Fisher's exact test (D, E, F, G, H and I) to evaluate the association between clinicopathological data and the mean macrophage categorized in dogs and women. The clinicopathological data are presented on the x-axis, the absolute frequency (n) on the y-axis and the proportion in percentage at the end of each bar. Association between histological grade (B, n=65) cell proliferation rate (D, n=65), local or metastatic disease (F, n=65), molecular subtype (H, n=65) and macrophages categorized as high or low infiltration based on a cut-off point of 400 macrophages in dogs. Association between histological grade (C, n=59) cell proliferation rate (E, n=59), local or metastatic disease (G, n=59), molecular subtype (I, n=59) and macrophages categorized as high or low infiltration based on a cut-off point of 250 macrophages in women. Error bar, not included because it is the evaluation of categorical data.

In the human cohort, it was not feasible to construct a cancer-specific survival curve using the same methodology as for the canine cohort. This is attributed to the fact that approximately 85% of the human patients in the study are currently alive and under medical follow-up. Consequently, median survival was not reached in any of the stratified groups, precluding further survival analysis. However, to highlight the clinical relevance of our findings in breast oncology, we investigated the association between macrophage infiltration and clinicopathological factors known to impact patient survival. The median macrophage infiltration value (250) was determined from the data and used to establish a cut-off point for categorizing patients.

The cut-off values of 400 infiltrating macrophages for the canine species and 250 infiltrating macrophages for the human species were used to stratify patients into two distinct groups. In the canine cohort, those diagnosed with carcinomas exhibiting more than 400 infiltrating macrophages were assigned to the first group, while those with fewer than 400 infiltrating macrophages were placed in the second group (Fig. 4B, 4D, 4F, 4H). Similarly, in the human cohort, women diagnosed with carcinomas with more than 250 infiltrating macrophages were categorized into the first group, while those with fewer than 250 infiltrating macrophages were assigned to the second group (Fig. 4C, 4E, 4G, 4I).

To examine the potential association or independence between macrophage infiltration and clinicopathological data, we conducted analyses using Fisher's Exact Test and the chi-square test. The results indicate that higher histological grade, elevated proliferative rate, presence of local and/or distant metastases, and the "triple-negative" and "Her2-overexpressed" molecular subtypes are associated with carcinomas exhibiting higher macrophage infiltration in both canine (Fig. 4B, 4D, 4F, and 4H) and human (Fig. 4C, 4E, 4G, 4I) subjects.

Intratumoral TAMs express M1 and M2 markers concurrently

After verifying that a higher infiltration of macrophages was associated with a worse prognosis in both dogs and women, and worse survival in dogs, we sought to identify the profile of intratumoural macrophages in the studied mammary neoplasms in dogs (Figure 05) and women (Figure 06). Figure 05 shows positive staining for DAPI (A, E, J, O), S100A8/A9 (B, F, K, P), CD206 (C, G, L, Q), iNOS (D, H, M, R) and visual representation of overlapping expression of DAPI, S100A8/A9, CD206 and iNOS (E, I, N, S) in carcinoma in mixed tumours, carcinoma with solid arrangement, invasive micropapillary carcinoma, and carcinosarcoma in dogs. Figure 06 shows positive staining for DAPI (A, E, J, O), S100A8/A9 (B, F, K, P), CD206 (C, G, L, Q), iNOS (D, H, M, R) and visual representation of overlapping expression of DAPI, S100A8/A9, CD206 and iNOS (E, I, N, S) in tubular carcinoma, invasive carcinoma grade I, invasive micropapillary carcinoma, and invasive carcinoma grade III in women. We identified four distinct patterns: S100A8/A9^{+}/iNOS^{-}/CD206^{-}, S100A8/A9^{+}/iNOS^{+}/CD206^{-}, S100A8/A9^{+}/iNOS^{-}/CD206^{+}, and S100A8/A9^{+}/iNOS^{+}/CD206^{+}.

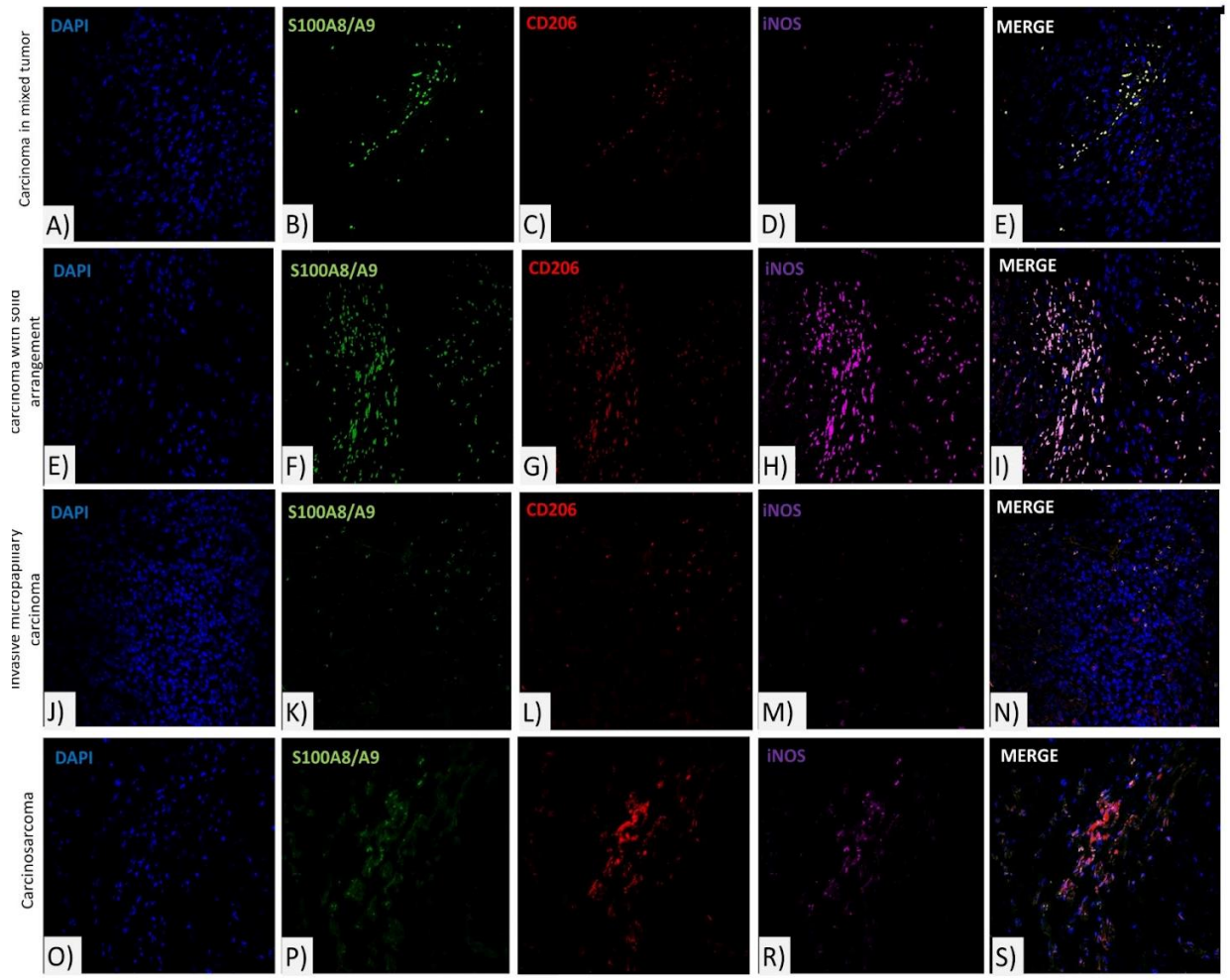

Figure 05: Macrophage profile in canine mammary carcinomas. Confocal immunofluorescence images of canine mammary carcinomas, showing inducible nitric oxide synthase (iNOS; magenta), CD206 (red), S100A8/A9 (green) and DAPI (blue) overlay images distinguishing between different macrophage phenotypes. DAPI (A, E, J, O), S100A8/A9 (B, F, K, P), CD206 (C, G, L, Q), iNOS (D, H, M, R) and merge of DAPI, S100A8/A9, CD206 and iNOS (E, I, N, S) in carcinoma in mixed tumours, carcinoma with solid arrangement, invasive micropapillary carcinoma, and carcinosarcoma. Nuclei were revealed by DAPI staining (blue) and merged images demonstrate the cytoplasmic localisation of the evaluated proteins. Images are representative of observations from three independent experiments.

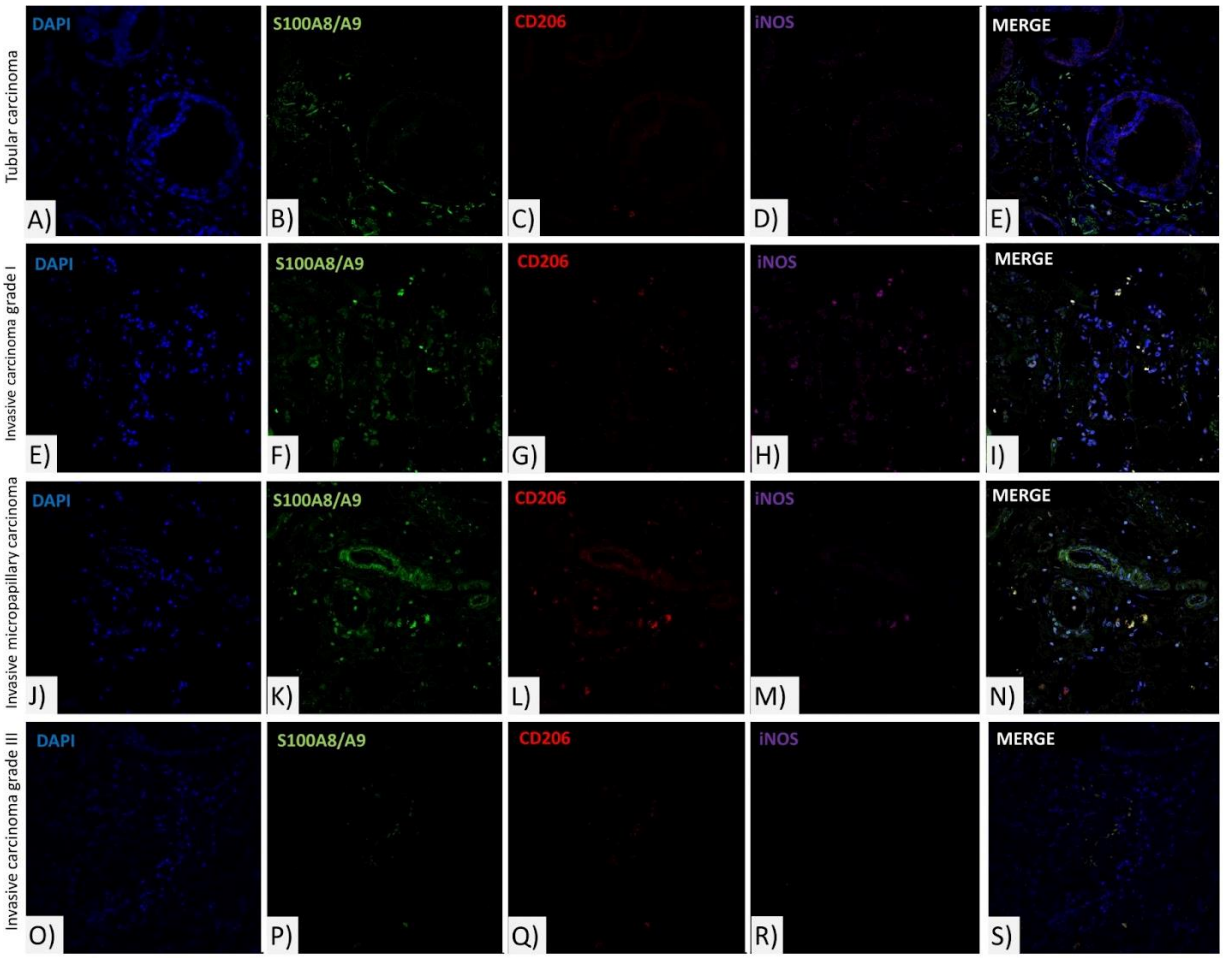

Figure 06: Macrophage profile in human mammary carcinomas. Confocal immunofluorescence images of human mammary carcinomas, showing inducible nitric oxide synthase (iNOS; magenta), CD206 (red), S100A8/A9 (green) and DAPI (blue) overlay images distinguishing between different macrophage phenotypes. DAPI (A, E, J, O), S100A8/A9 (B, F, K, P), CD206 (C, G, L, Q), iNOS (D, H, M, R) and merge of DAPI, S100A8/A9, CD206 and iNOS (E, I, N, S) in tubular carcinoma, invasive carcinoma grade I, invasive micropapillary carcinoma, and invasive carcinoma grade III. Nuclei were revealed by DAPI staining (blue) and merged images demonstrate the cytoplasmic localisation of the evaluated proteins. Images are representative of observations from three independent experiments.

Discussion

The present study establishes a strong correlation between the quantity of tumour-associated macrophages (TAMs) and the length of collagen fibres within tumours, suggesting that this

interaction plays a crucial role in disease progression. The negative correlation observed between macrophage infiltration and collagen fibre length indicates that the presence of macrophages may be linked to the remodelling of the extracellular matrix, resulting in a decrease in collagen fibre length. The remodelling of the extracellular matrix by TAMs is a complex process involving the secretion of various enzymes and cytokines, which can lead to the degradation and reorganisation of collagen fibres. The decrease in collagen fibre length observed in tumours with high macrophage infiltration could be attributed to the increased activity of matrix metalloproteases (MMPs) and other proteolytic enzymes secreted by TAMs. The degradation of collagen fibres may facilitate tumour cell invasion and metastasis by creating pathways for tumour cells to migrate through the extracellular matrix. Additionally, the altered collagen fibre architecture may promote angiogenesis and provide a supportive microenvironment for tumour growth.

Our results demonstrate that alterations in collagen fibres, such as decreased length and increased organisation, are associated with a poorer prognosis and reduced survival in both canine and human patients. The increase in the organisation and alignment of collagen fibres may create a physical barrier that hinders the penetration of immune cells and therapeutic agents into the tumour, contributing to treatment resistance and disease progression. Additionally, the altered collagen fibre architecture may promote tumour cell migration and invasion by providing tracks for cells to move along. These observations corroborate previous studies indicating that changes in collagen fibre organisation and density are associated with a worse prognosis in various cancer types, including breast cancer[57-76].

TAMs play a crucial role in metastasis by promoting extracellular matrix remodelling and tumour cell migration. In more advanced stages of cancer, the cytokine TGF-β, produced by TAMs, contributes to epithelial-to-mesenchymal transition, a fundamental process for the invasion and metastasis of cancer cells[77-80]. Studies in canine mammary carcinomas reinforce the role of TAMs in the progression and prognosis of breast cancer, showing that high TAM infiltration is associated with aggressive clinicopathological features, such as invasion and lymph node metastasis, as well as poorer overall survival. Although TAM infiltration is related to the progression of mammary carcinoma, no significant associations were found between increased TAM infiltration and tumour histological grade[54,55].

Furthermore, the study reveals a direct correlation between TAM infiltration and clinical stage, cell proliferation rate, molecular subtype, and histological grade in both canine and human

mammary carcinomas. This observation suggests that macrophage infiltration is linked to features indicative of heightened tumour aggressiveness. TAMs can promote tumour growth, angiogenesis, and metastasis through the secretion of various growth factors, cytokines, and chemokines[27,81-84]. The increased infiltration of TAMs in more aggressive tumours may contribute to the accelerated progression of the disease and a worse prognosis, as evidenced by the shorter survival observed in dogs with high macrophage infiltration. The comparative analysis between humans and dogs highlights the potential of the canine model for breast cancer research, demonstrating notable similarities in the relationship between macrophage infiltration, collagen fibre alterations, and clinicopathological parameters in both species. The spontaneous nature of canine mammary tumours and their similarities to human breast cancer in terms of clinical presentation, histological features, and molecular alterations make them a valuable model for translational research.[85-92.]

Depending on their polarisation, macrophages can be classified as M1 or M2. M1 macrophages, classically activated, are induced by factors such as IFN-γ and LPS and have cytotoxic effects on cancer cells. M1 macrophages express the S100A8/A9^{+}/iNOS^{+}/CD206^{-} pattern[27,29,93,94]. This combination of markers indicates a pro-inflammatory phenotype, with the presence of S100A8/A9 and iNOS, and the absence of CD206, which is a marker associated with M2 macrophages with an anti-inflammatory profile[55]. In contrast, M2 macrophages, alternatively activated, are stimulated by cytokines such as IL-4, IL-10, and TGF-β, and contribute to tumour promotion by providing a nutritional advantage for cancer cells and suppressing anti-tumour immune responses[27,29,83,95]. M2 macrophages express the S100A8/A9^{+}/iNOS^{-}/CD206^{+} pattern. This combination of markers suggests an anti-inflammatory phenotype, characterized by the presence of S100A8/A9 and CD206, and the absence of iNOS, a marker typically associated with pro-inflammatory M1 macrophages[55]. Generally, TAMs are predominantly polarised towards M2 macrophages, promoting tumour progression and metastasis[27,29,83,95-96].

Our findings demonstrate a clear association between macrophage phenotype and tumour prognosis in both canine and human mammary carcinomas. Carcinomas with a worse prognosis tend to express more CD206 than iNOS. Specifically, in canine mammary carcinomas, solid carcinomas, carcinosarcomas, and invasive micropapillary carcinomas exhibited a higher proportion of macrophages expressing CD206 compared to iNOS, in contrast to mixed tumours, which displayed fewer CD206+ macrophages. Similarly, in human breast carcinomas, invasive micropapillary carcinomas and invasive grade III carcinomas showed a predominance of CD206+ and iNOS- macrophages when compared to tubular carcinomas and invasive grade I

carcinomas. These findings highlight the association of a greater presence of CD206+ macrophages with more aggressive tumour subtypes, reinforcing their role in tumour progression and immune suppression[9,54,55,83,94,95,102].

Although S100A8/A9 is often associated with inflammatory processes and the recruitment of myeloid cells, its expression can also be detected in M2 macrophages in certain contexts, such as wound healing and some tumours[98-102]. CD206, a classical marker of M2 macrophages, is linked to tissue repair, angiogenesis, and immune suppression. In contrast, iNOS is a hallmark of M1 macrophages, which are primarily involved in inflammatory responses and tumour cell destruction. The predominance of CD206+ macrophages in more aggressive tumours suggests a significant shift towards the M2 phenotype, with decreased expression of iNOS in these contexts[29,83,94,95,102].

The polarization of macrophages into M1 or M2 phenotypes appears to be heavily influenced by the tumour microenvironment[29,35,83,94,95-102]. In tumours with a favourable prognosis, signals such as IFN-γ may favour the M1 phenotype, whereas in more aggressive tumours, the dominance of cytokines like IL-4, IL-10, and TGF-β favours the M2 phenotype. This shift not only reflects the immune evasion strategies of aggressive tumours but also underscores the role of macrophages in shaping the tumour's clinical behaviour[54,55,94,95-102].

In canine mammary tumours, the findings highlight the similarities and differences compared to human breast carcinomas. Both species exhibit a clear association between M2 macrophages and poor prognostic indicators, suggesting that the underlying mechanisms driving macrophage polarization and function are conserved across species. However, canine mammary tumors serve as a valuable model for investigating macrophage-tumor interactions, owing to their spontaneous development and remarkable histological heterogeneity. These features make them highly comparable to human breast cancer, offering significant insights into tumor biology and immune responses in a naturally occurring setting.

To further understand the phenotype of these TAMs, it is essential to conduct more detailed analyses of the different TAM subsets, considering their location within the tumour, to develop more effective therapies. Advanced technologies, such as multiplex IF and mass cytometry, are enabling a deeper understanding of TAM diversity and plasticity, revealing the complexity of their functions in the tumour microenvironment and providing insights for the development of new therapeutic strategies[104-107]. Furthermore, the comparative study of canine and human

mammary carcinomas may provide valuable insights into the translational potential of these approaches.

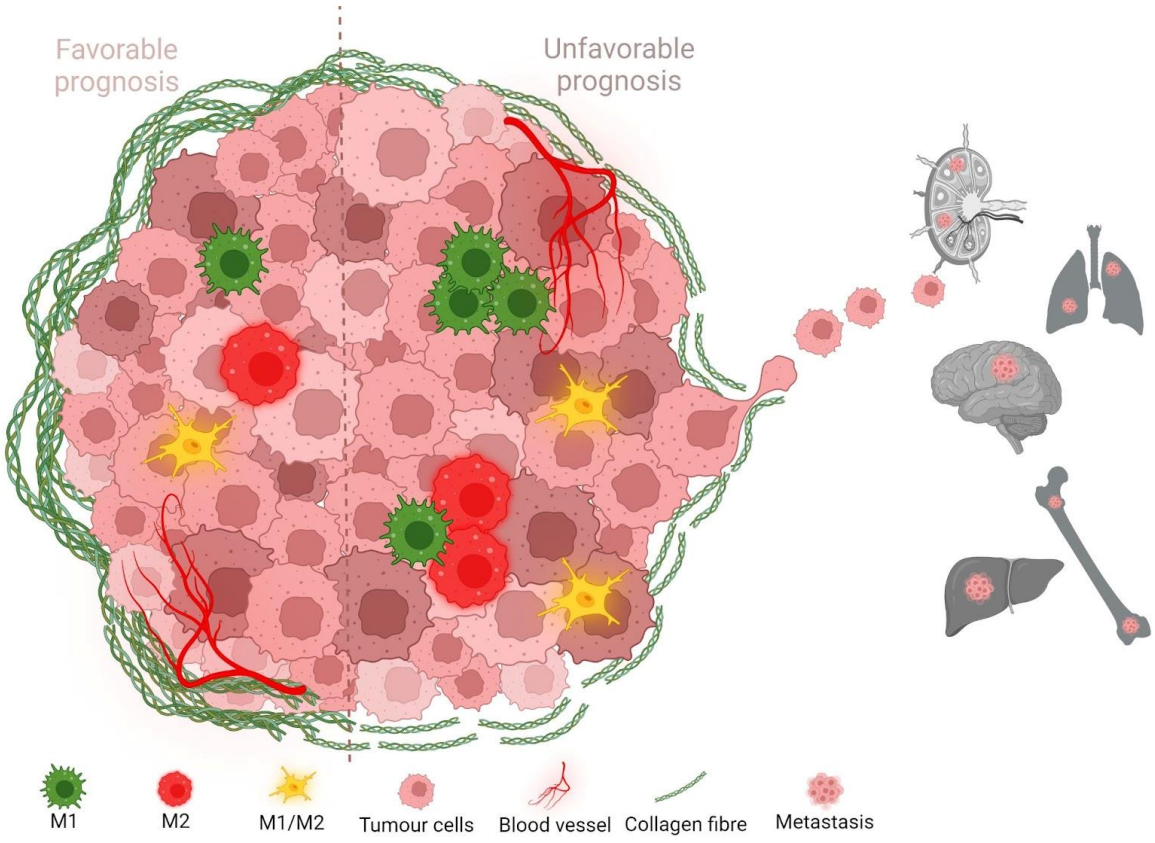

Figure 07: Carcinomas with an unfavourable prognosis have greater infiltration of tumor-associated macrophages and shorter fibres. Carcinomas with a favourable prognosis and low proliferative rate present longer collagen fibres and few infiltrating macrophages, capable of limiting neoplastic growth. In carcinomas with an unfavourable prognosis and high proliferative rates, collagen fibres are shorter and there is greater infiltration of macrophages. This is unable to limit this growth, allowing tumour expansion. The observed reduction in collagen fibre length within the tumour stroma may be attributed to the increased presence of tumor-associated macrophages and their active involvement in extracellular matrix remodelling. The resulting stiffening of the stromal microenvironment could potentially create tracks that facilitate the metastatic spread of cancer cells to lymph nodes and distant organs, such as the lungs, liver, brain, and bone. Created by BioRender.

Conclusions

This study provides robust evidence for the importance of the interplay between collagen fibres and TAMs in breast cancer progression, with significant prognostic implications. The infiltration of TAMs emerges as a promising biomarker for assessing tumour aggressiveness and the risk of disease progression. Our study highlights the significant role of macrophages and collagen fibres in the tumour microenvironment of canine and human mammary carcinomas. We observed that macrophage phenotypes are strongly associated with tumour prognosis, with M2-polarized macrophages predominating in aggressive tumours, while M1 macrophages were more frequent in tumours with a favourable prognosis. Additionally, alterations in collagen fibre length were linked to poorer prognostic indicators in both species, reinforcing the critical role of the extracellular matrix in tumour progression. It is important to note that while survival analysis was performed in canine cases, no survival analysis was conducted for the human samples in this study. Therefore, future research should aim to address this gap, evaluating the relationship between collagen alterations, macrophage polarization, and survival outcomes in human breast cancer. Such studies could provide deeper insights into the translational relevance of these findings and support the development of targeted therapeutic strategies for both species.

REFERENCES

1. Arnold, M., Morgan, E., Rumgay, H., Mafra, A., Singh, D., Laversanne, M., ... & Soerjomataram, I. (2022). Current and future burden of breast cancer: Global statistics for 2020 and 2040. *Breast, 66*, 15-23. doi:10.1016/j.breast.2022.06.002

2. Toss MS, Miligy IM, Gorringe K L et al. Geometric characteristics of collagen have independent prognostic significance in breast ductal carcinoma in situ: an image analysis study. Mod Pathol. 2019; 32:1473-85. doi: 10.1038/s41379-019-0296-7.

3. Piersma B, Hayward MK, Weaver VM. Fibrosis and cancer: A strained relationship. Biochim Biophys Acta Rev Cancer. 2020 1873 (2):188356. doi: 10.1016/j.bbcan.2020.188356.

4. Harbeck N, Penault-Llorca F, Cortes J. et al. Breast Cancer. Nat. Rev. Dis. Primers. 2019; 5:66. doi: 10.1038/s41572-019-0111-2.

5. Pollard JW. Macrophages define the invasive microenvironment in breast cancer. J Leukoc Biol. 2008. 84(3):623-30. doi: 10.1189/jlb.1107762.

6. Markkanen, E. Know thy model: charting molecular homology in stromal reprogramming between canine and human mammary tumors. Front. Cell Develop. Biol. 2019; 7:348. https://doi.org/10.3389/fcell.2019.00348.

7. Ajeti, V, Nadiarnykh O, Ponik SM, Keely PJ, Eliceiri KW, Campagnola PJ. Structural changes in mixed Col I/Col V collagen gels probed by SHG microscopy: implications for probing stromal alterations in human breast cancer. Biomed. Opt. Express. 2011; 2:2307-16. doi: 10.1364/BOE.2.002307.

8. Conklin MW, Eickhoff JC, Riching KM et al. Aligned collagen is a prognostic signature for survival in human breast carcinoma. 2011. Am. J. Pathol. 178, 1221-32. doi: 10.1016/j.ajpath.2010.11.076.

9. Garcia AM, Magalhaes FL, Soares JS et al. Second harmonic generation imaging of the collagen architecture in prostate cancer tissue. 2017. Biomed. Phys. Eng. Express 4, 025026. doi: 10.1088/2057-1976/aaa379.

10. Almici E, Arshakyan M, Carrasco JL et al. Quantitative Image Analysis of Fibrillar Collagens Reveals Novel Diagnostic and Prognostic Biomarkers and Histotype-Dependent Aberrant Mechanobiology in Lung Cancer. 2023; 36:100155. doi: 10.1016/j.modpat.2023.100155.

11. Hompland T, Erikson A, Lindgren M, Lindmo T, de Lange Davies C. Second-harmonic generation in collagen as a potential cancer diagnostic parameter. J. Biomed. Opt. 2008; 13(5):054050. doi: 10.1117/1.2983664.

12. Burke K, Tang P, Brown E B. Second harmonic generation reveals matrix alterations during breast tumor progression. J. Biomed. Opt. 2012; 18:031106. doi: 10.1117/1.JBO.18.3.031106.

13. Burke K, Smid M, Dawes RP et al. Using second harmonic generation to predict patient outcome in solid tumors. BMC Cancer. 2015; 15:929. doi: 10.1186/s12885-015-1911-8.

14. Golaraei A, Kontenis L, Cisek R et al. Changes of collagen ultrastructure in breast cancer tissue determined by second-harmonic generation double Stokes-Mueller polarimetric microscopy. Biomed. Opt. Express. 2016; 7:4054-68. doi: 10.1364/BOE.7.004054.

15. Barcus CE, O'Leary K, Brockman JL et al. Elevated collagen-I augments tumor progressive signals, intravasation and metastasis of prolactin-induced estrogen receptor alpha positive mammary tumour cells. Breast Cancer Res. 2017; 19:1-13. doi: 10.1186/s13058-017-0801-1.

16. Case A, Brisson BK, Durham AC. et al. Identification of prognostic collagen signatures and potential therapeutic stromal targets in canine mammary gland carcinoma. PLoS ONE. 2017; 12:1-19. doi: 10.1186/s12885-015-1911-8.

17. Conklin MW, Gangnon RE, Sprague BL et al. Collagen Alignment as a Predictor of Recurrence after Ductal Carcinoma *in situ.* Cancer Epidemiol Biomarkers Prev. 2018; 27(2):138-145. doi: 10.1158/1055-9965.EPI-17-0720.

18. Reis LA, Garcia APV, Gomes EFA et al. Canine mammary cancer diagnosis from quantitative properties of nonlinear optical images. Biomed. Opt. Express. 2020; 11, 6413-27. doi: 10.1364/BOE.400871.

19. Garcia APV, Reis LA, Nunes FC et al. Canine mammary cancer tumour behaviour and patient survival time are associated with collagen fibre characteristics. Sci Rep. 2021; 11:5668. doi: 10.1038/s41598-021-85104-w.

20. Natal RA, Vassalo J, Paiva GR et al. Collagen analysis by second-harmonic generation microscopy predicts outcome of luminal breast cancer. Tumor Biol. 2018; 40. doi: 1010428318770953.

20. Natal R A, Paiva GR, Pelegati VB et al. Exploring collagen parameters in pure special types of invasive breast cancer. Sci. Rep. 2019; 9:7715. doi: 10.1038/s41598-019-44156-9.

21. Garcia APV, Taborda DYO, Reis LA, de Paula AM, Cassali GD. Collagen modifications predictive of lymph node metastasis in dogs with carcinoma in mixed tumours. Front Vet Sci. 2024 Mar 6;11:1362693. doi: 10.3389/fvets.2024.1362693.

22. Hanahan, D., & Weinberg, R. A. (2011). Hallmarks of cancer: The next generation. *Cell, 144*(5), 646-674. doi:10.1016/j.cell.2011.02.013

23. Hanahan, D., & Coussens, L. M. (2012). Accessories to the crime: functions of cells recruited to the tumor microenvironment. *Cancer Cell, 21*(3), 309-322. doi:10.1016/j.ccr.2012.02.022

24. Joyce, J. A., & Pollard, J. W. (2009). Microenvironmental regulation of metastasis. *Nature Reviews Cancer, 9*(4), 239-252. doi:10.1038/nrc2618.

25. Noy, R., & Pollard, J. W. (2014). Tumor-associated macrophages: from mechanisms to therapy. *Immunity, 41*(1), 49-61. doi:10.1016/j.immuni.2014.06.010

26. Qian, B. Z., & Pollard, J. W. (2010). Macrophage diversity enhances tumor progression and metastasis. *Cell, 141*(1), 39-51. doi:10.1016/j.cell.2010.03.014

27. Mantovani, A., & Allavena, P. (2015). The interaction of anticancer therapies with tumor-associated macrophages. *Journal of Experimental Medicine, 212*(4), 435-445. doi:10.1084/jem.20150295

28. DeNardo, D. G., & Ruffell, B. (2019). Macrophages as regulators of tumour immunity and immunotherapy. *Nature Reviews Immunology, 19*(6), 369-382. doi:10.1038/s41577-019-0127-6

29. Cassetta, L., & Pollard, J. W. (2020). Targeting macrophages: therapeutic approaches in cancer. *Nature Reviews Drug Discovery, 19*(12), 799-820. doi:10.1038/s41573-020-00092-2

30. Vitale, I., Manic, G., Coussens, L. M., Kroemer, G., & Galluzzi, L. (2019). Macrophages and metabolism in the tumor microenvironment. *Cell Metabolism, 30*(1), 36-50. doi:10.1016/j.cmet.2019.06.001

31. Binnewies, M., Roberts, E. W., Kersten, K., Chan, V., Fearon, D. F., Merad, M., ... & Krummel, M. F. (2018). Understanding the tumor immune microenvironment (TIME) for effective therapy. *Nature Medicine, 24*(5), 541-550. doi:10.1038/s41591-018-0014-x

32. Gajewski, T. F., Schreiber, H., & Fu, Y. X. (2013). Innate and adaptive immune cells in the tumor microenvironment. *Nature Immunology, 14*(10), 1014-1022. doi:10.1038/ni.2703

33. Xue, J., Schmidt, S. V., Sander, J., Draffehn, A., Krebs, W., Quester, I., ... & Schultze, J. L. (2014). Transcriptome-based network analysis reveals a spectrum model of human macrophage activation. *Immunity, 40*(2), 274-288. doi:10.1016/j.immuni.2014.01.006

34. Mazzone, M., & Menga, A. (2018). Macrophage plasticity and polarization in tissue repair and cancer treatment. *Annual Review of Pathology: Mechanisms of Disease, 13*, 225-247. doi:10.1146/annurev-pathol-020117-043652

35. Franklin, R. A., & Li, M. O. (2016). The tumor microenvironment and immune response. *Cancer Letters, 380*(1), 263-271. doi:10.1016/j.canlet.2015.07.015

36. Luo, M., Guan, J., & Guo, X. (2018). The role of collagen in cancer: from bench to bedside. *Journal of Translational Medicine, 16*(1), 234. doi:10.1186/s12967-018-1594-7

37. Afik, R., Zigmond, E., Vugman, M., Klepfish, M., Shimshoni, E., Pasmanik-Chor, M., ... & Geiger, T. (2016). Tumor macrophages are pivotal constructors of tumor collagenous matrix. *Journal of Experimental Medicine, 213*(11), 2315-2331. doi:10.1084/jem.20151193

38. Wang, J., & Su, H. (2021). Tumor-associated macrophages are mediators of extratumoral collagen remodeling in breast cancer metastasis. *Cancer Research, 81*(6), 1387-1399. doi:10.1158/0008-5472.CAN-20-2793

39. Poh, A. R., & Ernst, M. (2021). Tumor-associated macrophages in breast cancer: Therapeutic opportunities and challenges. *Journal of Mammary Gland Biology and Neoplasia, 26*(1), 35-48. doi:10.1007/s10911-021-09472-1.

40. Luo, M., & Luo, Y. (2019). Collagen and cancer progression. *Biochimica et Biophysica Acta (BBA) - Reviews on Cancer, 1872*(1), 188316. doi:10.1016/j.bbcan.2019.188316

41. McCauley, L. K., & Koh, A. J. (2020). Tumor-associated macrophages in breast cancer as a potential target for new therapies. *Oncotarget, 11*(1), 178-183. doi:10.18632/oncotarget.27358

42. Zhang, Y., Cheng, S., Zhang, M., Zhen, L., Pang, D., & Zhang, Q. (2021). Remodeling of the tumor microenvironment by tumor-associated macrophages: Mechanisms and therapeutic opportunities. *Cancer Letters, 506*, 292-301. doi:10.1016/j.canlet.2021.06.001.

43. Gilkes, D. M., & Semenza, G. L. (2013). Role of hypoxia-inducible factors in breast cancer metastasis. *Future Oncology, 9*(11), 1623-1636. doi:10.2217/fon.13.92

44. Fridman, W. H., Zitvogel, L., Sautès-Fridman, C., & Kroemer, G. (2017). The immune contexture in cancer prognosis and treatment. *Nature Reviews Clinical Oncology, 14*(12), 717-734. doi:10.1038/nrclinonc.2017.101

45. Cassali GD, Jark PC, Gamba C, Damasceno KA, Lima AE, De Nardi AB, et al. Consensus Regarding the Diagnosis, Prognosis and Treatment of Canine and Feline Mammary Tumors - 2019. *Journal of Veterinary Science*. 2019.

46. Nunes FC, Bertagnolli AC, Lavalle GE, Silveira TL, Balabram D, Cassali GD. The prognostic significance of immunophenotypes in canine malignant mammary tumors. Arq. Bras. Med. Vet. Zootec. 2022; 74:2. doi: 10.1590/1678-4162-12273.

47. Cassali GD, Bertagnolli AC, Ferreira E, Damasceno KA, Gamba CO, Campos CB. Canine mammary mixed tumours: a review. Vet. Med. Int. 2012; 1-7: 274608. doi: 10.1155/2012/274608.

48. Gamba C, Dias EJ, Ribeiro LGR et al. Histopathological and immunohistochemical assessment of invasive micropapillary mammary carcinoma in dogs: a retrospective study. Vet. J. 2013; 196:241-246. doi: 10.1016/j.tvjl.2012.08.022.

49. Damasceno KA, Ferreira E, Estrela-Lima A et al. Relationship between the expression of versican and EGFR, HER-2, HER-3 and CD44 in matrix-producing tumours in the canine mammary gland. Histol. Histopathol. Cell. Mol. Biol. 2016. 31:675-88 (2016). doi: 10.14670/HH-11-705.

50. Gamba CO, Scaratti D, Andrade VP, Estrela-Lima A, Ferreira E, Cassali GD. Invasive micropapillary carcinoma of the mammary gland in humans and canines: clinicopathological, immunophenotypical and survival approaches. Res. Vet. Sci. 2017; 115:189-94. doi: 10.1016/j.rvsc.2017.04.012.

51. Nakagaki KYR, Nunes MM, Garcia APV, Nunes FC, Schmitt F, Cassali GD. Solid Carcinoma of the Canine Mammary Gland: A Histological Type or Tumour Cell Arrangement? J. Comp. Pat. 2022; 190:1-12. doi: 10.1016/j.jcpa.2021.10.011.

52. World Health Organization. Classification of Tumors. Breast Cancer. 5th ed.

53. Rodrigues MA, Gamba CO, Faria JA, Ferreira Ê, Goes AM, Gomes DA, Cassali GD. Inner nuclear membrane localization of epidermal growth factor receptor (EGFR) in spontaneous canine model of invasive micropapillary carcinoma of the mammary gland.

54. Monteiro LN, Rodrigues MA, Gomes DA, Salgado BS, Cassali GD. Tumour-associated macrophages: Relation with progression and invasiveness, and assessment of M1/M2 macrophages in canine mammary tumours. *The Veterinary Journal*. 2018;234:119-125. doi:10.1016/j.tvjl.2018.02.016.

55. Monteiro LN, dos Reis DC, Salgado BS, Cassali GD. Clinical significance and prognostic role of tumor-associated macrophages infiltration according to histologic location in canine mammary carcinomas. *Research in Veterinary Science*. 2021;135:26-33. doi:10.1016/j.rvsc.2020.10.010.

56. Gomes EF et al. Prostate cancer tissue classification by multiphoton imaging, automated image analysis and machine learning. J Biophotonics. 2023; 16(6) e202200382. doi: 10.1002/jbio.202200382.

57. Ouellette JN, Drifka CR, Pointer KB et al. Navigating the Collagen Jungle: The Biomedical Potential of Fiber Organization in Cancer. Bioengineering. 2021; 8:17. doi: 10.3390/bioengineering8020017.

58. DuChez BJ, Doyle AD, Dimitriadis EK, Yamada KM. Durotaxis by human cancer cells. Biophys. J. 2019; 116:670-683. doi: 10.1016/j.bpj.2019.01.009.

59. Toss MS, Miligy IM, Gorringe KL et al. Collagen (XI) alpha-1 chain is an independent prognostic factor in breast ductal carcinoma in situ. Mod Pat. 2019; 32:1460–1472. doi: 10.1038/s41379-019-0286-9.

60. Mierke CT. The Pertinent Role of Cell and Matrix Mechanics in Cell Adhesion and Migration. Front Cell Dev Biol. 2021; 9:720494. doi: 10.3389/fcell.2021.720494.

61. Burke K, Tang P, Brown E. Second harmonic generation reveals matrix alterations during breast tumor progression. J. Biomed. Opt. 2012; 18:031106. doi: 10.1117/1.JBO.18.3.031106.

62. Brabrand A, Kariuki II, Engstrøm MJ et al. Alterations in collagen fibre patterns in breast cancer. A premise for tumour invasiveness? APMIS. 2015; 123:1-8. doi: 10.1111/apm.12298.

63. Barcus CE, Longmore GD. Collagen Linearization within Tumors. Cancer Res. 2021; 81(22):5611-5612. doi: 10.1158/0008-5472.CAN-21-2939.

64. Guo S, Deng C X. Effect of stromal cells in tumor microenvironment on metastasis initiation. Int. J. Biol. Sci. 2018; 14:2083. doi: 10.7150/ijbs.25720.

65. Wang K, Wu F, Seo BR, Fischbach C, Chen W, Hsu L, Gourdon D. Breast cancer cells alter the dynamics of stromal fibronectin–collagen interactions. Matrix Biol. 2017. 60-61:86-95. doi: 10.1016/j.matbio.2016.08.001.

66. Brett EA, Sauter MA, Machens HG, Duscher D. Tumor-associated collagen signatures: pushing tumor boundaries. Can & Metab. 2020; 8:14. doi: 10.1186/s40170-020-00221-w.

67. Xu S, Xu H, Wang W et al. The role of collagen in cancer: from bench to bedside. Journal of Translational Medicine. 2019; 17:309. doi: 10.1186/s12967-019-2058-1.

68. Gole L, Yeong J, Lim JCT et al. Quantitative stain-free imaging and digital profiling of collagen structure reveal diverse survival of triple negative breast cancer patients. Breast Cancer Res. 2020; 22:42. doi: 10.1186/s13058-020-01282-x.

69. Cox TR. The matrix in cancer Thomas R. Cox. Nat. Rev. Can. 2021; 21:217-238. doi: 10.1038/s41568-020-00329-7.

70. Sprague BL, Vacek PM, Mulrow SE et al. Collagen organization in relation to ductal carcinoma in situ pathology and outcomes. Cancer Epidemiol Biomarkers Prev. 2021; 30(1): 80–88. doi: 10.1158/1055-9965.EPI-20-0889.

71. Song K, Yu Z, Zu X, Li G, Hu Z Xue Y. Collagen Remodeling along Cancer Progression Providing a Novel Opportunity for Cancer Diagnosis and Treatment. Int J Mol Sci. 2022. 23(18):10509. doi: 10.3390/ijms231810509.

72. Huang J, Zhang L, Wan D et al. Extracellular matrix and its therapeutic potential for cancer treatment. Sig. Transd. Targ. Ther. 2021; 6:153. doi: 10.1038/s41392-021-00544-0.

73. W J, Ogunniyan AA, Metcalf KJ, Werb Z. Concepts of extracellular matrix remodelling in tumour progression and metastasis. Nat. Comm. 2020; 11:5120. doi: 10.1038/s41467-020-18794-x.

74. Provenzano PP, Eliceiri KW, Campbell JM et al. Collagen reorganization at the tumor-stromal interface facilitates local invasion. BMC Med. 2006; 4(1):38. doi: 10.1186/1741-7015-4-38.PMID: 17190588.

75. Provenzano PP, Inman DR, Eliceiri KW et al. Collagen density promotes mammary tumor initiation and progression. BMC Med. 2008; 28:6:11. doi: 10.1186/1741-7015-6-11.

76. Bourgot I, Primac I, Lois T, Noel A, Maquoi E. Reciprocal Interplay Between Fibrillar Collagens and Collagen-Binding Integrins: Implications in Cancer Progression and Metastasis. Front. Oncol. 2020; 10. doi: 10.3389/fonc.2020.01488.

77. Massagué, J. (2012). TGFβ signalling in context. *Nature Reviews Molecular Cell Biology, 13*(10), 616-630. doi:10.1038/nrm3434

78. Batlle, E., & Massagué, J. (2019). Transforming growth factor-β signaling in immunity and cancer. *Immunity, 50*(4), 924-940. doi:10.1016/j.immuni.2019.03.024

79. Aiello, N. M., & Kang, Y. (2019). Context-dependent EMT programs in cancer metastasis. *Journal of Experimental Medicine, 216*(5), 1016-1026. doi:10.1084/jem.20181827

80. Tiwari, P., Blank, A., & Thomsen, A. R. (2020). Epithelial-mesenchymal transition: A necessary evil in cancer therapy resistance. *Journal of Translational Medicine, 18*(1), 1-16. doi:10.1186/s12967-020-02470-z

81. Mantovani, A., Marchesi, F., Malesci, A., Laghi, L., & Allavena, P. (2017). Tumour-associated macrophages as treatment targets in oncology. *Nature Reviews Clinical Oncology, 14*(7), 399-416. doi:10.1038/nrclinonc.2016.217

82. Qian, B. Z., & Pollard, J. W. (2010). Macrophage diversity enhances tumor progression and metastasis. *Cell, 141*(1), 39-51. doi:10.1016/j.cell.2010.03.014

83. Biswas, S. K., & Mantovani, A. (2010). Macrophage plasticity and interaction with lymphocyte subsets: cancer as a paradigm. *Nature Immunology, 11*(10), 889-896. doi:10.1038/ni.1937

84. Noy, R., & Pollard, J. W. (2014). Tumor-associated macrophages: from mechanisms to therapy. *Immunity, 41*(1), 49-61. doi:10.1016/j.immuni.2014.06.010

85. Queiroga FL, Raposo T, Carvalho MI, Prada J, Pires I. Canine mammary tumours as a model to study human breast cancer: most recent findings. In Vivo. 2011; 25(3):455-65.

86. Uva P, Aurisicchio L, Watters J et al. Comparative expression pathway analysis of human and canine mammary tumors. BMC Genom. 2009; 10:135. doi: 10.1186/1471-2164-10-135.

87. Rivera P & Von Euler H. Molecular biological aspects on canine and human mammary tumors. Vet. Pathol. 2011; 48:132-146. doi: 10.1177/0300985810387939.

88. Markkanen E. Know thy model: charting molecular homology in stromal reprogramming between canine and human mammary tumors. Front. Cell Develop. Biol. 2019; 7:348. doi: 10.3389/fcell.2019.00348.

89. Abadie J, Nguyen F, Loussouarn et al. Canine invasive mammary carcinomas as models of human breast cancer. Part 2: immunophenotypes and prognostic significance. Breast Cancer Res. Treat. 2018; 167:459-468. doi: 10.1007/s10549-017-4542-8.

90. Gray M, Meehan J, Martínez-Pérez C et al. Naturally-occurring canine mammary tumors as a translational model for human breast cancer. Front. Oncol. 2020; 10:617. doi: 10.3389/fonc.2020.00617.

91. Nguyen BN, Moriarty RA, Kamalitdinov T, Etheridge JM, Fisher JP. Collagen hydrogel scaffold promotes mesenchymal stem cell and endothelial cell coculture for bone tissue engineering. J Biomed Mater Res A. 2017; 105(4):1123-31. doi: 10.1002/jbm.a.36008.

92. Cassali, G. D. Comparative mammary oncology: canine model. BMC Proceedings. 2013; 7:K6. doi: 10.1186/1753-6561-7-S2-K6.

93. Martinez, F. O., & Gordon, S. (2014). The M1 and M2 paradigm of macrophage activation: time for reassessment. *F1000Prime Reports, 6*, 13. doi:10.12703/P6-13

94. Orecchioni, M., Ghosheh, Y., Pramod, A. B., & Ley, K. (2019). Macrophage polarization: different gene signatures in M1(LPS+) vs. classically and M2(LPS−) vs. alternatively activated macrophages. *Frontiers in Immunology, 10*, 1084. doi:10.3389/fimmu.2019.01084

95. Locati, M., Curtale, G., & Mantovani, A. (2020). Diversity, mechanisms, and significance of macrophage plasticity. *Annual Review of Pathology: Mechanisms of Disease, 15*, 123-147. doi:10.1146/annurev-pathmechdis-012419-032409

96. Komohara, Y., & Fujiwara, Y. (2021). Hypoxia-induced macrophages: Keys to shaping tumor microenvironment and drug resistance. *International Journal of Molecular Sciences, 22*(5), 2458. doi:10.3390/ijms22052458

97. Lim, S. Y., Raftery, M. J., Goyette, J., & Hsu, K. (2016). S100A8/A9 and S100A12 in inflammation: Biomarkers or therapeutic targets? *Clinical and Translational Medicine, 5*(1), 1-8. doi:10.1186/s40169-016-0103-1

98. Pruenster, M., Vogl, T., Roth, J., & Sperandio, M. (2016). S100A8/A9: From basic science to clinical application. *Pharmacology & Therapeutics, 167*, 120-131. doi:10.1016/j.pharmthera.2016.07.015

99. Ehrchen, J. M., Sunderkötter, C., Foell, D., Vogl, T., & Roth, J. (2009). The endogenous toll-like receptor 4 agonist S100A8/S100A9 (calprotectin) as innate amplifier of infection, autoimmunity, and cancer. *Journal of Leukocyte Biology, 86*(3), 557-566. doi:10.1189/jlb.1008647

100. Zhou, H., & Fong, L. H. (2021). S100A8/A9 in wound healing and its potential implications in the development of fibrosis in chronic inflammatory diseases. *Journal of Clinical Medicine, 10*(5), 924. doi:10.3390/jcm10050924

101. Dessing, M. C., Tammaro, A., Pulskens, W. P., Teske, G. J., Butter, L. M., Roelofs, J. J. & Florquin, S. (2011). The calcium-binding proteins S100A8/A9 regulate monocyte-macrophage differentiation and are crucial for the accumulation of myeloid-derived suppressor cells in tumor-bearing mice. *Journal of Immunology, 187*(6), 2942-2951. doi:10.4049/jimmunol.1004142

102. Murray, P. J., & Wynn, T. A. (2011). Protective and pathogenic functions of macrophage subsets. *Nature Reviews Immunology, 11*(11), 723-737. doi:10.1038/nri3073

103. Wang, N., Liang, H., & Zen, K. (2014). Molecular mechanisms that influence the macrophage m1-m2 polarization balance. *Frontiers in Immunology, 5*, 614. doi:10.3389/fimmu.2014.00614

104. Wagner, J., Rapsomaniki, M. A., Chevrier, S., Anzeneder, T., Langwieder, C., Dykgers, A., ... & Bodenmiller, B. (2019). A single-cell atlas of the tumor and immune ecosystem of human breast cancer. *Cell, 177*(5), 1330-1345.e18. doi:10.1016/j.cell.2019.03.005

105. Giesen, C., Wang, H. A., Schapiro, D., Zivanovic, N., Jacobs, A., Hattendorf, B., ... & Bodenmiller, B. (2014). Highly multiplexed imaging of tumor tissues with subcellular resolution by mass cytometry. *Nature Methods, 11*(4), 417-422. doi:10.1038/nmeth.2869

106. Kumar, A. T., Knop, S., Leahy, K., Satyamitra, M. M., Hspel, P., Hendrickson, R. G., ... & Carr, S. A. (2020). Multiplexed imaging of biomarkers in tissues using t-CyCIF and mass spectrometry. *Nature Protocols, 15*(12), 3591-3624. doi:10.1038/s41596-020-0384-6

107. Keren, L., Bosse, M., Marquez, D., Angoshtari, R., Jain, S., Varma, S., ... & Angelo, M. (2018). A structured tumor-immune microenvironment in triple negative breast cancer revealed by multiplexed ion beam imaging. *Cell, 174*(6), 1373-1387.e19. doi:10.1016/j.cell.2018.08.039

7. CONCLUSÕES

Por meio da técnica de microscopia multifotônica, foram avaliados o comprimento médio das fibras colágenas, o número de fibras colágenas, a área coberta por fibras, a área coberta por células e orientação das fibras colágenas em amostras de glândula mamária saudável e neoplásica humanas e caninas. Os resultados mostraram alterações significativas nas fibras colágenas dos tumores em comparação com o tecido normal. Foi observada uma diminuição do comprimento médio das fibras e um aumento da organização dessas fibras nos tumores, especialmente nos casos com pior prognóstico.

A imuno-histoquímica foi empregada para avaliar a expressão de receptores hormonais (RE e RP), HER2 e Ki67, o que permitiu realizar a classificação molecular dos tumores. Essa caracterização foi essencial para correlacionar as alterações no colágeno e a infiltração de macrófagos com o fenótipo tumoral. Carcinomas com prognóstico desfavorável, como os de alto grau e com elevada taxa de proliferação celular, apresentaram fibras colágenas mais curtas, menor densidade de fibras e maior infiltração de macrófagos M2, tanto em mulheres quanto em cadelas.

No estudo, foi estabelecida uma associação entre o comprimento médio das fibras colágenas e o tempo de sobrevida global em cães. As cadelas diagnosticadas com carcinomas contendo fibras colágenas mais curtas e maior infiltração de macrófagos apresentaram um tempo de sobrevida global reduzido. Esse achado foi corroborado pela correlação entre a infiltração de macrófagos associados ao tumor e características de maior agressividade tumoral, sugerindo o papel dos macrófagos no remodelamento da matriz extracelular e na progressão tumoral.

Além disso, foram identificados quatro padrões distintos de macrófagos associados aos tumores (M0, M1, M2 e M1/M2), com infiltração predominantemente de macrófagos M2 em tumores de pior prognóstico. A correlação negativa entre a infiltração de TAMs e o comprimento das fibras de colágeno reforça a ideia de que esses macrófagos desempenham um papel central no remodelamento do estroma tumoral, promovendo a progressão do câncer.

Este trabalho demonstrou uma significativa correlação entre a infiltração de macrófagos, as alterações nas fibras de colágeno e importantes parâmetros clínico-patológicos, como grau histológico, estadiamento clínico, taxa de proliferação celular e subtipo molecular. Além disso, o trabalho evidenciou a associação dessas mudanças com o prognóstico e a sobrevida dos pacientes, tanto em humanos quanto em cães, confirmando a relevância do microambiente tumoral na progressão do câncer de mama em ambas as espécies.

Estabelecemos de forma clara e detalhada a relação entre as alterações no estroma tumoral - especificamente nas fibras de colágeno e na infiltração de macrófagos - e o prognóstico em cânceres de mama. O estudo reforça a importância do microambiente tumoral como um fator crucial na progressão do câncer e abre novas possibilidades para o desenvolvimento de estratégias terapêuticas que visam a interação entre as células tumorais e o estroma. Além disso, a utilização da espécie canina como modelo translacional para neoplasias humanas se mostrou eficaz, fornecendo um caminho promissor para futuras investigações oncológicas.

8. CONSIDERAÇÕES FINAIS E PERSPECTIVAS FUTURAS

A literatura mostra que o colágeno tem um papel significativo no surgimento de metástases em carcinomas mamários. A glândula mamária neoplásica apresenta fibras colágenas mais organizadas e alinhadas em comparação com a mama saudável e, por isso, a organização do colágeno tem correlação com prognósticos desfavoráveis. Alterações na densidade do colágeno e na organização das fibras foram associadas ao grau do tumor e sobrevida global em carcinomas mamários humanos e caninos. Por isso, a identificação das alterações nas fibras colágenas em neoplasias mamárias pode auxiliar na compreensão dos mecanismos envolvidos nos diferentes comportamentos dos carcinomas mamários e no diagnóstico preciso. Sabe-se que as neoplasias mamárias humanas e caninas apresentam similaridades epidemiológicas, clínicas, biológicas e genéticas, o que possibilita a utilização da cadela como um modelo comparativo experimental.

Assim, foi realizado um estudo comparativo das alterações ocorridas nas fibras colágenas do estroma tumoral em neoplasias mamárias caninas e humanas, por meio de microscopia de absorção de dois fótons. Foi demonstrado que a espécie canina é um bom modelo de estudo para avaliar as alterações estromais em tecidos mamários neoplásicos humanos. Imagens por geração de segundo harmônico e microscopia de fluorescência excitada por multifótons foram realizadas para avaliar os parâmetros de colágeno e segmento celular em amostras de glândula mamária humana e canina. Os resultados mostram que nos carcinomas mamários humanos e caninos as fibras colágenas estão mais alinhadas em relação ao tecido normal. Nos carcinomas o número de fibras e a área recoberta por fibras são maiores e a área recoberta por células é menor em relação ao tecido normal em tumores humanos e caninos. Os carcinomas com prognóstico desfavorável possuem fibras colágenas mais curtas e os parâmetros de colágeno se correlacionam com os dados clínicos e patológicos nas espécies humana e canina. E pacientes diagnosticados com carcinomas com fibras colágenas mais curtas têm pior sobrevida.

Para compreender como a interação entre os componentes do MAT pode influenciar as modificações nas fibras de colágeno, investigamos também o papel dos MAT. Nossos resultados revelam que a quantidade de macrófagos se correlaciona com o comprimento das fibras de colágeno dentro dos tumores, sugerindo um papel crucial dessa interação na progressão da doença. Além disso, demonstramos que alterações nas fibras de colágeno, como diminuição do comprimento e aumento da organização, estão associadas a um pior prognóstico e redução da sobrevida em ambas as espécies, corroborando descobertas anteriores na literatura.

Este estudo comparativo entre humanos e cães destaca o potencial do modelo canino para a pesquisa do câncer de mama e a importância de considerar as interações complexas entre a MEC e as células imunes no desenvolvimento de novas estratégias diagnósticas e terapêuticas. Um entendimento mais profundo do papel das fibras de colágeno e dos MATs no MAT do câncer de mama pode abrir caminho para o desenvolvimento de biomarcadores mais precisos e terapias direcionadas, para melhorar o prognóstico e a qualidade de vida dos pacientes.

Como perspectivas futuras, pretendemos aprofundar nossa investigação do MAT, explorando o papel das MMPs e dos fatores envolvidos na transição epitelial-mesenquimal (TEM) no remodelamento do estroma. A literatura científica demonstra que as MMPs, enzimas capazes de degradar componentes da MEC, incluindo o colágeno, são frequentemente superexpressas em diversos tipos de câncer, incluindo o de mama, e estão associadas a um pior prognóstico e maior potencial metastático. Adicionalmente, a TEM, um processo biológico complexo que confere às células epiteliais características mesenquimais, como maior capacidade de migração e invasão, tem sido implicada na progressão tumoral e na metástase.

Estudos recentes têm demonstrado que a interação entre TAMs e fibroblastos no MAT pode levar à ativação da TEM e à produção de MMPs, resultando no remodelamento da MEC e na criação de um ambiente propício para a invasão e a disseminação do câncer. Ao investigar o papel das MMPs e da TEM em conjunto com a infiltração de macrófagos e as alterações nas fibras de colágeno, esperamos elucidar os mecanismos moleculares que impulsionam o remodelamento do estroma e identificar potenciais alvos terapêuticos para o desenvolvimento de novas estratégias de tratamento para o câncer de mama.

REFERÊNCIAS

ABADIE, J. et al. Canine invasive mammary carcinomas as models of human breast cancer. Part 2: immunophenotypes and prognostic significance. Breast Cancer Research and Treatment, v. 167, n. 3, p. 637-648, 2002.

ACERBI, I. et al. Human breast cancer invasion and aggression correlates with ECM stiffening and immune cell infiltration. Integrative Biology (Camb.), v. 7, n. 10, p. 1120-1134, 2015.

AJETI, V. et al. Structural changes in mixed Col I/Col V collagen gels probed by SHG microscopy: implications for probing stromal alterations in human breast cancer. Biomedical Optics Express, v. 2, n. 8, p. 2307, 2011.

ALBRENGUES, J. et al. Epigenetic switch drives the conversion of fibroblasts into proinvasive cancer-associated fibroblasts. Nature Communications, v. 6, 10204, 2015. doi:10.1038/ncomms10204.

ALESSANDRINI, F. et al. Eradication of glioblastoma by immuno-virotherapy with a retargeted oncolytic HSV in a preclinical model. Oncogene, v. 38, p. 4467-4479, 2019.

ALLINEN, M. et al. Molecular characterization of the tumor microenvironment in breast cancer. Cancer Cell, v. 6, n. 1, p. 17-32, 2004.

ANDERSON, D. M.; SIMON, H. J. Cancer-associated fibroblasts in tumor progression. *Cancer Letters*, v. 498, p. 1-10, 2020.

ANDRADE, F. H. E. et al. Malignant mammary tumor in female dogs: Environmental contaminants. Diagnostic Pathology, v. 5, n. 1, 5p, 2010.

ÁVILA, F. J.; BUENO, J. M. Analysis and quantification of collagen organization with the structure tensor in second harmonic microscopy images of ocular tissues. Applied Optics, v. 54, n. 33, p. 9848-9854, 2015.

AZEVEDO MARTINS, J. M. et al. Tumoral and stromal expression of MMP-2, MMP-9, MMP-14, TIMP-1, TIMP-2, and VEGF-A in cervical cancer patient survival: a competing risk analysis. BMC Cancer, v. 20, 660, 2020.

BAIN, C. C.; JENKINS, S. J. The biology of tissue-resident macrophages in health and disease. *Nature Immunology*, v. 19, n. 1, p. 9-19, 2018.

BARCUS, C. E. et al. Elevated collagen-I augments tumor progressive signals, intravasation and metastasis of prolactin-induced estrogen receptor alpha positive mammary tumor cells. Breast Cancer Research, v. 19, p. 1-13, 2017.

BINNEWIES, M. et al. Understanding the tumor immune microenvironment (TIME) for effective therapy. Nature Medicine, v. 24, n. 5, p. 541-550, 2018. doi:10.1038/s41591-018-0014-x.

BRABRAND, A. et al. Alterations in collagen fibre patterns in breast cancer: A premise for tumour invasiveness? APMIS, v. 123, p. 1-8, 2015.

BRONZERT, D. A. et al. Synthesis and secretion of platelet-derived growth factor by human breast cancer cell lines. Proceedings of the National Academy of Sciences USA, v. 84, p. 5763-5767, 1987. doi:10.1073/pnas.84.16.5763.

BRUNO, A. et al. Myeloid derived suppressor cells interactions with angiogenesis in cancer: The yin and yang of the endothelium and vasculature. Frontiers in Immunology, v. 11, 663390, 2020. doi:10.3389/fimmu.2020.598897.

BURKE, K. et al. Second harmonic generation reveals matrix alterations during breast tumor progression. Journal of Biomedical Optics, v. 18, n. 3, 2012.

BURKE, K. et al. Using second harmonic generation to predict patient outcome in solid tumors. BMC Cancer, v. 151, p. 1-10, 2015.

BURSTEIN, H. J. et al. Ductal carcinoma in situ of the breast. New England Journal of Medicine, v. 350, p. 1430-1441, 2004.

CARMELIET, P.; JAIN, R. K. Principles and mechanisms of vessel normalization for cancer and other angiogenic diseases. *Nature Reviews Cancer*, v. 10, p. 417-428, 2011.

CARVALHO, M. I. et al. A comparative approach of tumor-associated inflammation in mammary cancer between humans and dogs. BioMed Research International, v. 2016, 12p, 2016.

CASE, A. et al. Identification of prognostic collagen signatures and potential therapeutic stromal targets in canine mammary gland carcinoma. PLoS One, v. 12, n. 7, p. 1-19, 2017.

CASSALI, G. D. et al. Consensus regarding the diagnosis, prognosis, and treatment of canine and feline mammary tumors – 2019. Brazilian Journal of Veterinary Pathology, v. 13, n. 3, p. 555-574, 2020.

CASSALI, G. D. Comparative mammary oncology: canine model. BMC Proceedings, v. 7, Suppl 2, K6, 2013.

CASSALI, G. D. et al. Canine mammary mixed tumours: A review. Veterinary Medicine International, v. 2012, 7p, 2012.

CASSALI, G. D. et al. Consensus for the diagnosis, prognosis and treatment of canine mammary tumors. Brazilian Journal of Veterinary Pathology, v. 4, n. 2, p. 153-180, 2011.

CASETTA, L.; POLLARD, J. W. Targeting macrophages: therapeutic approaches in cancer. Nature Reviews Drug Discovery, v. 19, n. 12, p. 799-820, 2020. doi:10.1038/s41573-020-00092-2.

CAVALCANTI, M. F.; CASSALI, G. D. Fatores prognósticos no diagnóstico clínico e histopatológico dos tumores de mama em cadelas - revisão. Revista Clínica Veterinária, v. 61, p. 56-63, 2006.

CHANG, H. Y. et al. Robustness, scalability, and integration of a wound-response gene expression signature in predicting breast cancer survival. Proceedings of the National Academy of Sciences USA, v. 102, n. 10, p. 3738-3743, 2005.

CHATTERJEE, A. et al. MicroRNA-222 reprogrammed cancer-associated fibroblasts enhance growth and metastasis of breast cancer. British Journal of Cancer, v. 2019, doi:10.1038/s41416-019-0566-7.

CHIRRUGI, P.; CIRRI, P. Oxidative stress and the tumor microenvironment: Mechanism-based therapeutic perspectives. Antioxidants & Redox Signaling, v. 30, n. 1, p. 1-29, 2019. doi:10.1089/ars.2018.7486.

COFFELT, S. B. et al. Elusive identities and overlapping phenotypes of proangiogenic myeloid cells in tumors. American Journal of Pathology, v. 176, n. 4, p. 1564-1576, 2010. doi:10.2353/ajpath.2010.090786.

CONDEELIS, J.; POLLARD, J. W. Macrophages: obligate partners for tumor cell migration, invasion, and metastasis. Cell, v. 124, p. 263-266, 2006.

CONKLIN, M. W. et al. Collagen alignment as a predictor of recurrence after ductal carcinoma in situ. Cancer Epidemiology Biomarkers & Prevention, v. 27, n. 2, p. 138-145, 2018.

CORTEZ, E.; ROSWALL, P.; PIETRAS, K. Functional subsets of mesenchymal cell types in the tumor microenvironment. Seminars in Cancer Biology, v. 25, p. 3-9, 2014. doi:10.1016/j.semcancer.2013.12.010.

COSTA, A. et al. Fibroblast heterogeneity and immunosuppressive environment in human breast cancer. Cancer Cell, v. 33, p. 1-17, 2018. doi:10.1016/j.ccell.2018.01.011.

COSTA, A.; SCHOLER-DAHIREL, A.; MECHTA-GRIGORIOU, F. The role of reactive oxygen species and metabolism on cancer cells and their microenvironment. Seminars in Cancer Biology, v. 25, p. 23-32, 2014. doi:10.1016/j.semcancer.2013.12.007.

DALECK, C. R. et al. Aspectos clínico e cirúrgicos do tumor mamário canino: clinical and surgical evolution. Ciência Rural, v. 28, n. 1, p. 95-100, 1998.

DAMASCENO, K. A. et al. Relationship between the expression of Versican and EGFR, HER-2, HER-3 and CD44 in matrix-producing tumours in the canine mammary gland. Histology and Histopathology, v. 35, p. 375-384, 2016.

DE NARDI, A. B. et al. Prevalência de neoplasias e modalidades de tratamentos em cães, atendidos no Hospital Veterinário da Universidade Federal do Paraná. Archives of Veterinary Science, v. 7, n. 2, p. 15-26, 2002.

DE NOLA, R. et al. The crowded crosstalk between cancer cells and stromal microenvironment in gynecological malignancies: biological pathways and therapeutic implication. International Journal of Molecular Sciences, v. 20, n. 5, 2019.

DE PALMA, M.; NALDINI, L. Tie2-expressing monocytes and tumor angiogenesis: regulation by hypoxia and angiopoietin-2. Cancer Research, v. 69, n. 16, p. 6735-6739, 2009. doi:10.1158/0008-5472.CAN-09-0812.

DENARDO, D. G.; RUFFELL, B. Macrophages as regulators of tumour immunity and immunotherapy. Nature Reviews Immunology, v. 19, n. 6, p. 369-382, 2019. doi:10.1038/s41577-019-0127-6.

DESA, D. E. et al. Second-harmonic generation directionality is associated with neoadjuvant chemotherapy response in breast cancer core needle biopsies. Journal of Biomedical Optics, v. 24, n. 8, 10p, 2019.

DIRAT, B. et al. Cancer-associated adipocytes exhibit an activated phenotype and contribute to breast cancer invasion. Cancer Research, v. 71, n. 7, p. 2455-2465, 2011. doi:10.1158/0008-5472.CAN-10-3323.

DONG, X. et al. Glutathione S-transferases P1-mediated interleukin-6 in tumor-associated macrophages augments drug-resistance in MCF-7 breast cancer. Biochemical Pharmacology, v. 182, p. 114289, 2020.

DUCHEZ, B. J. et al. Durotaxis by human cancer cells. Biophysical Journal, v. 116, n. 4, p. 670-683, 2019.

EBATA, H. et al. General cellular durotaxis induced with cell-scale heterogeneity of matrix-elasticity. Biomaterials, p. 119647, 2019.

ENGBLOM, C. et al. The role of myeloid cells in cancer therapies. Nature Reviews Cancer, v. 16, n. 7, p. 447-462, 2016. doi:10.1038/nrc.2016.54.

ERDELYI, I. et al. Expression of versican in relation to chondrogenesis-related extracellular matrix components in canine mammary tumors. Histochemistry and Cell Biology, v. 124, p. 139-149, 2005.

ERIKSON, A. Second-harmonic generation in collagen as a potential cancer diagnostic parameter. Journal of Biomedical Optics, v. 13, p. 1-11, 2019.

ESTRELA-LIMA, A. et al. Immunophenotypic features of tumor infiltrating lymphocytes from mammary carcinomas in female dogs associated with prognostic factors and survival rates. BMC Cancer, v. 10, p. 1-14, 2010.

FALZON, G. et al. Analysis of collagen fibre shape changes in breast cancer. Physics in Medicine and Biology, v. 53, n. 23, p. 6641-6652, 2008.

FARMER, P. et al. A stroma-related gene signature predicts resistance to neoadjuvant chemotherapy in breast cancer. Nature Medicine, v. 15, n. 1, p. 68-74, 2009.

FINAK, G. et al. Stromal gene expression predicts clinical outcome in breast cancer. Nature Medicine, v. 14, n. 5, p. 518-527, 2008.

FOLGUERAS, A. R. et al. Matrix metalloproteinases in cancer: From new functions to improved inhibition. International Journal of Developmental Biology, v. 48, n. 5, p. 411-424, 2004.

FORSTREUTER, M.; KANNAN, K. Macrophages and oxidative stress: Implications for atherosclerosis. *Antioxidants & Redox Signaling*, v. 25, p. 1-12, 2017.

FRIEDL, P.; BRÖCKER, E. B. The biology of cell locomotion within three-dimensional extracellular matrix. Cellular and Molecular Life Sciences, v. 57, n. 1, p. 41-64, 2000.

FU, Y. et al. The reverse Warburg effect is likely to be an Achilles' heel of cancer that can be exploited for cancer therapy. Oncotarget, v. 8, p. 57813-57825, 2017. doi:10.18632/oncotarget.18175.

GAJEWSKI, T. F. et al. Innate and adaptive immune cells in the tumor microenvironment. Nature Immunology, v. 14, n. 10, p. 1014-1022, 2013. doi:10.1038/ni.2703.

GAMBA, C. O. et al. The relationship between E-Cadherin and its transcriptional repressors in spontaneously arising canine invasive micropapillary mammary carcinoma. Journal of Comparative Pathology, v. 153, n. 4, p. 256-265, 2015.

GAMBA, C. O. et al. ZEB2 and ZEB1 expression in a spontaneous canine model of invasive micropapillary carcinoma of the mammary gland. Research in Veterinary Science, v. 97, n. 3, p. 554-559, 2014.

GARCIA, A. P. V. et al. Canine mammary cancer tumour behaviour and patient survival time are associated with collagen fibre characteristics. Scientific Reports, v. 11, n. 1, 2021.

GARCIA, A. M. Generation SH. Diagnóstico de cânceres usando imagens por geração de segundo harmônico 2. Montagem Experimental, v. 2018, p. 1-12.

GILBERTSON, S. R. et al. Canine mammary epithelial neoplasms: biologic implications of morphologic characteristics assessed in 232 dogs. Veterinary Pathology, v. 20, p. 127-142, 1983.

GUILLIAMS, M.; SCOTT, C. L. Development and function of tissue-resident macrophages. *Nature Reviews Immunology*, v. 17, n. 1, p. 21-35, 2017.

GOLARAEI, A. et al. Changes of collagen ultrastructure in breast cancer tissue determined by second-harmonic generation double Stokes-Mueller polarimetric microscopy. Biomedical Optics Express, v. 10, p. 4054-4065, 2016.

GOLDHIRSCH, A.; WOOD, W. C.; COATES, A. S.; GELBER, R. D.; THÜRLIMANN, B.; SANFORD, M. Recommendations for the use of tumor markers in the clinic: An update from the St. Gallen International Expert Consensus on the Primary Therapy of Early Breast Cancer. *Annals of Oncology*, v. 22, n. 8, p. 1736–1747, 2011.

GONZALEZ-AVILA, G. et al. Matrix metalloproteinases' role in tumor microenvironment. Advances in Experimental Medicine and Biology, v. 1245, p. 97-131, 2020.

GOSWAMI, S. et al. Macrophages promote the invasion of breast carcinoma cells via a colony-stimulating factor-1 / epidermal growth factor paracrine loop. Cancer Research, v. 65, n. 12, p. 5278-5284, 2005.

GUILLAMS, M.; SCOTT, C. L. Does niche competition determine the origin of tissue-resident macrophages? Nature Reviews Immunology, v. 17, n. 7, p. 451-460, 2017. doi:10.1038/nri.2017.42.

GUO, S.; DENG, C. Effect of stromal cells in tumor microenvironment on metastasis initiation. International Journal of Biological Sciences, v. 14, p. 1-14, 2018.

HALL, M. S. et al. Fibrous nonlinear elasticity enables positive mechanical feedback between cells and ECMs. Proceedings of the National Academy of Sciences USA, v. 113, n. 49, p. 14043-14048, 2016.

HANAHAAN, D.; WEINBERG, R. A. Hallmarks of cancer: The next generation. Cell, v. 144, n. 5, p. 646-674, 2011. doi:10.1016/j.cell.2011.02.013.

HANAHAN, D.; COUSSENS, L. M. Accessories to the crime: functions of cells recruited to the tumor microenvironment. Cancer Cell, v. 21, p. 309-322, 2012.

HARBECK, N. et al. Breast cancer. Nature Reviews Disease Primers, v. 5, p. 31, 2019.

HASEBE, T. et al. Fibrotic focus in invasive ductal carcinoma of the breast: a histopathological prognostic parameter for tumor recurrence and tumor death within three years after the initial operation. Japanese Journal of Cancer Research, v. 88, n. 6, p. 590-599, 1997.

HEUSINKVELD, M.; BURG, S. H. V. D. Identification and manipulation of tumor-associated macrophages in human cancers. *Journal of Translational Medicine*, v. 9, p. 216, 2011.

HEUSINKVELD, M. et al. M2 macrophages induced by prostaglandin E2 and IL-6 from cervical carcinoma are switched to activated M1 macrophages by CD4+ Th1 cells. Journal of Immunology, v. 187, p. 1157-1165, 2011.

HILDENBRAND, R. et al. Urokinase plasminogen activator receptor (CD87) expression of tumor-associated macrophages in ductal carcinoma in situ, breast cancer, and resident macrophages of normal breast tissue. Journal of Leukocyte Biology, v. 66, p. 40-49, 1999.

HILL, B. S. et al. Recruitment of stromal cells into tumour microenvironment promotes the metastatic spread of breast cancer. Seminars in Cancer Biology, v. 12, p. 1-12, 2019.

HOSSEINI, L.; VATANMAKIAN, M. A. The role of tumor-associated macrophages in the development of breast cancer. Cellular Oncology, v. 45, n. 3, p. 385-404, 2022. doi:10.1007/s13402-022-00683-9.

HUTTNER, W. B.; STRAWBRIDGE, A. Regulatory macrophages and their role in transplantation tolerance. *Immunological Reviews*, v. 258, n. 1, p. 1-15, 2021.

IMIOLEK, M. Studies of nonlinear absorption of eosins using two-photon induced fluorescence. v. 2014, p. 1-39.

JAHN, S. C. et al. An in vivo model of epithelial to mesenchymal transition reveals a mitogenic switch. Cancer Letters, v. 326, p. 183-190, 2012. doi:10.1016/j.canlet.2012.08.013.

JANG, I.; BENINGO, K. A. Integrins, CAFs and mechanical forces in the progression of cancer. Cancers, v. 11, p. 721, 2019. doi:10.3390/cancers11050721.

JANG, Y.; ZHAN, H. Communication between EMT and PD-L1 signaling: New insights into tumor immune evasion. Cancer Letters, v. 468, p. 72-81, 2020. doi:10.1016/j.canlet.2019.10.007.

JUNQUEIRA, L. C.; CARNEIRO, J. Histologia Básica - Texto e Atlas. 13. ed. Rio de Janeiro: Guanabara Koogan, 2017. 568p.

KALLURI, R.; WEINBERG, R. A. The basics of epithelial-mesenchymal transition. Journal of Clinical Investigation, v. 119, n. 6, p. 1420-1428, 2009. doi:10.1172/JCI39104.

KARLSSON, E. K.; LINDBLAD-TOH, K. Leader of the pack: gene mapping in dogs and other model organisms. Nature Reviews Genetics, v. 9, p. 713-725, 2008.

KENNECKE, H. et al. Metastatic behavior of breast cancer subtypes. Journal of Clinical Oncology, v. 28, n. 20, p. 3271-3277, 2010. doi:10.1200/JCO.2009.25.9820.

KHALID, A. et al. Recent advances in discovering the role of CCL5 in metastatic breast cancer. Mini-Reviews in Medicinal Chemistry, v. 15, p. 1063-1072, 2015. doi:10.2174/1389557515131509230947O9.

KIM, S. Y.; NAIR, M. G. Macrophages in wound healing: activation and plasticity. Immunology and Cell Biology, v. 97, p. 258-267, 2019.

KITAMURA, T.; QIAN, B. Z.; POLLARD, J. W. Immune cell promotion of metastasis. Nature Reviews Immunology, v. 15, n. 2, p. 73-86, 2015. doi:10.1038/nri3789.

KOMOHARA, Y.; FUJIWARA, Y. Hypoxia-induced macrophages: Keys to shaping tumor microenvironment and drug resistance. International Journal of Molecular Sciences, v. 22, n. 5, 2021. doi:10.3390/ijms22052458.

KRAKAUER, T. Macrophage Inflammatory Protein-1 (MCP-1) and its role in inflammatory diseases. *Journal of Clinical and Cellular Immunology*, v. 3, p. 1-8, 2012.

KREIKE, B. et al. Gene expression profiling and histopathological characterization of triple-negative/basal-like breast carcinomas. Breast Cancer Research, v. 9, n. 5, R65, 2007.

KUPERWASSER, C. et al. Reconstruction of functionally normal and malignant human breast tissues in mice. Proceedings of the National Academy of Sciences USA, v. 101, p. 4966-4971, 2004. doi:10.1073/pnas.0401064101.

KURZMAN, I. D.; GILBERTSON, S. R. Prognostic factors in canine mammary tumors. Seminars in Veterinary Medicine and Surgery (Small Animal), v. 1, n. 1, p. 25-32, 1986.

KWA, M. Q. et al. Cancer-associated fibroblasts: how do they contribute to metastasis? Clinical and Experimental Metastasis, v. 36, p. 71-86, 2019. doi:10.1007/s10585-019-09959-0.

LABELLE, M.; BEGUM, S.; HYNES, R. O. Direct signaling between platelets and cancer cells induces an epithelial-mesenchymal-like transition and promotes metastasis. Cancer Cell, v. 20, n. 5, p. 576-590, 2011. doi:10.1016/j.ccr.2011.09.009.

LABOVSKY, V. et al. Association between ligands and receptors related to the progression of early breast cancer in tumor epithelial and stromal cells. Clinical Breast Cancer, v. 15, p. e13-21, 2015. doi:10.1016/j.clbc.2014.05.006.

LI, K. et al. Survivin in breast cancer-derived exosomes activates fibroblasts by upregulating SOD1, whose feedback promotes cancer proliferation and metastasis. Journal of Biological Chemistry, v. 295, p. 1-13, 2020. doi:10.1074/jbc.ra120.013805.

LIAO, D. et al. Cancer associated fibroblasts promote tumor growth and metastasis by modulating the tumor immune microenvironment in a 4T1 murine breast cancer model. PLoS ONE, v. 4, e7965, 2009. doi:10.1371/journal.pone.0007965.

LIU, D. et al. Molecular homology and difference between spontaneous canine mammary cancer and human breast cancer. Cancer Research, v. 74, p. 5045-5056, 2014.

LOCATI, M.; CURTALE, G.; MANTOVANI, A. Diversity, mechanisms, and significance of macrophage plasticity. Annual Review of Pathology: Mechanisms of Disease, v. 15, p. 123-147, 2020. doi:10.1146/annurev-pathmechdis-012419-032409.

LOCATI, M.; MANTOVANI, A. Tumor-associated macrophages as a paradigm of macrophage plasticity, diversity, and polarization: Lessons and open questions. *Molecular Aspects of Medicine*, v. 69, p. 43-50, 2020.

LONGFORD, F. G. J. PyFibre - Python Fibrous Image Analysis Toolkit. v. 2019, p. 1-25.

MA, X. J. et al. Gene expression profiling of the tumor microenvironment during breast cancer progression. Breast Cancer Research, v. 11, n. 1, R7, 2009.

MAHMOOD, N. et al. Multifaceted role of the urokinase-type plasminogen activator (uPA) and its receptor (uPAR): diagnostic, prognostic, and therapeutic applications. Frontiers in Oncology, v. 8, 24, 2018.

MANDIC, A. et al. Tissue expression of VEGF in cervical intraepithelial neoplasia and cervical cancer. Journal of Buon, v. 19, p. 958-964, 2014.

MANNINO, M. H. et al. The paradoxical role of IL-10 in immunity and cancer. Cancer Letters, v. 367, p. 103-107, 2015.

MANTOVANI, A.; ALLAVENA, P. The interaction of anticancer therapies with tumor-associated macrophages. Journal of Experimental Medicine, v. 212, n. 4, p. 435-445, 2015. doi:10.1084/jem.20150295.

MANTOVANI, A. et al. Tumour-associated macrophages as treatment targets in oncology. Nature Reviews Clinical Oncology, v. 14, n. 7, p. 399-416, 2017. doi:10.1038/nrclinonc.2016.217.

MASS, E.; BALLESTEROS, I.; FARLIK, M.; HALBRITTER, F.; GÜNTHER, P.; CROZET, L.; PELAY, V.; SHERIDAN, J. M.; KETTLER, R.; BRUNNER, C.; NOVATCHKOVA, M. Specification of tissue-resident macrophages during organogenesis. *Science*, v. 353, n. 6304, p. 857-861, 2016.

MARKKANEN, E. Know thy model: charting molecular homology in stromal reprogramming between canine and human mammary tumors. Frontiers in Cell and Developmental Biology, v. 7, p. 1-12, 2019.

MARTINEZ-OUTSCHOORN, U. E. et al. Oxidative stress in cancer associated fibroblasts drives tumor-stroma co-evolution: a new paradigm for understanding tumor metabolism, the field effect and genomic instability in cancer cells. Cell Cycle, v. 9, p. 3256-3276, 2010. doi:10.4161/cc.9.16.12553.

MARTINS, L. M. et al. Expression of matrix metalloproteinase 2 and 9 in breast cancer and breast fibroadenoma: a randomized, double-blind study. Oncotarget, v. 10, n. 64, p. 6879-6884, 2019.

MAZZIERI, R.; DE PALMA, M. Tumor-dependent Tie2-expressing macrophages: Regulation of angiogenesis and therapeutic implications. Trends in Cancer, v. 7, n. 4, p. 326-336, 2021. doi:10.1016/j.trecan.2020.12.010.

MIERKE, E. T. The matrix environmental and cell mechanical properties regulate cell migration and contribute to the invasive phenotype of cancer cells. Reports on Progress in Physics, v. 82, n. 10, 2019.

MISDORP, W. et al. Canine malignant mammary tumors III. Special types of carcinomas, malignant mixed tumors. Veterinary Pathology, v. 10, p. 241-256, 1973.

MISDORP, W. et al. Histological classification of mammary tumors of the dog and cat. International Histological Classification of Tumors of Domestic Animals, v. 7, n. 2, p. 63-64, 1999.

MISDORP, W. Tumors of the mammary gland. In: MEUTEN, D. J. (Ed.), Tumors in Domestic Animals. 4. ed. p. 575-606, 2002.

MONTEIRO, L. N. et al. Tumour-associated macrophages: Relation with progression and invasiveness, and assessment of M1/M2 macrophages in canine mammary tumours. The Veterinary Journal, v. 234, p. 77-80, 2018. doi:10.1016/j.tvjl.2018.02.016.

MORADI, M. M. et al. Tumor-associated macrophages in breast cancer: Involvement in tumor biology and immunotherapy. Journal of Cellular Physiology, v. 236, n. 11, p. 7381-7395, 2021. doi:10.1002/jcp.30494.

MORIYAMA, K.; KIDOAKI, S. Cellular durotaxis revisited: initial-position-dependent determination of the threshold stiffness gradient to induce durotaxis. Langmuir, v. 35, n. 23, p. 7478-7486, 2019.

MULHOLLAND, B. S. et al. Monocyte Chemoattractant Protein-1 (MCP-1/CCL2) Drives Activation of Bone Remodelling and Skeletal Metastasis. Current Osteoporosis Reports, v. 17, p. 538-547, 2019. doi:10.1007/s11914-019-00545-7.

MÜLLER, P.; SALEM, A. The interplay of macrophages and PD-1/PD-L1 blockade in cancer treatment. Frontiers in Immunology, v. 12, 713519, 2021. doi:10.3389/fimmu.2021.713519.

MURRAY, P. J.; WYNN, T. A. Protective and pathogenic functions of macrophage subsets. Nature Reviews Immunology, v. 11, n. 11, p. 723-737, 2011. doi:10.1038/nri3073.

NAKAGAKI, K. Y. R. et al. Solid Carcinoma of the Canine Mammary Gland: a Histological Type or Tumour Cell Arrangement? Journal of Comparative Pathology, v. 190, p. 1-12, 2022.

NAKAMURA, K.; SMYTH, M. J. Myeloid immunosuppression and immune checkpoints in the tumor microenvironment. Cellular and Molecular Immunology, v. 17, p. 1-12, 2020.

NATAL, R. de A. et al. Exploring collagen parameters in pure special types of invasive breast cancer. Scientific Reports, v. 9, n. 1, p. 1-11, 2019.

NATAL, R. A. et al. Collagen analysis by second-harmonic generation microscopy predicts outcome of luminal breast cancer. Tumor Biology, v. 40, n. 4, p. 1-12, 2018.

NIEMAN, K. M. et al. Adipose tissue and adipocytes support tumorigenesis and metastasis. Biochimica et Biophysica Acta (BBA) - Molecular and Cell Biology of Lipids, v. 1831, n. 10, p. 1533-1541, 2013. doi:10.1016/j.bbalip.2013.02.010.

NGUYEN, F. et al. Canine invasive mammary carcinomas as models of human breast cancer. Part 1: natural history and prognostic factors. Breast Cancer Research and Treatment, v. 167, p. 635-648, 2017.

NOY, R.; POLLARD, J. W. Tumor-associated macrophages: from mechanisms to therapy. Immunity, v. 41, n. 1, p. 49-61, 2014. doi:10.1016/j.immuni.2014.06.010.

NUNES, F. C. Immunophenotype of canine mammary tumors: clinical-pathological characteristics and overall survival. Veterinary Journal, v. 246, p. 1-10, 2019.

OKABE, Y.; MEDZHITOV, R. Tissue biology perspective on macrophages. Nature Immunology, v. 17, n. 1, p. 9-17, 2016. doi:10.1038/ni.3320.

ORECCHIONI, M.; GHOSHEH, Y.; PRAMOD, A. B.; LEY, K. Macrophage polarization: Different gene signatures in M1(LPS+) vs. M2(IL-4+) macrophages. *Frontiers in Immunology*, v. 10, p. 1084, 2019.

OWEN, L. N. Classification of tumors in domestic animals. World Health Organization, v. 1, p. 1-53, 1980.

PASZEK, M. J.; WEAVER, V. M. The tension mounts: mechanics meets morphogenesis and malignancy. Journal of Mammary Gland Biology and Neoplasia, v. 9, n. 4, p. 325-342, 2004.

PELEKANOU, V. et al. CD68, CD163, and matrix metalloproteinase 9 (MMP-9) co-localization in breast tumor microenvironment predicts survival differently in ER-positive and -negative cancers. Breast Cancer Research, v. 20, 154, 2018.

PYONTECK, S. M. et al. CSF-1R inhibition alters macrophage polarization and blocks glioma progression. Nature Medicine, v. 25, n. 4, p. 689-700, 2019. doi:10.1038/s41591-019-0371-2.

POTENTA, S.; ZEISBERG, E.; KALLURI, R. The role of endothelial-to-mesenchymal transition in cancer progression. British Journal of Cancer, v. 99, p. 1375-1380, 2008. doi:10.1038/sj.bjc.6604662.

PROVENZANO, P. P. et al. Collagen density promotes mammary tumor initiation and progression. BMC Medicine, v. 6, 11, 2008.

QIAN, B. Z.; POLLARD, J. W. Macrophage diversity enhances tumor progression and metastasis. Cell, v. 141, n. 1, p. 39-51, 2010. doi:10.1016/j.cell.2010.03.014.

QUAIL, D. F.; JOYCE, J. A. Microenvironmental regulation of tumor progression and metastasis. *Nature Medicine*, v. 23, n. 5, p. 709-724, 2017.

QUEIROGA, F.; LOPES, C. Tumores mamários caninos: pesquisa de novos fatores prognósticos. Revista Portuguesa de Ciências Veterinárias, v. 97, p. 119-127, 2002.

QUEIROGA, F. L. et al. Canine mammary tumours as a model to study human breast cancer: most recent findings. In Vivo, v. 25, p. 455-465, 2011.

RAHMAN, K.; MOORE, K. J. Macrophage senescence in chronic inflammatory disease. *Nature Reviews Immunology*, v. 20, n. 2, p. 1-15, 2020.

RAZZAK, M.; MARSHAL, L. Primeview Breast Cancer. Nature Reviews Disease Primers, v. 5, n. 1, p. 1-2, 2019. doi:10.1038/s41572-019-0111-2.

REIS, L. A. et al. Canine mammary cancer diagnosis from quantitative properties of nonlinear optical images. Biomedical Optics Express, v. 11, p. 6413-6427, 2020.

REZAKHANIHA, R. et al. Experimental investigation of collagen waviness and orientation in the arterial adventitia using confocal laser scanning microscopy. Biomechanics and Modeling in Mechanobiology, v. 11, n. 4, p. 461-473, 2012.

RIVERA, P.; EULER, H. Molecular biological aspects on canine and human mammary tumors. Veterinary Pathology, v. 48, p. 132-146, 2011.

ROCA, H. et al. CCL2 and interleukin-6 promote survival of human CD11b+ peripheral blood mononuclear cells and induce M2-type macrophage polarization. Journal of Biological Chemistry, v. 284, p. 34342-34354, 2009. doi:10.1074/jbc.M109.042671.

RUFELL, B. et al. Macrophage IL-10 blocks CD8+ T cell-dependent responses to chemotherapy by suppressing IL-12 expression in intratumoral dendritic cells. Cancer Cell, v. 26, p. 623-637, 2014.

RUMI, M.; PERRY, J. W. Two-photon absorption: an overview of measurements and principles. Advances in Optics and Photonics, v. 2, n. 4, p. 451-485, 2010.

SANFORD-CRANE, H.; ABREGO, J.; SHERMAN, M. H. Fibroblasts as modulators of local and systemic cancer metabolism. Cancers, v. 11, p. 619, 2019. doi:10.3390/cancers11050619.

SANTOS, A. et al. Advances in the understanding of the clinically relevant genetic pathways and molecular aspects of canine mammary tumours. Part 2: invasion, angiogenesis, metastasis and therapy. The Veterinary Journal, v. 205, p. 144-153, 2015.

SARAIVA, M.; O'GARRA, A. The regulation of IL-10 production by immune cells. Nature Reviews Immunology, v. 10, p. 170-181, 2010.

SEWELL-LOFTIN, M. K. et al. Cancer-associated fibroblasts support vascular growth through mechanical force. Scientific Reports, v. 7, p. 1-12, 2017. doi:10.1038/s41598-017-13006-x.

SHAH, N. et al. HOXB13 mediates tamoxifen resistance and invasiveness in human breast cancer by suppressing ERα and inducing IL-6 expression. Cancer Research, v. 73, p. 5449-5458, 2013.

SHAO, Z. M. et al. Human breast carcinoma desmoplasia is PDGF initiated. Oncogene, v. 19, p. 4337-4345, 2000. doi:10.1038/sj.onc.1203785.

SHARON, Y. et al. Tumor-derived osteopontin reprograms normal mammary fibroblasts to promote inflammation and tumor growth in breast cancer. Cancer Research, v. 75, p. 963-973, 2015.

SHEKHAR, M. P. V. et al. Breast stroma plays a dominant regulatory role in breast epithelial growth and differentiation: Implications for tumor development and progression. Cancer Research, v. 61, p. 1320-1326, 2001.

SHI, Y. et al. Tumour-associated mesenchymal stem/stromal cells: Emerging therapeutic targets. Nature Reviews Drug Discovery, v. 16, p. 35-52, 2016. doi:10.1038/nrd.2016.193.

SIMPSON, P. T. et al. Molecular evolution of breast cancer. Journal of Pathology, v. 205, p. 248-254, 2005.

SMID, M. et al. Subtypes of breast cancer show preferential site of relapse. Cancer Research, v. 68, n. 9, p. 3108-3114, 2008. doi:10.1158/0008-5472.CAN-07-5644.

SORENMO, K. U. Canine mammary gland tumors. Veterinary Clinics of North America: Small Animal Practice, v. 33, p. 573-596, 2003.

SORENMO, K. U. et al. Canine mammary gland tumors: a histological continuum from benign to malignant; clinical and histopathological evidence. Veterinary and Comparative Oncology, v. 7, n. 3, p. 162-172, 2009.

SPAETH, E. et al. Inflammation and tumor microenvironments: defining the migratory itinerary of mesenchymal stem cells. Gene Therapy, v. 15, p. 730-738, 2008. doi:10.1038/gt.2008.39.

SUH, J. et al. Fibroblast growth factor-2, derived from cancer-associated fibroblasts, stimulates growth and progression of human breast cancer cells via FGFR1 signaling. Molecular Carcinogenesis, v. 59, n. 1-3, 2020. doi:10.1002/mc.23233.

SWAMYDAS, M. et al. Mesenchymal stem cell-derived CCL-9 and CCL-5 promote mammary tumor cell invasion and the activation of matrix metalloproteinases. Cell Adhesion & Migration, v. 7, p. 315-324, 2013. doi:10.4161/cam.25138.

TAN, W. J. et al. Second harmonic generation microscopy is a novel technique for differential diagnosis of breast fibroepithelial lesions. Journal of Clinical Pathology, v. 68, n. 12, p. 1033-1035, 2015.

TILBURY, K.; CAMPAGNOLA, P. J. Applications of second-harmonic generation imaging microscopy in ovarian and breast cancer. Perspectives in Medicinal Chemistry, v. 7, p. 21-32, 2015.

TORÍBIO, J. M. et al. Caracterização clínica, diagnóstico histopatológico e distribuição geográfica das neoplasias mamárias em cadelas de Salvador, Bahia. Revista Ceres, v. 59, n. 4, p. 427-433, 2012.

TUER, A. E. et al. Nonlinear optical properties of type I collagen fibers studied by polarization dependent second harmonic generation microscopy. Journal of Physical Chemistry B, v. 115, n. 44, p. 12759-12769, 2011.

TURNER, A. P.; LUCKEY, C. J. Regulatory macrophages: Therapeutic applications in transplantation and autoimmunity. *Frontiers in Immunology*, v. 4, p. 1-10, 2013.

UENO, T. et al. Significance of macrophage chemoattractant protein-1 in macrophage recruitment, angiogenesis, and survival in human breast cancer. Clinical Cancer Research, v. 6, p. 3282-3289, 2000.

UNGEFROREN, H. et al. Interaction of tumor cells with the microenvironment. Cell Communication and Signaling, v. 9, 18p, 2011.

UVA, P. et al. Comparative expression pathway analysis of human and canine mammary tumors. BMC Genomics, v. 10, p. 1-20, 2009.

VAN DEN BOSSCHE, J.; O'NEILL, L. A.; MENON, D. Macrophage immunometabolism: where are we (going)? Trends in Immunology, v. 38, n. 5, p. 395-406, 2017.

VAYSSE, C. et al. Metabolic reprogramming during the progression of cancers: Role of adipocytes. World Journal of Clinical Oncology, v. 5, n. 2, p. 158-164, 2014. doi:10.5306/wjco.v5.i2.158.

VENNERI, M. A. et al. Identification of proangiogenic Tie2-expressing monocytes (TEMs) in human peripheral blood and cancer. Blood, v. 109, n. 12, p. 5276-5285, 2007. doi:10.1182/blood-2006-10-053504.

VIEIRA, T. C.; OLIVEIRA, E. A.; SANTOS, B. J.; SOUZA, F. R.; VELOSO, E. S.; NUNES, C. B.; DEL PUERTO, H. L.; CASSALI, G. D. COX-2 expression in mammary invasive micropapillary carcinoma is associated with prognostic factors and acts as a potential therapeutic target in comparative oncology. *Frontiers in Veterinary Science*, v. 9, 2022.

VITALE, I.; SHEMBERGER, M.; APOSTOLIDIS, C.; KEITH, J. E. Immunoregulation in the tumor microenvironment. Frontiers in Immunology, v. 10, p. 1234-1249, 2019. Disponível em: <https://pubmed.ncbi.nlm.nih.gov/31269428/>. Acesso em: 5 dez. 2024.

VIOLA, A.; MUNARI, F.; SANCHEZ-RODRIGUEZ, R.; SCOLARO, T.; CASTEGNA, A. The metabolic signature of macrophage responses. Frontiers in Immunology, v. 10, 1462, 2019.

VU, L. T. et al. Tumor-secreted extracellular vesicles promote the activation of cancer-associated fibroblasts via the transfer of microRNA-125b. Journal of Extracellular Vesicles, v. 8, 1599680, 2019. doi:10.1080/20013078.2019.1599680.

WANG, B. et al. Breast fibroblasts in both cancer and normal tissues induce phenotypic transformation of breast cancer stem cells: a preliminary study. PeerJ, v. 6, e4805, 2018. doi:10.7717/peerj.4805.

WANG, D. D. et al. miR-222 confers the resistance of breast cancer cells to Adriamycin through suppression of p27kip1 expression. Gene, v. 590, p. 44-50, 2016. doi:10.1016/j.gene.2016.06.013.

WEIGELT, B.; PETERSE, J. L.; VAN 'T VEER, L. J. Breast cancer metastasis: markers and models. Nature Reviews Cancer, v. 5, n. 8, p. 591-602, 2005. doi:10.1038/nrc1670.

WEBER, J. S.; SANBORN, R. E.; AMIN, A. PD-1 blockade: the tale of the tail. Nature Medicine, v. 24, n. 12, p. 1839-1840, 2018. doi:10.1038/s41591-018-0226-0.

WORLD HEALTH ORGANIZATION. Classification of Tumors. 5. ed. 368p, 2019.

WYCKOFF, J. B. et al. A paracrine loop between tumor cells and macrophages is required for tumor cell migration in mammary tumors. Cancer Research, v. 64, p. 7022-7029, 2004.

WYNN, T. A.; CHAWLA, A.; POLLARD, J. W. Macrophage biology in development, homeostasis and disease. Nature, v. 496, n. 7446, p. 445-455, 2013. doi:10.1038/nature12034.

XING, F.; SAIDOU, J.; WATABE, K. Cancer-associated fibroblasts (CAFs) in tumor microenvironment. Frontiers in Bioscience (Landmark Edition), v. 15, p. 166-179, 2010. doi:10.2741/3613.

XU, T. et al. Dysregulated tumor-associated macrophages in carcinogenesis, progression, and targeted therapy of gynecological and breast cancers. Biomedicine & Pharmacotherapy, v. 120, 109431, 2020.

XUE, J. et al. Transcriptome-based network analysis reveals a spectrum model of human macrophage activation. Immunity, v. 40, n. 2, p. 274-288, 2014. doi:10.1016/j.immuni.2014.01.006.

YAO, X. et al. Targeting interleukin-6 in inflammatory autoimmune diseases and cancers. Pharmacology & Therapeutics, v. 141, p. 125-139, 2014.

YEON, J. H. et al. Cancer-derived exosomes trigger endothelial to mesenchymal transition followed by the induction of cancer-associated fibroblasts. Acta Biomaterialia, v. 76, p. 146-153, 2018. doi:10.1016/j.actbio.2018.07.001.

YONA, S.; GORDON, S. From the reticuloendothelial to mononuclear phagocyte system – the unaccounted years. Frontiers in Immunology, v. 6, 328, 2015. doi:10.3389/fimmu.2015.00328.

ZEISBERG, E. M. et al. Discovery of endothelial to mesenchymal transition as a source for carcinoma-associated fibroblasts. Cancer Research, v. 67, p. 10123-10128, 2007. doi:10.1158/0008-5472.CAN-07-3127.

ZHANG, K. et al. The collagen receptor discoidin domain receptor 2 stabilizes SNAIL1 to facilitate breast cancer metastasis. Nature Cell Biology, v. 15, n. 6, p. 677-687, 2013.

ZHONG, Q. et al. CPEB3 inhibits epithelial-mesenchymal transition by disrupting the crosstalk between colorectal cancer cells and tumor-associated macrophages via IL-6R/STAT3 signaling. Journal of Experimental & Clinical Cancer Research, v. 39, 132, 2020.

ZHU, Y. et al. Tissue-resident macrophages in pancreatic ductal adenocarcinoma originate from embryonic hematopoiesis and promote tumor progression. Immunity, v. 47, n. 3, p. 597-613.e8, 2017. doi:10.1016/j.immuni.2017.08.018.

ZHU, J.; THOMPSON, C. B. Metabolic regulation of cell growth and proliferation. Nature Reviews Molecular Cell Biology, v. 20, n. 8, p. 436-450, 2019. doi:10.1038/s41580-019-0123-6.

ZHU, Y.; HERNDON, J. M.; SOJKA, D. K.; KIM, K. W.; KNOLHOFF, B. L.; ZUO, C. Tissue-resident macrophages in pancreatic ductal adenocarcinoma originate from embryonic hematopoiesis and promote tumor progression. *Immunity*, v. 51, n. 4, p. 786-801, 2019.

ZHU, Y.; WANG, L. Role of tumor-associated macrophages in promoting angiogenesis in hepatocellular carcinoma. Cellular and Molecular Life Sciences, v. 78, n. 8, p. 2909-2919, 2021. doi:10.1007/s00018-021-03756-5.

APÊNDICES

APÊNDICE A - Outras atividades desenvolvidas durante o período de doutoramento

Artigos publicados

GARCIA, A. P. V.; REIS, LUANA A.; RIBEIRO, B. R. M.; NUNES, C. B.; DE PAULA, ANA M.; CASSALI, GEOVANNI D. Comparative evaluation of collagen modifications in breast cancer in human and canine carcinomas. Scientific Reports, 14(1):28846, 2024.

GARCIA, A. P. V.; REIS, LUANA A.; NUNES, FERNANDA C.; LONGFORD, FRANCIS G. J.; FREY, JEREMY G.; DE PAULA, ANA M.; CASSALI, GEOVANNI D. Canine mammary cancer tumour behaviour and patient survival time are associated with collagen fibre characteristics. Scientific Reports, v. 11, p. 5668, 2021

GARCIA, ANA PAULA VARGAS; TABORDA, DAIANA YIVELY OSORIO; REIS, LUANA APARECIDA; DE PAULA, ANA MARIA; CASSALI, GEOVANNI DANTAS. Collagen modifications predictive of lymph node metastasis in dogs with carcinoma in mixed tumours. FRONTIERS IN VETERINARY SCIENCE, v. 11, p. 01-10, 2024.

NAKAGAKI, KAREN YUMI RIBEIRO; NUNES, MAÍRA MEIRA; **GARCIA, ANA PAULA VARGAS**; DE BROT, MARINA; CASSALI, GEOVANNI DANTAS. Neuroendocrine Carcinomas of the Canine Mammary Gland: Histopathological and Immunohistochemical Characteristics. FRONTIERS IN VETERINARY SCIENCE, v. 7, p. 621714, 2021.

GONÇALVES, ROSÂNGELA MAYER; DELGOBO, MARINA; AGNES, JONATHAN PAULO; DAS NEVES, RAQUEL NASCIMENTO; FALCHETTI, MARCELO; CASAGRANDE, TUANY; **GARCIA, ANA PAULA VARGAS**; VIEIRA, THAYNAN CUNHA; SOMENSI, NAUANA; BRUXEL, MACIEL ALENCAR; MENDES, DANIEL AUGUSTO GASPARIN BUENO; RAFACHO, ALEX; BÁFICA, ANDRÉ; GELAIN, DANIEL PENS; MOREIRA, JOSÉ CLÁUDIO FONSECA; CASSALI, GEOVANNI DANTAS; BISHOP, ALEXANDER JAMES ROY; ZANOTTO-FILHO, ALFEU. COX-2 promotes mammary adipose tissue inflammation, local estrogen biosynthesis, and carcinogenesis in high-sugar/fat diet treated mice. CANCER LETTERS, v. 502, p. 44-57, 2021.

SENA, ISADORA F. G.; ROCHA, BEATRIZ G. S.; PICOLI, CAROLINE C.; SANTOS, GABRYELLA S. P.; COSTA, ALINNE C.; GONÇALVES, BRYAN O. P.; **GARCIA, ANA PAULA V.**; SOLTANI-ASL, MARYAM; COIMBRA-CAMPOS, LEDA M. C.; SILVA, WALISON N.; COSTA, PEDRO A. C.; PINTO, MAURO C. X.; AMORIM, JAIME H.; AZEVEDO, VASCO A. C.; RESENDE, RODRIGO R.; HELLER, DEBORA; CASSALI, GEOVANNI D.; MINTZ, AKIVA; BIRBRAIR, ALEXANDER. C(3)1-TAg in C57BL/6 J background as a model to study mammary tumor development. HISTOCHEMISTRY AND CELL BIOLOGY, v. 155, p. 1-18, 2021.

CARVALHO, THAYNARA PARENTE DE; OLIVEIRA, AYISA RODRIGUES DE; SANTOS, DANIEL OLIVEIRA DOS; CASSALI, GEOVANNI DANTAS; **GARCIA, ANA PAULA VARGAS**; PEREIRA, FERNANDA MARA ARAGÃO MACEDO; SOARES'NETO, LAURO LEITE; SILVA, MONIQUE FERREIRA; PAIXÃO, TATIANE

ALVES; SANTOS, RENATO LIMA. Histopathologic and immunophenotypic profile of a spontaneous mammary carcinoma in a male Humboldt's white-fronted capuchin (Cebus albifrons). JOURNAL OF MEDICAL PRIMATOLOGY, v. 01, p. 01-04, 2021.

NUNES, M. M.; **GARCIA, A. P. V.**; NAKAGAKI, K. Y. R.; CASSALI, G. D. Histopathological and immunohistochemical characteristics of malignant adenomyoepithelioma in a cat: case report. ARQUIVO BRASILEIRO DE MEDICINA VETERINÁRIA E ZOOTECNIA (ONLINE), v. 73, p. 1351-1356, 2021.

NAKAGAKI, KAREN YUMI RIBEIRO; NUNES, M. M.; **GARCIA, ANA P. V.**; NUNES, F. C. ; SCHIMITT, F. ; CASSALI, G. D. . CANINE MAMMARY GLAND SOLID CARCINOMA: A HISTOLOGICAL TYPE OR TUMOR CELL ARRANGEMENT? JOURNAL OF COMPARATIVE PATHOLOGY, v. 190, p. 1-12, 2021.

REIS, LUANA A.; **GARCIA, ANA P. V.**; GOMES, EGLEIDSON F. A.; LONGFORD, FRANCIS G. J.; FREY, JEREMY G.; CASSALI, GEOVANNI D.; DE PAULA, ANA M. Canine mammary cancer diagnosis from quantitative properties of nonlinear optical images. Biomedical Optics Express, v. 11, p. 6413, 2020.

Capítulos de livros publicados

CASSALI, G. D.; SOUZA, F. R.; **GARCIA, ANA PAULA VARGAS**; CAMPOS, C. B.; SOUSA, A. A.; RIBEIRO, C. B.; NAKAGAKI, K. Y. R. Metástases. In: Geovanni Dantas Cassali; Fernanda Rezende Souza; Ana Paula Vargas Garcia; Cecília Bonolo de Campos; Ana Augusta de Sousa; Catarina Brenha Ribeiro; Karen Yumi Ribeiro Nakagaki. (Org.). Patologia Mamária Canina e Felina do Diagnóstico ao Tratamento. 2ed.São Paulo: Editora Medvet LTDA., 2023, p. 223-244.

2. CASSALI, G. D.; FERREIRA, E.; **GARCIA, ANA PAULA VARGAS**; NAKAGAKI, K. Y. R. Marcadores Prognósticos e Preditivos no Câncer de Mama. In: Geovanni Dantas Cassali; Enio Ferreira; Ana Paula Vargas Garcia; Karen Yumi Ribeiro Nakagaki. (Org.). Patologia Mamária Canina e Felina do Diagnóstico ao Tratamento. 2ed.São Paulo: Editora Medvet LTDA., 2023, p. 301-327.

MATA, L. C. C.; **GARCIA, ANA PAULA VARGAS**; SENHORELLO, I. L. S. Marcadores Séricos no Câncer de Mama. In: Liliane Cunha Campos da Mata; Ana Paula Vargas Garcia; Igor Luiz Salardani Senhorello. (Org.). Patologia Mamária Canina e Felina do Diagnóstico ao Tratamento. 2ed.São Paulo: Editora Medvet LTDA., 2023, p. 407-416.

DAMASCENO, K. A.; **GARCIA, ANA PAULA VARGAS**; SOUZA, F. R.; FLECHER, M. C.; CASSALI, G. D. Microambiente Tumoral. In: Karine Araújo Damasceno; Ana Paula Vargas Garcia; Fernanda Rezende Souza; Mayra Cunha Flecher; Geovanni Dantas Cassali. (Org.). Patologia Mamária Canina e Felina do Diagnóstico ao Tratamento. 2ed.São Paulo: Editora Medvet LTDA., 2023, p. 455-478.

Premiações

Premiação 01:
Nome: Prêmio Washington Tafuri. Premiação concedida ao artigo original de Mestrado do programa de Pós-graduação em Patologia da UFMG publicado em periódico de maior impacto entre 2023 e 2024.

Artigo: **Garcia APV,** Taborda DYO, Reis LA, de Paula AM, Cassali GD. Collagen modifications predictive of lymph node metastasis in dogs with carcinoma in mixed tumours. Frontiers in Veterinary Science, v. 11, p. 01-10, 2024.

Evento: Encontro de Patologia da UFMG.

Associação: Programa de Patologia da UFMG.

Premiação 02:
Nome: Prêmio Washington Tafuri. Premiação concedida ao artigo original de Mestrado do programa de Pós-graduação em Patologia da UFMG publicado em periódico de maior impacto entre 2021 e 2022.

Artigo: **Garcia APV,** Reis LA., Nunes FC., Longford FGJ, Frey JG, De Paula AM, Cassali GD. Canine mammary cancer tumour behaviour and patient survival time are associated with collagen fibre characteristics. Scientific Reports, v. 11, p. 5668, 2021.

Evento: Encontro de Patologia da UFMG.

Associação: Programa de Patologia da UFMG.

Premiação 03:
Nome: Menção Honrosa pelo resumo "Alinhamento, ondulação, número e comprimento médio das fibras colágenas estão associados ao comportamento tumoral em neoplasias mamárias humanas e caninas".

Evento: 7º Congresso Brasileiro de Patologia Veterinária e XXI Encontro Nacional de Patologia Veterinária.

Associação: Associação Brasileira de Medicina Veterinária.

Colaborações em Projetos de Pesquisa

Projeto 01
Título: Utilização da elipsometria espectroscópica de ângulo variável associada a *machine learning* para a identificação de alterações neoplásicas na glândula mamária canina.

Período: outubro/2023 - atual.

Pesquisador responsável: Prof. Dr. Juan Carlos Gonzalez (ICEx/ UFMG).

Projeto 02
Título: Estudo morfométrico das áreas de invasão nos carcinomas em tumores mistos da glândula mamária canina e sua correlação com a sobrevida específica

Período: março/ 2022- abril/2024.

Aluna de mestrado: Fernanda Freitas Miranda.

Orientador: Prof. Dr. Geovanni Dantas Cassali (ICB/ UFMG).

Projeto 03
Título: Avaliação das fibras colágenas em tumores mistos mamários de cadelas pela microscopia por geração de segundo harmônico.

Período: agosto/2020 - julho/2022.

Aluna de mestrado: Daiana Osório Taborda.

Orientador: Prof. Dr. Geovanni Dantas Cassali (ICB/ UFMG).

Projeto 04
Título: Avaliação da participação do colágeno na progressão do melanoma cutâneo.

Período: agosto/2022 - atual.

Aluna de doutorado: Fernanda Luíza Menezes Bello.

Orientadora: Profa. Dra. Sara Santos Bernardes (ICB/ UFMG).

Participação em projetos de extensão

Projeto 01
Título: Exames cito e histopatológicos de tumores mamários da cadela.

Coordenador: Prof. Dr. Geovanni Dantas Cassali (ICB/ UFMG).

Período: março/2018 - dezembro/2022.

Projeto 02
Título: Patologia Interativa e Integrativa.

Coordenadora: Profa. Dra. Helen Lima del Puerto (ICB/ UFMG).

Período: agosto/2021 - dezembro/2022.

Integração de corpo editorial de periódicos

Período 01
Nome: Biomedinar (ISSN: 2965-8446)
Período: 02/2024-atual

Periódico 02
Nome: Cancer Research Journal (ISSN: 2330-8214)
Período: 03/2024-atual

Participação como Revisora de Periódicos

Periódico 01
Nome: INTERFACES - Revista de Extensão da UFMG
Período: 01/2021 - atual

Periódico 02
Nome: Pesquisa Veterinária Brasileira
Período: 01/2021 - atual

Periódico 03
Nome: Biomedinar
Período: 02/2024-atual

Periódico 04
Nome: Cancer Research Journal
Período: 03/2024-atual

Atividades de docência

Atividade 01
Período: março/2020 a julho/2020.

- **Local:** Pontifícia Universidade Católica de Minas Gerais.
- **Disciplina:** Saúde Ambiental.

Atividade 02
Período: agosto/2022 a dezembro/2022

- **Local:** Pontifícia Universidade Católica de Minas Gerais.
- **Disciplina:** Citologia e Histologia
- **Cursos:** Biomedicina *campus* Betim (Teórica: 40 horas).
  Enfermagem/Fonoaudiologia *campus* Coração Eucarístico (Teórica: 40 horas).

- **Local:** Pontifícia Universidade Católica de Minas Gerais.
- **Disciplina:** Histotecnologia Clínica.
- **Curso:** Biomedicina *campus* Contagem (Teórico-prática: 60 horas).

- **Local:** Pontifícia Universidade Católica de Minas Gerais.
- **Disciplina:** Microscopia Celular e dos Tecidos.
- **Curso:** Farmácia *campus* Coração Eucarístico (Prática: 20 horas).

- **Local:** Pontifícia Universidade Católica de Minas Gerais.
- **Disciplina:** Técnicas de Coleta.
- **Curso:** Biomedicina unidade Praça da Liberdade (Teórico-prática: 40 horas).

Período: fevereiro/2023 a julho/2023

- **Disciplina:** Citologia e Histologia.
- **Cursos:** Biomedicina *campus* Betim (Teórico-prática: 80 horas).
  Biomedicina *campus* Contagem (Teórico-prática: 80 horas).
  Enfermagem *campus* Coração Eucarístico (Teórica: 40 horas).

- **Disciplina:** Histotecnologia Clínica.
- **Curso:** Biomedicina *campus* Contagem (Teórico-prática: 60 horas).

Período: fevereiro/2024 - atual

- **Disciplina:** Citologia Oncótica, Imunologia, Técnicas de Coleta
- **Cursos:** Biomedicina *campus* Betim (Teórico-prática: 80 horas).
  Enfermagem *campus* Coração Eucarístico (Teórica: 40 horas).

Membro examinador de bancas

Banca da defesa do Trabalho de Conclusão de Curso:

Aluna: Amanda Gabrielle de Sousa

Orientadora: Profa. Dra. Letícia da Conceição Braga

Título do Trabalho: "Biomarcadores associados à terapia alvo como perspectiva para o tratamento quimioterápico do câncer de mama em cães".

Local: Centro Universitário Metodista Izabela Hendrix

Alunas: Bruna Marcandali Junqueira Campos, Jéssica Souza Guimarães e Karine Fonseca Souza

Orientadora: Profa. Dra. Andreia Teixeira

Título do Trabalho: "Insuficiência cardíaca associada a Anomalia de Ebstein e a influência da alimentação e das alterações emocionais na evolução da doença: relato de caso".

Local: Pontifícia Universidade Católica de Minas Gerais, *campus* Betim.

Apresentação de trabalhos e resumos publicados em Anais de Congressos

I Congresso Latino-Americano de Patologia Mamária Canina e Felina & V Encontro de Patologia Mamária. Histopathological, immunohistochemical and imaging features of bone metastasis of mammary neoplasm in female dog: case report. 2023. (Congresso).

I Congresso Latino-Americano de Patologia Mamária Canina e Felina & V Encontro de Patologia Mamária. Changes in the collagen organization may be related to lymph node metastasis in canine mammary carcinomas. 2023. (Congresso).

Evaluation of cancer biopsies by multiphoton imaging and machine learning techniques. In: Encontro de Outono da SBF 2023, 2023, Ouro Preto. Livro de resumos do Encontro de Outono da SBF 2023. São Paulo: SBF, 2023. v. 1. p. R0919-1-R0919-1.

Levantamento dos Casos de Tumores Cutâneos Caninos do LPC-UFMG. In: VIII Encontro Pathos UFMG, 2022, Belo Horizonte. Patologia ConsCiência, 2022. v. 01. p. 14-14.

Levantamento dos Casos de Mastocitomas no LPC UFMG. In: VIII Encontro Pathos UFMG, 2022, Belo Horizonte. Patologia ConsCiência, 2022. v. 01. p. 19-19.

Levantamento de Imuno-Histoquímica das Neoplasias Malignas da Glândula Mamária das Cadelas Realizados no LPC- UFMG. In: VIII Encontro Pathos UFMG, 2022, Belo Horizonte. Patologia ConsCiência, 2022. v. 01. p. 25-25.

A Imuno-Histoquímica como Ferramenta Diagnóstica do Linfoma Intestinal em Felinos Domésticos. In: VIII Encontro Pathos UFMG, 2022, Belo Horizonte. Patologia ConsCiência, 2022. v. 01. p. 26-26.

Levantamento das neoplasias ovarianas em cadelas - LPC - UFMG. In: VIII Encontro Pathos UFMG, 2022, Belo Horizonte. Patologia ConsCiência, 2022. v. 01. p. 31-31.

Avaliação da expressão proteica de CD26 e GAPDH em tumores colorretais para definição de potencial prognóstico. In: VIII Encontro Pathos UFMG, 2022, Belo Horizonte. Patologia ConsCiência, 2022. v. 01. p. 37-37.

Alterações das fibras colágenas podem estar relacionadas com metástase regional nos carcinomas em tumores mistos caninos. In: VIII Encontro Pathos UFMG, 2022, Belo Horizonte. Patologia ConsCiência, 2022. v. 01. p. 39-39.

Multiphoton imaging on cancer biopsies. In: 51a. Reunião Anual da Sociedade Brasileira de Bioquímica e Biologia Molecular (SBBq) e 46o. Congresso da Sociedade Brasileira de Biofísica (SBBf), 2022, Águas de Lindóia. Livro de resumos: 51a. Reunião Anual da Sociedade Brasileira de Bioquímica e Biologia Molecular (SBBq) e 46o. Congresso da Sociedade Brasileira de Biofísica (SBBf), 2022. v. 1. p. 1-1.

Changes in the collagen organization may be related to lymph node metastasis in canine mammary carcinomas. Congresso da Sociedade Brasileira de Biofísica (SBBf), 2022, Águas de Lindóia. Livro de resumos: 51a. Reunião Anual da Sociedade Brasileira de Bioquímica e

Biologia Molecular (SBBq) e 46o. Congresso da Sociedade Brasileira de Biofísica (SBBf), 2022. v. 1. p. 1-1.

Carcinoma sólido da glândula mamária canina: características morfológicas e imunohistoquímicas. In: 6º Congresso Brasileiro de Patologia Veterinária e XX Encontro Brasileiro de Patologia Veterinária, 2021. 6º Congresso Brasileiro de Patologia Veterinária e XX Encontro Brasileiro de Patologia Veterinária, 2021.

Expressão de marcadores prognósticos e preditivos em carcinomas em tumores mistos da glândula mamária de cadelas. In: 6º Congresso Brasileiro de Patologia Veterinária e XX Encontro Brasileiro de Patologia Veterinária, 2021. 6º Congresso Brasileiro de Patologia Veterinária e XX Encontro Brasileiro de Patologia Veterinária, 2021.

Female dog mammary cancer diagnosis by nonlinear optical images. In: Encontro de Outono 2021, 2021, São Paulo. Encontro de Outono 2021. São Paulo: SBF, 2021. v. 1. p. 1-1.

Nonlinear imaging of biological tissues. In: 2021 SBFoton International Optics and Photonics Conference, 2021, 2021, São Paulo. 2021 SBFoton International Optics and Photonics Conference, 2021, 2021. v. 1. p. 1-1.

Canine mammary cancer tumor behavior and patient survival rate based on collagen fibre characteristics. In: VII Encontro de Patologia da UFMG, 2020, Belo Horizonte. Um Olhar Sobre a Construção do Pesquisador em Patologia, 2020. p. 35-35. (Apresentação Oral).

Nível de informação da população a respeito da influência ambiental na disseminação de doenças. In: VI Mostra de Pesquisa e Extensão da PUC Minas, 2020, Betim. Revista Sinapse Múltipla, 2020. p. 79-80.

Microambiente Tumoral: o que sabemos a seu respeito? 2021. IX Semana da Biomedicina da PUC Minas. (Palestra).

Roda de Conversa com Ex-alunos. 2021. VIII Jornada da Biomedicina da PUC Minas. (Palestra).

Participação em cursos relacionados à tese

I Curso de Histopatologia Mamária Canina e Felina

Período: 04 e 05 de dezembro de 2020.

Carga Horária: 12 horas.

Organizador: Prof. Dr. Geovanni Dantas Cassali.

Organização de eventos técnico-científicos

I Congresso Brasileiro de Oncologia Translacional (2024).
Coordenação: Prof. Dr. Geovanni Dantas Cassali.
Organização: ReMITRIBIC

I Congresso Latino-Americano de Patologia Mamária Canina e Felina & V Encontro de Patologia Mamária (2023).
Coordenação: Prof. Dr. Geovanni Dantas Cassali.
Organização: Laboratório de Patologia Comparada/ UFMG.

Outubro Rosa Pet 2022 (2022).
Coordenação: Prof. Dr. Geovanni Dantas Cassali.
Organização: Laboratório de Patologia Comparada/ UFMG.

Outubro Rosa Pet 2021 (2021).
Coordenação: Prof. Dr. Geovanni Dantas Cassali.
Organização: Laboratório de Patologia Comparada/ UFMG.

Outubro Rosa Pet Brasil 2020 (2020).
Coordenação: Prof. Dr. Geovanni Dantas Cassali.
Organização: Laboratório de Patologia Comparada/ UFMG.

VII Encontro de Patologia da UFMG (2020).
Coordenação: Profa. Dra. Tatiane Alves Paixão.
Organização: Programa de Pós-graduação em Patologia da UFMG.

Participação em eventos, congressos, exposições e feiras

I Congresso Latino-Americano de Patologia Mamária Canina e Felina & V Encontro de Patologia Mamária. (2023)

Next Frontiers to Cure Cancer 2023. (2023)

Outubro Rosa Pet 2022. (2022)

VIII Encontro de Patologia da UFMG. (2022)

I Congresso Internacional de Histotecnologia. (2021)

Outubro Rosa Pet 2021. (2021)

I Simpósio Online de Oncologia. (2020)

Masterclass imunocitoquímica. (2020)

Minicurso Oncologia Multiprofissional. (2020)

Neoplasias de células redondas: características clinico-patológicas e métodos diagnósticos. (2020)

Outubro Rosa Pet Brasil 2020. (2020)

Semana de Comportamento e bem-estar felinos. (2020)

VII Encontro de Patologia da UFMG. (2020)

I Webinar Saúde Única: Relevância dos estudos em Patologia Mamária Comparada. (2020)

ANEXOS

ANEXO A - Publicação do artigo 01 da tese

www.nature.com/scientificreports

scientific reports

OPEN

Comparative evaluation of collagen modifications in breast cancer in human and canine carcinomas

Ana Paula Vargas Garcia[1], Luana Aparecida Reis[2], Bárbara Regina Melo Ribeiro[2], Cristiana Buzelin Nunes[3], Ana Maria de Paula[2,4]✉ & Geovanni Dantas Cassali[1]

New diagnostic and therapeutic approaches have been increasingly demanded due to the high morbidity and mortality associated with breast cancer. Recently, changes in the collagen fibres in mammary neoplasms have been shown to provide information that can be helpful for more accurate diagnosis. We aimed to conduct a comparative analysis of the tumour stroma in human and canine mammary neoplasms to assess the relationship between collagen modifications and the behaviour of carcinomas in both species, by multiphoton microscopy. We present a retrospective study of 70 cases of human mammary tumour and 74 cases of canine mammary tumour. We analysed sections stained with haematoxylin and eosin from 1,200 representative areas of normal mammary tissue, fibroadenoma, grade I invasive carcinoma, grade III invasive carcinoma and invasive micropapillary carcinoma in human species and 1,304 representative areas of normal mammary tissue, benign mixed tumour, mixed carcinoma, carcinosarcoma, invasive micropapillary carcinoma and solid carcinoma in canine species. We obtained that both human and canine mammary carcinomas present lower density of collagen fibres, higher density of cells and the collagen fibres are more aligned than in normal tissue. For human mammary carcinomas, the collagen fibres are more linear as compared to normal tissue. In addition, we demonstrated that the carcinomas with unfavourable prognosis present shorter collagen fibres, and these collagen changes correlate with the clinical and pathological data in human and canine species. For dogs, there is a correlation between the mean fibre length with the specific survival times. Thus, we demonstrate that dogs provide an excellent comparative perspective for studying how changes in the tumour stroma affect patient survival.

Keywords Collagen fibre, Collagen alignment, Tumour microenvironment, Breast cancer, Matrix remodelling, Tumour-associated stroma

Mammary gland neoplasms are characterized by collagen deposition, remodelling, and linearisation of the extracellular matrix, leading to fibrosis that promotes malignancy[1,2]. The stiffened stroma enhances tumour cell growth, survival, and migration, driving an epithelial-mesenchymal transition. A rigid stroma also induces angiogenesis, hypoxia, and compromises antitumour immunity[3]. It is a well-established fact that the tumour microenvironment, also known as the tumour-associated stroma, is composed of a diverse combination of non-tumour cells, such as fibroblasts, macrophages and other immune cells, vascular cells, adipocytes, and others, in addition to the extracellular matrix. Studies demonstrated that tumour-associated stroma plays a key role in the initiation and progression of a wide variety of neoplasms, having multiple roles in tumour biology[4,5]. Collagen, specifically, plays a crucial role in metastasis development in breast cancer, as well as in matrix metalloprotease activity, that has been the subject of a considerable number of planned and therapeutic studies of many types of cancer[6–9] and specifically in breast cancer[10–15]. It has been shown that the neoplastic mammary glands present more organized and defined collagen fibres when compared to the healthy breast. Therefore, collagen organization is correlated with unfavourable prognosis[1,15–21]. Furthermore, changes in collagen density and fibre organization were associated with tumour grade and overall survival in human[15] and canine[18] breast carcinomas.

[1]Department of General Pathology, Institute of Biological Sciences, Federal University of Minas Gerais, Av. Pres. Antônio Carlos, 6627, Pampulha, Belo Horizonte 31270-901, MG, Brazil. [2]Department of Physics, Institute of Exact Sciences, Federal University of Minas Gerais, Av. Pres. Antônio Carlos, 6627, Pampulha, Belo Horizonte 31270-901, MG, Brazil. [3]Department of Anatomic Pathology, Faculty of Medicine, Federal University of Minas Gerais, Av. Prof. Alfredo Balena, 190, Santa Efigênia, Belo Horizonte 30130-100, MG, Brazil. [4]Present address: Institute of Physics "Gleb Wataghin", University of Campinas, Campinas, SP, Brazil. ✉email: ana@fisica.ufmg.br

Neoplasms naturally developed in domestic dogs have increasingly been used as a valuable source of information to better understand the biology of breast cancer development in women. The canine species presents pathophysiological similarities with the human species and can help in research for new diagnoses and therapies related to this neoplasm[22–28]. The field of comparative oncology aims to approach some existing research deficiency, broadening its focus from classic rodent models to spontaneous tumours that develop in animals. This additional perspective is perceived as a chance to complement and improve the understanding of complex diseases, such as cancer, in relation to tumour development, risk factors and mechanisms of tumourigenesis. Due to the many similarities shared between dogs and humans, the domestic dog has been considered one of the best examples of comparative oncology[21,22,25,26,28–30]. Thus, the aim of this study was to carry out a comparative analysis of the tumour stroma in human and canine mammary neoplasms to evaluate the links between changes in collagen fibres and the behaviour of carcinomas in both species. The study was based on morphological, clinicopathological, immunophenotypic data and imaging by second harmonic generation (SHG) and two-photon excited fluorescence (TPEF) microscopy in cases of human mammary and canine mammary tumour.

Materials and methods

Case selection

This retrospective study involved the analysis of 70 cases of human mammary neoplasms, 74 samples of canine mammary tumours, 20 healthy samples of human mammary tissue, and 12 healthy samples of canine mammary tissue. The canine mammary tissue samples were obtained from the archives of the Comparative Pathology Laboratory at the Federal University of Minas Gerais (UFMG), Brazil. The human mammary tissue samples were collected from the biopsy sector archives of the Faculty of Medicine at the Federal University of Minas Gerais (UFMG), Brazil. Both the canine and human samples were sourced from naturally occurring tumours in patients undergoing treatment at the UFMG Veterinary Hospital and the UFMG Hospital das Clínicas. Healthy canine mammary tissue samples were acquired from mammary tissues without mammary chain abnormalities received at the Comparative Pathology Laboratory. Healthy samples of human breast tissue were obtained from breast reduction surgeries performed at the Hospital das Clínicas of UFMG. The selection process encompassed samples with comprehensive information regarding tumour size, presence or absence of regional or distant metastasis, and histological grade.

The two-photon microscopy images were performed on histological slides stained with haematoxylin and eosin (H&E). The slides were prepared using sections of healthy or neoplastic mammary tissue sourced from biopsies involving procedures such as setorectomy, simple mastectomy, or unilateral/bilateral radical mastectomy, determined by factors including tumour size, tumour site, lymphatic involvement, and clinical stage. The selected canine samples were collected between 2009 and 2020 and submitted to histological classification according to the Classification and Grading of Canine Mammary Tumors[31,32] and Consensus for the Diagnosis, Prognosis and Treatment of Canine and Feline Mammary Tumours[33–36]. The selected human samples were collected from 2010 to 2020 a were classified histologically based on the criteria described in the World Health Organization[37]. For correlations between collagen fibre organization parameters, number, waviness and mean fibre length, collagen density and cell density and patient-specific survival, only data from patients treated with surgery alone were included. Score 1 was assigned to patients who died from breast cancer and 0 to living patients. Patients who died for reasons other than mammary cancer were not included.

The canine sample study was performed in view of the fundamental ethical principles under law no. 11.794, of October 8, 2008 and of decree no. 6.899 of July 2009, and with the rules issued by the National Council for the Control of Animal Experimentation (CONCEA) and the international Animal Research: Reporting of In Vivo Experiments (ARRIVE). All experimental protocols were approved by the "Ethics Committee on the Use of Animals" at UFMG, under number 83/2021.

The research on human tissue sample was previously approved by the "Research Ethics Committee" at UFMG (COEP-UFMG) under No. 43947521.3.0000.5149/2021. All experiments were carried out in accordance with the Declaration of Helsinki. As a retrospective study, performed on archive histopathological slides, the need for informed consent from all subjects and/or their legal guardian(s) was waived by the COEP-UFMG.

Performing immunohistochemistry

Histological sections, measuring 4 µm thick, were prepared for immunohistochemical analysis. A commercial anti-mouse/anti-rabbit detection kit (Novolink Polymer Detection System, Leica Biosystems, Newcastle Upon Tyne, United Kingdom, REF RE7158, LOT 6092583), was used following the manufacturer's instructions. Antigen retrieval for estrogen receptor (ER), progesterone receptor (PR), Ki67 and HER2 was performed using steam heat (*Pascal*®) with citrate pH 6.0 (Invitrogen by Thermo Fisher Scientific, 10X low pH, REF 00-4955-58, LOT 2410220, Life Technologies' Corp., 5781 Van Allen Way, Carlsbad, CA92008). The histological sections were incubated with the corresponding primary antibodies for 1 h in a humid chamber at 4 °C. Primary antibodies used included ER (Dako Cat# ER-14-0481, RRID: AB_1545347, goat anti-human EP1 receptor, PTGER1 antibody, unconjugated, LOT 11303512, REF IR084, ready-to-use), PR (LSBio LifeSpan Cat# LS-C26712, RRID: AB_2283822, progesterone receptor (PGR) mouse monoclonal (hPRa2 + hPRa3) antibody, anti-human/mouse/rat, unconjugated, LOT X13703736, REF MA512642, 0.4 mg/mL, 1:50), HER2 (Dako Cat# AP7629e, RRID: AB_2262284, rabbit anti-human HER2, polyclonal antibody, unconjugated, REF A0485, LOT 00060381, 0.50 g/mL, 1:200), and Ki67 (Thermo Fisher Scientific Cat# MA5-31796, RRID: AB_2787419, mouse anti-human MIB1 receptor, 2A7B1 antibody, unconjugated, LOT 20067572, REF M7240, 46 mg/mL, 1:50). Immunoreactivity was visualized using 3,3′-diaminobenzidine chromogen (Novolink Polymer Detection System, Leica Biosystems, Newcastle Upon Tyne, United Kingdom, REF RE7158, LOT 6092583) and counterstained with Mayer's haematoxylin. Positive controls for the reactions consisted of fragments of canine and human mammary tissues positive for HER-2, ER, PR and Ki67. The primary antibody was omitted and chromogen was added to both

for negative controls. The evaluation of the slides, the quantification of immunoreactive and the classification of immunophenotypes were carried out in accordance with the World Health Organization[32] guidelines (for human samples) and the criteria established by Nunes et al.[33] (for dog samples). The antibodies used were standardized in our laboratory routine, and their antigenic specificity was confirmed through our own research and by reference to others published studies[33–38].

Image acquisition and analyses

The imaging system employed in this study combined SHG and TPEF imaging using a custom setup comprising an Olympus FV300 confocal scanning laser unit connected to a BX61- upright microscope. The SHG images allow to extract information from the collagen fibres and the TPEF allows to extract details of the cell arrangements in the tissue. Details of the image acquisition methodology is described in our previous publications[17,18,39]. In brief, we used 140 fs pulses centred at the wavelength of 800 nm. The beam is focused on the sample microscope slab by a 20X objective with a high numerical aperture (NA = 0.9) and the images are obtained in back scattering geometry. The SHG is measured at 400 nm using a filter with bandwidth of 20 nm by directing the signal to a non-descanned detector placed just above the objective. The fluorescence signal from the eosin dye staining the tissue is measured by the standard de-scanned detector of the confocal unit at the wavelength band of 560 to 600 nm. The transmitted laser image is also collected by the condenser of the microscope. We measured images at the optimized focus position and at ± 1 µm from this position to allow for noise filtering by the software. The images were acquired for areas of 0.47 ×0.47 mm2. For human samples, 1,200 representative sections of normal human breast tissue (NMTh) and evaluated human histological types were chosen from H&E-stained slides. For canine samples, 1,304 representative sections of normal mammary tissue (NMTc) and canine histological types evaluated from sections stained with H&E were defined. In cases where histological slides included normal mammary regions, images of the 10 most representative areas in human and canine samples were captured. Regarding neoplastic tissues, 10 to 15 highly representative intratumoural regions were selected for measurements. SHG and TPEF signals from selected areas were measured for further analyses. Additionally, brightfield microscopy images of H&E-stained tissue were acquired from the same measured areas using the Olympus BX41 microscope coupled to the *SPOT Insight Color* camera for comparative purposes. The capture software used was *SPOT Advanced*.

Our quantitative analyses of collagen fibre and cell segment parameters utilized PyFibre, an open-source software package (Python Fibrous Image Analysis Toolkit), that we specifically designed for automated segmentation of images into cellular and collagen regions, allowing extraction of pertinent parameters. PyFibre is openly accessible on GitHub[40]. During the analyses process, the integration of SHG and TPEF signals along with laser transmission data was employed to improve the accurate identification of collagen fibres and cellular features in the images. This approach utilized the TPEF and SHG signals, in addition to a copy of the laser transmission data, to better discern collagen fibres and cellular features in the images. Data were extracted and analysed according to Reis et al.[17], Garcia et al.[18] and Gomes et al.[39].

Statistical analysis

The Shapiro-Wilk test was employed to assess normality in small sample groups, while the Kolmogorov-Smirnov test was used for larger sample groups. Due to the non-parametric nature of the data, the Kruskal Wallis test and the Dunn test were performed for multiple comparisons of the medians between groups. We employed Spearman's Correlation Coefficient and linear regression statistical tests to establish correlations between clinicopathological data of patients and collagen fibre parameters. The cancer-specific survival rate was estimated using the Kaplan–Meier curve, and the comparisons between groups were performed using the Mantel–Cox log rank test. To evaluate the independence or association between the categorical variables mean fibre length and histological grading, clinical staging, cell proliferation and significant molecular subtype between categorical variables using the chi-square test and Fisher's Exact Test. The graphs were presented in contingency graphs. These analyses were performed using *Prism* (version 8.0, GraphPad, San Diego, CA, United States). A value of $p < 0.05$ was considered statistically significant for all analyses. The p values less than 0.001 are denoted by (***), p less than 0.01 are denoted by (**) and p less than (0.05) are denoted by (*).

Results

Details of the analysed samples

Table 1 presents the details of the histological subtypes analysed, number of samples, patient age, clinical staging, histological grading, molecular subtype and survival information for human breast neoplasms. Table 2 provides equivalent details for canine mammary neoplasms. The analysis of correlations between collagen fibre parameters and clinicopathological data did not include Fibroadenoma (Fb) in women and benign mixed tumours (BMT) in dogs. It should be noted that the canine data presented in this article comprise a different data set from that used in our previously published works. Importantly, there is no overlap between the samples included in this study and those analysed in our previous publications[18,41]. For this study, we selected more recent cases, ensuring a more accurate assessment of potential changes in the genetic, environmental, and social conditions of the animals involved. Additionally, we prioritised cases with comprehensive descriptions of clinical-pathological data, which allowed us to deepen the analysis of additional prognostic factors. Nonetheless, due to the low occurrence of carcinosarcomas in clinical practice, we used some of the same carcinosarcoma cases described in our previous publication[18]. However, all the other cases selected are new, and the analyses performed in this work are original, providing new insights into tumour progression.

The women were followed up for a minimum of 05 years and a maximum of 10 years. At the conclusion of the study, we completed the follow-up of 43 patients. Of these, 06 women had died and 37 were still alive. Follow-up was not possible for 11 patients. The distribution of women based on clinical staging was as follows: 04 women

Histological type	n	Age (year)	Staging (TNM)				Histological grades			Molecular subtype			Survival (months)
			I	II	III	IV	I	II	III	HR+/ Ki67< 20%	HR+ Ki67> 20%	HR+/- HER2+	HR-/HER2-	
Fb	12	34.2	NA	NA	NA	NA	NA	NA	NA	NA	NA	NA	NA	NA
TC	4	71.3	2	2	0	0	4	0	0	4	0	0	0	66.0
IcgI	16	68.4	5	7	0	3	1	16	0	13	3	0	0	86.3
IcgIII	21	59.6	5	2	2	10	2	0	0	21	2	12	4	3	79.1
IMC	17	52.3	4	3	1	9	0	3	8	2	3	8	6	0	59.5
Total	70	-	16	14	3	22	3	23	8	23	22	23	9	4	-

Table 1. Clinicopathological features of human mammary neoplasms. For the age and the survival, the data are the mean values with the standard deviation in brackets. Fibroadenoma (Fb), tubular carcinoma (TC), grade I invasive carcinoma (IcgI), grade III invasive carcinoma (IcgIII), invasive micropapillary carcinoma (IMC). N = number of cases; NA = not evaluated. HR = hormonal receptor.

Histological type	n	Age (year)	Staging (TNM)				Histological grades			Molecular subtype			Survival (days)
			I	II	III	IV	I	II	III	HR+/ Ki67 < 20%	HR+/ Ki67 >20%	HR+/-/HER2+	HR-/HER2-	
BMT	15	10	NA	NA	NA	NA	NA	NA	NA	NA	NA	NA	NA	NA
MC	14	11	7	3	4	0	11	2	1	13	1	0	0	11162
CS	6	8.5	0	0	4	2	0	0	6	2	4	0	0	321.8
IMC	16	10.8	0	1	2	10	3	2	9	5	1	7	3	5	230.9
SC	23	11.8	5	4	4	9	1	2	10	11	3	17	2	1	229.5
Total	74	-	12	8	14	19	6	13	21	25	19	29	5	6	-

Table 2. Clinicopathological features of canine mammary neoplasms. For the age and the survival, the data are the mean values with the standard deviation in brackets. Benign mixed tumour (BMT), mixed carcinoma (MC), invasive micropapillary carcinoma (IMC), carcinosarcoma (CS), solid carcinoma (SC). N= number of cases, NA = not evaluated.

with TC (02 alive, 02 not followed up), 16 women with ICgI (01 died, 14 alive, 01 not followed up), 21 women with ICgIII (18 alive, 03 not followed up), and 17 women with IMC (05 died, 09 alive, 03 not followed up). All patients had complete information on clinical staging.

The female dogs were followed up for a minimum of 02 years and a maximum of 05 years. At the conclusion of the study, we completed the follow-up of 55 bitches. Of these, 46 patients had died and 09 were still alive. Follow-up was not possible for 04. The distribution of patients based on clinical staging was as follows: 14 patients with MC (07 died, 07 alive), 16 with IMC (14 died, 02 not followed up), 06 with CS (all died), and 23 with SC (19 died, 02 alive, 02 not followed up). Three patients with IMC did not have complete information to define the clinical staging. Women with Fb and dogs with BMT were not followed up.

Images and extract parameters

Figure 1 present representative images of the human histological sections studied to illustrate the imaging procedure. The histological types in the columns are indicated as NMTh (Fig. 1A, E, I and M), Fb (1B, 1 F, 1 J and 1 N), ICgI (1 C, 1G, 1 K and 1O) and IMC (1D, 1 H, 1 L, 1P) for the normal mammary gland, fibroadenoma, grade I invasive carcinoma and invasive micropapillary carcinoma, respectively. The fourth row presents images of individual fibres, displayed in varying colours, extracted using our image analysis methodology (1M-1P). The SHG signal is from the collagen fibres, that are non-centrosymmetric fibres, and the TPEF signal corresponds to the fluorescence emission of the dye eosin. The SHG and TPEF represent false colour representations of normalized intensity maps to accentuate various features. Comparing the two images allows to segment the tissue into collagen and cellular regions, and thus extract quantitative parameters. The images of the extracted collagen fibres are presented in Fig. 1M and N 1O 1P. For the canine samples, the methodology for acquiring the images and extracting the parameters has already been thoroughly exemplified in previous articles[17,18,39]. More details about measurements and image analyses can be found in the 'Materials and Methods' section.

Human mammary tissue (NNMTh, Fig. 1) is composed of lobes, ducts, and an interconnected network of connective tissue (indicated by the asterisk in Fig. 1A), connective tissue, abundant collagen fibres are found surrounding the parenchyma, which exhibit different orientations within the breast tissue (Fig. 1E). In benign neoplasms of the mammary gland, such as fibroadenoma (Fb) in women (Fig. 1B), and also benign mixed tumours (BMT) in dogs, an abundance of collagen fibres is visible in the adjacent connective tissue, exhibiting a pattern of diverse orientation similar to that of NNMTh (Fig. 1F) and NMTc. However, in grade I invasive carcinoma (ICgI) and invasive micropapillary carcinoma (IMC), there is a reduction in collagen density and collagen fibres are organized in a preferential direction (Fig. 1G, H, O and P). ICgI has a favourable prognosis, while IMC is associated with an unfavourable prognosis[17,23,29]. Mixed carcinomas (MC) originates from the malignant transformation of benign mixed tumours, presenting a complex histological pattern and favourable prognosis[31–36,42,43]. On the other hand, carcinosarcoma (CS) is characterized by the coexistence of malignant epithelial and mesenchymal components, presenting an extremely aggressive biological behaviour, with a high incidence of metastases to regional lymph nodes and lower overall survival[29,31,34,36]. In IMC and SC, decrease in collagen density and an increased alignment of collagen fibres in the surrounding connective tissue are also noticeable.

Our image analysis and fibre and cell extraction procedures allowed the quantification of many of these microscopic features described. Collagen fibre organization parameters (fibre segment SHG coherence), number of collagen fibres (no. fibres), mean fibre length, collagen density (fibre segment coverage) and cell density (cell segment coverage) for all histological types of human and canine mammary neoplasms and for NMTh and NMTc that are presented in Fig. 2.

Carcinomas present aligned fibres, lower fibre density and higher cell density

The collagen fibre organization parameter assesses the degree of alignment of collagen fibres within the tissue, with values spanning from zero (indicating a random arrangement) to one (indicating highly oriented and aligned fibres along a specific direction). As depicted in Fig. 2A human mammary carcinomas exhibit a greater degree of collagen fibre alignment when compared to NMTh. Canine neoplastic tissues exhibit the same behaviour (see Supplementary Fig. S1). These results clearly delineate a distinction between normal and carcinomatous tissue in both species.

Figure 2B show the waviness of the collagen fibres for human mammary tissues. This parameter evaluates the straightness of the collagen fibres extracted from the stromal regions, where 1 means perfectly linear fibres and 0 means perfectly wavy fibres. In human mammary tissues, carcinomas present more linear fibres compared to NBTh and Fb. In canine mammary tissue (see Supplementary Fig. S1), it was not possible to verify this same behaviour. We observed that none of the histological types present statistically significant differences with NBTc. SC has more linear collagen fibres compared to BMT and ICM, and CS has more linear fibres compared to BMT and IMC.

The number of collagen fibres, the fibre coverage area and the cell coverage area determine the collagen density and cell density in the measured regions. These are important parameters to evaluate changes related to the stromal and epithelial components of human (Fig. 2C and E) and canine (see Supplementary Fig. S1) mammary carcinomas. Figure 2C and D show that the number of collagen fibres and the area covered by fibres decrease in carcinomas compared to NMTh and neoplastic tissues benign. Comparatively, Fig. 2E show that carcinomas present a larger area covered by cells compared to NMTh and benign neoplastic tissues. We observed similar behaviour in the canine species (see Supplementary Fig. S1), however we did not observe significant differences in the number of collagen fibres, area covered by fibres and area covered by cells between CS with NMTc and BMT.

Furthermore, the collagen fibre length is an important parameter for evaluating the stromal changes that occur in neoplastic mammary tissues[1,9,18,44]. Figure 2 F show that the mean fibre length is different between

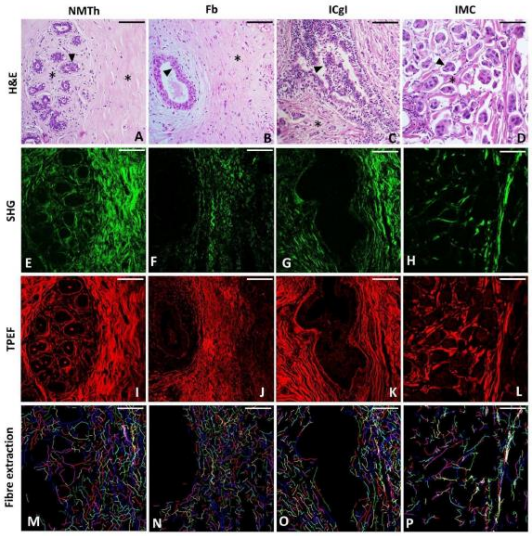

Fig. 1. Acquired images (20X objective). The optical microscopy H&E (**A**-**D**), second harmonic generation microscopy (**E**-**H**), two-photon excited fluorescence microscopy (**I**-**L**) and the extracted collagen fibres with each fibre in a random colour (**M**-**P**) for the human normal mammary tissue (**A**, **E**, **I** and **M**), fibroadenoma (**B**, **F**, **J** and **N**), grade I invasive carcinoma (**C**, **G**, **K** and **O**) and invasive micropapillary carcinoma (**D**, **H**, **L** and **P**). Asterisk HE: stroma. HE arrowhead: epithelial cells. The scale bar is 100 µm.

the histological types in humans. Carcinomas with favourable prognosis (TC and ICgI) present a higher mean fibre length as compared to carcinomas with unfavourable prognosis (ICgIII and IMC). In canine mammary carcinomas, we identified the same behaviour (see Supplementary Fig. S1 online). Carcinoma with favourable prognosis (MC) presents the highest average fibre length as compared to carcinomas with reserved to unfavourable prognosis (CS, IMC and SC).

More aggressive carcinomas present lower fibre density, higher cell density and shorter collagen fibres

To evaluate the influence of the tumour stroma on the behaviour of human and canine mammary carcinomas, we verified whether the density of collagen fibres, cell density and fibre length correlate with the clinicopathological data. Immunohistochemistry was performed on a sample of 58 human and 59 canine mammary tissue samples, all diagnosed with mammary carcinoma. Figure 3 shows these correlations. Here, the increased aggressiveness

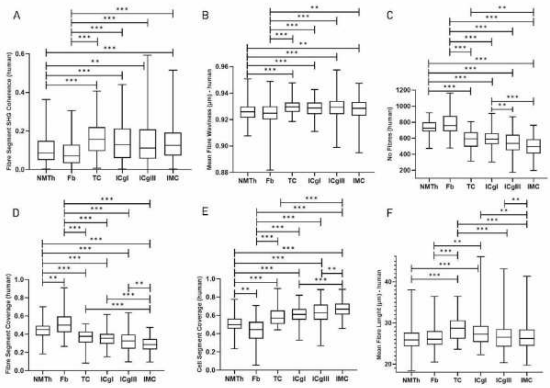

Fig. 2. Parameters of the human mammary gland analysed by second harmonic generation and two-photon excited fluorescence techniques. Kruskal Wallis test and the Dunn test. Boxplot graphics showing the calculated parameters for the fibre segment SHG coherence, mean fibre waviness, mean fibre length, number of fibres, fibre segment coverage and cell segment coverage for human normal mammary tissue (NMTh, $n = 20$), fibroadenoma (Fb, $n = 12$), tubular carcinoma (TC, $n = 04$), invasive carcinoma grade I (ICgI, $n = 16$), invasive carcinoma grade III (ICgIII, $n = 21$), invasive micropapillary carcinoma (IMC, $n = 17$) in human samples ($n = 90$). The centre lines show the medians, the box limits indicate the 25th and 75th percentiles, the whiskers extend 1.5 times the interquartile range from the 25th and 75th percentiles and the outliers are represented by dots. The p values less than 0.001 denoted by (***), p less than 0.01 are denoted by (**) and p less than (0.05) are denoted by (*).

of carcinomas was associated with cases that presented the following characteristics: higher histological grade, larger probability of developing local and/or distant metastases, higher rate of cellular proliferation and larger probability of presenting molecular expressions of the "triple-negative" and "Her2 overexpressed". For the correlations, the cell proliferation rate was obtained from the Ki67 count and the molecular subtype of human and canine mammary carcinomas were categorized as follows: 1 for luminal A (positive hormone receptors, negative HER-2 and proliferative rate less than 20%), 2 for luminal B (positive hormone receptors, negative HER-2 and proliferative rate greater than 20%), 3 for HER-2 positive (positive or negative hormone receptors and positive HER-2 independent of the proliferative rate) and 4 for triple negative (negative hormone receptors, negative HER2 regardless of proliferative rate).

We note that the mean fibre length inversely correlates with histological grade (Fig. 3A and B), clinical staging (Fig. 3C and D), cell proliferation (Fig. 3E and F) and molecular subtype (Fig. 3G and H) in women and dogs. Here, we show data correlating the increased tumour aggressiveness with the smaller collagen mean fibre length. It is important to note that while human molecular subtypes have been adapted for use in canine mammary carcinomas, their prognostic value in dogs remains controversial, particularly for HER2 overexpression. Conflicting results in the literature have made it difficult to establish a consistent correlation between HER2 status and clinical outcome in dogs. Despite this limitation, we found that mean fibre length inversely correlates with histological grade (Fig. 3A and B), clinical staging (Fig. 3C and D), cell proliferation (Fig. 3E and F) and molecular subtype (Fig. 3G and H) in both women and dogs. Here, we show data correlating the increased tumour aggressiveness with the smaller collagen mean fibre length.

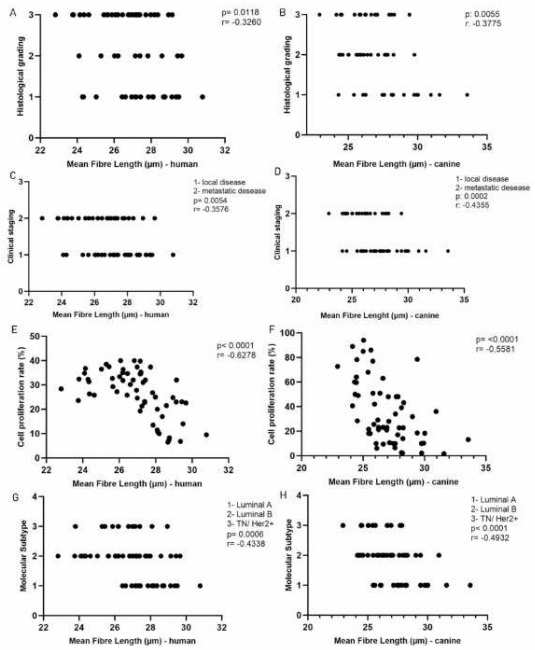

Fig. 3. Correlation between clinicopathological parameters and mean fibre length in women and dogs. Spearman's correlation between histological grading and mean fibre length in women (**A**, $n = 58$) and dogs (**B**, $n = 59$). Spearman's correlation between clinical standing and mean fibre length in women (**C**, $n = 58$) and dogs (**D**, $n = 59$). Linear regression between cell proliferation and mean fibre length in women (**E**, $n = 58$) and dogs (**F**, $n = 59$). Spearman's correlation between molecular subtype and mean fibre length in women (**G**, $n = 58$) and dogs (**H**, $n = 59$).

To determine the influence of mean fibre length on patient survival, we established a cut-off point disregarding histological subtype, histological grade, clinical staging, cell proliferation rate and molecular subtype. For this, the data were organized in ascending order and the median fibre length value was calculated. Therefore, the value 27 µm was determined as the cut-off point, categorizing patients into two groups based on this cut-off point. Those diagnosed with carcinomas with fibres smaller than 27 µm were grouped in the first category, while those with carcinomas with collagen fibres larger than 27 µm were grouped in the second category. We assigned 0 to patients alive at the end of the study and 1 to patients who died from mammary carcinoma. For those diagnosed with carcinomas with collagen fibres larger than 27 µm (represented by the red line), the average survival was 150 days. On the other hand, patients with carcinomas with fibres larger than 27 µm (shown by the blue line) had a median survival of 849 days. Notably, more aggressive carcinomas with an unfavourable prognosis had shorter collagen fibres compared to less aggressive carcinomas with a favourable prognosis. In Fig. 4A, we show survival curves for dogs. We extend this method to define cut-off points for SHG coherence, mean fibre waviness, number of fibres, fibre segment coverage, and cell segment coverage. However, no significant correlations were observed between these metrics and dog-specific survival. These findings support the data from our current study and are in line with our previously published work[18]. It should be noted that the canine dataset examined in this study differs from our previous assessment.

In humans, it was not possible to establish a specific survival curve for cancer using the same methodology as used for dogs. This is because approximately 85% of the patients in the study are alive and still under medical supervision. Thus, the median survival was not reached in any of the stratified groups, making it impossible to carry out and evaluate the analysis. However, to demonstrate the clinical importance of these findings for breast oncology, we established an association between the mean fibre length and clinicopathological data[30] that directly influence patient survival. For this analysis, the same cut-off point defined for the analysis of the dog's survival curve (Fig. 4A) was considered. Using the cut-off point of 27 µm, women and dogs were stratified into two groups: those diagnosed with carcinomas with collagen fibres smaller than 27 µm were categorized into the first group, while those diagnosed with carcinomas with collagen fibres larger than 27 µm were grouped into the second group (Fig. 4B and I). To verify the association or independence between the mean fibre length and the clinicopathological data, we performed an analysis using the Fisher's Exact Test and the chi-square test. The data indicate that a higher proliferative rate, higher histological grade, presence of local and/or distant metastases and the "triple negative" and "Her2 overexpressed" molecular subtypes are associated with carcinomas with collagen fibres smaller than 27 µm in women (Fig. 4B, D, F and H) and dogs (Fig. 4C, E, G and I). Finally, we observed that collagen density presents an inverse correlation with histological grade (Fig. 5A and B), cell proliferation rate (Fig. 5C and D) and molecular subtype (Fig. 5E) in human breast carcinomas. Cell density has a direct correlation with molecular subtype (Fig. 5F). The same correlations were established for dogs, but no statistically significant correlations were obtained.

Discussion

Numerous studies indicate that collagen plays a key role in the tumour micro-environment, playing a critical role in the regulation of neoplastic growth and tumour cell dissemination, due to its ability to provide physical, biochemical, and biomechanical guidance for tumour and non-tumour cells[18,45–51]. Tumours can actively remodel the surrounding extracellular matrix. Type 1 and type 3 collagen fibres, when aligned, increase the stiffness of the extracellular matrix and this predicts worse outcomes[28,52] and the expression of COL11A1 may have a potential role in the aggressiveness of carcinoma in situ in women through collagen remodelling and regulation of the cellular stimulation mechanism[1]. Recent studies have described that this stiffness of the extracellular matrix is fundamental in the process of cell migration, invasion, and metastasis of tumour cells[18,44–49,51–63]. Here, we demonstrated that in human and canine mammary carcinomas, collagen fibres orient themselves in a preferential direction, becoming more organized.

In human mammary carcinomas, we observed that collagen fibres are more linear compared to NMTh and Fb. We did not observe this behaviour in canine mammary carcinomas. The composition of carcinomas in mixed tumours and carcinosarcomas may explain this difference. As previously stated, the MC arises from epithelial malignant transformation into benign mixed tumours[31,42,43]. It has components of malignant epithelial origin and normal or benign mesenchymal components. CS are characterized by malignant components of epithelial and mesenchymal origin, leading to intense proliferation of the extracellular matrix. MC and CS exhibit a complex histological pattern[31,33,34,36]. Thus, we noticed that canine mammary carcinomas exhibit significant heterogeneity in their composition, unlike mammary carcinomas in women, which exhibit homogeneity in epithelial and mesenchymal components. Despite exhibiting distinct features, we selected these tumours for our study because they commonly affect the female dogs, as we aim to understand the behaviour of these carcinomas in regard to the more common breast carcinomas in women.

The larger organization and alignment of collagen fibres in the tumour and peritumoural areas collected in the evaluated samples makes the stroma more rigid. We believe that this increased alignment and linearity of collagen fibres in carcinomas is associated with extracellular matrix remodelling and increased stromal stiffness. The rigid extracellular stroma, which surrounds neoplastic cells, may offer a durotactic escape route from the potentially hypoxic and necrotic environment for tumour cells. Inhospitable conditions can induce an innate mechanical sensitivity to direct cancer cells to an environment where conditions are more favourable[17,49]. The study by Toss et al., 2019[1] and Sprague et al., 2021[66] showed that the deposition and reorganization of collagen around breast carcinoma in situ plays a role in tumour progression and recurrence. The larger linearity of collagen fibres was associated with an increased risk of breast cancer recurrence in these women. Several studies show that the stiffness of the extracellular matrix and the high contractility of tumour cells severely disturb tumoural homeostasis. Matrix remodelling and cross-linking stiffens the extracellular matrix as positive feedback to further stiffen, remodel and reorient the matrix. In a transformed epithelium, increased cell tension

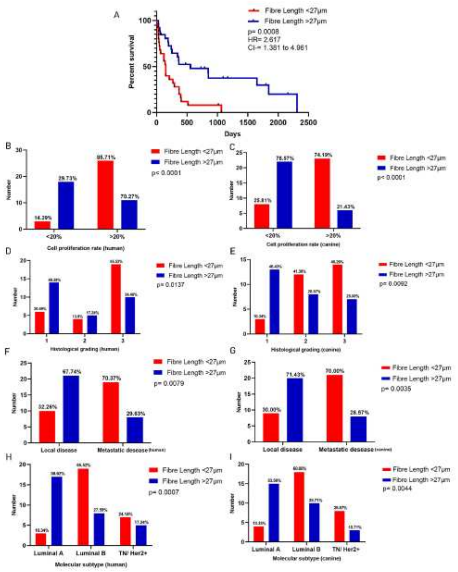

Fig. 4. Survival curve for dogs and association between clinicopathological parameters and mean fibre length in women and dogs. Kaplan–Meier curve showing the separation of cases by mean fibre length in dogs; red line for fibre length < 27 µm and blue line for fibre length > 27. (**A**, $n = 59$). Contingency plots presenting data from chi-square analysis (**D**, **E**, **H** ad **I**) and Fisher's exact test (**B**, **C**, **F** and **G**) to evaluate the association between clinicopathological data and the mean fibre length categorized in women and dogs. The clinicopathological data are presented on the x-axis, the absolute frequency (n) on the y-axis and the proportion in percentage at the end of each bar. Association between cell proliferation rate (**B**, $n = 58$), histological grade (**D**, $n = 58$), local or metastatic disease (F, $n = 58$), molecular subtype (**H**, $n = 58$) and mean fibre length categorized by the 27 µm cut-off point in women. Association between cell proliferation rate (**C**, $n = 58$), histological grade (**E**, $n = 58$), presence or absence of metastatic disease (**G**, $n = 58$) and molecular subtype (**I**, $n = 58$) and mean fibre length categorized by the cut-off point 27 µm in dogs. Error bar not included because it is the evaluation of categorical data.

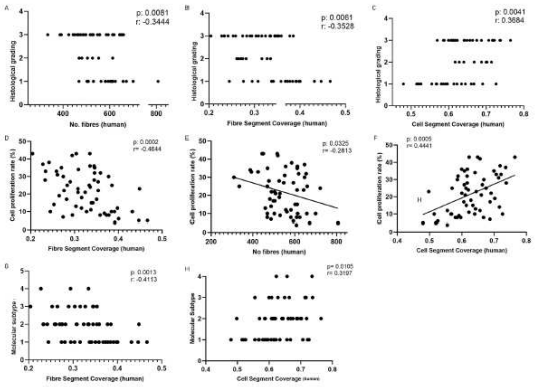

Fig. 5. Correlation between clinicopathological parameters and metrics extracted by second harmonic generation and two-photon fluorescence techniques in women. Spearman's correlation between the number of fibres (**A**, $n = 58$), fibre segment coverage (**B**, $n = 58$), cell segment coverage (**C**, $n = 58$) and histological grading. Spearman's correlation between fibre segment coverage (**G**, $n = 58$) and cell segment coverage (**H**, $n = 58$) and molecular subtype. Linear regression between the fibre segment coverage (**D**, $n = 58$), number of fibres (**E**, $n = 58$) and cell segment coverage (**F**, $n = 58$) and cell proliferation rate.

stimulates cell growth, disturbs cell-cell adhesion, compromises tissue polarity, and promotes stromal invasion by tumour cells[66–70].

We observed that in human and canine mammary carcinomas there is an exacerbated growth of epithelial components contributing to the loss of balance between stromal and parenchymal components. Therefore, the tumours present lower density of collagen fibres and higher cell density. CS does not follow this growth pattern because it has malignant epithelial and mesenchymal components. Thus, a malignant mesenchymal component induces exaggerated deposition of stromal components[33]. We therefore observed higher stromal density and lower cell density compared to other canine mammary carcinomas. In Pb, we observed higher collagen density and lower cell density compared to other histological types and NMT in humans, since the deposition of stromal elements is increased in this tumour[32].

Correlating the parameters, number of fibres, area covered by fibres and area covered by cells with the histological grade, TNM, cell proliferation rate and molecular subtype, we observed that the most aggressive human mammary carcinomas[32] present lower density of collagen fibres and higher cell density (Fig. 3). Maller et al., 2013[32] showed that the abundance of collagen in the extracellular matrix of pregnant rats was associated with reduced tumour growth and invasion compared to the tumour micro-environment of nulliparous rats. Using methods including second harmonic generation imaging, the authors showed that the abundant collagen in the mammary glands of pregnant rats is less linearised and that high-density collagen induces tumour suppressive attributes[60]. Other authors have also shown that the decrease in collagen density and increase in fibre organization is correlated with more aggressive tumour behaviour[9,61].

Another important characteristic of collagen fibres that stood out was the identification that shorter collagen fibres are associated with an unfavourable prognosis (Figs. 2F, 3A, F, A and F and 4B, I, B and I). In addition, we demonstrated that canine mammary carcinomas with shorter collagen fibres are associated with lower patient survival (Fig. 4A). Unlike women, most dogs diagnosed with mammary carcinoma are treated exclusively with surgery, without the use of chemotherapy. This fact is important to allow the study of progression of spontaneous

breast carcinomas, without the interference of chemotherapy drugs that impact the growth and development of neoplasms. Furthermore, studying mammary carcinomas in dogs avoids the bias associated with induced experimental models that are carried out within controlled environments. Thus, a comparative study using dogs as a model provides accurate data on patient survival and the behaviour of mammary carcinomas in a short period of time, since these tumours progress more quickly compared to tumours in women.

Although we were unable to plot survival curves for women, we established correlations between the number of collagen fibres, collagen fibre density, and cell density with clinicopathological data that are known to play a crucial role in patients' survival[32]. Similarly, to what occurs in the canine species, we observed that a lower number and density of fibres, a higher cell density, and shorter collagen fibres are associated with carcinomas with an unfavourable prognosis. These are important findings. It can be hypothesized that this behaviour is related to the stromal changes that occur during tumour progression, as shown in our previous work[18]. TC and ICgI in humans and MTC in dogs are carcinomas that present well-defined tubular structures, differentiated cells, low mitotic rate and low cellular and nuclear pleomorphism. The stromal component is preserved and the rate of epithelial proliferation is low. These characteristics are associated with local growth, low probability of local and/or distant metastases and favourable prognosis[31–34]. In contrast, ICgII and IMC in humans and CS, IMC and SC in dogs present expansive growth, undifferentiated cells, high mitotic rate and high cellular and nuclear pleomorphism. The stromal component is replaced by epithelial growth because the proliferation rate of these components is high. CS does not present this behaviour because the mesenchymal component is also malignant, making it more aggressive. Thus, these carcinomas are commonly associated with local and/or distant metastases and with an unfavourable prognosis[31,32,35].

We believe that in carcinomas with a favourable prognosis and low proliferative rate, collagen fibres are larger because they limit neoplastic growth. However, in carcinomas with an unfavourable prognosis, with loss of cellular differentiation and a high proliferative rate, the collagen fibres are unable to limit this growth, and thus they rupture, allowing the tumour to expand. In this way, the fibres become fragmented and shorter compared to the fibres of carcinomas with less aggressive behaviour. Furthermore, we believe that this "shortening" of collagen fibres is associated with remodelling of the extracellular matrix to guide the metastatic invasion of tumour cells (Fig. 6). Studies show that while collagen can potentially form a protective barrier and prevent cancer cells from escaping their original location, collagen fibres also serve as a "highway" that facilitates the migration of cancer cells to remote locations, impacting survival of patients[7,9,14,62–73].

Conclusions

In conclusion, our study revealed similarities in collagen changes between human and canine mammary neoplasms, showing the association of these changes with clinicopathological factors in both species. Employing second harmonic generation, two-photon excited fluorescence techniques, and automated image analysis, we identified similar changes in the tumour stroma of human and canine mammary neoplasms. We observed that human and canine mammary carcinomas present more organized fibres. Carcinomas with higher histological grade, higher cell proliferation rate, with local and/or distant metastasis and molecular classifications of triple negative type and overexpressed Her2 present lower collagen density and higher cell density. We have also

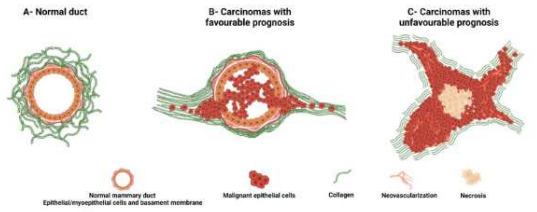

Fig. 6. Carcinomas with an unfavourable prognosis present shorter fibre. Mammary carcinomas present more organized fibres (**B** and **C**) compared to normal mammary tissue (**A**). Carcinomas with a favourable prognosis and low proliferative rate present longer collagen fibres, capable of limiting neoplastic growth (**B**). In carcinomas with an unfavourable prognosis and high proliferative rates, collagen fibres are shorter and unable to limit this growth, allowing tumour expansion (**C**). This "shortening" of collagen fibres may be associated with remodelling of the tumour stroma that creates rigid pathways to help cancer cells escape necrotic and hypoxic environments. Thus, the fibres become capable of guiding tumour cells towards locations with greater vascularization (**C**). Created by BioRender.